Generation of 2-D Analog and Digital Lowpass, Highpass and Bandpass Filters with Monotonic Amplitude-Frequency Response

Ajit Singh Sandhu

A Thesis

in

The Department

of

Electrical and Computer Engineering

Presented in Partial Fulfillment of the Requirements
for the Degree of Master of Applied Science at
Concordia University,
Montreal, Quebec, Canada

April 2005

Your file Votre référence
ISBN: 0-494-04392-X
Our file Notre référence
ISBN: 0-494-04392-X

ABSTRACT

Generation of 2-D Analog and Digital Lowpass, Highpass and Bandpass Filters with Monotonic Amplitude-Frequency Response

Ajit Singh Sandhu

A significant amount of research work has been done in 1-D filters with monotonic amplitude-frequency response, e.g., Butterworth, Papoulis, Filanovsky, Thomson-Bessel filters, etc, to name a few.

In this work, we have discussed design methodologies for generation of polynomial Butterworth, Papoulis and Filanovsky lowpass filters of different orders with arbitrary flatness, and also Thomson-Bessel lowpass filters, with monotonic amplitude-frequency response. We have shown how other monotonic responses can be obtained either by choosing lower order responses and/or by suitable combinations of these monotonic responses. We have proposed extraction of all possible lower order 1-D lowpass filters from the designed higher order lowpass filters, and segregate the filters with monotonic amplitude-frequency response. Furthermore, we cascaded the proposed extracted monotonic 1-D lowpass filters to realize higher order 1-D lowpass filters with monotonic characteristics, and studied combinations of the same.

We have proposed 2-D fourth and fifth order Papoulis, Butterworth and Thomson-Bessel filters, and fifth order Filanovsky analog and digital lowpass filters, with monotonic amplitude-frequency response. Furthermore, by appropriately cascading lower order extracted 1-D lowpass filters from the above mentioned types, 2-D monotonic filters of different orders are realized. Also, a few combination 1-D lowpass filters having monotonic amplitude-frequency response are cascaded to realize 2-D monotonic lowpass filters of different orders.

Another approach to generate 2-D filters is to start with a doubly terminated network. So, we considered a Continued Fractional Expansion, defined its stability, conditions for monotonicity, and implemented it as stable 2-D analog and digital lowpass filters, with monotonic amplitude-frequency response. The generalized 2-D analog filter has been implemented, and constraints on the coefficients to attain monotonic characteristics are defined, and verified by simulation results. Furthermore, the coefficients of the generalized 2-D analog lowpass filter required to generate 2-D Butterworth analog lowpass filter are derived, and the corresponding 2-D filter have been implemented. The 2-D lowpass filters have been implemented in digital domain by applying generalized bilinear transformation. The effects of the coefficients to achieve monotonic characteristics are discussed.

We also proposed 2-D digital Papoulis, Butterworth, Filanovsky and Thomson-Bessel highpass and bandpass filters, with monotonic amplitude-frequency response, by utilizing the equivalent generated 2-D lowpass filters, and studied their characteristics. In the end, we have shown some basic examples of implementation of 2-D digital lowpass, highpass and bandpass filters in image and video processing. The examples includes reducing added Gaussian noise from images/frames of videos, by using 2-D lowpass filtering, and extraction of different frequency bands from images.

ACKNOWLEDGEMENTS

I would like to express my gratitude to my supervisor, Dr. V. Ramachandran, for his expert guidance and support that made this research work possible. He has been extremely helpful, understanding and extra-ordinarily patient in the critical review of my thesis. It has been a great privilege to work with him which has resulted in the writing of a few invaluable research papers which we will submit in future. I sincerely thank Dr. E. I. Plotkin, Dr. Aishy Amer, Dr. C.S. Gargour, and Dr. Amir G. Aghdam for insightful discussions on related topics/courses at one point or other during the tenure of this thesis.

I am heartly grateful to my parents and sister for their encouragement and support which have always been the key factor behind every success in my life. I would like to thank them for their love and sacrifices. Many thanks are due to my close relatives and friends, especially to Debashis Sen, Ayushya Bangur, Harun Prasad, Nikhil Gupta, Amitabh & Aditi Barua, and my loving sister Jolly Sandhu for their constant help and encouragement.

Ajit Singh Sandhu, April 2005

I dedicate this work to my parents and sister ...

Contents

List of Figures

List of Tables

List of Algorithms

List of Symbols and Abbreviations

s_1, s_2	:	Laplace domain parameter in two dimensions.
z_1, z_2	:	Z-domain parameter in two dimensions.
H_a	:	Transfer function of a filter in analog domain
H_d	:	Transfer function of a filter in digital domain
$\sum$	:	Summation.
$\in$	:	Belongs to.
m	:	Order of filter.
i	:	Degree of flatness.
$f_{m,i}$	:	Filtering function of order m and degree of flatness i.
$F_{m,i}$	:	1-D filter transfer function with order m and degree of flatness i.
$A_{m,i}$	:	Amplitude frequency response of a filter with order m and degree of flatness i.
$P_k^{(0,i)}$	:	Jacobi polynomial with degree of flatness i.
b_k	:	Coefficients required for the filtering function.
a_{00}, a_{01}, a_{10}, a_{11}	:	Coefficients of the generalized doubly terminated network
b_{00}, b_{01}, b_{10}, b_{11}		considered by using the CFE.
k_1, k_2	:	Bandwidth effecting coefficients of generalized bilinear transformation.
a_{1L}, a_{2L}	:	Gain effecting coefficients of generalized bilinear transformation for Lowpass filters.
a_1, a_2	:	Gain effecting coefficients of generalized bilinear transformation.

b_1, b_2	:	Polarity effecting coefficients of generalized bilinear transformation.
Pi	:	Lower order 1-D analog lowpass filters obtained from 1-D Papoulis lowpass filter (i=1 to 8).
Bi	:	Lower order 1-D analog lowpass filters obtained from 1-D Butterworth lowpass filter (i=1 to 8).
TBi	:	Lower order 1-D analog lowpass filters obtained from 1-D Thomson-Bessel lowpass filter (i=1 to 8).
Fi	:	Lower order 1-D analog lowpass filters obtained from 1-D Filanovsky lowpass filter (i=1 to 6).
Ci	:	Cascaded combinational 1-D analog lowpass filters with monotonic amplitude-frequency response (i=1 to 31).
FLi	:	Cascaded combinational 2-D analog lowpass filters with monotonic amplitude-frequency response (i=1 to 22).
μ	:	Mean of average value of the noise function.
σ	:	Standard deviation of the noise function.
w_{1c}, w_{2c}	:	Cutoff frequencies of the 2-D analog lowpass filter.
M, N	:	Number of columns and rows of a digital image.
$*$	:	Convolution.
N-D	:	N-Dimensional, where N is positive integer, e.g., 2-D for Two-Dimensional.
D_a	:	Denominator of a transfer function.
N_a	:	Numerator of a transfer function.
SHP	:	Strictly Hurwitz Polynomial.
VSHP	:	Very Strict Hurwitz Polynomial.
CFE	:	Continued Fraction Expansion.
BIBO	:	Bounded Input Bounded Output.
FIR	:	Finite Impulse Response.

IIR	:	Infinite Impulse Response.
DFT	:	Discrete Fourier Transform.
IDFT	:	Inverse Discrete Fourier Transform.
MSE	:	Mean Square Error.
$PSNR$	:	Peak Signal-to-Noise Ratio.
PDF	:	Power Density Function.

Chapter 1

Introduction

Digital filters are a fundamental tool in Digital Signal Processing (DSP) applications, and in general in data acquisition and processing applications. There are many problems in science and engineering whose solution involves use of multi-dimensional (M-D) digital filters. It is observed that due to merits and requirement of M-D digital filtering, its design is coming up as a key aspect in implementation of various stable digital systems.

The computational efficiency of M-D signal processing algorithms plays a crucial role in design and implementation of digital systems. Phenomenal advances in digital integrated circuit technology during the past few years have made the digital processing approach economically practical, flexible and reliable in many diverse fields. The design and implementation of M-D digital filters require considerable research effort over many years, in both M-D FIR and M-D IIR filters. Over the past few years, researchers have shown particular interest in two-dimensional (2-D) filters, due to increasing requirements in various applications.

1.1 Importance of two-dimensional filtering

Recent growth in two dimensional (2-D) signal processing activities for example, image processing, has stimulated active research in area of 2-D circuits and systems, both recur-

sive and non-recursive. There are various problems that call for digital filtering of sampled two-dimensional data to process and analyze various digital systems. For example, 2-D variable recursive digital filters are applied in signal processing, imaging processing, video processing processes, as well as communication systems where the frequency-domain characteristics of digital filters are required to be adjusted, and also in the geophysical industry uses 2-D filtering for processing seismic records, gravity and magnetic data, enhancement of photographic data such as weather photos, air photos and medical X-rays, etc. The uses of digital filters range from simple noise reduction to the complex spectral processing and analysis used in speech processing and recognition, audio, and communications.

The applications vary from filter banks in image coding via fan filtering in seismology to modeling of physical systems such as fluid flow. Due to the rapidly increasing interest in High-Definition TV, Multimedia, etc., the processing of still and motion, monochrome and color pictures has become of great importance. 2-D linear phase FIR filters have been used particularly in scanning rate converters, PAL decoders and digital video codecs based on the Discrete Cosine Transform (DCT), subband and pyramidal coding schemes.

It is observed that recursive filters based on the allpass subfilter offer strong competition to FIR filters because they require less computation per sample. Although the structures are recursive, stability is assured given certain conditions and furthermore, unlike other recursive filters, approximately linear phase can be achieved easily.

There are many works concentrating on the use of 2-D filters in image and video signal processing problems. The first application area is image enhancement. 2-D highpass filters can be used to increase local contrast and sharpen an image, 2-D lowpass filters can improve noisy images. The second application area of 2-D filter is image coding. Because of the need to transmit pictures using existing speech transmission channels, for example in video conferencing, many new techniques for coding the image have been developed. One of these techniques is subband coding in which the image is split into a number of frequency bands and, as a result, the sampling rate can be reduced (decimation). After transmission

and/or storage, these subbands are recombined (interpolation) to reconstruct the image and these require 2-D digital filtering. There are many applications in the video field for M-D filters. Some of these were discussed in early BBC and IBA technical reports. Principally they are used in pre-filtering and post-filtering of high definition signals so as to reduce the data rate for digital transmission. 2-D filters used for pattern recognition operations permit the extraction of significant information and configuration from the images for final interpretation and utilization. Hence, 2-D filters have various applications associated with image enhancement, pattern recognition and restoration [25, 26].

In addition, seismic data is two-dimensional in nature. The structure of subsurface ground formations can be explored by using the so-called seismic reflection method. Seismic waveforms consist of two distinct components: a component due to reflections from subsurface formations and a surface component called ground roll. The frequency of the ground roll is lower than that of the reflected component and can be removed using a 2-D filter whose response contour is in the shape of a fan having a specified angle. With high definition television (HDTV) and improved quality television (IQTV) now in use around the world, multi-dimensional digital filters are used in video signal processing circuits. Therefore, 2-D filters with certain type of symmetry, e.g., circular, quadrantal, etc, are often required depending upon the application.

Similarly, it is observed that 2-D filtering is having various applications in data communication , speech processing , CAT (Computer Aided Tomography) like spectral analysis, weather predictions, the processing of radar and sonar arrays, array processing applications, such as, X-Ray enhancements, etc, to name just a few.

1.2 Conditions to be satisfied in design of 2-D filters

In one-dimensional (1-D) systems (both analog and discrete), one can use suitably chosen transfer functions having no common factors between the numerator and denominator in

order to design a filter having required specifications. Let $H_a(s) = \frac{N_a(s)}{D_a(s)}$ be a transfer function in the analog domain with $N_a(s)$ and $D_a(s)$ being relatively prime. For the transfer function $H_a(s)$ to be stable, $D_a(s)$ should be a Strictly Hurwitz Polynomial (SHP). A SHP contains its zeros strictly in the left-half of the s-plane. Similarly, if $H_d(s) = \frac{N_d(z)}{D_d(z)}$ be a transfer function in the discrete domain with $N_d(z)$ and $D_d(z)$ being relatively prime, then $D_d(z)$ should be a Schur polynomial in order that the function $H_d(z)$ shall be stable. A Schur polynomial contains its zeros strictly within the unit circle.

In case of 2-D analog systems, it is possible that both the even and odd parts of a polynomial may become zero simultaneously at specified sets of points, but not in their neighbourhood. If this occurs in the denominator of the transfer function, it is called a non-essential singularity of the first kind. In addition, in 2-D transfer functions, both the numerator and the denominator polynomials can become zero simultaneously at a given set of points. When this happens, it is known as non-essential singularity of the second kind. A 2-D analog transfer function may be represented as

$$H_a(s_1, s_2) = \frac{N_a(s_1, s_2)}{D_a(s_1, s_2)} \tag{1.1}$$

and hence, the above two cases may be expressed as :

(a) $D_a(s_1, s_2)$=0 and $N_a(s_1, s_2) \neq 0$ constitute non-essential singularity of the first kind at (s_1, s_2).

(b) $D_a(s_1, s_2)$=0 and $N_a(s_1, s_2)$=0 constitute non-essential singularity of the second kind at (s_1, s_2).

A similar situation exists in the case of 2-D discrete systems also. A well known method to obtain 2-D digital transfer function is by applying generalized bilinear transformation [19] to a given analog filter transfer function.

The occurrence of non-essential singularity of the first kind in the transfer function (eqn. 1.1) always result in an unstable filter, and hence, cannot be used in design of stable

filters. The occurrence of the non-essential singularities of the second-kind in a transfer function may or may not cause instability. It is not possible to determine the possibility of instability by inspections only [1, 2].

The most commonly used stability criterion is based on Bounded-Input Bounded-Output (BIBO) stability condition [28]. It states that the output 2-D sequence of the filter remain bounded for all possible, bounded input sequences. Mathematically, it is possible to show that for casual linear shift-invariant systems, the BIBO stability is ensured if the impulse response coefficients $h(n_1, n_2)$ of the filter are absolutely summable, i.e.,

$$\sum_{n_1=0}^{\infty} \sum_{n_2=0}^{\infty} |h(n_1, n_2)| < \infty \tag{1.2}$$

The 2-D filters can be classified into two main categories, namely, the Finite Impulse Response (FIR) and Infinite Impulse Response Filters (IIR). This condition (eqn. 1.2) is automatically satisfied by a bounded 2-D FIR filter, as it has only a finite number of nonzero impulse response coefficients. On the other hand, it is substantially more difficult to ensure that the above condition holds for a 2-D IIR filter.

In the 1-D filters, BIBO stability condition can be related to the positions of the z-domain transfer function poles which have to be within the unit circle and it is possible to get the stability by determining the roots of the denominator polynomial. Considerable efforts have been done by a number of authors in developing stability theorems for IIR filters and formulating practical tests based on these theorems. Some references of the earliest proposed theorems in two-dimensional digital signal processing are available in [21]. A theorem relating the stability of the 2-D filters by utilizing the denominator polynomial was formulated by [20]. The proposed theorem shows that for 2-D IIR causal quarter-plane filters, if $B(z_1, z_2)$ is a polynomial in z_1 and z_2, the real transfer function of the form $\frac{1}{B(z_1,z_2)}$ is stable if and only if

$$B(z_1, z_2) \neq 0 \; for \; |z_1| \geq 1, |z_2| \geq 1$$

A widely used approach involves the design of two-variable stable analog transfer function and use bilinear transformations to obtain digital transfer function. For example, [22, 23] first design a two-variable passive (hence guaranteed stable) analog filter via a computer - aided optimization technique and then obtained a 2-D IIR transfer function by applying a double bilinear transformation on the transfer function of the analog filter. The 2-D filter stability testing problem can also be avoided by designing a separable 2-D IIR filter approximating the frequency response characteristic.

For separable filter, the 2-D transfer function $H(z_1, z_2)$ can be expressed as a product of two 1-D transfer functions, i.e., $H(z_1, z_2) = H(z_1).H(z_2)$. In this case, the stability testing reduces to that of checking the stability of the 1-D filters, which is considerably simpler. Moreover, a separable filter is also more economical to implement. For example, [24] describe a computer-aided method of designing separable filters.

Therefore, from the point of view of stability tests in designing an IIR filter, first approach can be to carry out the stability test in every stage of the filter design. Another approach can be to design a filter with a required magnitude squared transfer function and the stability can be assured by checking the location of poles in the stability region.

1.3 Suitable remedies to ensure stability, like VSHP

To ensure stability of 2-D digital filters (for example [18]), the polynomial of the denominator of the transfer function is a key factor. A major area of application of Hurwitz polynomials is the study of the stability of linear systems. As a result of the varied applications of Hurwitz polynomials in the analysis and design of two-dimensional circuits and systems, over the years, several different classes of two-variable Hurwitz polynomials have been defined.

Stable 2-D digital transfer function can be generated by using two-variable Hurwitz polynomials [8, 9, 10, 11]. Analog Hurwitz polynomials are used to characterize stable con-

tinuous domain systems, hybrid Hurwitz polynomial for delay differential and distributed parameter systems and discrete Hurwitz polynomials for discrete domain systems. In discrete domain, considerable research has been carried out on the definition of 2-D system stability, the procedure to test system functions for stability, and the generation of stable system functions.

The author in [6] considered definitions of eight types of Hurwitz polynomials on the basis of zero-free regions in the (s_1, s_2) biplane and relationship of the principal Hurwitz polynomials to other types of Hurwitz polynomials. Based on a continuity property of the zeros of two-variable polynomials, test procedures for five types of Hurwitz polynomials are also discussed. Hurwitz polynomials in $(z_1, z_2)$and (s_1, z_2) domains are presented and lastly, their applications in stability analysis of 2-D systems and study of properties of two-variable passive networks are also discussed.

A class of polynomials which does not contain singularities (discussed in Sec.1.2) is called Very Stable Hurwitz Polynomials (VSHP) [6, 7]. A VSHP is defined as follows:

"$D_a(s_1, s_2)$ is a VSHP , if $\frac{1}{D_a(s_1,s_2)}$ does not possess any singularities in the region $\{(s_1, s_2) \mid \text{Re } s_1 \geq 0, \text{Re } s_2 \geq 0, |s_1| \leq \infty \text{ and } |s_2| \leq \infty\}$. "

In view of this definition, a VSHP has to be necessarily a Strictly Hurwitz Polynomial (SHP) [7]. After ensuring that a given two-variable polynomial is SHP, one can proceed further to ascertain the absence of singularities at points of infinity. The points of infinity are studied by considering the reciprocal of the variable. In view of two variables considered, the following possibilities exist:

(a) $s_1 \rightarrow \infty$, $s_2 =$ finite.

(b) $s_1 =$ finite, $s_2 \rightarrow \infty$.

(c) $s_1 \rightarrow \infty$, and $s_2 \rightarrow \infty$.

That is, in (a) and (b), only one of the variables goes to infinity, while the other remains finite, whereas in (c), both the variables reach infinity simultaneously. Another alternate definition for a VSHP is proposed by Fettweis and Basu in [12].

A relatively prime two-variable function, $H(s_1, s_2) = \frac{A(s_1,s_2)}{B(s_1,s_2)}$, having no second kind singularities is a reactance function if and only if $A(s_1, s_2) + B(s_1, s_2)$ is a VSHP. Such functions are called proper reactance functions [8] and are useful as transformation functions to generate a (structurally stable) 2-D network from a stable 1-D network. This is one of the main applications of VSHPs and is utilized in design of 2-D stable digital filters.

1.4 Some review of the properties of VSHP

In this section, we shall discuss some of the properties of VSHP. For proof of the properties and a comprehensive study of two-variable Hurwitz polynomials refer [6, 7].

Property 1.

The transfer function $H_a(s_1, s_2)$ (defined in [3]) does not possess any singularity in the closed right-half of the (s_1, s_2)- biplane, if and only if $D_a(s_1, s_2)$ is a VSHP.

In the above, the closed right-half biplane is

$\{(s_1, s_2) \mid \text{Re } s_1 \geq 0, \text{Re } s_2 \geq 0, |s_1| \leq \infty \text{ and } |s_2| \leq \infty\}$.

Property 2.

$D(s_1, s_2) = [D_1(s_1, s_2)] \,.\, [D_2(s_1, s_2)]$ shall be a VSHP, if and only if $[D_1(s_1, s_2)]$ and $[D_2(s_1, s_2)]$ are individually VSHPs.

This property demonstrates clearly that a product of two VSHPs results in a VSHP. Also, if a VSHP is product-separable, the individual factors shall be VSHPs.

Property 3.

If $D_a(s_1, s_2)$ is a VSHP, $\frac{\partial D_a(s_1,s_2)}{\partial s_1}$ and $\frac{\partial D_a(s_1,s_2)}{\partial s_2}$ are also VSHPs.

Property 4.

The polynomials $E_i(s_2)$, i=0,1,.2,...,p and $F_j(s_1)$, j=0,1,2,...,q defined in [4] are SHPs (Strictly Hurwitz Polynomials) in $s_1$and s_2 respectively.

Property 5.

Each of the functions $\frac{E_i(s_2)}{E_{i-1}(s_2)}$, i=1,2,...,p is a minimum reactive positive real function in s_2 (where a positive real function $E(s)$ is called minimum reactive (susceptive), if it has no poles or zeros on the imaginary axis of s). Similarly, each of the functions $\frac{F_j(s_1)}{F_{j-1}(s_1)}$, j=1,2,...,q is a minimum reactive positive real function in s_1.

1.5 Types of symmetries and their importance

It is observed (for example in [13, 27]) that by taking into account the symmetry constraints, considerable reduction in multiplications can be achieved in implementation of 2-D filters. Symmetries can also be used to reduce the number of variables in optimization procedure [13]. It is observed that monotonic response helps in catering certain types of symmetries. 2-D or M-D systems may possess different types of symmetries. Most of the applications require 2-D digital filter to have certain symmetry in its magnitude response.

Symmetry concept is extended to mathematical functions. Consider a real function $f(x_1, x_2)$ with $x_1$and x_2 as two independent variables. $f(x_1, x_2)$ gets a unique value in accordance to the values of x_1 and x_2 which can be represented as a three-dimensional object having the (x_1, x_2) plane as the base and the value of the function at each point in the plane as the height. It can be said that a function possesses a symmetry, if a pair of operations, performed simultaneously, one on the base of the function object (i.e. (x_1, x_2) plane), and the other on the height of the object leaves the function undisturbed. Existence of symmetry in a function implies that the value of the function at (x_{1a}, x_{2a}) meets a certain requirement or condition, where (x_{1a}, x_{2a}) is obtained by some operation on (x_1, x_2), and

this condition being satisfied for all the points in the region. A brief review of different types of symmetries are as follows.

Displacement(Identity) Symmetry

If a function possesses displacement identity symmetry with a displacement of d, the symmetry conditions on the function can be expressed as

$f(x+d) = f(x)$ for all $x \in X$ (random variable)

Rotational Symmetry

Choosing the rotational center as the origin and rotation angle as $\pi/2$ radians, we get the four-fold rotational symmetry condition as

$f(x_1, x_2) = f(-x_2, x_1)$ for all x $\in$X

following which we have

$f(x_1, x_2) = f(-x_1, x_2) = f(-x_1, -x_2) = f(x_1, -x_2)$

Centro-Symmetry

In the two-variable case, two fold rotational symmetry (rotation by π radians) is called centro-symmetry. The required condition for centro-symmetry is

$f(-x_1, -x_2) = f(x_1, x_2)$ for all x $\in$X

Centro-Anti Symmetry

In the two-variable case, the required condition for centro-anti symmetry is

$f(-x_1, -x_2) = -f(x_1, x_2)$ for all x $\in$X

Centro-Conjugate Symmetry

In the two-variable case, the required condition for centro-conjugate symmetry is

$f(-x_1, -x_2) = [f(x_1, x_2)]^*$ for all x $\in$X

Centro-Conjugate Anti symmetry

In the two-variable case, the required condition for centro-conjugate anti-symmetry is

$f(-x_1, -x_2) = [-f(x_1, x_2)]^*$ for all x $\in$X

Reflection Symmetry

Reflection about the x_1 axis, the x_2 axis, and the diagonals $x_1 = x_2$ and $x_1 = -x_2$ line, respectively, results in reflection symmetries which could be anyone of the following:

x_1 axis reflection $\rightarrow f(x_1, -x_2) = f(x_1, x_2)$

x_2 axis reflection $\rightarrow f(-x_1, x_2) = f(x_1, x_2)$

$x_1 = x_2$ line intersection $\rightarrow f(x_2, x_1) = f(x_1, x_2)$

$x_1 = -x_2$ line intersection $\rightarrow f(-x_2, -x_1) = f(x_1, x_2)$

180^o rotation about the origin $\rightarrow f(-x_1, -x_2) = f(x_1, x_2)$

90^o rotation about the origin $\rightarrow f(x_2, -x_1) = f(x_1, x_2)$

Quadrantal Symmetry

The condition on the function to possess quadrantal identity symmetry is

$f(x_1, x_2) = f(-x_1, x_2) = f(-x_1, -x_2) = f(x_1, -x_2)$

It is easy to verify that the four quadrants of the X-plane correspond to the four symmetry regions. Hence this symmetry is called quadrantal symmetry.

Diagonal Fourfold Reflection Symmetry

Similar to the quadrantal case, if the function possesses reflection symmetry with respect to $x_1 = x_2$ line and the $x_1 = -x_2$ line simultaneously, it is supposed to possess diagonal fourfold reflection symmetry

$f(x_1, x_2) = f(x_2, x_1) = f(-x_2, -x_1) = f(-x_1, -x_2)$

As in quadrantal symmetry, the function possesses two-fold rotational symmetry when it has diagonal fourfold reflection symmetry.

Octagonal Symmetry

In this case the function possesses quadrantal symmetry and diagonal symmetry simultaneously. The conditions for a function to possess octagonal symmetry are given by

$f(x_1, x_2) = f(x_1, -x_2) = f(-x_1, x_2) = f(x_2, x_1)$

$= f(-x_2, -x_1) = f(-x_1, -x_2) = f(x_2, -x_1) = f(-x_2, x_1)$

Circular Symmetry

Mathematically, circular symmetry in 2-D filter responses can be defined as the filter response being able to satisfy the general equation of a circle, according to which, $w_1^2 + w_2^2 = M$, where, w_1 and w_2 are the frequencies in the two dimensions, and M is the magnitude response which need to be a constant in order to satisfy the circular symmetry property.

The function relation for circular symmetric response in w plane is given by [13]

$$H_1(w_1^2)H_2(w_2^2) = H_s(w_1^2 + w_2^2) \tag{1.3}$$

It has been clearly proved in [5, 13] that, it is not possible to obtain exact circular symmetric stable rational transfer function with denominator other than unity in the analog domain. In order to approximate circular symmetry, a product separable function given by, $H(s_1, s_2) = h_1(s_1)h_2(s_2)$ is considered. Therefore the following can be deduced:

1. Any separable function $H(s_1, s_2) = h_1(s_1)h_2(s_2)$ is quadrantally symmetric.

2. When $h_1(.) = h_2(.)$, $H(s_1, s_2)$ is also octagonally symmetric, where $h_1(.)$ is a single variable function.

3. For the magnitude of circular symmetry being the main criterion, $|h_1(jw_2)|^2$ should approximate $\lambda e^{\alpha w_1^2}$ for suitable values of λ and α.

4. When stable, all-pole 2-D transfer functions are considered to possess quadrantal symmetry, they turn out to be separable.

5. $H(s_1, s_2)$ is said to possess elliptical (rectangular) symmetry if its magnitude is invariant on a set of specified elliptical (rectangular) paths around the origin in the w plane.

Elliptical Symmetry

Similar to the circular case, elliptical symmetry in 2-D filter responses can be defined as the filter response being able to satisfy the general equation of an ellipse, according to which,

$$\frac{w_1^2}{a^2} + \frac{w_2^2}{b^2} = 1$$

where w_1 and w_2 are the frequencies in the two dimensions, and M is the magnitude response which needs to be constant in order to satisfy the elliptical symmetry property. The magnitude M takes both the axes (major and minor) into account when a constant value for it is chosen and a & b corresponding to a magnitude M.

By replacing w_1 by αw_1 and w_2 by βw_2 in eqn.1.3, we obtain the function relation for elliptic symmetric functions. Thus an ideal elliptical symmetric 2-D magnitude squared function is given by [13]

$$H(w_1^2, w_2^2) = \lambda e^{(\alpha w_1^2 + \beta w_2^2)}$$

1.6 Scope of the thesis

Monotonic amplitude-frequency response in the passband and transition band of the filters have been given lots of importance in various application. Hence, various researchers have proposed different types of filters like Butterworth, Papoulis, Filanovsky, Thomson-Bessel filters, etc, having monotonic amplitude-frequency response. Most of the work proposed by various authors is based on the frequency response of 1-D filters having different orders and nature of amplitude-frequency response. For example, Papoulis, Filanovsky and Fukada

[14, 15, 16, 17] proposed 1-D filters satisfying certain conditions, and hence, resulting in different types of monotonic amplitude-frequency response in the passband, depending on the order and degree of freedom of the filter.

To the best of our knowledge the monotonic response have not been explored in multi-dimensional filters till now. In this thesis, keeping the monotonic amplitude-frequency response as the primary aspect, we have explored various possibilities in 2-D case. The monotonic behavior of various types (and different orders) of 1-D filters will be studied and it will be extended to 2-D filters by cascade combination of the 1-D filters (having monotonic amplitude-frequency response). Various possibilities will be explored in both analog and digital domain for realization of 1-D and 2-D lowpass filters with monotonic amplitude-frequency response, and the constraints/conditions to achieve them will be discussed. Furthermore, we will consider generalized doubly terminated network, define its stability, condition of monotonicity, for realizing 2-D filter with monotonic characteristics. This will be extended to other types of filter response, namely, highpass and bandpass filters. In the end, we will also show a few basic examples of 2-D digital filter implementation in image and video processing.

In Chapter 2, 1-D lowpass filters namely, Butterworth, Papoulis and intermediate stages of Filanovsky filters obtained from the methodology proposed in [14], having monotonic amplitude-frequency response with different order and degree of freedom will be designed and studied. Thomson-Bessel filters derived in [43] will also be studied. After studying these standard 1-D lowpass analog filters, we will propose two concepts for monotonic 1-D filters. Firstly, we will propose extraction of all possible lower order 1-D lowpass filters from the higher order filters realized. The lower order 1-D filters with monotonic characteristics will be segregated. Secondly, a few cascaded combinations of the extracted monotonic lower order filters to attain higher order 1-D monotonic lowpass filters of different order will be proposed.

In Chapter 3, the concept proposed in Chapter 2 will be furthermore utilized to de-

sign 2-D lowpass filters with monotonic amplitude-frequency response, by cascading 1-D derived lowpass filters. We will derive, implement and study the Butterworth, Papoulis, Filanovsky and Thomson-Bessel 2-D analog lowpass filters. The 2-D analog transfer function will be realized for various possibilities in digital domain by applying generalized bilinear transformation [19]. We will also generate all possible first to fourth order 2-D analog lowpass filters with monotonic characteristics, by cascade combination of the corresponding extracted lower order 1-D lowpass filters (proposed in Chapter 2) with monotonic amplitude-frequency response. Furthermore, we will realize few fourth, sixth and eighth order 2-D analog lowpass filters, by cascading higher order combinational monotonic 1-D lowpass filters derived in Chapter 2, with monotonic amplitude-frequency response. The 3-D magnitude response and contour plots of all the 2-D digital filters will be studied by varying various possible combinations of constants in the bilinear transformation.

In Chapter 4, we will consider a generalized doubly terminated network, define its stability, condition for monotonicity and its possible realization as different types of 2-D analog and digital lowpass filters, e.g., Butterworth filter, having monotonic amplitude-frequency response. The stability of the 2-D filter is defined by verifying the denominator of the transfer function to be a VSHP. Furthermore, some conditions to be satisfied by the 2-D filter coefficients for monotonic characteristics will be derived. The condition of the coefficients to obtain 2-D Butterworth analog lowpass filter (with monotonic amplitude-frequency response) will be obtained for the considered 2-D analog filter by utilizing Koga's technique [29]. The 2-D analog lowpass filters will be implemented in digital domain by applying generalized lowpass bilinear transformation. The affect of the 2-D digital filter coefficients to achieve monotonic amplitude-frequency response will be studied. Overall in this Chapter, we shall propose a methodology to obtain monotonic analog and digital 2-D lowpass filters by considering a generalized doubly terminated network.

In Chapter 5, we will propose 2-D digital Papoulis, Butterworth, Filanovsky and Thomson-Bessel highpass and bandpass filters, with monotonic amplitude-frequency response, by

utilizing the 2-D lowpass filters proposed in Chapter 3 and 4. We will implement fifth order 2-D digital Papoulis, Butterworth, Filanovsky and Thomson-Bessel highpass and bandpass filters with monotonic characteristics by utilizing the 2-D lowpass filter transfer functions proposed in Chapter 3. We will also implement second order 2-D monotonic digital Butterworth highpass and bandpass filter by utilizing the 2-D lowpass filter transfer function proposed in Chapter 4. We will use generalized bilinear transformation for the highpass and bandpass 2-D digital filter design. The affect of digital filter coefficients on the 2-D highpass and bandpass filter design to obtain monotonic characteristics will be studied.

In Chapter 6, we have shown some basic examples of implementation of 2-D digital lowpass, highpass and bandpass filters in image and video processing. The examples will include recovering standard images/frames of videos corrupted by the added Gaussian noise, by using 2-D lowpass filtering, and extraction of different frequency bands from images [44, 45].

Chapter 7 will give summary of the thesis, conclusion, and some directions for the future work.

The basic goal, underlying all the above study, is to emphasise on realizing novel 2-D analog and digital filters with monotonic amplitude-frequency response. These may be obtained from cascade combinations of stable standard 1-D filters with monotonic amplitude-frequency response, namely, Butterworth, Papoulis, Filanovsky and Thomson-Bessel filters. We will be defining certain conditions to be satisfied while designing these novel 2-D monotonic amplitude-frequency response filters. We will also explore the properties of the generalized doubly terminated network (2-D filter) considered, analyse and implement it in the form of standard 2-D filter, e.g., Butterworth filter, and hence, resulting in a stable 2-D IIR filter both in analog and digital domain, having monotonic amplitude-frequency response.

Chapter 2

Generation of analog 1-D lowpass filters with monotonic amplitude-frequency response and arbitrary flatness

2.1 Review

Monotonic behavior of amplitude-frequency response in a filter is often required in various applications, such as, image and video processing. For example, we need monotonic characteristic of frequency response in processing of digital audio systems. The goal of any digital audio system is to sample and reconstruct an analog audio signal, without noticeable changes to the original signal. Currently, two major types of reconstruction filters, brickwall and monotonic filters, are used to smooth a sampled analog audio signal during its reconstruction. The monotonic filters are the best ones for reconstruction of transient signals.

Several kind of filters such as Butterworth filter, the Chebychev filter, Filanovsky filters, Thomson-Bessel filters, the class L of filters (proposed by Papoulis), etc, with the maximum cutoff rate under the condition of a monotonically decreasing response (the L filter), etc,

have been proposed and implemented [14, 15, 16, 17, 30, 31, 32, 33, 34, 35, 37, 41, 42, 43]. In this section, we will review some proposed filters with monotonic amplitude-frequency response.

The Butterworth filter with the maximum degrees of flatness in the passband gives better time response than the Chebychev filter, for instance the ringing of the step response is small [30, 38, 39, 40]. However, cutoff properties of the Butterworth filter are constrained because it utilizes all degrees of freedom for flatness in the passband. The Chebychev filter with equi-ripple amplitude-frequency response in the passband gives us the greatest cutoff rate among all filters, namely, Butterworth filter, Filanovsky filter and Papoulis (class L) Filters, for a given order. However, the ringing of the step response in Chebychev filter becomes large, as there are ripples in the frequency response. Therefore, if the only requirement in amplitude characteristics of a filter is to have the maximum possible attenuation for a given variation in passband, the Chebychev filter is optimal. But, in such applications, as the time response is also considered, high ripples in the passband are often not tolerated, and then the Butterworth filter is sometimes used as a simple compromise.

In [41], a new class of IIR digital filters that unifies the classical digital Butterworth filter and the well-know maximally flat FIR filters is introduced. New closed-form expressions are provided, and a straightforward design technique is described. The new IIR digital filters have more zeros than poles away from the origin, and their monotonic square magnitude-frequency responses are maximally flat at $w = 0$ and at $w = \pi$. Their technique also permits continuous variation of the cutoff frequency. It should be noted that IIR filters having more zeros than poles are of interest because often to obtain a good trade off between performance and implementation complexity, just a few poles are best.

In [15, 16], Papoulis developed a new class L of filters, which has the maximum cutoff rate under the condition of monotonically-decreasing response. This class of filters has a greater attenuation in the stop band than that of the Butterworth class of the same order, by giving up the requirement of maximum flatness in the passband. But, it still holds sat-

isfactory time response because of the monotonicity property in its frequency response. Papoulis has given formulas for the optimum polynomials of odd degrees [15], from which these filters were derived. Fukada [17] proposed general formulas for the optimum polynomials of even degrees and showed that from these polynomials, class L filters can actually be designed.

Therefore, the class L of filters has been developed by combining the desirable features of both Butterworth and Chebychev filters, whose amplitude-frequency response has no ripple but the minimum degree of flatness in the passband and a high rate of attenuation in the stopband. In brief, frequency and time response of the Class L filters are in-between. Furthermore, the transfer function of the L filter is given with Legendre's polynomials of the first kind in a mathematically closed form separately for even or odd orders. In [42], Papoulis also provides a methodology for attenuation limits for filters with monotonic step response.

Halpern [32] extended the work of Papoulis [15, 16] to attain monotonic lowpass filters. The author generalized the magnitude-square characteristic of a lowpass filter as

$$H_n(w) = \frac{1}{1 + \epsilon T_n(w^2)}$$

where $T_n(w^2)$ approximates zero in some manner for $0 \leq w < 1$ and grows as large as quickly as possible for $w > 1$. The tolerance in the passband is controlled by ϵ. The Butterworth filter is monotonic ($T_n(w^2) = w^{2n}$, where n is the order of the filter) and concentrates its flatness at $w = 0$. The Chebyshev filters have the sharpest cutoff frequencies but have ripples in the passband. The author solved two primary problems by proposing two criterias. Firstly, optimize the rate of change of $T_n(w^2)$ at $w = 1$ under the constraint of monotonic response. Secondly, optimize the asymptotic growth of $T_n(w^2)$ under the constraint of monotonic response. Furthermore, the author listed table of seven optimum polynomials for each criterion, and in addition listed the odd and even polynomials from

which they were derived. It showed that there is considerable improvement over the Butterworth filter provided that it is available for greater than second-order transfer functions.

In [33], the authors proposed least square monotonic lowpass filters with sharp cutoff frequency. They also proposed monotonic passband lowpass filters with Chebyshev stopband attenuation in [37]. The author proposed, a class of non-maximally flat monotonic lowpass filters with sharp cutoff frequencies. It is shown to provide better magnitude response both in the passband and in the stopband than their maximally flat counterparts. The normalized pole and zero locations are tabulated for filters of order 3 to 11 and different values of the minimum stopband attenuation. In [34], a methodology of lowpass filters with critical monotonic magnitude-frequency response is proposed.

Furthermore, in [35], sensitivity of all pole filters with critical monotonic magnitude characteristic is optimized in a mini-max sense and a new class of transitional monotonic filters is introduced. Comparison of the proposed filter with other monotonic filters, namely, Butterworth filter, Papoulis filter, Halpern filter and Least square monotonic lowpass filter is also given. It includes comparison of the magnitude characteristics of eighth order filter, attenuations at normalized frequency $w = 2$, etc.

In analog lowpass filters with a monotonically decreasing amplitude-frequency response, there is also a large disparity of flatness in the passband between the Butterworth filter and the class L filters. The same is reflected in digital filters too. Therefore, in [31], filters are proposed with arbitrary flatness characteristics whose frequency and time response are in-between Butterworth filter and the class L filters. They proposed a closed form transfer function of analog lowpass filters with monotonic response and arbitrary flatness characteristics by using the Jacobi polynomials. By using their methodology, we can decide a degree of flatness arbitrarily for the order of a filter. With this approach, we will get the transfer function of the Butterworth filter, if we take the maximum possible degrees of flatness, and we will get the transfer function of the L filter for the minimum degree of flatness. In addition, the transfer function is easily realizable because of its closed form regardless of

even or odd orders.

Filanovsky [14] proposed polynomial lowpass filters with monotonic amplitude-frequency responses in the passband based on the concepts proposed in [15, 16, 17, 31]. Filanovsky filters have characteristics intermediate between Butterworth and Papoulis filters (with these two classes as limiting) and are obtained starting from the filters of the fifth order. The number of intermediate characteristics increases with the order of the filter. The author provided design methodology and tables for the filters of the fifth, sixth and seventh orders which showed that by decreasing the passband flatness degree, one can obtain an additional attenuation in the stop band. The work also includes the derivation of the required monotonic polynomial.

Bessel polynomials are also used to generate transfer functions with monotonic amplitude-frequency response, often called as Thomson-Bessel response [43]. The procedure to generate Bessel polynomial is explained in [43]. The Bessel polynomials (B_n for any value of n) can also be generated by using the recursion formula,

$$B_n = (2n-1)B_{n-1} + s^2 B_{n-2} \tag{2.1}$$

In general, the transfer function, $F_n(s)$, with denominator polynomial, $D_n(s)$ (which defines the stability of the filter), can be defined as

$$F_n(s) = \frac{D_n(0)}{D_n(s)} \tag{2.2}$$

where, $s = jw$ and the numerator of $F_n(s)$ is chosen so that $F_n(j0) = 1$ [14, 43]. It is also our objective to achieve another flatness, namely, that of the magnitude function, $A_n(w)$, which is found as follows,

$$A_n(w) = |F_n(jw)| = \left|\frac{D_n(0)}{D_n(jw)}\right| \tag{2.3}$$

In this Chapter, we will design analog 1-D lowpass filters, namely, Butterworth, Papoulis, Filanovsky and Thomson-Bessel filters, of different order with monotonic response, arbitrary flatness, and study their characteristics. In Sec. 2.2, we will explain a design method to generate polynomial lowpass filters of different order with arbitrary flatness. In Sec. 2.3, we will generate the monotonic polynomial, i.e., filtering function with arbitrary flatness, which will eventually be used to generate analog 1-D lowpass filters of fourth and fifth order in Sec. 2.4. In Sec. 2.5, we will generate Thomson-Bessel filters having monotonic characteristics by using Bessel polynomials [43]. Comparison of the implemented filters will be done in Sec. 2.6. In Sec. 2.2 to 2.6, we shall review the mentioned methods. In Sec. 2.7 and 2.8, we shall show how other monotonic responses can be obtained either by choosing lower order responses and/or by suitable combinations of these monotonic responses. We will propose extraction of all possible lower order 1-D lowpass filters from the designed higher order 1-D lowpass filters, and segregate the filters with monotonic amplitude-frequency response in Sec. 2.7. Furthermore, we will cascade the proposed extracted monotonic 1-D lowpass filters to realize higher order 1-D lowpass filters with monotonic amplitude-frequency response in Sec. 2.8, and study a few possible combinations of the same. Our primary emphasis is to define and implement a methodology for designing analog 1-D lowpass filters of any order with monotonic amplitude-frequency response and arbitrary flatness.

2.2 Design Method

After going through different methodologies reviewed in Sec. 2.1, we have to decide about the design technique to be adopted for implementing 1-D filters with monotonic characteristics. The amplitude-frequency response of a polynomial lowpass filter, which has no finite zeros, can be written by the formula

$$A(w) = \frac{A_0}{\sqrt{1 + f(w^2)}} \tag{2.4}$$

where,

$$f(0) = 0 \tag{2.5}$$

$$f(1) = 1 \tag{2.6}$$

and, the filtering function, $f(w^2)$, is a $2m^{th}$ degree polynomial of w for the filter of the m^{th} order. The exact expression of $f(w^2)$ is determined by approximation conditions. If we want amplitude-frequency response of the lowpass filter to be monotonically decreasing, the filtering transfer function, $f(w^2)$, should increase monotonically. Hence, the condition to satisfy the requirement of monotony of $A(w)$ can be given by

$$\frac{\partial f(w^2)}{\partial w} \geq 0, (0 \leq w \leq 1) \tag{2.7}$$

. The most known filters with monotonic amplitude-frequency response are Butterworth or maximally flat filters. In case of Butterworth filter, $f(w^2) = w^{2m}$ and all the first $m - 1$ derivatives are equal to zero at $w = 0$, i.e,

$$\left.\frac{\partial f^j}{\partial (w^2)^j}\right|_{w=0} = 0$$

Since the derivative $\partial f/\partial(w^2)$, calculated at the bandpass edge, i.e., $w = 1$, is relatively low, this results in a wide transition band for a given order of filter (in comparison with filters of non-monotonic amplitude-frequency response). To overcome this deficiency, [15, 16, 17] introduced the polynomial filters (frequently called Papoulis filters) with monotonic amplitude-frequency responses, and with the derivative $\partial f/\partial(w^2)$ maximized at $w = 1$. It should be noted that the amplitude frequency responses for these filters are not flat and even the first derivative $\partial f/\partial(w^2)$, calculated at $w = 0$, is not equal to zero.

Two most recent work proposed in [14, 31] which were extensions of investigations of

Papoulis [15, 16] and Fukada [17], provides an appropriate criterion to implement Butterworth filter, Papoulis (Class L) filter and Filanovsky filter [14], of a given order by varying flatness degree. In [14], a generalization of monotonic amplitude-frequency response is described, and hence, came into existence the Filanovsky filters which have characteristics in-between Butterworth and Papoulis filters. In this section, we will illustrate the design of polynomial lowpass filter which will inhibit monotonic amplitude-frequency response, based on the concepts proposed in [14, 15, 16, 17, 31].

The problem of designing analog lowpass filters with monotonic response and arbitrary flatness characteristics is to determine a positive increasing polynomial, $f(w^2)$, of degree $2m$ in w^2, with arbitrary flatness characteristics in the passband, such that, its slope at the point $w = 1$ is maximum. The amplitude-frequency responses of filters are monotonic in the passband, with first consecutive i derivatives equal to zero at $w = 0$, i.e.,

$$\left.\frac{\partial^j f\left(w^2\right)}{\partial w^j}\right|_{w=0} = 0, (j = 0, 1, \cdots, 2i+1) \tag{2.8}$$

Hence, the number $i < m$ becomes a flatness degree for the amplitude characteristics given by eqn. 2.4. Furthermore, we can define our problem as finding among all positive polynomials of degree $2m$ satisfying eqn. 2.4, 2.5, 2.6, 2.7 and 2.8, such that

$$\left.\frac{\partial f\left(w^2\right)}{\partial w}\right|_{w=1} = M \tag{2.9}$$

is maximum, where M is maximal at the stated condition.

The filtering function polynomial is given by

$$f\left(w^2\right) = \int_{-1}^{2w^2-1} (x+1)^i u^2\left(x\right) dx \tag{2.10}$$

where, $u\left(x\right)$ is an arbitrary polynomial of l-th order and is represented as the sum of Jacobi

polynomials [36].

$$u(x) = \sum_{k=0}^{l} b_k P_k^{(0,i)}(x) \tag{2.11}$$

where, $P_k^{(0,i)}$ denotes the Jacobi Polynomials,

$$P_k^{(0,i)}(x) = 2^{-k} \sum_{n=0}^{k} \binom{k}{n} \binom{k+i}{k-n} (x-1)^{k-n} (x+1)^n \tag{2.12}$$

and the coefficients b_k's are given by

$$b_k = \frac{(2k+i+1)}{\sqrt{2^{i-1}(m+1+i)(m+1-i)}} \tag{2.13}$$

The above expression shows that the coefficients b_k's will be determined uniquely by the filter of order m and flatness i. Furthermore, the relation of l to the filter of order m and flatness i is given by

$$\begin{aligned} m &= 2l + i + 1 \\ l &= \frac{m-1-i}{2} \end{aligned} \tag{2.14}$$

Therefore, from eqn. 2.10 and 2.11, we get the filtering function,

$$f_{m,i}\left(w^2\right) = \int_{-1}^{2w^2-1} (1+x)^i \left[\sum_{k=0}^{l} b_k P_k^{(0,i)}(x)\right]^2 dx \tag{2.15}$$

The derivative will be maximized based on eqn. 2.9, hence, we have

$$\left.\frac{\partial f_{m,i}(w^2)}{\partial w}\right|_{w=1} = \frac{(m+1+i)(m+1-i)}{2} \tag{2.16}$$

Therefore, the transfer function of analog lowpass filters with monotonic response and arbitrary flatness characteristics, whose slope at cutoff frequency is maximum can be obtained from eqn. 2.4, 2.12, 2.13 and 2.15 in mathematically closed form.

The pole locations of the lowpass filter transfer functions, $F_{m,i}(s)$, can be found using the relationship,

$$F_{m,i}(s)F_{m,i}(-s)\Big|_{s=jw} = \frac{1}{1+f_{m,i}(w^2)} \tag{2.17}$$

where, the poles can be separated in the left half of the s plane to ensure stability.

2.3 Generation of monotonic polynomial - filtering function with arbitrary flatness

To find the filtering function polynomial, $f\,(w^2)$, with the degree $2m$ and the degree of flatness i, in Sec. 2.2 we introduced the eqn. 2.11, 2.12, 2.13 and 2.15. In this section, we will find all possible monotonic filtering transfer functions for the analog 1-D lowpass filters of the fourth and fifth order. The fourth order transfer function, will result in two values of degree of flatness (i), hence, two lowpass filters, namely, Butterworth filter and Papoulis filter will be possible. Filanovsky filters [14] are realizable from fifth order onwards. Filtering functions for the Filanovsky filters will also be generated, and the implemented filters will be studied in subsequent sections.

2.3.1 Generation of filtering transfer functions for fourth order lowpass filters

When filter order is four, i.e, $m = 4$, one can choose flatness degree $i = 1, 3$. The lower bound of degree of freedom ($i = 1$) corresponds to Papoulis filter and upper bound ($i = 3$) corresponds to Butterworth filter. Since there are only two values of degree of freedom, the intermediate stage(s) between Butterworth filter and Papoulis filter are not realizable, hence, Filanovsky filter(s) does not exist.

2.3.1.1 Generation of filtering function for fourth order Papoulis filter

When $i = 1$, substituting the value of i in eqn. 2.14, we obtain $l = 1$. So, integer k varies from 0 to l, i.e., 0 to 1. Utilizing the formula's in eqn. 2.12 and 2.13, we simplify the following two cases:

Case I: When $k = 0$,

$$b_0 = \frac{(1+1)}{\sqrt{2^{1-1}\,(4+1+1)\,(4+1-1)}} = \frac{1}{\sqrt{6}} \tag{2.18}$$

$$P_0^{(0,1)}(x) = 1 \tag{2.19}$$

Case II: When $k = 1$,

$$b_1 = \frac{(2+1+1)}{\sqrt{2^{1-1}\,(4+1+1)\,(4+1-1)}} = \frac{2}{\sqrt{6}} \tag{2.20}$$

$$P_1^{(0,1)}(x) = \frac{2\,(x-1)+(x+1)}{2} = \frac{(3x-1)}{2} \tag{2.21}$$

After substituting the values from eqn. 2.18, 2.19, 2.20 and 2.21 in eqn. 2.15, the filtering function can be expressed as the following,

$$f_{4,1}\left(w^2\right) = \int_{-1}^{2w^2-1} (1+x)^1 \left[\frac{1}{\sqrt{6}} + \frac{2}{\sqrt{6}}\frac{(3x-1)}{2}\right]^2 dx$$

$$= 6w^8 - 8w^6 + 3w^4 \tag{2.22}$$

Therefore, the filtering function for the fourth order Papoulis filter is given by eqn. 2.22.

2.3.1.2 Generation of filtering function for fourth order Butterworth filter

When $i = 3$, substituting the value of i in eqn. 2.14, we obtain $l = 0$. So, integer k varies from 0 to l, i.e., only one value 0. Utilizing the formula's in eqn. 2.12 and 2.13, we get the following :

When $k = 0$,

$$b_0 = \frac{(3+1)}{\sqrt{2^{3-1}(4+1+3)(4+1-3)}} = \frac{1}{2} \tag{2.23}$$

$$P_0^{(0,3)}(x) = 1 \tag{2.24}$$

After substituting the values of b_0 and $P_0^{(0,3)}(x)$ in eqn. 2.15, the filtering function can be expressed as the following,

$$f_{4,3}\left(w^2\right) = \int_{-1}^{2w^2-1} (1+x)^3 \left[\frac{1}{2}\right]^2 dx = w^8 \tag{2.25}$$

Therefore, the filtering function for the fourth order Butterworth filter is given by eqn. 2.25.

2.3.2 Generation of filtering transfer functions for fifth order lowpass filters

When filter order is five, i.e, $m = 5$, one can choose flatness degree $i = 0, 2, 4$. The lower bound of degree of freedom ($i = 0$) corresponds to Papoulis filter and upper bound ($i = 4$) corresponds to Butterworth filter. Since there are three values of degree of freedom, the intermediate stage (value) between Butterworth filter and Papoulis filter is $i = 2$, hence, corresponds to filtering function for Filanovsky filter.

2.3.2.1 Generation of filtering function for fifth order Papoulis filter

When $i = 0$, substituting the value of i in eqn. 2.14, we obtain $l = 2$. So, integer k varies from 0 to l, i.e., 0 to 2. Utilizing the formula's in eqn. 2.12 and 2.13, we simplify the following three cases:

Case I: When $k = 0$,

$$b_0 = \frac{1}{\sqrt{2^{0-1}(5+1+0)(5+1-0)}} = \frac{1}{\sqrt{18}} \tag{2.26}$$

$$P_0^{(0,0)}(x) = 1 \tag{2.27}$$

Case II: When $k = 1$,

$$b_1 = \frac{(2+1)}{\sqrt{2^{0-1}(5+1+0)(5+1-0)}} = \frac{3}{\sqrt{18}} \tag{2.28}$$

$$P_1^{(0,0)}(x) = \frac{(x-1)+(x+1)}{2} = x \tag{2.29}$$

Case III: When $k = 2$,

$$b_2 = \frac{(4+1)}{\sqrt{2^{0-1}(5+1+0)(5+1-0)}} = \frac{5}{\sqrt{18}} \tag{2.30}$$

$$P_2^{(0,0)}(x) = \frac{(x-1)^2 + 4(x-1)(x+1) + (x+1)^2}{2} = \frac{3x^2-1}{2} \tag{2.31}$$

After substituting the values of eqn. 2.26, 2.27, 2.28, 2.29, 2.30 and 2.31 in eqn. 2.15, the filtering function can be expressed as the following,

$$f_{5,0}\left(w^2\right) = \int_{-1}^{2w^2-1} (1+x)^0 \left[\frac{1}{\sqrt{18}} + \frac{3x}{\sqrt{18}} + \frac{5}{\sqrt{18}}\frac{(3x-1)}{2}\right]^2 dx$$

$$= 20w^{10} - 40w^8 + 28w^6 - 8w^4 + w^2 \tag{2.32}$$

Therefore, the filtering function for the fifth order Papoulis filter is given by eqn. 2.32.

2.3.2.2 Generation of filtering function for fifth order Filanovsky filter

When $i = 2$, substituting the value of i in eqn. 2.14, we obtain $l = 1$. So, integer k varies from 0 to l, i.e., 0 to 1. Utilizing the formula's in eqn. 2.12 and 2.13, we simplify the following two cases:

Case I: When $k = 0$,

$$b_0 = \frac{(2+1)}{\sqrt{2^{2-1}(5+1+2)(5+1-2)}} = \frac{3}{8} \tag{2.33}$$

$$P_0^{(0,2)}(x) = 1 \tag{2.34}$$

Case II: When $k = 1$,

$$b_1 = \frac{(2+2+1)}{\sqrt{2^{2-1}(5+1+2)(5+1-2)}} = \frac{5}{8} \tag{2.35}$$

$$P_0^{(0,2)}(x) = 2x - 1 \tag{2.36}$$

After substituting the values of eqn. 2.33, 2.34, 2.35 and 2.36 in eqn. 2.15, the filtering function can be expressed as the following,

$$f_{5,2}\left(w^2\right) = \int_{-1}^{2w^2-1} (1+x)^2 \left[\frac{3}{8} + \frac{5(2x-1)}{8}\right]^2 dx$$

$$= 10w^{10} - 15w^8 + 6w^6 \tag{2.37}$$

Therefore, the filtering function for the fifth order Filanovsky filter is given by eqn. 2.37.

2.3.2.3 Generation of filtering function for fifth order Butterworth filter

When $i = 4$, substituting the value of i in eqn. 2.14, we obtain $l = 0$. So, integer k varies from 0 to l, i.e., only one value 0. Utilizing the formula's in eqn. 2.12 and 2.13, we get the following :

When $k = 0$,

$$b_0 = \frac{(4+1)}{\sqrt{2^{4-1}(5+1+4)(5+1-4)}} = \frac{5}{4\sqrt{10}} \tag{2.38}$$

$$P_0^{(0,4)}(x) = 1 \tag{2.39}$$

After substituting the values of b_0 and $P_0^{(0,4)}(x)$ in eqn. 2.15, the filtering function can be expressed as the following,

$$f_{5,4}\left(w^2\right) = \int_{-1}^{2w^2-1} (1+x)^4 \left[\frac{5}{4\sqrt{10}}\right]^2 dx = w^{10} \tag{2.40}$$

Therefore, the filtering function for the fifth order Butterworth filter is given by eqn. 2.40.

2.4 Generation of 1-D lowpass filters with arbitrary flatness, monotonic response and study their characteristics

Considering an analog 1-D lowpass filter of a specific order, the degree of flatness of the filter will characterise type of filter, namely, Butterworth filter, Papoulis filter or Filanovsky filter [14]. In this section, we will implement the fourth and fifth order analog 1-D lowpass filters, namely, Papoulis, Butterworth and Filanovsky filters, study their characteristics based on the discussions in Sec. 2.1, 2.2 and 2.3, and compare their results.

2.4.1 Generation of analog 1-D Papoulis lowpass filters and study their characteristics

We will generate fourth and fifth order analog 1-D Papoulis lowpass filters, study their characteristics and compare the amplitude-frequency responses, by utilizing the filtering functions derived in Sec. 2.3.

2.4.1.1 Generation of 1-D Papoulis lowpass filter of fourth order

The amplitude-frequency response (eqn. 2.4) of the fourth order (i.e., $m = 4$) Papoulis filter, having flatness degree one (i.e., $i = 1$), (and by utilizing the filter polynomial function

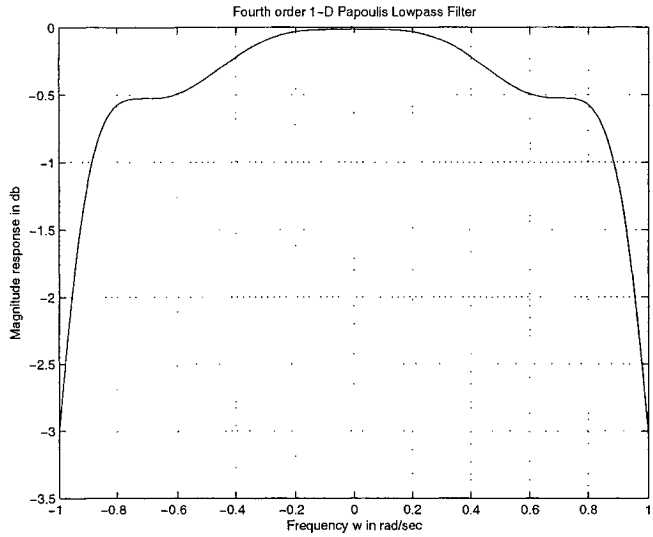

Figure 2.1: Amplitude-frequency response of the fourth order Papoulis Lowpass filter

derived in Sec. 2.3.1.1, i.e., eqn. 2.22), can be given by

$$A_{4,1}(w) = \frac{A_0}{\sqrt{1 + 6w^8 - 8w^6 + 3w^4}}$$

The pole locations of the lowpass filter transfer function, $F_{4,1}(s)$, can be found using the eqn. 2.17. Hence, we get the poles,

$$s = jw = \pm 0.2317 \pm j0.9445, \pm 0.5497 \pm j0.3586$$

To ensure stability, we will separate the poles in the left half of the s plane and discard the rest. Therefore, the transfer function of the fourth order 1-D Papoulis lowpass filter (eqn. 2.17 and 2.2) is

$$F_{4,1}(s) = \frac{0.4075}{\begin{array}{ll}(s + 0.5497 + j0.3586) & (s + 0.5497 - j0.3586) \\ (s + 0.2317 + j0.9445) & (s + 0.2317 - j0.9445)\end{array}}$$

and, after simplification we get,

$$F_{4,1}(s) = \frac{0.4075}{(s^2 + 1.0994s + 0.4308)(s^2 + 0.4634s + 0.9458)} \tag{2.41}$$

Hence, we get the amplitude-frequency response (eqn. 2.3) in the form

$$A_{4,1}(w) = \left| \frac{0.4075}{(0.4308 - w^2 + 1.0994jw)(0.9458 - w^2 + 0.4634jw)} \right| \tag{2.42}$$

The amplitude-frequency response of the fourth order Papoulis lowpass filter (eqn. 2.41 and 2.42) is shown in the fig. 2.1. We can observe that the response is monotonically decreasing, and at -3db gain value the cutoff frequency is 1 rad/s.

2.4.1.2 Generation of 1-D Papoulis lowpass filter of fifth order

The amplitude-frequency response (eqn. 2.4) of the fifth order (i.e., $m = 5$) Papoulis filter, having flatness degree zero (i.e., $i = 0$), (and by utilizing the filter polynomial function derived in Sec. 2.3.2.1, i.e., eqn. 2.32), can be given by

$$A_{5,0}(w) = \frac{A_0}{\sqrt{1 + 20w^{10} - 40w^8 + 28w^6 - 8w^4 + w^2}}$$

The pole locations of the lowpass filter transfer function, $F_{5,0}(s)$, can be found using the eqn. 2.17. Hence, we get the poles,

$$s = jw = -0.4681, \pm 0.3881 \pm j0.5886, \pm 0.1536 \pm j0.9681$$

To ensure stability, we will separate the poles in the left half of the s plane and discard the rest. Therefore, the transfer function of the fifth order 1-D Papoulis lowpass filter (eqn.

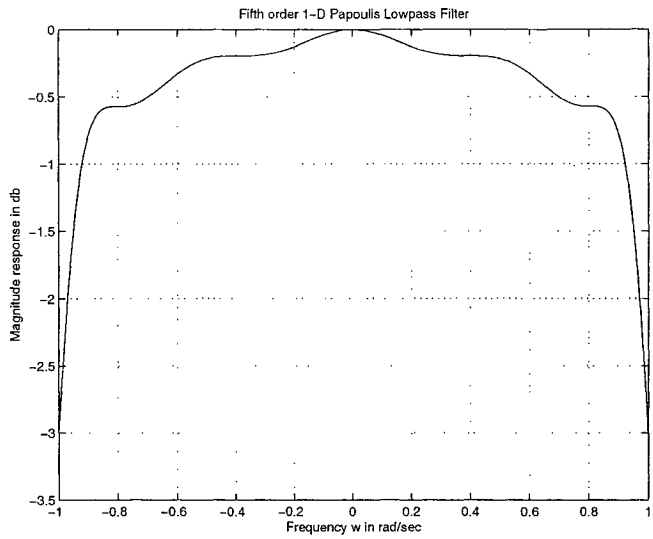

Figure 2.2: Amplitude-frequency response of the fifth order Papoulis lowpass filter

2.17 and 2.2) is

$$F_{5,0}(s) = \frac{0.2235}{(s+0.4681)\,(s+0.3881+j0.5886)\,(s+0.3881-j0.5886)\,(s+0.1536+j0.9681)\,(s+0.1536-j0.9681)}$$

and, after simplification we get,

$$F_{5,0}(s) = \frac{0.2235}{(s+0.4681)\,(s^2+0.7762s+0.4971)\,(s^2+0.3072s+0.9608)} \tag{2.43}$$

Hence, we get the amplitude-frequency response (eqn. 2.3) in the form

$$A_{5,0}(w) = \left| \frac{0.2235}{(0.4681+jw)\,(0.4971-w^2+0.7762jw)\,(0.9608-w^2+0.3072jw)} \right| \tag{2.44}$$

The amplitude-frequency response of the fifth order Papoulis lowpass filter (eqn. 2.44

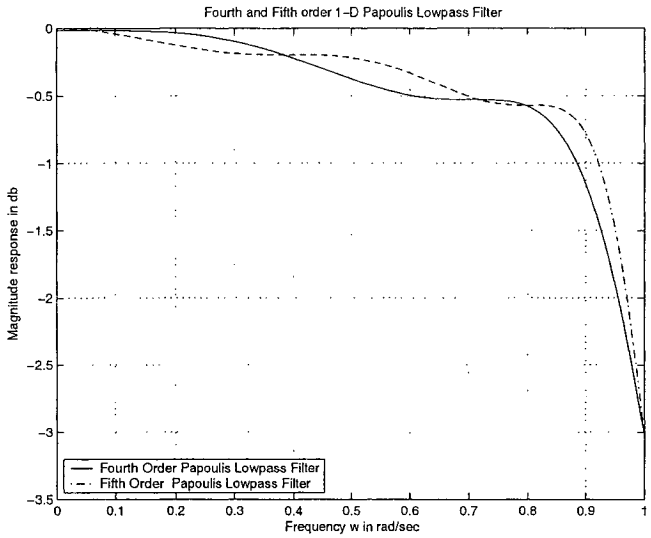

Figure 2.3: Amplitude-frequency response of the fourth and fifth order Papoulis lowpass filters.

and 2.43) is shown in the fig. 2.2. We can observe that the response is monotonically decreasing, and at -3db gain value the cutoff frequency is 1 rad/s.

2.4.1.3 Comparison of the derived fourth and fifth order analog 1-D Papoulis lowpass filters

Fig. 2.3 shows the amplitude-frequency response of the fourth and fifth order 1-D Papoulis lowpass filter for frequency range of $0 \leq w \leq 1$. It is observed that the fifth order Papoulis filter has steeper transition band as compared to the fourth order filter. The response in the passband for the fourth and fifth order filters often overlaps but maintains the monotonic characteristic of the corresponding filter, with cutoff frequency, $w = 1$. There is trade off between flatness of the filter in the passband to the sharpness of the response in the transition band. (Discussions based on comparison of all the 1-D lowpass filters implemented will be done in Sec. 2.6). The MATLAB code to plot the amplitude-frequency response of the fourth and fifth order Papoulis lowpass filters is in algorithm 1.

Algorithm 1 MATLAB Code to plot Amplitude-Frequency response of the fourth and fifth order 1-D Papoulis lowpass filters

```
% Under Guidance of Prof. Dr. V. Ramachandran
% Student's name : Ajit Singh Sandhu..... ID:4841492.
clear all; clc;
%Least count size of the frequency axes
step=0.00001;
% Frequency varying from -1 to 1 rad/sec
w=[-1:step:1]; s=j.*w;
% Generation of transfer function for fourth order 1-D Papoulis Lowpass filter
ha1D=(s+0.2317+0.9455i).*(s+0.2317-0.9455i);
ha2D=(s+0.5497+0.3586i).*(s+0.5497-0.3586i);
ha0D=0.4075; h_1D=abs(ha0D./(ha1D.*ha2D));
% Final transfer function for fourth order 1-D Papoulis Lowpass filter
h_1D_pop_order4=20*log10(h_1D);
%Plotting the fourth order 1-D Papoulis Lowpass filter
figure(1);
plot(w,h_1D_pop_order4,'k');
title('Fourth order 1-D Papoulis Lowpass Filter');
xlabel('Frequency w in rad/sec');
ylabel('Magnitude response in db'); grid on;
% Generation of transfer function for fifth order 1-D Papoulis Lowpass filter
ha_1D=(s+0.4681).*(s+0.3881+0.5886i).*(s+0.3881-0.5886i);
ha_2D=(s+0.1536+0.9681i).*(s+0.1536-0.9681i);
ha_0D=0.2235; h_1D_p=abs(ha_0D./(ha_1D.*ha_2D));
% Final transfer function for fifth order 1-D Papoulis Lowpass filter
h_1D_pop_order5=20*log10(h_1D_p);
%Plotting the fifth order 1-D Papoulis Lowpass filter
figure(2);
plot(w,h_1D_pop_order5,'k');
title('Fifth order 1-D Papoulis Lowpass Filter');
xlabel('Frequency w in rad/sec');
ylabel('Magnitude response in db'); grid on;
clear all; step=0.00001;
ww=[0:step:1]; s=j.*ww;
ha1D=(s+0.2317+0.9455i).*(s+0.2317-0.9455i);
ha2D=(s+0.5497+0.3586i).*(s+0.5497-0.3586i);
ha0D=0.4075; h_1D=abs(ha0D./(ha1D.*ha2D));
h_1D_pop_order4=20*log10(h_1D);
ha_1D=(s+0.4681).*(s+0.3881+0.5886i).*(s+0.3881-0.5886i);
ha_2D=(s+0.1536+0.9681i).*(s+0.1536-0.9681i);
ha_0D=0.2235; h_1D_p=abs(ha_0D./(ha_1D.*ha_2D));
h_1D_pop_order5=20*log10(h_1D_p);
%Plotting the fourth and fifth order 1-D Papoulis Lowpass filter with
%reduced axes together on the same figure
figure(3);
plot(ww,h_1D_pop_order4,'k-',ww,h_1D_pop_order5,'k-.');
legend('Fourth Order Papoulis Lowpass Filter','Fifth Order Papoulis Lowpass Filter',3);
title('Fourth and Fifth order 1-D Papoulis Lowpass Filter');
xlabel('Frequency w in rad/sec');
ylabel('Magnitude response in db'); grid on;
```

2.4.2 Generation of analog 1-D Butterworth lowpass filters and study their characteristics

We will generate fourth and fifth order analog 1-D Butterworth lowpass filters, study their characteristics and compare the amplitude-frequency responses, by utilizing the filtering functions derived in Sec. 2.3.

2.4.2.1 Generation of 1-D Butterworth lowpass filter of fourth order

The amplitude-frequency response (eqn. 2.4) of the fourth order (i.e., $m = 4$) Butterworth filter, having flatness degree three (i.e., $i = 3$), (and by utilizing the filter polynomial function derived in Sec. 2.3.1.2 ,i.e., eqn. 2.25), can be given by

$$A_{4,3}(w) = \frac{A_0}{\sqrt{1 + w^8}}$$

The pole locations of the lowpass filter transfer function, $F_{4,3}(s)$, can be found using the eqn. 2.17. Hence, we get the poles,

$$s = jw = \pm 0.9239 \pm j0.3827, \pm 0.3827 \pm j0.9239$$

To ensure stability, we will separate the poles in the left half of the s plane and discard the rest. Therefore, the transfer function of the fourth order 1-D Butterworth lowpass filter (eqn. 2.17 and 2.2) is

$$F_{4,3}(s) = \frac{1}{\begin{matrix}(s + 0.9239 + j0.3827) & (s + 0.9239 - j0.3827) \\ (s + 0.3827 + j0.9239) & (s + 0.3827 - j0.9239)\end{matrix}}$$

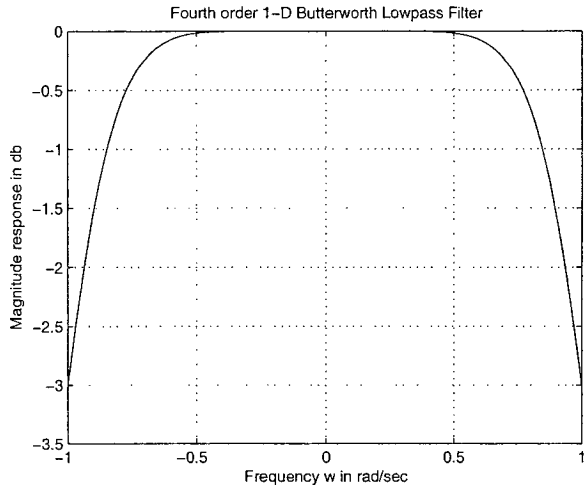

Figure 2.4: Amplitude-frequency response of the fourth order Butterworth Lowpass filter

and, after simplification we get,

$$F_{4,3}(s) = \frac{1}{(s^2 + 1.8478s + 1)(s^2 + 0.7654s + 1)} \tag{2.45}$$

Therefore, we get the amplitude-frequency response (eqn. 2.3) in the form

$$A_{4,3}(w) = \left| \frac{1}{(1 - w^2 + 1.8478jw)(1 - w^2 + 0.7654jw)} \right| \tag{2.46}$$

The amplitude-frequency response of the fourth order Butterworth lowpass filter (eqn. 2.45 and 2.46) is shown in the fig. 2.4. We can observe that the response is monotonically decreasing and, at -3db gain value the cutoff frequency is 1 rad/s.

2.4.2.2 Generation of 1-D Butterworth lowpass filter of fifth order

The amplitude-frequency response (eqn. 2.4) of the fifth order (i.e., $m = 5$) Butterworth filter, having flatness degree four (i.e., $i = 4$), (and by utilizing the filter polynomial func-

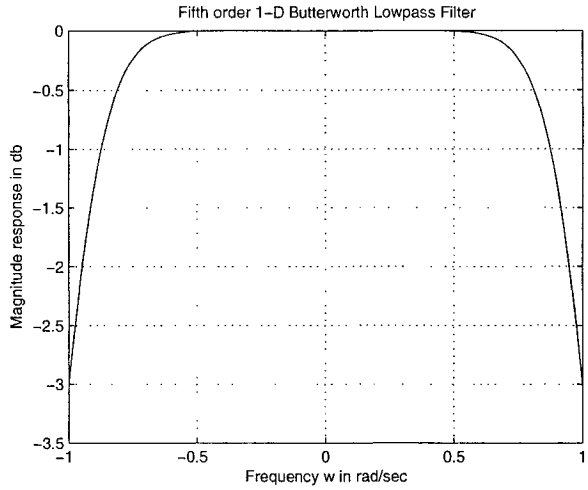

Figure 2.5: Amplitude-frequency response of the fifth order Butterworth lowpass filter

tion derived in Sec. 2.3.2.3, i.e., eqn. 2.40), can be given by

$$A_{5,4}(w) = \frac{A_0}{\sqrt{1+w^{10}}}$$

The pole locations of the lowpass filter transfer function, $F_{5,4}(s)$, can be found using the eqn. 2.17. Hence, we get the poles,

$$s = jw = -1.0000, \pm 0.8090 \pm j0.5878, \pm 0.3090 \pm j0.9511$$

To ensure stability, we will separate the poles in the left half of the s plane and discard the rest. Therefore, the transfer function of the fifth order 1-D Butterworth lowpass filter (eqn. 2.17 and 2.2) is

$$F_{5,4}(s) = \frac{1}{(s+1)(s+0.8090+j0.5878)(s+0.8090-j0.5878)} \\ (s+0.3090+j0.9511)(s+0.3090-j0.9511)$$

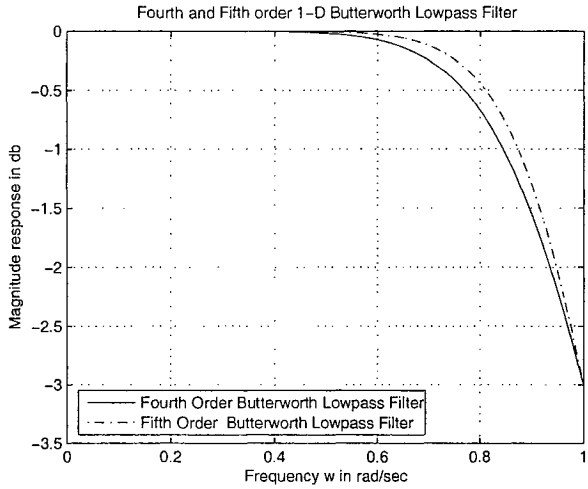

Figure 2.6: Amplitude-frequency response of the fourth and fifth order Butterworth lowpass filters.

and, after simplification we get,

$$F_{5,4}(s) = \frac{1}{(s+1)\left(s^2+1.618s+1\right)\left(s^2+0.618s+1\right)} \tag{2.47}$$

Hence, we get the amplitude-frequency response (eqn. 2.3) in the form

$$A_{5,4}(w) = \left| \frac{1}{(1+jw)\left(1-w^2+1.618jw\right)\left(1-w^2+0.618jw\right)} \right| \tag{2.48}$$

The amplitude-frequency response of the fifth order Butterworth lowpass filter (eqn. 2.47 and 2.48) is shown in the fig. 2.5. We can observe that the response is monotonically decreasing, and at -3db gain value the cutoff frequency is 1 rad/s.

2.4.2.3 Comparison of the derived fourth and fifth order analog 1-D Butterworth lowpass filters

Fig. 2.6 shows the amplitude-frequency response of the fourth and fifth order 1-D Butterworth lowpass filter for frequency range of $0 \leq w \leq 1$. It is observed that the fifth order Butterworth filter has sharper transition band as compared to the fourth order filter.

Algorithm 2 MATLAB Code to plot Amplitude-Frequency response of the fourth and fifth order 1-D Butterworth lowpass filters

```
% Under Guidance of Prof. Dr. V. Ramachandran
% Student's name : Ajit Singh Sandhu..... ID:4841492.
clear all; clc;
%Least count size of the frequency axes
step=0.00001;
% Frequency varying from -1 to 1 rad/sec
w=[-1:step:1]; s=j.*w;
% Generation of transfer function for fourth order 1-D Butterworth Lowpass filter
ha1D=(s+0.9239+0.3827i).*(s+0.9239-0.3827i);
ha2D=(s+0.3827+0.9239i).*(s+0.3827-0.9239i);
% Final transfer function for fourth order 1-D Butterworth Lowpass filter
h_1D_but_4=20*log10(abs(1./(ha1D.*ha2D)));
%Plotting the fourth order 1-D Butterworth Lowpass filter
figure(1);
plot(w,h_1D_but_4,'k');
title('Fourth order 1-D Butterworth Lowpass Filter');
xlabel('Frequency w in rad/sec');
ylabel('Magnitude response in db');
grid on;
% Generation of transfer function for fifth order 1-D Butterworth Lowpass filter
ha_1D=(s+1).*(s+0.8090+0.5878i).*(s+0.8090-0.5878i);
ha_2D=(s+0.3090+0.9511i).*(s+0.3090-0.9511i);
% Final transfer function for fifth order 1-D Butterworth Lowpass filter
h_1D_but_5=20*log10(abs(1./(ha_1D.*ha_2D)));
%Plotting the fifth order 1-D Butterworth Lowpass filter
figure(2);
plot(w,h_1D_but_5,'k');
title('Fifth order 1-D Butterworth Lowpass Filter');
xlabel('Frequency w in rad/sec');
ylabel('Magnitude response in db');
grid on;
clear all;
step=0.00001;
ww=[0:step:1];
s=j.*ww;
ha1D=(s+0.9239+0.3827i).*(s+0.9239-0.3827i);
ha2D=(s+0.3827+0.9239i).*(s+0.3827-0.9239i);
h_1D_but_4=20*log10(abs(1./(ha1D.*ha2D)));
ha_1D=(s+1).*(s+0.8090+0.5878i).*(s+0.8090-0.5878i);
ha_2D=(s+0.3090+0.9511i).*(s+0.3090-0.9511i);
h_1D_but_5=20*log10(abs(1./(ha_1D.*ha_2D)));
%Plotting the fourth and fifth order 1-D Butterworth Lowpass filter with
%reduced axes together on the same figure
figure(3);
plot(ww,h_1D_but_4,'k-',ww,h_1D_but_5,'k-.');
legend('Fourth Order Butterworth Lowpass Filter','Fifth Order Butterworth Lowpass Fil-
ter','Location','SouthWest');
title('Fourth and Fifth order 1-D Butterworth Lowpass Filter');
xlabel('Frequency w in rad/sec');
ylabel('Magnitude response in db');
grid on;
```

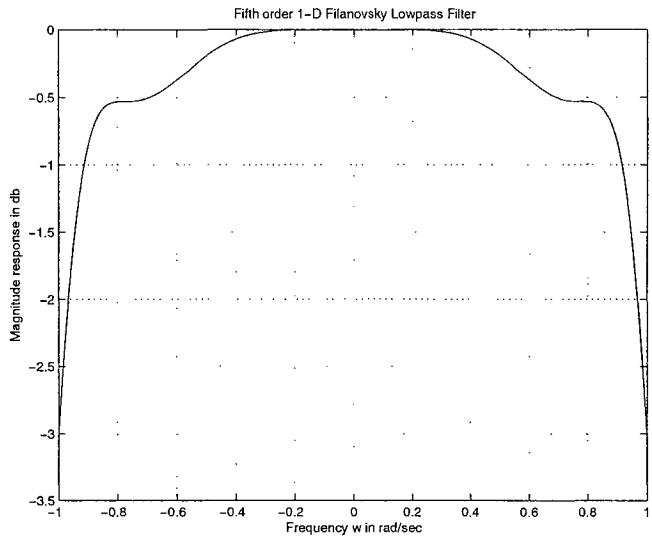

Figure 2.7: Amplitude-frequency response of the fifth order Filanovsky Lowpass filter

The response in the passband for the fifth order filters is flatter and wider than that of the fourth order, and they maintain the monotonic characteristic of the corresponding filter, with cutoff frequency, $w = 1$. (Discussions based on comparison of all the 1-D lowpass filters implemented will be done in Sec. 2.6). The MATLAB code to plot the amplitude-frequency response of the fourth and fifth order Butterworth filters is in algorithm 2.

2.4.3 Generation of analog 1-D Filanovsky lowpass filter and study its characteristics

Filanovsky filters are realizable for order five onwards [14], hence, we cannot have filter of fourth order. We will generate fifth order analog 1-D Filanovsky lowpass filter and study its characteristics. The amplitude-frequency response (eqn. 2.4) of the fifth order (i.e., $m = 5$) Filanovsky filter, having flatness degree two (i.e., $i = 2$), (and by utilizing the filter polynomial function derived in Sec. 2.3.2.2, i.e., eqn. 2.37), we get

$$A_{5,2}(w) = \frac{A_0}{\sqrt{1 + 10w^{10} - 15w^8 + 6w^6}}$$

The pole locations of the lowpass filter transfer function, $F_{5,2}(s)$, can be found using the eqn. 2.17. Hence, we get the poles,

$$s = jw = -0.6445, \pm 0.4754 \pm j0.5344, \pm 0.1746 \pm j0.9637$$

To ensure stability, we will separate the poles in the left half of the s plane and discard the rest. Therefore, the transfer function of the fifth order 1-D Filanovsky lowpass filter (eqn. 2.17 and 2.2) is

$$F_{5,2}(s) = \frac{0.3162}{(s+0.6445)(s+0.4754+j0.5344)(s+0.4754-j0.5344)} \\ (s+0.1746+j0.9637)(s+0.1746-j0.9637)$$

and, after simplification we get,

$$F_{5,2}(s) = \frac{0.3162}{(s+0.6445)(s^2+0.9508s+0.5116)(s^2+0.3492s+0.9592)} \tag{2.49}$$

Hence, we get the amplitude-frequency response (eqn. 2.3) in the form

$$A_{5,2}(w) = \left| \frac{0.3162}{(0.6445+jw)(0.5116-w^2+0.9508jw)} \\ (0.9592-w^2+0.3492jw) \right| \tag{2.50}$$

The amplitude-frequency response of the fifth order Filanovsky lowpass filter (eqn. 2.49 and 2.50) is shown in the fig. 2.7. We can observe that the response is monotonically decreasing, and at -3db gain value the cutoff frequency is 1 rad/s. The MATLAB code to plot the amplitude-frequency response of the fifth order Filanovsky filter is in algorithm 3.

Algorithm 3 MATLAB Code to plot amplitude-frequency response of the fifth order 1-D Filanovsky lowpass filter

```
% Under Guidance of Prof. Dr. V. Ramachandran
% Student's name : Ajit Singh Sandhu..... ID:4841492.
clear all; clc;
%Least count size of the frequency axes
step=0.00001;
% Frequency varing from -1 to 1 rad/sec
w=[-1:step:1];
s=j.*w;
% Generation of transfer function for fifth order 1-D Papoulis Lowpass
% filter
ha1D=(s+0.6445).*(s+0.4754+0.5344i).*(s+0.4754-0.5344i);
ha2D=(s+0.1746+0.9637i).*(s+0.1746-0.9637i);
h_1D=abs(0.3162./(ha1D.*ha2D));
% Final transfer function for fifth order 1-D Papoulis Lowpass filter
h_1D_fila_order5=20*log10(h_1D);
%Plotting the fifth order 1-D Papoulis Lowpass filter
figure(1);
plot(w,h_1D_fila_order5,'k');
title('Fifth order 1-D Filanovsky Lowpass Filter');
xlabel('Frequency w in rad/sec');
ylabel('Magnitude response in db');
grid on;
```

2.5 Generation of 1-D Thomson-Bessel lowpass filters with monotonic response and study their characteristics

In [43], Bessel polynomials are used to generate the Thomson-Bessel lowpass analog filters. The Bessel Polynomials are written in general form as $\sum_{j=0}^{n-1} a_j s^j$, where $a_n = 1$. The coefficients are tabulated with values to $n = 8$ and the roots of the resulting polynomials are also tabulated in [43]. The Bessel polynomial forms the denominator of the transfer function (eqn. 2.2) of the Thomson-Bessel filter. In this section, we will generate fourth and fifth order analog 1-D Thomson-Bessel lowpass filters (utilizing the results of Bessel polynomials in [43]), study their characteristics and compare the amplitude-frequency responses.

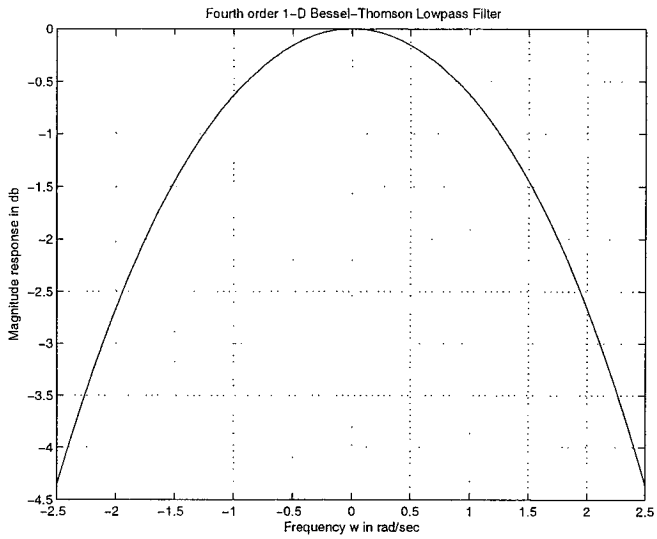

Figure 2.8: Amplitude-frequency response of the fourth order Thomson-Bessel Lowpass filter

2.5.1 Generation of 1-D Thomson-Bessel lowpass filter of fourth order

The pole locations of the fourth order Thomson-Bessel lowpass filter transfer function [43] are,

$$s = jw = \pm 2.8962 \pm j0.8672, \pm 2.1038 \pm j2.6574$$

To ensure stability, we will separate the poles in the left half of the s plane and discard the rest. Therefore, the transfer function of the fourth order 1-D Thomson-Bessel lowpass filter (eqn. 2.2 and [43]) is

$$F_4(s) = \frac{105}{(s^4 + 10s^3 + 45s^2 + 105s + 105)} \tag{2.51}$$

Hence, we get the amplitude-frequency response (eqn. 2.3) in the form:

$$A_4(w) = \left| \frac{105}{(w^4 - 45w^2 + 105) + j\left(-10w^3 + 105w\right)} \right| \tag{2.52}$$

The amplitude-frequency response of the fourth order Thomson-Bessel lowpass filter (eqn. 2.51 and 2.52) is shown in the fig. 2.8. We can observe that the response is monoton-

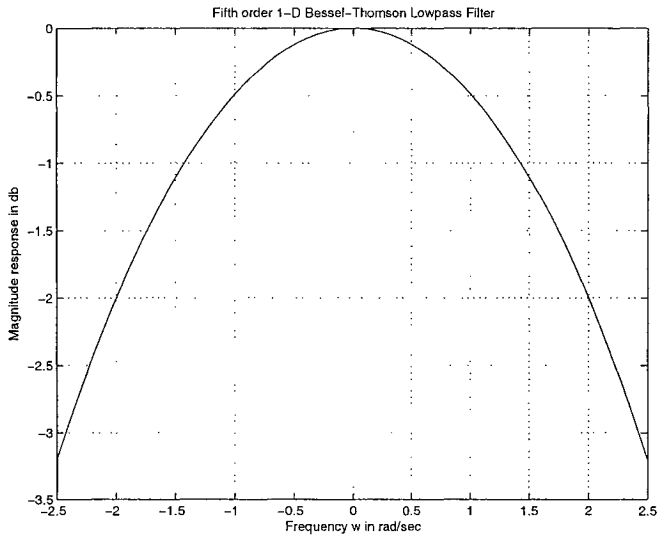

Figure 2.9: Amplitude-frequency response of the fifth order Thomson-Bessel Lowpass filter

ically decreasing.

2.5.2 Generation of 1-D Thomson-Bessel lowpass filter of fifth order

The pole locations of the fifth order Thomson-Bessel lowpass filter transfer function ([43]) are,

$$s = jw = -3.6467, \pm 3.3520 \pm j1.7427, \pm 2.3247 \pm j3.5710$$

To ensure stability, we will separate the poles in the left half of the s plane and discard the rest. Therefore, the transfer function of the fifth order 1-D Thomson-Bessel lowpass filter (refer eqn. 2.2 and [43]) is

$$F_5(s) = \frac{945}{(s^5 + 15s^4 + 105s^3 + 420s^2 + 945s + 945)} \tag{2.53}$$

Hence, we get the amplitude-frequency response (eqn. 2.3) in the form:

$$A_5(w) = \left| \frac{945}{(15w^4 - 420w^2 + 945) + j\,(w^5 - 105w^3 + 945w)} \right| \tag{2.54}$$

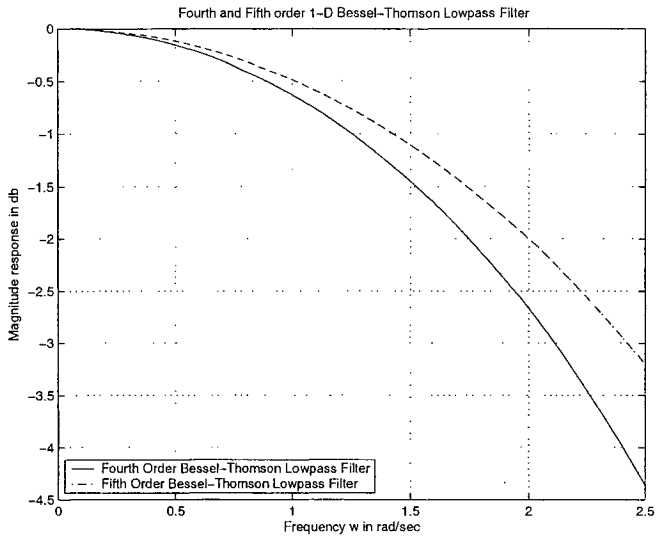

Figure 2.10: Amplitude-frequency response of the fourth and fifth order Thomson-Bessel lowpass filters.

The amplitude-frequency response of the fifth order Thomson-Bessel lowpass filter (eqn. 2.53 and 2.54) is shown in the fig. 2.9. We can observe that the response is monotonically decreasing.

2.5.3 Comparison of the derived fourth and fifth order analog 1-D Thomson-Bessel lowpass filters

Fig. 2.10 shows the amplitude-frequency response of the fourth and fifth order 1-D Thomson-Bessel lowpass filter. It is observed that the fifth order Thomson-Bessel filter has flatter and wider passband as compared to the fourth order filter. With larger order of filter, we will get larger band of frequencies for flat response. (Discussions based on comparison of all the 1-D lowpass filters implemented will be done in Sec. 2.6). The MATLAB code to plot the amplitude-frequency response of the fourth and fifth order Thomson-Bessel filters is in algorithm 4.

Algorithm 4 MATLAB Code to plot Amplitude-Frequency response of the fourth and fifth order 1-D Thomson-Bessel lowpass filters

```
% Under Guidance of Prof. Dr. V. Ramachandran
% Student's name : Ajit Singh Sandhu..... ID:4841492.
clear all; clc;
%Least count size of the frequency axes
step=0.00001;
% Frequency varing from -1 to 1 rad/sec
w=[-2.5:step:2.5];
s=j.*w;
% Generation of transfer function for fourth order 1-D Thomson-Bessel Lowpass filter
ha0D=105;
h_1D=abs(ha0D./(s.^4+10.*s.^3+45.*s.^2+105.*s+105));
h_1D_bes_order4=20*log10(h_1D);
%Plotting the fourth order 1-D Papoulis Lowpass filter
figure(1);
plot(w,h_1D_bes_order4,'k');
title('Fourth order 1-D Bessel-Thomson Lowpass Filter');
xlabel('Frequency w in rad/sec');
ylabel('Magnitude response in db');
grid on;
% Generation of transfer function for fifth order 1-D Thomson-Bessel Lowpass filter
ha_0D=945;
ha_1D=abs(ha_0D./(s.^5+15.*s.^4+105.*s.^3+420.*s.^2+945.*s+945));
ha_1D_bes_order5=20*log10(ha_1D);
%Plotting the fifth order 1-D Papoulis Lowpass filter
figure(2);
plot(w,ha_1D_bes_order5,'k');
title('Fifth order 1-D Bessel-Thomson Lowpass Filter');
xlabel('Frequency w in rad/sec');
ylabel('Magnitude response in db');
grid on;
clear all;
step=0.00001;
ww=[0:step:2.5];
s=j.*ww;
ha0D=105;
h_1D=abs(ha0D./(s.^4+10.*s.^3+45.*s.^2+105.*s+105));
h_1D_bes_order4=20*log10(h_1D);
ha_1D=(s+3.6467).*(s+3.3520+1.7427i).*(s+3.3520-1.7427i);
ha_2D=(s+2.3247+3.5710i).*(s+2.3247-3.5710i);
ha_0D=945.01;
h_1D_p=abs(ha_0D./(ha_1D.*ha_2D));
h_1D_bes_order5=20*log10(h_1D_p);
%Plotting the fourth and fifth order 1-D Thomson-Bessel Lowpass filter with
%reduced axes together on the same figure
figure(3);
plot(ww,h_1D_bes_order4,'k-',ww,h_1D_bes_order5,'k-.');
legend('Fourth Order Bessel-Thomson Lowpass Filter','Fifth Order Bessel-Thomson Lowpass Filter',3);
title('Fourth and Fifth order 1-D Bessel-Thomson Lowpass Filter');
xlabel('Frequency w in rad/sec');
ylabel('Magnitude response in db');
grid on;
```

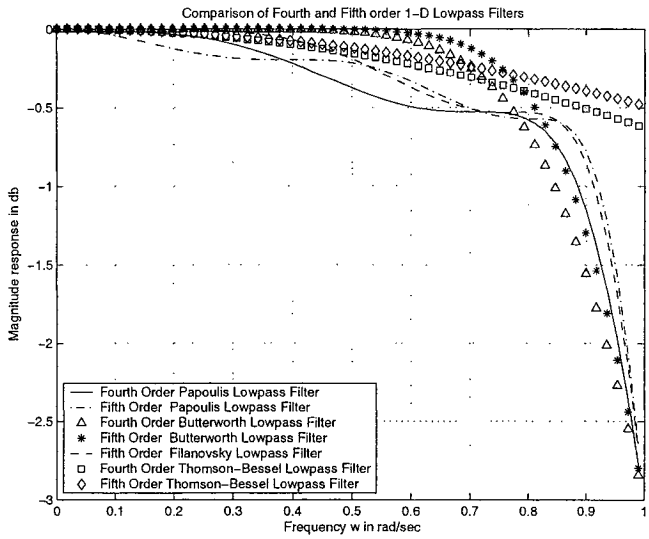

Figure 2.11: Amplitude-frequency response of the fourth and fifth order 1-D lowpass filters with monotonic response and arbitrary flatness

2.6 Comparison of the implemented fourth and fifth order analog 1-D lowpass filters with monotonic response and arbitrary flatness

Fig. 2.11 shows amplitude-frequency response of analog 1-D Butterworth, Papoulis and Thomson-Bessel lowpass filters of fourth and fifth order. It also shows the amplitude-frequency response of fifth order 1-D Filanovsky lowpass filter. The variation in amplitude-frequency response of all the filters can be easily observed. In the case of the Butterworth filters, the derivative calculated at the passband edge at $w = 1$, is relatively low and this results in a wider transition band for a given order filter, in comparison with the other filters. To overcome this deficiency, the derivative must be maximized at $w = 1$. It is observed in fig. 2.11 that the cutoff frequency (at -3db gain) for all the filters (except for Thomson-Bessel filters) is $w = 1$rad/sec.

Papoulis filters have much steeper transition band due to maximized derivative at $w = 1$ but less flatter amplitude-frequency response in the passband, in comparison to the Butter-

Algorithm 5 MATLAB Code to plot amplitude-frequency response of all the implemented fourth and fifth order 1-D lowpass filters

```
% Under Guidance of Prof. Dr. V. Ramachandran
% Student's name : Ajit Singh Sandhu..... ID:4841492.
clear all; clc;
%Least count size of the frequency axes
step=0.018;
% Frequency varing from -1 to 1 rad/sec
w=[0:step:1];
s=j.*w;
% Generation of transfer function for fifth order 1-D Papoulis Lowpass
% filter
fha1D=(s+0.6445).*(s+0.4754+0.5344i).*(s+0.4754-0.5344i);
fha2D=(s+0.1746+0.9637i).*(s+0.1746-0.9637i);
fh_1D=abs(0.3162./(fha1D.*fha2D));
% Final transfer function for fifth order 1-D Papoulis Lowpass filter
h_1D_fila_order5=20*log10(fh_1D);
%Transfer function for fourth order 1-D Butterworth lowpass Filter.
bha1D=(s+0.9239+0.3827i).*(s+0.9239-0.3827i);
bha2D=(s+0.3827+0.9239i).*(s+0.3827-0.9239i);
h_1D_but_4=20*log10(abs(1./(bha1D.*bha2D)));
%Transfer function for fifth order 1-D Butterworth lowpass Filter.
bha_1D=(s+1).*(s+0.8090+0.5878i).*(s+0.8090-0.5878i);
bha_2D=(s+0.3090+0.9511i).*(s+0.3090-0.9511i);
h_1D_but_5=20*log10(abs(1./(bha_1D.*bha_2D)));
%Transfer function for fourth order 1-D Papoulis lowpass Filter.
pha1D=(s+0.2317+0.9455i).*(s+0.2317-0.9455i);
pha2D=(s+0.5497+0.3586i).*(s+0.5497-0.3586i);
ph_1D=abs(0.4075./(pha1D.*pha2D));
h_1D_pop_order4=20*log10(ph_1D);
%Transfer function for fifth order 1-D Papoulis lowpass Filter.
pha_1D=(s+0.4681).*(s+0.3881+0.5886i).*(s+0.3881-0.5886i);
pha_2D=(s+0.1536+0.9681i).*(s+0.1536-0.9681i);
ph_1D_pop=abs(0.2235./(pha_1D.*pha_2D));
h_1D_pop_order5=20*log10(ph_1D_pop);
%Transfer function for fourth order 1-D Thomson-Bessel lowpass Filter.
ha0D=105;
h_1D=abs(ha0D./(s.^4+10.*s.^3+45.*s.^2+105.*s+105));
h_1D_bes_order4=20*log10(h_1D);
%Transfer function for fifth order 1-D Thomson-Bessel lowpass Filter.
ha_0D=945;
ha_1D=abs(ha_0D./(s.^5+15.*s.^4+105.*s.^3+420.*s.^2+945.*s+945));
ha_1D_bes_order5=20*log10(ha_1D);
%Plotting the fourth and fifth order Lowpass filters
figure(1);
plot(w,h_1D_pop_order4,'k-',w,h_1D_pop_order5,'k-.',w,h_1D_but_4,'k^',w,h_1D_but_5,'k*',
w,h_1D_fila_order5,'k-',w,h_1D_bes_order4,'ks',w,ha_1D_bes_order5,'kd');
legend('Fourth Order Papoulis Lowpass Filter','Fifth Order Papoulis Lowpass Filter',
'Fourth Order Butterworth Lowpass Filter','Fifth Order Butterworth Lowpass Filter',
'Fifth Order Filanovsky Lowpass Filter','Fourth Order Thomson-Bessel Lowpass Filter',
'Fifth Order Thomson-Bessel Lowpass Filter',3);
title('Comparison of Fourth and Fifth order 1-D Lowpass Filters');
xlabel('Frequency w in rad/sec');
ylabel('Magnitude response in db'); grid on;
```

worth filters. The amplitude-frequency response of analog 1-D Filanovsky lowpass filter is intermediate between Butterworth and Papoulis filter of the same order. In fig. 2.11, considering the fifth order filters, Filanovsky filter response can be seen intermediate between the Butterworth and Papoulis filter, especially as it approaches the transition region.

In general, the amplitude-frequency response of Papoulis and Filanovsky filters are not flat and even the first derivative, calculated at $w = 0$, is not equal to zero. On the other hand, Butterworth filter response is much flatter than compared to other filters and has its first derivative equal to zero, at $w = 0$. It can also be seen that as the order of the filter increases the passband becomes wider and transition band sharpens. This is verified by observing the fourth and fifth order Butterworth filter and Papoulis filter response in fig. 2.11. It can be seen that the Butterworth filter of fifth order is having sharper transition band than that of the fourth order. The same is observed for Papoulis filters too. It is interesting to note that Papoulis filter of fourth order is still having steeper transition of amplitude-frequency response than fifth order Butterworth filter, in the transition region. The nature of response of the Papoulis, Butterworth and Filanovsky filters in fig. 2.11 are similar to the work proposed in [14].

The Thomson-Bessel filters are not derived to have cutoff frequency of $w = 1$ rad/sec in [43]. Their magnitude response is much flatter and have higher cut off frequencies than Butterworth, Filanovsky and Papoulis filters [14] (derived in Sec. 2.2, 2.3 and 2.4). The fifth order Thomson-Bessel filters have much flatter response than the fourth order. The MATLAB code to plot the amplitude-frequency response of the fourth and fifth order Papoulis, Butterworth, Filanovsky and Thomson-Bessel filters is in algorithm 5.

In the next two sections, we will show how by proper choice of poles of each of these filters and also by judicious combinations, other types of monotonic responses (not available in the literature so far) can be generated.

2.7 Extracting lower order analog 1-D lowpass filters from higher order 1-D lowpass filters having monotonic response and study their characteristics

The higher order lowpass 1-D filter can be expressed as a product separable lower order 1-D filter transfer functions in the frequency domain, also termed as cascading of filters in series. Keeping this into consideration, we can study the 1-D filters with each filter having poles on the left side of the s-plane (to ensure stability). If the poles are complex then they should be in conjugate pairs. Our primary emphasis will be to propose a methodology to extract the lower order 1-D lowpass filters from higher order, and segregate the one bearing monotonic characteristics.

In this section, we will study the characteristics of all the possible lower order 1-D filters obtained from the fourth and fifth order Papoulis, Butterworth and Thomson-Bessel filters designed earlier in Sec. 2.4.1, 2.4.2, 2.5, and also fifth order Filanovsky filter designed in Sec. 2.4.3. We will study the amplitude-frequency response of the filters and characterise (segregate) the filters bearing monotonic behavior.

2.7.1 Extracting lower order 1-D lowpass filters from 1-D Papoulis lowpass filters and study their characteristics

In Sec. 2.4.1, we generated and studied stable fourth and fifth order analog 1-D Papoulis lowpass filters, in which all poles are on the left side of the s-plane. By observing the nature of the poles, we can realize it in the form of cascaded lower order 1-D lowpass filters (which are having transfer functions obtained from the implemented analog 1-D Papoulis lowpass filters).

F.No.	*Poles*	$F(s)$	$A(w)$
P1	$-0.2317 \pm j0.9445$	$\frac{0.9458}{s^2+0.4634s+0.9458}$	$\frac{0.9458}{\sqrt{\left(0.9458-w^2\right)^2+(0.4634w)^2}}$
P2	$-0.5497 \pm j0.3586$	$\frac{0.4308}{s^2+1.0994s+0.4308}$	$\frac{0.4308}{\sqrt{\left(0.4308-w^2\right)^2+(1.0994w)^2}}$

Table 2.1: Second order 1-D lowpass filters obtained from the fourth order 1-D Papoulis lowpass filter

F.No.	*Order*	*-3db freq.*	*slope at -3db*
P1	2	1.45	-1.4482
P2	2	0.5394	-0.9544

Table 2.2: Slope and frequency at -3db magnitude of second order 1-D lowpass filters obtained from the fourth order 1-D Papoulis lowpass filter

2.7.1.1 Extracting lower order lowpass filters from fourth order 1-D Papoulis lowpass filter

In Sec. 2.4.1.1, we generated and studied stable fourth order 1-D Papoulis lowpass filters. The poles of the filter are in complex conjugate pairs. By observing the nature of the poles, we can realize it in the form of two cascaded second order 1-D lowpass filters, with the transfer functions having denominator polynomials of second order each.

Table: 2.1 shows the extracted second order analog 1-D lowpass filters with, *(i)* the transfer function (eqn. 2.2), $F(s)$, *(ii)* amplitude-frequency response (eqn. 2.3), $A(w)$, *(iii) Poles* corresponding to each filter, and *(iv)* the filter number, *F.No* (where, Pi, with i as integer varying from 1 to 2, corresponds to analog 1-D lowpass filter obtained from Papoulis lowpass filter).

Table: 2.2 shows, *(i)* the filter number, *F.No, (ii) Order* of the extracted lower order analog 1-D lowpass filters, *(iii)* the cutoff frequency at magnitude response of $\frac{1}{\sqrt{2}}$, i.e., -3db value and, *(iv) Slope at -3db* magnitude value of the frequency response.

The amplitude-frequency response of the extracted analog 1-D lowpass filter, P1 and P2 (refer table: 2.1) is shown in fig. 2.12. Filter P2 is having monotonic amplitude-frequency response, as its complex conjugate poles are further away from the origin. Since poles of

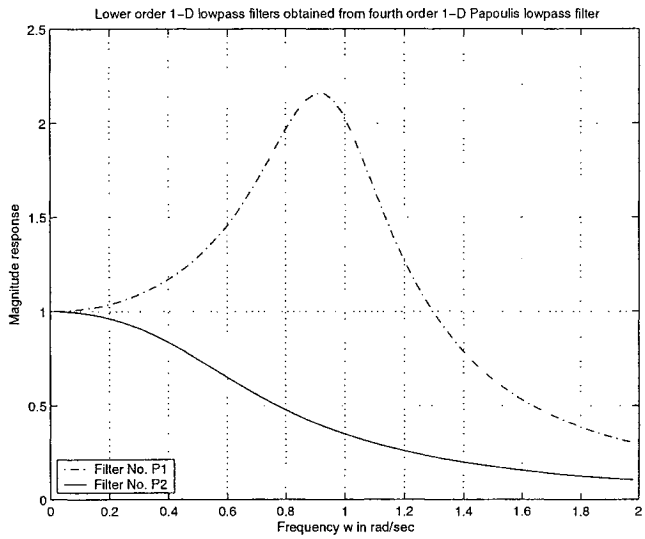

Figure 2.12: Plot of two lower order 1-D lowpass filters obtained from the fourth order 1-D Papoulis lowpass filter (Refer Table: 2.1)

P1 are closer to the origin with magnitude of real part less than imaginary part, it is having ripple in the passband, hence, does not inhibit the monotonic behavior. The MATLAB code written to plot the response of the filters in table: 2.1 is in algorithm 6.

2.7.1.2 Extracting lower order 1-D lowpass filters from the fifth order 1-D Papoulis lowpass filter

In Sec. 2.4.1.2, we generated and studied stable fifth order 1-D Papoulis lowpass filters. The poles of the filter are real as well as in complex conjugate pairs. By observing the nature of the poles, we can realize it in the form of cascaded first, second, third and fourth order 1-D lowpass filters, with the transfer functions having denominator polynomials of the corresponding order.

Table: 2.3 shows the extracted analog 1-D lowpass filters with, *(i)* the transfer function (eqn. 2.2), $F(s)$, *(ii)* amplitude-frequency response (eqn. 2.3), $A(w)$, *(iii) Poles* corresponding to each filter and, *(iv)* the filter number, *F.No* (where, Pi, with i as integer varying from 3 to 8, corresponds to analog 1-D lowpass filter obtained from Papoulis lowpass filter).

Table: 2.4 shows, *(i)* the filter number, *F.No, (ii) Order* of the extracted lower order

Algorithm 6 MATLAB Code to plot second order 1-D lowpass filters obtained from fourth order 1-D Papoulis filter (Refer Table: 2.1)

```
% Under Guidance of Prof. Dr. V. Ramachandran
% Student's name : Ajit Singh Sandhu..... ID:4841492.
clear all; clc;
%Defining the step size of the frequency axis.
step=0.03;
%Defining the frequency range
w=[0:step:2];
s=j.*w;
%Transfer function for Filter No. P1
ha1D=(s+0.2317+0.9445i).*(s+0.2317-0.9445i);
ha1D=abs(0.9458./ha1D);
%Transfer function for Filter No. P2
ha2D=(s+0.5497+0.3586i).*(s+0.5497-0.3586i);
ha2D=abs(0.4308./ha2D);
%Plotting all the 1-D lowpass filters on the same figure
figure(1);
plot(w,ha1D,'k-.',w,ha2D,'k-');
legend('Filter No. P1','Filter No. P2',3);
title('Lower order 1-D lowpass filters obtained from fourth order 1-D Papoulis lowpass filter');
xlabel('Frequency w in rad/sec');
ylabel('Magnitude response');
grid on;
```

F.No.	*Poles*	$F(s)$	$A(w)$
P3	-0.4681	$\frac{0.4681}{s+0.4681}$	$\frac{0.4681}{\sqrt{(0.4681)^2+w^2}}$
P4	$-0.1536 \pm j0.9681$	$\frac{0.9608}{s^2+0.3072s+0.9608}$	$\frac{0.9608}{\sqrt{(0.9608-w^2)^2+(0.3072w)^2}}$
P5	$-0.3881 \pm j0.5886$	$\frac{0.4971}{s^2+0.7762s+0.4971}$	$\frac{0.4971}{\sqrt{(0.4971-w^2)^2+(0.7762w)^2}}$
P6	-0.4681, $-0.3881 \pm j0.5886$	$\frac{0.2327}{s^3+1.2443s^2+0.8604s+0.2327}$	$\frac{0.2327}{\sqrt{(0.2327-1.2443w^2)^2+(0.8604w-w^3)^2}}$
P7	-0.4681, $-0.1536 \pm j0.9681$	$\frac{0.4498}{s^3+0.7753s^2+1.1046s+0.4498}$	$\frac{0.4498}{\sqrt{(0.4498-0.7753w^2)^2+(1.1046w-w^3)^2}}$
P8	$-0.3881 \pm j0.5886$, $-0.1536 \pm j0.9681$	$\frac{0.4776}{s^4+1.0834s^3+1.6963s^2+0.8985s+0.4776}$	$\frac{0.4776}{\sqrt{(w^4-1.6963w^2+0.4776)^2+(0.8985w-1.0834w^3)^2}}$

Table 2.3: First to fourth order 1-D lowpass filters obtained from fifth order 1-D Papoulis lowpass filter

F.No.	*Order*	*-3db freq.*	*slope at -3db*
P3	1	0.4682	−0.7551
P4	2	1.4965	−1.5196
P5	2	0.8545	−1.3064
P6	3	0.531	−1.0484
P7	3	1.153	−3.1213
P8	4	1.1675	−3.7811

Table 2.4: Slope and frequency at -3db magnitude of first to fourth order 1-D lowpass filters obtained from fifth order 1-D Papoulis lowpass filter

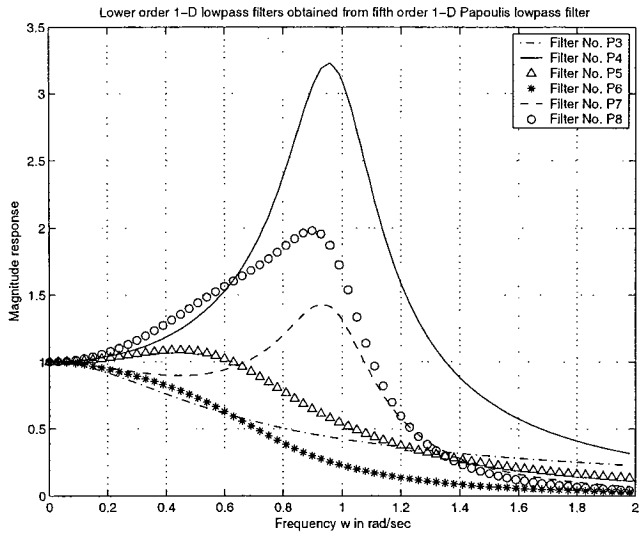

Figure 2.13: Plot of lower order 1-D lowpass filters obtained from the fifth order 1-D Papoulis lowpass filter (Refer Table: 2.3)

Algorithm 7 MATLAB Code to plot lower order 1-D lowpass filters obtained from fifth order 1-D Papoulis filter (Refer Table: 2.3)

```
% Under Guidance of Prof. Dr. V. Ramachandran
% Student's name : Ajit Singh Sandhu..... ID:4841492.
clear all; clc;
%Defining the step size of the frequency axis.
step=0.03;
%Defining the frequency range
w=[0:step:2];
s=j.*w;
%Transfer function for Filter No. P3
ha1D=(s+0.4681);
ha1D=abs(0.4681./ha1D);
%Transfer function for Filter No. P4
ha2D=(s+0.1536+0.9681i).*(s+0.1536-0.9681i);
ha2D=abs(0.9608./ha2D);
%Transfer function for Filter No. P5
ha3D=(s+0.3881+0.5886i).*(s+0.3881-0.5886i);
ha3D=abs(0.4971./ha3D);
%Transfer function for Filter No. P6
ha4D=(s+0.4681).*(s+0.3881+0.5886i).*(s+0.3881-0.5886i);
ha4D=abs(0.2327./ha4D);
%Transfer function for Filter No. P7
ha5D=(s+0.4681).*(s+0.1536+0.9681i).*(s+0.1536-0.9681i);
ha5D=abs(0.4498./ha5D);
%Transfer function for Filter No. P8
ha6D=(s+0.3881+0.5886i).*(s+0.3881-0.5886i).*(s+0.1536+0.9681i).*(s+0.1536-0.9681i);
ha6D=abs(0.4776./ha6D);
%Plotting all the 1-D lowpass filters on the same figure
figure(1);
plot(w,ha1D,'k-.',w,ha2D,'k-',w,ha3D,'k^',w,ha4D,'k*',w,ha5D,'k--',w,ha6D,'ko');
legend('Filter No. P3','Filter No. P4','Filter No. P5','Filter No. P6','Filter No. P7','Filter No. P8',1);
title('Lower order 1-D lowpass filters obtained from fifth order 1-D Papoulis lowpass filter');
xlabel('Frequency w in rad/sec');
ylabel('Magnitude response');
grid on;
```

analog 1-D lowpass filters, *(iii)* the cutoff frequency at magnitude response of $\frac{1}{\sqrt{2}}$, i.e., -3db value and, *(iv) Slope at -3db* magnitude value of the frequency response.

The amplitude-frequency response of the extracted analog 1-D lowpass filters, P3, P4, P5, P6, P7 and P8 (refer table: 2.3) is shown in fig. 2.13. Filters P3 and P6 are having monotonic amplitude-frequency response. P6 is having a wider passband and steeper transition band as compared to P3. This is primarily because P6 transfer function is of higher order than P3.

Filters P4, P5, P7 and P8 are having ripples in the pass band, hence, does not inhibit

the monotonic behavior. This is primarily because the poles are closer to the origin with magnitude of real part less than imaginary part. Since P4 is having only two complex conjugate poles much closer to the origin, the ripple of amplitude-frequency response in the passband is having maximum deviation. Filter P7 transfer function is having poles of P3 and P4, with real pole of P3 further away from origin as compared to poles of P4. Therefore, the combination filter (P7) is having reduced ripples in comparison to P4. Filter P5 have two complex-conjugate poles which are not as close to origin as in case of P4, hence, its magnitude response ripple in the passband is much less. Since, filter P8 is combination filter of P4 and P5 (having poles of P4 and P5), its amplitude-frequency response is intermediate between response of P4 and P5. It is furthermore observed that, the small ripple in the passband of P5 is not present in P6, as the latter is combination filter of P3 and P5. The MATLAB code to plot the amplitude-frequency response of the filters in table: 2.3 is in algorithm 7.

2.7.2 Extracting lower order 1-D lowpass filters from 1-D Butterworth lowpass filters and study their characteristics

In Sec. 2.4.2, we generated and studied stable fourth and fifth order analog 1-D Butterworth lowpass filters, in which all poles are on the left side of the s-plane. By observing the nature of the poles, we can realize it in the form of cascaded lower order 1-D lowpass filters (which are having transfer functions obtained from the implemented analog 1-D Butterworth lowpass filters).

2.7.2.1 Extracting lower order lowpass filters from fourth order 1-D Butterworth lowpass filter

In Sec. 2.4.2.1, we generated and studied stable fourth order 1-D Butterworth lowpass filters. The poles of the filter are in complex conjugate pairs. By observing the nature of the poles, we can realize it in the form of two cascaded second order 1-D lowpass filters,

F.No.	*Poles*	$F(s)$	$A(w)$
B1	$-0.9239 \pm j0.3827$	$\frac{1}{s^2+1.8478s+1}$	$\frac{1}{\sqrt{\left(1-w^2\right)^2+(1.8478w)^2}}$
B2	$-0.3827 \pm j0.9239$	$\frac{1}{s^2+0.7654s+1}$	$\frac{1}{\sqrt{\left(1-w^2\right)^2+(0.7654w)^2}}$

Table 2.5: Second order 1-D lowpass filters obtained from fourth order 1-D Butterworth lowpass filter

F.No.	*Order*	*-3db freq.*	*slope at -3db*
B1	2	0.7195	-0.623
B2	2	1.39	-1.2032

Table 2.6: Slope and frequency at -3db magnitude of second order 1-D lowpass filters obtained from fourth order 1-D Butterworth lowpass filter

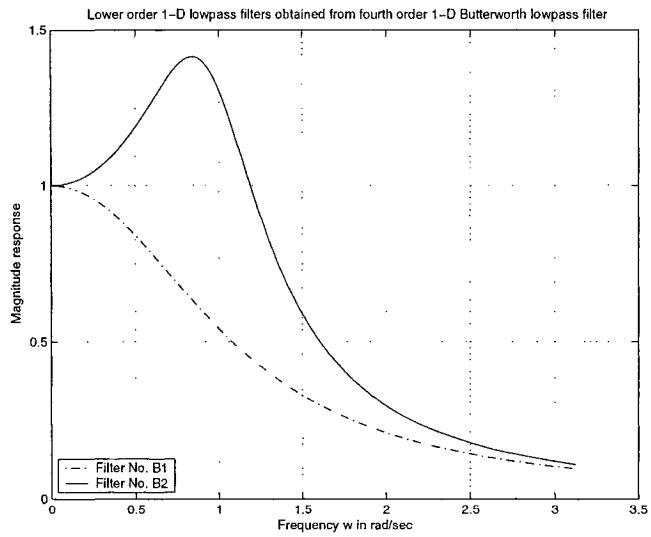

Figure 2.14: Plot of two lower order 1-D lowpass filters obtained from the fourth order 1-D Butterworth lowpass filter (Refer Table: 2.5)

with the transfer functions having denominator polynomials of second order each.

Table: 2.5 shows the extracted second order analog 1-D lowpass filters with, *(i)* the transfer function (eqn. 2.2), $F(s)$, *(ii)* amplitude-frequency response (eqn. 2.3), $A(w)$, *(iii) Poles* corresponding to each filter and, *(iv)* the filter number, *F.No* (where, Bi, with i as integer varying from 1 to 2, corresponds to analog 1-D lowpass filter obtained from Butterworth lowpass filter).

Table: 2.6 shows, *(i)* the filter number, *F.No, (ii) Order* of the extracted lower order analog 1-D lowpass filters, *(iii)* the cutoff frequency at magnitude response of $\frac{1}{\sqrt{2}}$, i.e., -3db value and, *(iv) Slope at -3db* magnitude value of the frequency response.

The amplitude-frequency response of the extracted analog 1-D lowpass filters, B1 and B2 (refer table: 2.5) is shown in fig. 2.14. Filter B1 is having monotonic amplitude-frequency response, as its complex conjugate poles are further away from the origin. Since poles of B2 are closer to the origin with magnitude of real part less than imaginary part, it is having ripple in the passband, hence, does not inhibit the monotonic behavior. The MATLAB code written to plot the response of the filters in table: 2.5 is in algorithm 8.

2.7.2.2 Extracting lower order 1-D lowpass filters from the fifth order 1-D Butterworth lowpass filter

In Sec. 2.4.2.2, we generated and studied stable fifth order 1-D Butterworth lowpass filters. The poles of the filter are real as well as in complex conjugate pairs. By observing the nature of the poles, we can realize it in the form of cascaded first, second, third and fourth order 1-D lowpass filters, with the transfer functions having denominator polynomials of the corresponding order.

Table: 2.7 shows the extracted analog 1-D lowpass filters with, *(i)* the transfer function (eqn. 2.2), $F(s)$, *(ii)* amplitude-frequency response (eqn. 2.3), $A(w)$, *(iii) Poles* corresponding to each filter and, *(iv)* the filter number, *F.No* (where, Bi, with i as integer varying from 3 to 8, corresponds to analog 1-D lowpass filter obtained from Butterworth lowpass

Algorithm 8 MATLAB Code to plot second order 1-D lowpass filters obtained from fourth order 1-D Butterworth filter (Refer Table: 2.5)

```
% Under Guidance of Prof. Dr. V. Ramachandran
% Student's name : Ajit Singh Sandhu..... ID:4841492.
clear all; clc;
%Defining the step size of the frequency axis.
step=0.03;
%Defining the frequency range
w=[0:step:pi];
s=j.*w;
%Transfer function for Filter No. B1
ha1D=(s+0.9239+0.3827i).*(s+0.9239-0.3827i);
ha1D=abs(1./ha1D);
%Transfer function for Filter No. B2
ha2D=(s+0.3827+0.9239i).*(s+0.3827-0.9239i);
ha2D=abs(1./ha2D);
%Plotting all the 1-D lowpass filters on the same figure
figure(1);
plot(w,ha1D,'k-.',w,ha2D,'k-');
legend('Filter No. B1','Filter No. B2',3);
title('Lower order 1-D lowpass filters obtained from fourth order 1-D Butterworth lowpass filter');
xlabel('Frequency w in rad/sec');
ylabel('Magnitude response');
grid on;
```

F.No.	*Poles*	$F(s)$	$A(w)$
B3	-1.0000	$\frac{1}{s+1.0000}$	$\frac{1}{\sqrt{1+w^2}}$
B4	$-0.8090 \pm j0.5878$	$\frac{1}{s^2+1.618s+1}$	$\frac{1}{\sqrt{(1-w^2)^2+(1.618w)^2}}$
B5	$-0.3090 \pm j0.9511$	$\frac{1}{s^2+0.618s+1}$	$\frac{1}{\sqrt{(1-w^2)^2+(0.618w)^2}}$
B6	-1.0000, $-0.3090 \pm j0.9511$	$\frac{1}{s^3+1.618s^2+1.618s+1}$	$\frac{1}{\sqrt{(1-1.618w^2)^2+(1.618w-w^3)^2}}$
B7	-1.0000, $-0.8090 \pm j0.5878$	$\frac{1}{s^3+2.618s^2+2.618s+1}$	$\frac{1}{\sqrt{(1-2.618w^2)^2+(2.618w-w^3)^2}}$
B8	$-0.3090 \pm j0.9511$, $-0.8090 \pm j0.5878$	$\frac{1}{s^4+2.236s^3+3s^2+2.236s+1}$	$\frac{1}{\sqrt{(w^4-3w^2+1)^2+(2.236w-2.236w^3)^2}}$

Table 2.7: First to fourth order 1-D lowpass filters obtained from fifth order 1-D Butterworth lowpass filter

F.No.	*Order*	*-3db freq.*	*slope at -3db*
B3	1	1.0001	−0.3535
B4	2	0.8589	−0.6356
B5	2	1.4476	−1.3161
B6	3	1.2193	−1.7980
B7	3	0.6394	−0.7782
B8	4	1.1362	−2.0808

Table 2.8: Slope and frequency at -3db magnitude of first to fourth order 1-D lowpass filters obtained from fifth order 1-D Butterworth lowpass filter

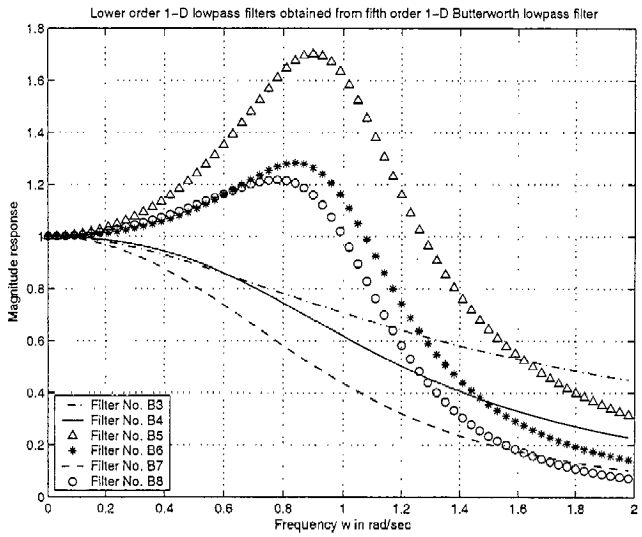

Figure 2.15: Plot of lower order 1-D lowpass filters obtained from the fifth order 1-D Butterworth lowpass filter (Refer Table: 2.7)

Algorithm 9 MATLAB Code to plot lower order 1-D lowpass filters obtained from fifth order 1-D Butterworth filter (Refer Table: 2.7)

```
% Under Guidance of Prof. Dr. V. Ramachandran
% Student's name : Ajit Singh Sandhu..... ID:4841492.
clear all; clc;
%Defining the step size of the frequency axis.
step=0.03;
%Defining the frequency range
w=[0:step:2];
s=j.*w;
%Transfer function for Filter No. B3
ha1D=(s+1);
ha1D=abs(1./ha1D);
%Transfer function for Filter No. B4
ha2D=(s+0.8090+0.5878i).*(s+0.8090-0.5878i);
ha2D=abs(1./ha2D);
%Transfer function for Filter No. B5
ha3D=(s+0.3090+0.9511i).*(s+0.3090-0.9511i);
ha3D=abs(1./ha3D);
%Transfer function for Filter No. B6
ha4D=(s+1).*(s+0.3090+0.9511i).*(s+0.3090-0.9511i);
ha4D=abs(1./ha4D);
%Transfer function for Filter No. B7
ha5D=(s+1).*(s+0.8090+0.5878i).*(s+0.8090-0.5878i);
ha5D=abs(1./ha5D);
%Transfer function for Filter No. B8
ha6D=(s+0.8090+0.5878i).*(s+0.8090-0.5878i).*(s+0.3090+0.9511i).*(s+0.3090-0.9511i);
ha6D=abs(1./ha6D);
%Plotting all the 1-D lowpass filters on the same figure
figure(1);
plot(w,ha1D,'k-.',w,ha2D,'k-',w,ha3D,'k^',w,ha4D,'k*',w,ha5D,'k–',w,ha6D,'ko');
legend('Filter No. B3','Filter No. B4','Filter No. B5','Filter No. B6','Filter No. B7','Filter No. B8',3);
title('Lower order 1-D lowpass filters obtained from fifth order 1-D Butterworth lowpass filter');
xlabel('Frequency w in rad/sec');
ylabel('Magnitude response');
grid on;
```

filter).

Table: 2.8 shows, *(i)* the filter number, *F.No, (ii) Order* of the extracted lower order analog 1-D lowpass filters, *(iii)* the cutoff frequency at magnitude response of $\frac{1}{\sqrt{2}}$, i.e., -3db value and, *(iv) Slope at -3db* magnitude value of the frequency response.

The amplitude-frequency response of the extracted analog 1-D lowpass filters, B3, B4, B5, B6, B7 and B8 (refer table: 2.7) is shown in fig. 2.15. Filters B3, B4 and B7 are having monotonic amplitude-frequency response. B3 is having only one real pole, hence, have less steeper transition band. B7 transfer function is of higher order (than B3 and B4)

and therefore, is having steeper transition band. Since B4 is having two complex conjugate poles further away from the origin, it also bears monotonic response.

Filters B5, B6, and B8 are having ripples in the pass band, hence, does not inhibit the monotonic behavior. This is primarily because the poles are closer to the origin with magnitude of real part less than imaginary part. Since B5 is having only two complex conjugate poles much closer to the origin, the ripple of amplitude-frequency response in the passband is having maximum deviation. Filter B8 transfer function is having poles of B4 and B5, with two complex conjugate poles of B4 further away from origin as compared to poles of B5. Therefore, the combination filter (B8) is having reduced ripples, in comparison to B5, and steeper transition band. Similarly, B6 transfer function is having poles of B3 and B5, with real pole of B3 further away from origin, as compared to complex conjugate poles of B5. Hence, the combination filter (B6) is having reduced ripples, in comparison to B5, and steeper transition band. The MATLAB code to plot the amplitude-frequency response of the filters in table: 2.7 is in algorithm 9.

2.7.3 Extracting lower order 1-D lowpass filters from the fifth order 1-D Filanovsky lowpass filter and study their characteristics

In Sec. 2.4.3, we generated and studied stable fifth order 1-D Filanovsky lowpass filters. The poles of the filter are real as well as in complex conjugate pairs. By observing the nature of the poles, we can realize it in the form of cascaded first, second, third and fourth order 1-D lowpass filters, with the transfer functions having denominator polynomials of the corresponding order.

Table: 2.9 shows the extracted analog 1-D lowpass filters with, *(i)* the transfer function (eqn. 2.2), $F(s)$, *(ii)* amplitude-frequency response (eqn. 2.3), $A(w)$, *(iii) Poles* corresponding to each filter and, *(iv)* the filter number, *F.No* (where, Fi, with i as integer varying from 1 to 6, corresponds to analog 1-D lowpass filter obtained from Filanovsky lowpass filter).

F.No.	*Poles*	$F(s)$	$A(w)$
F1	-0.6445	$\frac{0.6445}{s+0.6445}$	$\frac{0.6445}{\sqrt{(0.6445)^2+w^2}}$
F2	$-0.4754 \pm j0.5344$	$\frac{0.5116}{s^2+0.9508s+0.5116}$	$\frac{0.5116}{\sqrt{(0.5116-w^2)^2+(0.9508w)^2}}$
F3	$-0.1746 \pm j0.9637$	$\frac{0.9592}{s^2+0.3492s+0.9592}$	$\frac{0.9592}{\sqrt{(0.9592-w^2)^2+(0.3492w)^2}}$
F4	-0.6445, $-0.1746 \pm j0.9637$	$\frac{0.6182}{s^3+0.9937s^2+1.1843s+0.6182}$	$\frac{0.6182}{\sqrt{(0.6182-0.9937w^2)^2+(1.1843w-w^3)^2}}$
F5	-0.6445, $-0.4754 \pm j0.5344$	$\frac{0.3297}{s^3+1.5953s^2+1.1244s+0.3297}$	$\frac{0.3297}{\sqrt{(0.3297-1.5953w^2)^2+(1.1244w-w^3)^2}}$
F6	$-0.1746 \pm j0.9637$, $-0.4754 \pm j0.5344$	$\frac{0.4907}{s^4+1.3s^3+1.8028s^2+1.0907s+0.4907}$	$\frac{0.4907}{\sqrt{(w^4-1.8028w^2+0.4907)^2+(1.0907w-1.3w^3)^2}}$

Table 2.9: First to fourth order 1-D lowpass filters obtained from fifth order 1-D Filanovsky lowpass filter

F.No.	*Order*	*-3db freq.*	*slope at -3db*
F1	1	0.6445	-0.5486
F2	2	0.7581	-1.0547
F3	2	1.4874	-1.5021
F4	3	1.2017	-2.7118
F5	3	0.5354	-1.0942
F6	4	1.1377	-3.4733

Table 2.10: Slope and frequency at -3db magnitude of first to fourth order 1-D lowpass filters obtained from fifth order 1-D Filanovsky lowpass filter

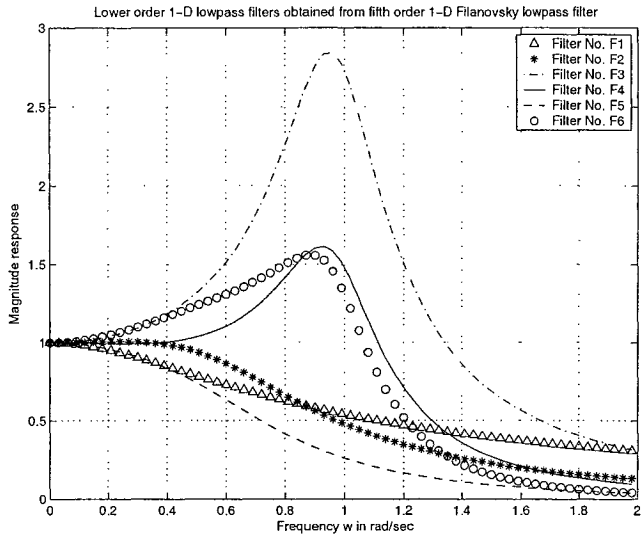

Figure 2.16: Plot of lower order 1-D lowpass filters obtained from the fifth order 1-D Filanovsky lowpass filter (Refer Table: 2.9)

Table: 2.10 shows, *(i)* the filter number, *F.No, (ii) Order* of the extracted lower order analog 1-D lowpass filters, *(iii)* the cutoff frequency at magnitude response of $\frac{1}{\sqrt{2}}$, i.e., -3db value and, *(iv) Slope at -3db* magnitude value of the frequency response.

The amplitude-frequency response of the extracted analog 1-D lowpass filters, F1, F2, F3, F4, F5 and F6 (refer table: 2.9) is shown in fig. 2.16. Filter F1 and F5 are having monotonic amplitude-frequency response. F1 is having only one real pole, hence, have less steeper transition band. F5 transfer function is of higher order (than F1) and therefore, is having steeper transition band.

Filters F2, F3, F4 and F6 are having ripples in the pass band, hence, does not inhibit the monotonic behavior. This is primarily because the poles are closer to the origin with magnitude of real part less than imaginary part. F2 is having only two complex conjugate poles not too closer to the origin, but not far enough to give it monotonic frequency response. There is a small ripple in amplitude-frequency response in the passband. Since F3 is having only two complex conjugate poles much closer to the origin, the ripple in the amplitude-frequency response in the passband is having maximum deviation. Filter F4 transfer function is having poles of F1 and F3, with real pole of F1 further away from ori-

Algorithm 10 MATLAB Code to plot lower order 1-D lowpass filters obtained from fifth order 1-D Filanovsky filter (Refer Table: 2.9)

```
% Under Guidance of Prof. Dr. V. Ramachandran
% Student's name : Ajit Singh Sandhu..... ID:4841492.
clear all; clc;
%Defining the step size of the frequency axis.
step=0.03;
%Defining the frequency range
w=[0:step:2];
s=j.*w;
%Transfer function for Filter No. F1
ha1D=(s+0.6445);
ha1D=abs(0.6445./ha1D);
%Transfer function for Filter No. F2
ha2D=(s+0.4754+0.5344i).*(s+0.4754-0.5344i);
ha2D=abs(0.5116./ha2D);
%Transfer function for Filter No. F3
ha3D=(s+0.1746+0.9637i).*(s+0.1746-0.9637i);
ha3D=abs(0.9592./ha3D);
%Transfer function for Filter No. F4
ha4D=(s+0.6445).*(s+0.1746+0.9637i).*(s+0.1746-0.9637i);
ha4D=abs(0.6182./ha4D);
%Transfer function for Filter No. F5
ha5D=(s+0.6445).*(s+0.4754+0.5344i).*(s+0.4754-0.5344i);
ha5D=abs(0.3297./ha5D);
%Transfer function for Filter No. F6
ha6D=(s+0.1746+0.9637i).*(s+0.1746-0.9637i).*(s+0.4754+0.5344i).*(s+0.4754-0.5344i);
ha6D=abs(0.4907./ha6D);
%Plotting all the 1-D lowpass filters on the same figure
figure(1);
plot(w,ha1D,'k^',w,ha2D,'k*',w,ha3D,'k-.',w,ha4D,'k-',w,ha5D,'k–',w,ha6D,'ko');
legend('Filter No. F1','Filter No. F2','Filter No. F3','Filter No. F4','Filter No. F5','Filter No. F6',1);
title('Lower order 1-D lowpass filters obtained from fifth order 1-D Filanovsky lowpass filter');
xlabel('Frequency w in rad/sec');
ylabel('Magnitude response');
grid on;
```

F.No.	*Poles*	$F(s)$	$A(w)$
TB1	$-2.8962 \pm j0.8672$	$\frac{9.14}{s^2+5.7924s+9.14}$	$\frac{9.14}{\sqrt{\left(9.14-w^2\right)^2+(5.7924w)^2}}$
TB2	$-2.1038 \pm j2.6574$	$\frac{11.4878}{s^2+4.2076s+11.4878}$	$\frac{11.4878}{\sqrt{\left(11.4878-w^2\right)^2+(4.2076w)^2}}$

Table 2.11: Second order 1-D lowpass filters obtained from the fourth order 1-D Thomson-Bessel lowpass filter

gin as compared to complex conjugate poles of F3. Therefore, the combination filter (F4) is having reduced ripples, in comparison to F3, and steeper transition band. Similarly, F6 transfer function is having poles of F2 and F3, with complex conjugate poles of F2 away from origin, as compared to complex conjugate poles of F3. Hence, the combination filter (F6) is having reduced ripples, in comparison to F3, and steeper transition band. The MATLAB code to plot the amplitude-frequency response of the filters in table: 2.9 is in algorithm 10.

2.7.4 Extracting lower order 1-D lowpass filters from 1-D Thomson-Bessel lowpass filters and study their characteristics

In Sec. 2.5, we generated and studied stable fourth and fifth order analog 1-D Thomson-Bessel lowpass filters, in which all poles are on the left side of the s-plane. By observing the nature of the poles, we can realize it in the form of cascaded lower order 1-D lowpass filters (which are having transfer functions obtained from the implemented analog 1-D Thomson-Bessel lowpass filters).

2.7.4.1 Extracting lower order lowpass filters from fourth order 1-D Thomson-Bessel lowpass filter

In Sec. 2.5.1, we generated and studied stable fourth order 1-D Thomson-Bessel lowpass filters. The poles of the filter are in complex conjugate pairs. By observing the nature of

F.No.	*Order*	*-3db freq.*	*slope at -3db*
TB1	2	2.07	-0.2082
TB2	2	3.81	-0.2385

Table 2.12: Slope and frequency at -3db magnitude of second order 1-D lowpass filters obtained from the fourth order 1-D Thomson-Bessel lowpass filter

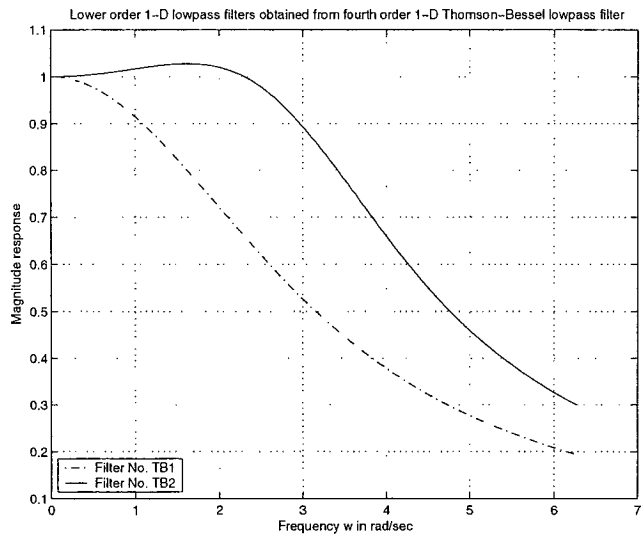

Figure 2.17: Plot of two lower order 1-D lowpass filters obtained from the fourth order 1-D Thomson-Bessel lowpass filter (Refer Table: 2.11)

the poles, we can realize it in the form of two cascaded second order 1-D lowpass filters, with the transfer functions having denominator polynomials of second order each.

Table: 2.11 shows the extracted second order analog 1-D lowpass filters with, *(i)* the transfer function (eqn. 2.2), $F(s)$, *(ii)* amplitude-frequency response (eqn. 2.3), $A(w)$, *(iii) Poles* corresponding to each filter and, *(iv)* the filter number, *F.No* (where, TBi, with i as integer varying from 1 to 2, corresponds to analog 1-D lowpass filter obtained from Thomson-Bessel lowpass filter).

Table: 2.12 shows, *(i)* the filter number, *F.No, (ii) Order* of the extracted lower order analog 1-D lowpass filters, *(iii)* the cutoff frequency at magnitude response of $\frac{1}{\sqrt{2}}$, i.e., -3db value and, *(iv) Slope at -3db* magnitude value of the frequency response.

The amplitude-frequency response of the extracted analog 1-D lowpass filters, TB1 and TB2 (refer table: 2.11) is shown in fig. 2.17. Filter TB1 is having monotonic amplitude-frequency response and TB2 does not inhibit the monotonic behavior. Though the poles in both TB1 and TB2 are far away from the origin but in TB2 the real part is less in magnitude than imaginary part, hence resulting in small ripple in its response. The MATLAB code written to plot the magnitude response of the filters in table: 2.11 is in algorithm 11.

2.7.4.2 Extracting lower order 1-D lowpass filters from the fifth order 1-D Thomson-Bessel lowpass filter

In Sec. 2.5.2, we generated and studied stable fifth order 1-D Thomson-Bessel lowpass filters. The poles of the filter are real as well as in complex conjugate pairs. By observing the nature of the poles, we can realize it in the form of cascaded first, second, third and fourth order 1-D lowpass filters, with the transfer functions having denominator polynomials of the corresponding order.

Table: 2.13 shows the extracted analog 1-D lowpass filters with, *(i)* the transfer function (eqn. 2.2), $F(s)$, *(ii)* amplitude-frequency response (eqn. 2.3), $A(w)$, *(iii) Poles* corresponding to each filter and, *(iv)* the filter number, *F.No* (where, TBi, with i as integer

Algorithm 11 MATLAB Code to plot second order 1-D lowpass filters obtained from fourth order 1-D Thomson-Bessel filter (Refer Table: 2.11)

```
% Under Guidance of Prof. Dr. V. Ramachandran
% Student's name : Ajit Singh Sandhu..... ID:4841492.
clear all; clc;
%Defining the step size of the frequency axis.
step=0.03;
%Defining the frequency range
w=[0:step:2*pi];
s=j.*w;
%Transfer function for Filter No. TB1
ha1D=s.^2+5.7924.*s+9.14;
ha1D=abs(9.14./ha1D);
%Transfer function for Filter No. TB2
ha2D=s.^2+4.2076.*s+11.4878;
ha2D=abs(11.4878./ha2D);
%Plotting all the 1-D lowpass filters on the same figure
figure(1);
plot(w,ha1D,'k-.',w,ha2D,'k-');
legend('Filter No. TB1','Filter No. TB2',3);
title('Lower order 1-D lowpass filters obtained from fourth order 1-D Thomson-Bessel lowpass filter');
xlabel('Frequency w in rad/sec');
ylabel('Magnitude response');
grid on;
```

F.No.	*Poles*	$F(s)$	$A(w)$
TB3	-3.6467	$\frac{3.6467}{s+3.6467}$	$\frac{3.6467}{\sqrt{(3.6467)^2+w^2}}$
TB4	$-3.3520 \pm j1.7427$	$\frac{14.2729}{s^2+6.704s+14.2729}$	$\frac{14.2729}{\sqrt{(14.2729-w^2)^2+(6.704w)^2}}$
TB5	$-2.3247 \pm j3.5710$	$\frac{18.1563}{s^2+4.6494s+18.1563}$	$\frac{18.1563}{\sqrt{(18.1563-w^2)^2+(4.6494w)^2}}$
TB6	-3.6467, $-3.3520 \pm j1.7427$	$\frac{52.0490}{s^3+10.3507s^2+38.7204s+52.0490}$	$\frac{52.0490}{\sqrt{(52.0490-10.3507w^2)^2+(38.7204w-w^3)^2}}$
TB7	-3.6467, $-2.3247 \pm j3.5710$	$\frac{66.2106}{s^3+8.2961s^2+35.1113s+66.2106}$	$\frac{66.2106}{\sqrt{(66.2106-8.2961w^2)^2+(35.1113w-w^3)^2}}$
TB8	$-3.3520 \pm j1.7427$, $-2.3247 \pm j3.5710$	$\frac{259.1431}{s^4+11.3534s^3+63.5988s^2+188.0802s+259.1431}$	$\frac{259.1431}{\sqrt{(w^4-63.5988w^2+259.1431)^2+(188.0802w-11.3534w^3)^2}}$

Table 2.13: First to fourth order 1-D lowpass filters obtained from fifth order 1-D Thomson-Bessel lowpass filter

F.No.	*Order*	*-3db freq.*	*slope at -3db*
TB3	1	3.6468	−0.0969
TB4	2	2.8743	−0.1642
TB5	2	5.1899	−0.2180
TB6	3	2.158	−0.2150
TB7	3	3.7485	−0.2077
TB8	4	3.1879	−0.2195

Table 2.14: Slope and frequency at -3db magnitude of first to fourth order 1-D lowpass filters obtained from fifth order 1-D Thomson-Bessel lowpass filter

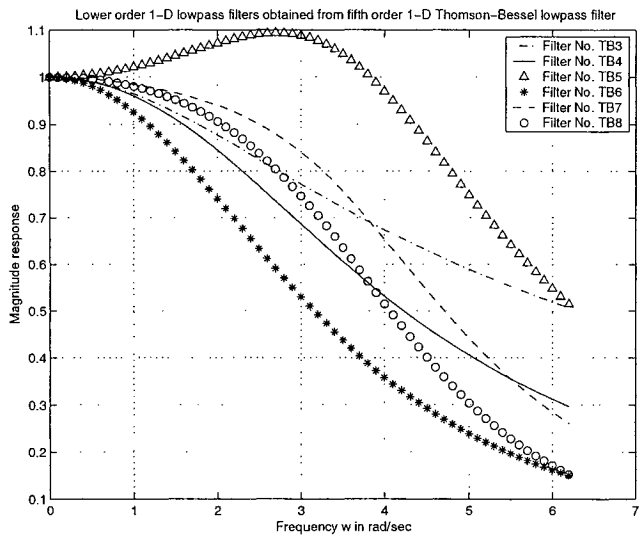

Figure 2.18: Plot of lower order 1-D lowpass filters obtained from the fifth order 1-D Thomson-Bessel lowpass filter (Refer Table: 2.13)

varying from 3 to 8, corresponds to analog 1-D lowpass filter obtained from Papoulis lowpass filter).

Table: 2.14 shows, *(i)* the filter number, *F.No, (ii) Order* of the extracted lower order analog 1-D lowpass filters, *(iii)* the cutoff frequency at magnitude response of $\frac{1}{\sqrt{2}}$, i.e., -3db value and, *(iv) Slope at -3db* magnitude value of the frequency response.

The amplitude-frequency response of the extracted analog 1-D lowpass filters, TB3, TB4, TB5, TB6, TB7 and TB8 (refer table: 2.13) is shown in fig. 2.18. Filters TB3, TB4, TB6, TB7 and TB8 are having monotonic amplitude-frequency response. TB5 is having two complex conjugate poles, with magnitude of real part less than imaginary part, hence, resulting in ripple in the passband. Though TB7 and TB8 also includes the TB5 poles, but the presence of other poles which are further away from origin with magnitude of real value greater than imaginary part (for each pole), results in monotonic filters. The MATLAB code to plot the amplitude-frequency response of the filters in table: 2.13 is in algorithm 12.

2.8 Cascading lower order 1-D lowpass filters to realize higher order 1-D lowpass filter with monotonic characteristics

In Sec. 2.7, we segregated lower order 1-D filters, derived from the Butterworth, Filanovsky and Papoulis filters, having monotonic amplitude-frequency response. We know that higher order filters can be obtained by cascading lower order filters in the frequency domain. Hence, we will utilize the derived filters with monotonic behavior, and cascade them to realize few higher order analog 1-D lowpass filters. We will study the amplitude-frequency response of few combinations of cascaded analog 1-D filters with different orders, and verify that they still inhibit the monotonic characteristic.

Algorithm 12 MATLAB Code to plot lower order 1-D lowpass filters obtained from fifth order 1-D Thomson-Bessel filter (Refer Table: 2.13)

```
% Under Guidance of Prof. Dr. V. Ramachandran
% Student's name : Ajit Singh Sandhu..... ID:4841492.
clear all; clc;
%Defining the step size of the frequency axis.
step=0.1;
%Defining the frequency range
w=[0:step:2*pi];
s=j.*w;
%Transfer function for Filter No. TB3
ha1D=(s+3.6467);
ha1D=abs(3.6467./ha1D);
%Transfer function for Filter No. TB4
ha2D=(s.^2+6.704.*s+14.2729);
ha2D=abs(14.2729./ha2D);
%Transfer function for Filter No. TB5
ha3D=(s+2.3247+3.5710i).*(s+2.3247-3.5710i);
%ha3D=((s.^2)+(4.6494.*s)+18.1563);
ha3D=abs(18.1563./ha3D);
%Transfer function for Filter No. TB6
ha4D=(s+3.6467).*(s.^2+6.704.*s+14.2729);
ha4D=abs(52.0490./ha4D);
%Transfer function for Filter No. TB7
ha5D=(s+3.6467).*(s.^2+4.6494.*s+18.1563);
ha5D=abs(66.2106./ha5D);
%Transfer function for Filter No. TB8
ha6D=(s.^2+6.704.*s+14.2729).*(s.^2+4.6494.*s+18.1563);
ha6D=abs(259.1431./ha6D);
%Plotting all the 1-D lowpass filters on the same figure
figure(1);
plot(w,ha1D,'k-.',w,ha2D,'k-',w,ha3D,'k^',w,ha4D,'k*',w,ha5D,'k–',w,ha6D,'ko');
legend('Filter No. TB3','Filter No. TB4','Filter No. TB5','Filter No. TB6','Filter No. TB7','Filter No. TB8',1);
title('Lower order 1-D lowpass filters obtained from fifth order 1-D Thomson-Bessel lowpass filter');
xlabel('Frequency w in rad/sec');
ylabel('Magnitude response');
grid on;
```

F.No.	*Order*	*F. Combination*	*Transfer Func. $F(s)$*
C1	4	P2.P2	$\frac{0.1856}{s^4+2.1988s^3+2.0703s^2+0.9472s+0.1856}$
C2	4	P3.P6	$\frac{0.1089}{s^4+1.7124s^3+1.4429s^2+0.6355s+0.1089}$
C3	6	P2.P2.P2	$\frac{0.08}{s^6+3.2982s^5+4.9184s^4+4.1706s^3+2.1189s^2+0.6121s+0.08}$
C4	6	P2.P3.P6	$\frac{0.0469}{s^6+2.8118s^5+3.7563s^4+2.9594s^3+1.4291s^2+0.3935s+0.0469}$
C5	8	P2.P2.P3.P6	$\frac{0.0202}{s^8+3.9112s^7+7.2784s^6+8.3004s^5+6.3009s^4+3.2396s^3+1.0952s^2+0.2211s+0.0202}$
C6	8	P2.P2.P2.P2	$\frac{0.0344}{s^8+4.3976s^7+8.9753s^6+10.9988s^5+8.8228s^4+4.7383s^3+1.6657s^2+0.3516s+0.0344}$

Table 2.15: Cascading 1-D lowpass filters obtained from 1-D Papoulis lowpass filter

2.8.1 Cascading 1-D lowpass filters, derived from Papoulis filters and study their characteristics

We will utilize the segregated analog 1-D lowpass filters, P2, P3 and P6, obtained from the fourth and fifth order Papoulis lowpass filters (Sec. 2.7.1), having monotonic amplitude-frequency response, to get few cascaded analog 1-D lowpass filters of different order. Table: 2.15 shows, few cascaded analog 1-D lowpass filters with, *(i)* the transfer function (eqn. 2.2), $F(s)$, *(ii)* filter combination (*F. Combination*), *(iii)* order of the filter (*order*) and, *(iv)* the filter number, *F.No* (where, Ci, with i as integer varying from 1 to 6, corresponds to cascaded analog 1-D lowpass filter).

Table: 2.16 shows, *(i)* the filter number, *F.*, *(ii)* amplitude-frequency response (eqn. 2.3), $A(w)$, *(iii)* the cutoff frequency at magnitude response of $\frac{1}{\sqrt{2}}$, i.e., -3db value and, *(iv) Slope at -3db* magnitude value of the frequency response.

The amplitude-frequency response of the cascaded analog 1-D lowpass filters, C1, C2, C3, C4, C5 and C6 (refer table: 2.15) is shown in fig. 2.19. All the filters are having monotonic amplitude-frequency response. The sharpness of the transition band increases as the order of the filter increases. The MATLAB code to plot the amplitude-frequency

F.	$A(w)$	*-3db freq.*	*slope at -3db*
C1	$\frac{0.1856}{\sqrt{(w^4-2.0703w^2+0.1856)^2+(0.9472w-2.1988w^3)^2}}$	0.392	-1.3815
C2	$\frac{0.1089}{\sqrt{(w^4-1.4429w^2+0.1089)^2+(0.6355w-1.7124w^3)^2}}$	0.3355	-1.2470
C3	$\frac{0.08}{\sqrt{\begin{matrix}(-w^6+4.9184w^4-2.1189w^2+0.08)^2\\+(3.2982w^5-4.1706w^3+0.6121w)^2\end{matrix}}}$	0.3265	-1.6587
C4	$\frac{0.0469}{\sqrt{\begin{matrix}(-w^6+3.7563w^4-1.4291w^2+0.0469)^2\\+(2.8118w^5-2.9594w^3+0.3935w)^2\end{matrix}}}$	0.2845	-1.5970
C5	$\frac{0.0202}{\sqrt{\begin{matrix}(w^8-7.2784w^6+6.3009w^4-1.0952w^2+0.0202)^2\\+(-3.9112w^7+8.3004w^5-3.2396w^3+0.2211w)^2\end{matrix}}}$	0.2536	-1.8598
C6	$\frac{0.0344}{\sqrt{\begin{matrix}(w^8-8.9753w^6+8.8228w^4-1.6657w^2+0.0344)^2\\+(-4.3976w^7+10.9988w^5-4.7383w^3+0.3516w)^2\end{matrix}}}$	0.2858	-1.8652

Table 2.16: Slope and frequency at -3db magnitude of cascaded 1-D lowpass filters obtained from 1-D Papoulis lowpass filter

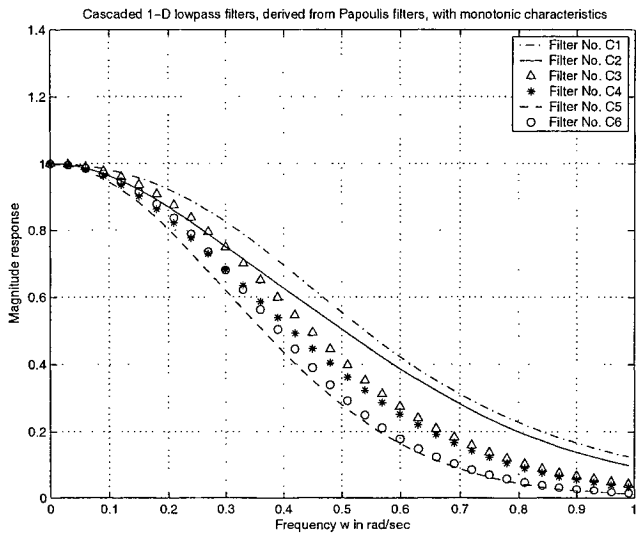

Figure 2.19: Plot of cascaded 1-D lowpass filters obtained from 1-D Papoulis lowpass filter. (Refer Table: 2.15)

Algorithm 13 MATLAB Code to plot few possible cascaded 1-D lowpass filters, derived from 1-D Papoulis filter, having monotonic characteristics. (Refer Table: 2.15)

```
% Under Guidance of Prof. Dr. V. Ramachandran
% Student's name : Ajit Singh Sandhu..... ID:4841492.
clear all; clc;
%Defining the step size of the frequency axis.
step=0.03;
%Defining the frequency range
w=[0:step:1];
s=j.*w;
%Transfer function for Filter No. C1=P2.P2
ha1D=(s+0.5497+0.3586i).*(s+0.5497-0.3586i).*(s+0.5497+0.3586i).*(s+0.5497-0.3586i);
ha1D=abs(0.1856./ha1D);
%Transfer function for Filter No. C2=P3.P6
ha2D=(s+0.4681).*(s+0.4681).*(s+0.3881+0.5886i).*(s+0.3881-0.5886i);
ha2D=abs(0.1089./ha2D);
%Transfer function for Filter No. C3=P2.P2.P2
ha3D=(s+0.5497+0.3586i).*(s+0.5497-0.3586i).*(s+0.5497+0.3586i).*(s+0.5497-
0.3586i).*(s+0.5497+0.3586i).*(s+0.5497-0.3586i);
ha3D=abs(0.08./ha3D);
%Transfer function for Filter No. C4=P2.P3.P6
ha4D=(s+0.5497+0.3586i).*(s+0.5497-0.3586i).*(s+0.4681).*(s+0.4681).*(s+0.3881+0.5886i).*(s+0.3881-
0.5886i);
ha4D=abs(0.0469./ha4D);
%Transfer function for Filter No. C5=P2.P2.P3.P6
ha5D=(s+0.5497+0.3586i).*(s+0.5497-0.3586i).*(s+0.5497+0.3586i).*(s+0.5497-0.3586i)
.*(s+0.4681).*(s+0.4681).*(s+0.3881+0.5886i).*(s+0.3881-0.5886i);
ha5D=abs(0.0202./ha5D);
%Transfer function for Filter No. C3=P2.P2.P2.P2
ha6D=(s+0.5497+0.3586i).*(s+0.5497-0.3586i).*(s+0.5497+0.3586i).*(s+0.5497-0.3586i)
.*(s+0.5497+0.3586i).*(s+0.5497-0.3586i).*(s+0.5497+0.3586i).*(s+0.5497-0.3586i);
ha6D=abs(0.0344./ha6D);
%Plotting all the cascaded 1-D lowpass filters on the same figure
figure(1);
plot(w,ha1D,'k-.',w,ha2D,'k-',w,ha3D,'k^',w,ha4D,'k*',w,ha5D,'k--',w,ha6D,'ko');
legend('Filter No. C1','Filter No. C2','Filter No. C3','Filter No. C4','Filter No. C5','Filter No. C6',1);
title('Cascaded 1-D lowpass filters, derived from Papoulis filters, with monotonic characteristics');
xlabel('Frequency w in rad/sec');
ylabel('Magnitude response');
grid on;
```

F.No.	*Order*	*F. Combination*	*Transfer Func.* $F(s)$
C7	4	B1.B4	$\frac{1}{s^4+3.4658s^3+4.9897s^2+3.4658s+1}$
C8	4	B3.B7	$\frac{1}{s^4+3.618s^3+5.2360s^2+3.618s+1}$
C9	6	B3.B4.B7	$\frac{1}{s^6+5.2365s^5+12.0899s^4+15.7078s^3+12.0899s^2+5.236s+1}$
C10	6	B1.B3.B7	$\frac{1}{s^6+5.4658s^5+12.9213s^4+16.9111s^3+12.9213s^2+5.4658s+1}$
C11	8	B1.B3.B4.B7	$\frac{1}{s^8+7.0838s^7+22.765s^6+43.2836s^5+53.2048s^4+43.2836s^3+22.765s^2+7.0838s+1}$
C12	8	B1.B1.B4.B4	$\frac{1}{s^8+6.9316s^7+21.9913s^6+41.5185s^5+50.9210s^4+41.5185s^3+21.9913s^2+6.9316s+1}$

Table 2.17: Cascading 1-D lowpass filters obtained from 1-D Butterworth lowpass filter

response of the filters in table: 2.15 is in algorithm 13.

2.8.2 Cascading 1-D lowpass filters, derived from Butterworth filters and study their characteristics

We will utilize the segregated analog 1-D lowpass filters, B1, B3, B4 and B7, obtained from the fourth and fifth order Butterworth lowpass filters (Sec. 2.7.2), having monotonic amplitude-frequency response, to get few cascaded analog 1-D lowpass filters of different order. Table: 2.17 shows, few cascaded analog 1-D lowpass filters with, *(i)* the transfer function (eqn. 2.2), $F(s)$, *(ii)* filter combination (*F. Combination*), *(iii)* order of the filter (*order*) and, *(iv)* the filter number, *F.No* (where, Ci, with i as integer varying from 7 to 12, corresponds to cascaded analog 1-D lowpass filter).

Table: 2.18 shows, *(i)* the filter number, *F.*, *(ii)* amplitude-frequency response (eqn. 2.3), $A(w)$, *(iii)* the cutoff frequency at magnitude response of $\frac{1}{\sqrt{2}}$, i.e., -3db value and, *(iv) Slope at -3db* magnitude value of the frequency response.

The amplitude-frequency response of the cascaded analog 1-D lowpass filters, C7, C8, C9, C10, C11 and C12 (refer table: 2.17) is shown in fig. 2.20. All the filters are having

F.	$A(w)$	*-3db freq.*	*slope at -3db*
C7	$\frac{1}{\sqrt{(w^4-4.9897w^2+1)^2+(3.4658w-3.4658w^3)^2}}$	0.5616	-0.9083
C8	$\frac{1}{\sqrt{(w^4-5.236w^2+1)^2+(3.618w-3.618w^3)^2}}$	0.5197	-0.9219
C9	$\frac{1}{\sqrt{\begin{array}{c}(-w^6+12.0899w^4-12.0899w^2+1)^2\\+(5.236w^5-15.7078w^3+5.236w)^2\end{array}}}$	0.4555	-1.1015
C10	$\frac{1}{\sqrt{\begin{array}{c}(-w^6+12.9213w^4-12.9213w^2+1)^2\\+(5.4658w^5-16.9111w^3+5.4658w)^2\end{array}}}$	0.4169	-1.1595
C11	$\frac{1}{\sqrt{\begin{array}{c}(w^8-22.765w^6+53.2048w^4-22.765w^2+1)^2\\+(-7.0838w^7+43.2836w^5-43.2836w^3+7.0838w)^2\end{array}}}$	0.3832	-1.293
C12	$\frac{1}{\sqrt{\begin{array}{c}(w^8-21.9913w^6+50.921w^4-21.9913w^2+1)^2\\+(-6.9316w^7+41.5185w^5-41.5185w^3+6.9316w)^2\end{array}}}$	0.4026	-1.2645

Table 2.18: Slope and frequency at -3db magnitude of cascaded 1-D lowpass filters obtained from 1-D Butterworth lowpass filter

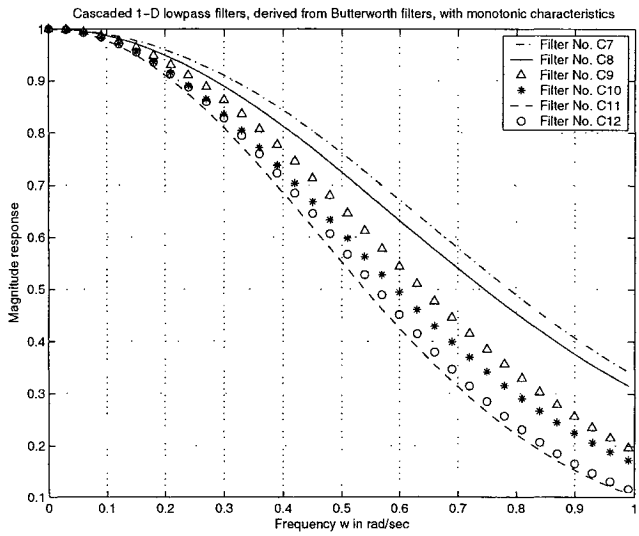

Figure 2.20: Plot of cascaded 1-D lowpass filters obtained from 1-D Butterworth lowpass filter. (Refer Table: 2.17)

Algorithm 14 MATLAB Code to plot few possible cascaded 1-D lowpass filters, derived from 1-D Butterworth filter, having monotonic characteristics. (Refer Table: 2.17)

```
% Under Guidance of Prof. Dr. V. Ramachandran
% Student's name : Ajit Singh Sandhu..... ID:4841492.
clear all; clc;
%Defining the step size of the frequency axis.
step=0.03;
%Defining the frequency range
w=[0:step:1]; s=j.*w;
%Transfer function for Filter No. C7= B1.B4
ha1D=(s+0.9239+0.3827i).*(s+0.9239-0.3827i).*(s+0.8090+0.5878i).*(s+0.8090-0.5878i);
ha1D=abs(1./ha1D);
%normalizing with the maximum value.
ha1D=ha1D/max(max(ha1D));
%Transfer function for Filter No. C8=B3.B7
ha2D=(s+1).*(s+1).*(s+0.8090+0.5878i).*(s+0.8090-0.5878i);
ha2D=abs(1./ha2D);
%normalizing with the maximum value.
ha2D=ha2D/max(max(ha2D));
%Transfer function for Filter No. C9=B3.B4.B7
ha3D=(s+1).*(s+0.8090+0.5878i).*(s+0.8090-0.5878i).*(s+1).*(s+0.8090+0.5878i).*(s+0.8090-0.5878i);
ha3D=abs(1./ha3D);
%normalizing with the maximum value.
ha3D=ha3D/max(max(ha3D));
%Transfer function for Filter No. C10=B1.B3.B7
ha4D=(s+0.9239+0.3827i).*(s+0.9239-0.3827i).*(s+1).*(s+1).*(s+0.8090+0.5878i).*(s+0.8090-0.5878i);
ha4D=abs(1./ha4D);
%normalizing with the maximum value.
ha4D=ha4D/max(max(ha4D));
%Transfer function for Filter No. C11= B1.B3.B4.B7
ha5D=(s+0.9239+0.3827i).*(s+0.9239-0.3827i).*(s+1).*(s+0.8090+0.5878i).*(s+0.8090-
0.5878i).*(s+1).*(s+0.8090+0.5878i).*(s+0.8090-0.5878i);
ha5D=abs(1./ha5D);
%normalizing with the maximum value.
ha5D=ha5D/max(max(ha5D));
%Transfer function for Filter No. C12=B1.B1.B4.B4
ha6D=(s+0.9239+0.3827i).*(s+0.9239-0.3827i).*(s+0.9239+0.3827i).*(s+0.9239-
0.3827i).*(s+0.8090+0.5878i).*(s+0.8090-0.5878i).*(s+0.8090+0.5878i).*(s+0.8090-0.5878i);
ha6D=abs(1./ha6D);
%normalizing with the maximum value.
ha6D=ha6D/max(max(ha6D));
%Plotting all the cascaded 1-D lowpass filters on the same figure
figure(1);
plot(w,ha1D,'k-.',w,ha2D,'k-',w,ha3D,'k^',w,ha4D,'k*',w,ha5D,'k–',w,ha6D,'ko');
legend('Filter No. C7','Filter No. C8','Filter No. C9','Filter No. C10','Filter No. C11','Filter No.
C12','Location','NorthEast');
title('Cascaded 1-D lowpass filters, derived from Butterworth filters, with monotonic characteristics');
xlabel('Frequency w in rad/sec');
ylabel('Normalized Magnitude frequency response');
grid on;
```

F.No.	*Order*	*F. Combination*	*Transfer Func.* $F(s)$
C13	4	F1.F5	$\frac{0.2125}{s^4+2.2398s^3+2.1526s^2+1.0544s+0.2125}$
C14	6	F5.F5	$\frac{0.1087}{s^6+3.1906s^5+4.7938s^4+4.2469s^3 +2.3162s^2+0.7414s+0.1087}$
C15	6	F1.F1.F1.F5	$\frac{0.0883}{s^6+3.5288s^5+5.4551s^4+4.7594s^3 +2.4657s^2+0.7119s+0.0883}$
C16	8	F1.F1.F5.F5	$\frac{0.0452}{s^8+4.4796s^7+9.3218s^6+11.7514s^5+9.7817s^4 +5.4911s^3+2.0265s^2+0.4481s+0.0452}$

Table 2.19: Cascading 1-D lowpass filters obtained from 1-D Filanovsky lowpass filter

monotonic amplitude-frequency response. The sharpness of the transition band increases as the order of the filter increases. The MATLAB code to plot the amplitude-frequency response of the filters in table: 2.17 is in algorithm 14.

2.8.3 Cascading 1-D lowpass filters, derived from Filanovsky filters and study their characteristics

We will utilize the segregated analog 1-D lowpass filters, F1 and F5, obtained from the fifth order Filanovsky lowpass filter (Sec. 2.7.3), having monotonic amplitude-frequency response, to get few cascaded analog 1-D lowpass filters of different order. Table: 2.19 shows, few cascaded analog 1-D lowpass filters with, *(i)* the transfer function (eqn. 2.2), $F(s)$, *(ii)* filter combination (*F. Combination*), *(iii)* order of the filter (*order*) and, *(iv)* the filter number, *F.No* (where, Ci, with i as integer varying from 13 to 16, corresponds to cascaded analog 1-D lowpass filter).

Table: 2.20 shows, *(i)* the filter number, *F.*, *(ii)* amplitude-frequency response (eqn. 2.3), $A(w)$, *(iii)* the cutoff frequency at magnitude response of $\frac{1}{\sqrt{2}}$, i.e., -3db value and, *(iv) Slope at -3db* magnitude value of the frequency response.

The amplitude-frequency response of the cascaded analog 1-D lowpass filters, C13, C14, C15, and C16 (refer table: 2.19) is shown in fig. 2.21. All the filters are having monotonic amplitude-frequency response. The sharpness of the transition band increases

F.	$A(w)$	*-3db freq.*	*slope at -3db*
C13	$\frac{0.2125}{\sqrt{(w^4-2.1526w^2+0.2125)^2+(1.0544w-2.2398w^3)^2}}$	0.4050	-1.1582
C14	$\frac{0.1087}{\sqrt{\left(-w^6+4.7938w^4-2.3162w^2+0.1087\right)^2+\left(3.1906w^5-4.2469w^3+0.7414w\right)^2}}$	0.398	-1.3965
C15	$\frac{0.0883}{\sqrt{\left(-w^6+5.4551w^4-2.4657w^2+0.0883\right)^2+\left(3.5288w^5-4.7594w^3+0.7119w\right)^2}}$	0.2832	-1.6472
C16	$\frac{0.0452}{\sqrt{\left(w^8-9.3218w^6+9.7817w^4-2.0265w^2+0.0452\right)^2+\left(-4.4796w^7+11.7514w^5-5.4911w^3+0.4481w\right)^2}}$	0.2859	-1.7699

Table 2.20: Slope and frequency at -3db magnitude of cascaded 1-D lowpass filters obtained from 1-D Filanovsky lowpass filter

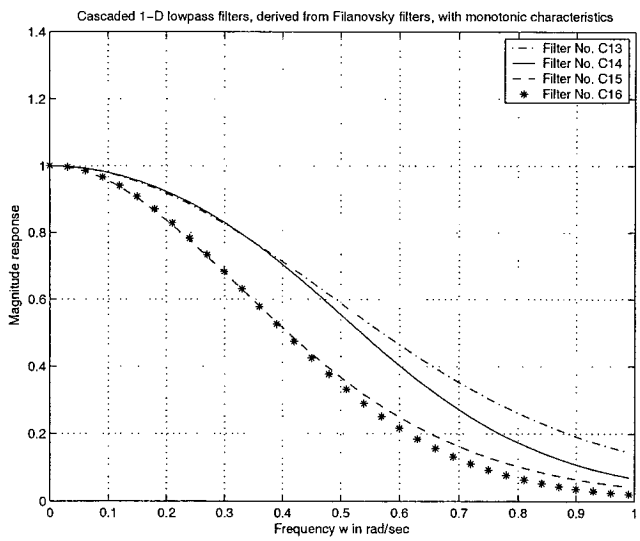

Figure 2.21: Plot of cascaded 1-D lowpass filters obtained from 1-D Filanovsky lowpass filter. (Refer Table: 2.19)

Algorithm 15 MATLAB Code to plot few possible cascaded 1-D lowpass filters, derived from 1-D Filanovsky filter, having monotonic characteristics. (Refer Table: 2.19)

```
% Under Guidance of Prof. Dr. V. Ramachandran
% Student's name : Ajit Singh Sandhu..... ID:4841492.
clear all; clc;
%Defining the step size of the frequency axis.
step=0.03;
%Defining the frequency range
w=[0:step:1];
s=j.*w;
%Transfer function for Filter No. C13=F1.F3
ha1D=(s+0.6445).*(s+0.6445).*(s+0.4754+0.5344i).*(s+0.4754-0.5344i);
ha1D=abs(0.2125./ha1D);
%Transfer function for Filter No. C14=F5.F5
ha2D=(s+0.6445).*(s+0.4754+0.5344i).*(s+0.4754-0.5344i).*(s+0.6445).*(s+0.4754+0.5344i).*(s+0.4754-
0.5344i);
ha2D=abs(0.1087./ha2D);
%Transfer function for Filter No. C15=F1.F1.F1.F5
ha3D=(s+0.6445).*(s+0.6445).*(s+0.6445).*(s+0.6445).*(s+0.4754+0.5344i).*(s+0.4754-0.5344i);
ha3D=abs(0.0883./ha3D);
%Transfer function for Filter No. C16=F1.F1.F5.F5
ha4D=(s+0.6445).*(s+0.6445).*(s+0.6445).*(s+0.4754+0.5344i).*(s+0.4754-
0.5344i).*(s+0.6445).*(s+0.4754+0.5344i).*(s+0.4754-0.5344i);
ha4D=abs(0.0452./ha4D);
%Plotting all the 1-D lowpass filters on the same figure
figure(1);
plot(w,ha1D,'k-.',w,ha2D,'k-',w,ha3D,'k--',w,ha4D,'k*');
legend('Filter No. C13','Filter No. C14','Filter No. C15','Filter No. C16',1);
title('Cascaded 1-D lowpass filters, derived from Filanovsky filters, with monotonic characteristics');
xlabel('Frequency w in rad/sec');
ylabel('Magnitude response');
grid on;
```

F.No.	*Order*	*F. Combination*	*Transfer Func. $F(s)$*
C17	4	TB1.TB1	$\frac{83.5396}{s^4+11.5848s^3+51.8319s^2+105.8851s+83.5396}$
C18	4	TB3.TB6	$\frac{189.8071}{s^4+13.9974s^3+76.4663s^2+193.2507s+189.8071}$
C19	6	TB1.TB1.TB1	$\frac{763.6}{s^6+17.4s^5+128.1s^4+512s^3+1170.6s^2+1451.7s+763.6}$
C20	6	TB6.TB7	$\frac{3446.2}{s^6+18.6s^5+159.7s^4+802.9s^3+2476.7s^2+4391.2s+3446.2}$
C21	8	TB3.TB4.TB4.TB7	$\frac{49187}{s^8+25s^7+299s^6+2140s^5+10139s^4+32455s^3+68234s^2+85779s+49187}$
C22	8	TB8.TB8	$\frac{67155}{s^8+23s^7+256s^6+1820s^5+8834s^4+29808s^3+68337s^2+97479s+67155}$

Table 2.21: Cascading 1-D lowpass filters obtained from 1-D Thomson-Bessel lowpass filter

as the order of the filter increases. The MATLAB code to plot the amplitude-frequency response of the filters in table: 2.19 is in algorithm 15.

2.8.4 Cascading 1-D lowpass filters, derived from Thomson-Bessel filters and study their characteristics

We will utilize the segregated analog 1-D lowpass filters, TB1, TB3, TB4, TB6, TB7 and TB8, obtained from the fourth and fifth order Thomson-Bessel lowpass filters (Sec. 2.7.4), having monotonic amplitude-frequency response, to get few cascaded analog 1-D lowpass filters of different order. Table: 2.21 shows, few cascaded analog 1-D lowpass filters with, *(i)* the transfer function (eqn. 2.2), $F(s)$, *(ii)* filter combination (*F. Combination*), *(iii)* order of the filter (*order*) and, *(iv)* the filter number, *F.No* (where, Ci, with i as integer varying from 17 to 22, corresponds to cascaded analog 1-D lowpass filter).

Table: 2.22 shows, *(i)* the filter number, *F.*, *(ii)* amplitude-frequency response (eqn. 2.3), $A(w)$, *(iii)* the cutoff frequency at magnitude response of $\frac{1}{\sqrt{2}}$, i.e., -3db value and, *(iv) Slope at -3db* magnitude value of the frequency response.

The amplitude-frequency response of the cascaded analog 1-D lowpass filters, C17,

F.	$A(w)$	*-3db freq.*	*slope at -3db*
C17	$\frac{83.5396}{\sqrt{(w^4-51.8319w^2+83.5396)^2+(105.8851w-11.5848w^3)^2}}$	1.4154	-0.3265
C18	$\frac{189.8071}{\sqrt{(w^4-76.4663w^2+189.8071)^2+(193.2507w-13.9974w^3)^2}}$	1.7801	-0.2606
C19	$\frac{763.6}{\sqrt{\begin{array}{c}(-w^6+128.1w^4-1170.6w^2+763.6)^2\\+(17.4w^5-512w^3+1451.7w)^2\end{array}}}$	1.1444	-0.4126
C20	$\frac{3446.2}{\sqrt{\begin{array}{c}(-w^6+159.7w^4-2476.7w^2+3446.2)^2\\+(18.6w^5-802.9w^3+4391.2w)^2\end{array}}}$	1.9565	-0.2461
C21	$\frac{49187}{\sqrt{\begin{array}{c}(w^8-299w^6+10139w^4-68234w^2+49187)^2\\+(-25w^7+2140w^5-32455w^3+85779w)^2\end{array}}}$	1.6149	-0.3021
C22	$\frac{67155}{\sqrt{\begin{array}{c}(w^8-256w^6+8834w^4-68337w^2+67155)^2\\+(-23w^7+1820w^5-29808w^3+97479w)^2\end{array}}}$	2.4827	-0.2676

Table 2.22: Slope and frequency at -3db magnitude of cascaded 1-D lowpass filters obtained from 1-D Thomson-Bessel lowpass filter

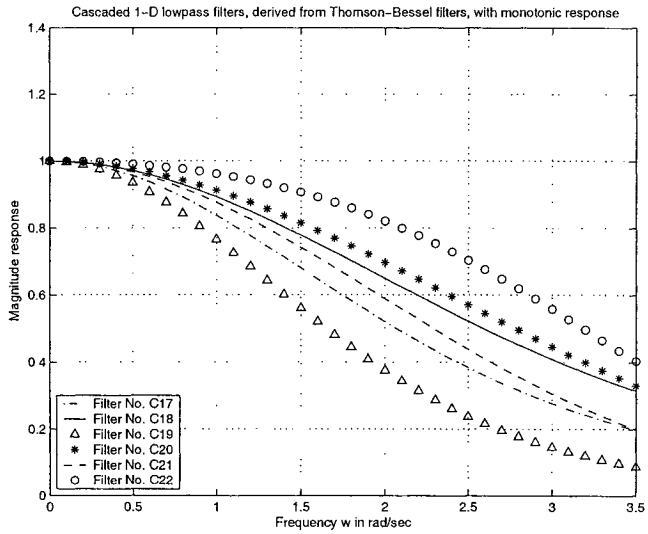

Figure 2.22: Plot of cascaded 1-D lowpass filters obtained from 1-D Thomson-Bessel lowpass filter. (Refer Table: 2.21)

Algorithm 16 MATLAB Code to plot few possible cascaded 1-D lowpass filters, derived from 1-D Thomson-Bessel filter, having monotonic characteristics. (Refer Table: 2.21)

```
% Under Guidance of Prof. Dr. V. Ramachandran
% Student's name : Ajit Singh Sandhu..... ID:4841492.
clear all; clc;
%Defining the step size of the frequency axis.
step=0.1;
%Defining the frequency range
w=[0:step:3.5];
s=j.*w;
%Transfer function for Filter No. C17=TB1.TB1
ha1D=(s.^2+5.7924.*s+9.14).*(s.^2+5.7924.*s+9.14);
ha1D=abs(83.5396./ha1D);
%Transfer function for Filter No. C18=TH3.TH6
ha2D=(s+3.6467).*(s+3.6467).*(s.^2+6.704.*s+14.2729);
ha2D=abs(189.8071./ha2D);
%Transfer function for Filter No. C19=TB1.TB1.TB1
ha3D=(s.^2+5.7924.*s+9.14).*(s.^2+5.7924.*s+9.14).*(s.^2+5.7924.*s+9.14);
ha3D=abs(763.5519./ha3D);
%Transfer function for Filter No. C20=TB6.TB7
ha4D=(s+3.6467).*(s.^2+6.704.*s+14.2729).*(s+3.6467).*(s.^2+4.6494.*s+18.1563);
ha4D=abs(3446.1955./ha4D);
%Transfer function for Filter No. C21=TB3.TB4.TB4.TB7
ha5D=(s+3.6467).*(s.^2+6.704.*s+14.2729).*(s.^2+6.704.*s+14.2729).*(s+3.6467).*(s.^2+4.6494.*s
+18.1563);
ha5D=abs(49187.1893./ha5D);
%Transfer function for Filter No. C22=TB8.TB8
ha6D=(s.^2+6.704.*s+14.2729).*(s.^2+4.6494.*s+18.1563).*(s.^2+6.704.*s+14.2729).*(s.^2
+4.6494.*s+18.1563);
ha6D=abs(67155.1463./ha6D);
%Plotting all the cascaded 1-D lowpass filters on the same figure
figure(1);
plot(w,ha1D,'k-.',w,ha2D,'k-',w,ha3D,'k^',w,ha4D,'k*',w,ha5D,'k–',w,ha6D,'ko');
legend('Filter No. C17','Filter No. C18','Filter No. C19','Filter No. C20','Filter No. C21','Filter No.
C22',3);
title('Cascaded 1-D lowpass filters, derived from Thomson-Bessel filters, with monotonic response');
xlabel('Frequency w in rad/sec');
ylabel('Magnitude response');
grid on;
```

F.No.	*Order*	*F. Combination*	*Transfer Func. $F(s)$*
C23	4	P3.P3.B3.F1	$\frac{0.1412}{s^4+2.5807s^3+2.4032s^2+0.9637s+0.1412}$
C24	4	P3.B1.F1	$\frac{0.3017}{s^4+2.9604s^3+3.3576s^2+1.6701s+0.3017}$
C25	4	B4.TB4	$\frac{14.2729}{s^4+8.322s^3+26.12s^2+29.7976s+14.2729}$
C26	6	P2.B1.F1.F1	$\frac{0.1789}{s^6+4.2362s^5+7.6766s^4+7.5825s^3+4.3122s^2+1.3426s+0.1789}$
C27	6	P3.B4.F5	$\frac{0.1543}{s^6+3.6814s^5+6.2097s^4+5.947s^3+3.4106s^2+1.1057s+0.1543}$
C28	6	P2.TB1.TB4	$\frac{56.1997}{s^6+13.5958s^5+76.4145s^4+217.7647s^3+315.5269s^2+205.4347s+56.1997}$
C29	8	P6.B1.F5	$\frac{0.0767}{s^8+4.6874s^7+10.2168s^6+13.5091s^5+11.8795s^4+7.111s^3+2.8333s^2+0.6871s+0.0767}$
C30	8	P6.B4.B7	$\frac{0.2327}{s^8+5.48037s^7+13.9852s^6+21.5039s^5+21.7519s^4+14.8560s^3+6.7166s^2+1.8461s+0.2327}$
C31	8	B4.P2.TB8	$\frac{111.6}{s^8+14.1s^7+97.7s^6+399.1s^5+995.2s^4+1427s^3+1197s^2+546.6s+111.6}$

Table 2.23: Cascading 1-D lowpass filters, obtained from 1-D Butterworth, Filanovsky, Papoulis and Thomson-Bessel lowpass filters

C18, C19, C20, C21 and C22 (refer table: 2.21) is shown in fig. 2.22. All the filters are having monotonic amplitude-frequency response. The MATLAB code to plot the amplitude-frequency response of the filters in table: 2.21 is in algorithm 16.

2.8.5 Cascading 1-D lowpass filters, derived from Butterworth, Papoulis, Filanovsky, Thomson-Bessel filters, and study their monotonic characteristics

We will utilize all the segregated analog 1-D lowpass filters, namely, P2, P3, P6, B1, B3, B4, B7, F1, F5, TB1, TB3, TB4, TB6, TB7 and TB8 obtained from the Butterworth, Papoulis, Filanovsky and Thomson-Bessel lowpass filters (Sec. 2.7.1, 2.7.2, 2.7.3 and 2.7.4), having monotonic amplitude-frequency response, to get few cascaded analog 1-D lowpass filters of different order. Table: 2.23 shows, few cascaded analog 1-D lowpass filters with,

F.	$A(w)$	*-3db freq.*	*slope at -3db*
C23	$\frac{0.1412}{\sqrt{(w^4-2.4032w^2+0.1412)^2+(0.9637w-2.5807w^3)^2}}$	0.2481	-1.7833
C24	$\frac{0.3017}{\sqrt{(w^4-3.3576w^2+0.3017)^2+(1.6701w-2.9604w^3)^2}}$	0.3065	-1.4219
C25	$\frac{14.2729}{\sqrt{(w^4-26.12w^2+14.2729)^2+(29.7976w-8.322w^3)^2}}$	0.8274	-0.6627
C26	$\frac{0.1789}{\sqrt{\begin{array}{c}(-w^6+7.6766w^4-4.3122w^2+0.1789)^2\\+(4.2362w^5-7.5825w^3+1.3426w)^2\end{array}}}$	0.2962	-1.6142
C27	$\frac{0.1543}{\sqrt{\begin{array}{c}(-w^6+6.2097w^4-3.4106w^2+0.1543)^2\\+(3.6814w^5-5.947w^3+1.1057w)^2\end{array}}}$	0.3262	-1.4117
C28	$\frac{56.1997}{\sqrt{\begin{array}{c}(-w^6+76.4145w^4-315.5269w^2+56.1997)^2\\+(13.5958w^5-217.7647w^3+205.4347w)^2\end{array}}}$	0.5133	-1.0104
C29	$\frac{0.0767}{\sqrt{\begin{array}{c}(w^8-10.2168w^6+11.8795w^4-2.8333w^2+0.0767)^2\\+(-4.6874w^7+13.5091w^5-7.111w^3+0.6871w)^2\end{array}}}$	0.3401	-1.4305
C30	$\frac{0.2327}{\sqrt{\begin{array}{c}(w^8-13.9852w^6+21.7519w^4-6.7166w^2+0.2327)^2\\+(-5.4803w^7+21.5039w^5-14.8560w^3+1.8461w)^2\end{array}}}$	0.3799	-1.2814
C31	$\frac{111.6}{\sqrt{\begin{array}{c}(w^8-97.7w^6+995.2w^4-1197w^2+111.6)^2\\+(-14.1w^7+399.1w^5-1427w^3+546.6w)^2\end{array}}}$	0.4696	-1.15

Table 2.24: Slope and frequency at -3db magnitude of cascaded 1-D lowpass filters, obtained from 1-D Butterworth, Filanovsky, Papoulis and Thomson-Bessel lowpass filters

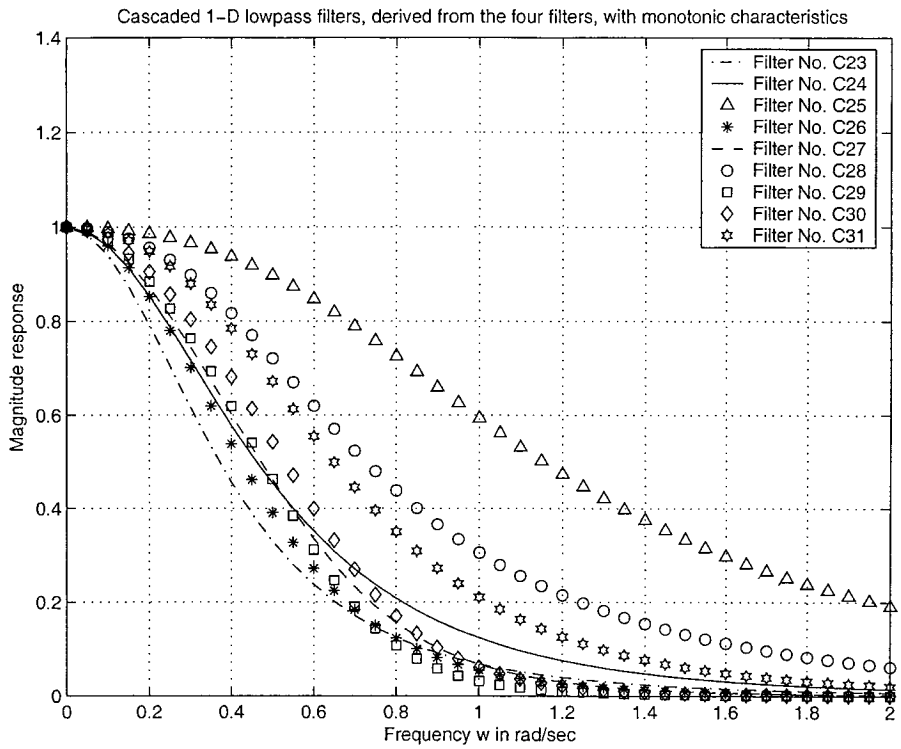

Figure 2.23: Plot of cascaded 1-D lowpass filters obtained from 1-D Butterworth, Filanovsky, Papoulis and Thomson-Bessel lowpass filters. (Refer Table: 2.23)

(i) the transfer function (eqn. 2.2), $F(s)$, *(ii)* filter combination (*F. Combination*), *(iii)* order of the filter (*order*) and, *(iv)* the filter number, *F.No* (where, Ci, with i as integer varying from 23 to 31, corresponds to cascaded analog 1-D lowpass filter).

Table: 2.24 shows, *(i)* the filter number, *F.*, *(ii)* amplitude-frequency response (eqn. 2.3), $A(w)$, *(iii)* the cutoff frequency at magnitude response of $\frac{1}{\sqrt{2}}$, i.e., -3db value and, *(iv) Slope at -3db* magnitude value of the frequency response.

The amplitude-frequency response of the cascaded analog 1-D lowpass filters, C23, C24, C25, C26, C27, C28, C29, C30 and C31 (refer table: 2.23) is shown in fig. 2.23. All the filters are having monotonic amplitude-frequency response. The MATLAB code to plot the amplitude-frequency response of the filters in table: 2.23 is in algorithm 17.

Algorithm 17 MATLAB Code to plot few possible cascaded 1-D lowpass filters, derived from 1-D Butterworth, Filanovsky, Papoulis and Thomson-Bessel filter, having monotonic characteristics. (Refer Table: 2.23)

```
% Under Guidance of Prof. Dr. V. Ramachandran
% Student's name : Ajit Singh Sandhu..... ID:4841492.
clear all; clc;
%Defining the step size of the frequency axis.
step=0.05;
%Defining the frequency range
w=[0:step:2];
s=j.*w;
%Transfer function for Filter No. C23=P3.P3.B3.F1
ha1D=(s+0.4681).*(s+0.4681).*(s+1).*(s+0.6445);
ha1D=abs(0.1412./ha1D);
%Transfer function for Filter No. C24=P3.B1.F1
ha2D=(s+0.4681).*(s+0.9239+0.3827i).*(s+0.9239-0.3827i).*(s+0.6445);
ha2D=abs(0.3017./ha2D);
%Transfer function for Filter No. C25=B4.TB4
ha3D=(s+0.8090+0.5878i).*(s+0.8090-0.5878i).*(s.^2+6.704.*s+14.2729);
ha3D=abs(14.2729./ha3D);
%Transfer function for Filter No. C26=P2.B1.F1.F1
ha4D=(s+0.5497+0.3586i).*(s+0.5497-0.3586i).*(s+0.9239+0.3827i).*(s+0.9239-
0.3827i).*(s+0.6445).*(s+0.6445);
ha4D=abs(0.1790./ha4D);
%Transfer function for Filter No. C27=P3.B4.F5
ha5D=(s+0.4681).*(s+0.8090+0.5878i).*(s+0.8090-0.5878i).*(s+0.6445).*(s+0.4754+0.5344i).*(s+0.4754-
0.5344i);
ha5D=abs(0.1543./ha5D);
%Transfer function for Filter No. C28=P2.TB1.TB4
ha6D=(s+0.5497+0.3586i).*(s+0.5497-0.3586i).*(s.^2+5.7924.*s+9.14).*(s.^2+6.704.*s+14.2729);
ha6D=abs(56.1997./ha6D);
%Transfer function for Filter No. C29=P6.B1.F5
ha7D=(s+0.4681).*(s+0.3881+0.5886i).*(s+0.3881-0.5886i).*(s+0.9239+0.3827i)
.*(s+0.9239-0.3827i).*(s+0.6445).*(s+0.4754+0.5344i).*(s+0.4754-0.5344i);
ha7D=abs(0.0767./ha7D);
%Transfer function for Filter No. C30=P6.B4.B7
ha8D=(s+0.4681).*(s+0.3881+0.5886i).*(s+0.3881-0.5886i).*(s+0.8090+0.5878i)
.*(s+0.8090-0.5878i).*(s+1).*(s+0.8090+0.5878i).*(s+0.8090-0.5878i);
ha8D=abs(0.2327./ha8D);
%Transfer function for Filter No. C31=B4.P2.TB8
ha9D=(s+0.8090+0.5878i).*(s+0.8090-0.5878i).*(s+0.5497+0.3586i)
.*(s+0.5497-0.3586i).*(s.^2+6.704.*s+14.2729).*(s.^2+4.6494.*s+18.1563);
ha9D=abs(111.6388./ha9D);
%Plotting all the cascaded 1-D lowpass filters on the same figure
figure(1);
plot(w,ha1D,'k-.',w,ha2D,'k-',w,ha3D,'k^',w,ha4D,'k*',w,ha5D,'k--',w,ha6D,'ko',w,ha7D,'ks',w,ha8D
,'kd',w,ha9D,'kh');
legend('Filter No. C23','Filter No. C24','Filter No. C25','Filter No. C26','Filter No. C27','Filter No.
C28','Filter No. C29','Filter No. C30','Filter No. C31',0);
title('Cascaded 1-D lowpass filters, derived from the three filters, with monotonic characteristics');
xlabel('Frequency w in rad/sec');
ylabel('Magnitude response');
grid on;
```

2.9 Summary

In this Chapter, we have generated analog 1-D lowpass filters with monotonic amplitude-frequency response and studied their characteristics. We started with literature review of few monotonic filters, and then implemented Butterworth, Papoulis and Thomson-Bessel filters of fourth and fifth order, and Filanovsky filters of fifth order.

We discussed a design technique for generation of Butterworth, Papoulis and Filanovsky lowpass filters of any order with arbitrary flatness. We derived the filtering transfer function for the fourth and fifth order Butterworth and Papoulis filters, and also for the fifth order Filanovsky filters. By using the filtering functions, the corresponding 1-D analog stable lowpass filters with monotonic amplitude-frequency response were designed, implemented, and their results were compared. Furthermore, Thomson-Bessel filters of fourth and fifth order with monotonic response were also designed and their characteristics were studied. After designing all the mentioned 1-D filters, their characteristics were compared and results were discussed.

Furthermore, we proposed extraction of all possible lower order 1-D lowpass filters from the implemented filters, namely, Butterworth, Papoulis, Filanovsky and Thomson-Bessel Filters. They were based on the real or complex conjugate poles of the higher order 1-D filters implemented. The characteristics of all the lower order 1-D filters were studied and the filters with monotonic amplitude-frequency response were segregated. Higher order filters can be realized by cascading lower order filters. Therefore, few cascaded combinations of the extracted monotonic filters were realized to attain fourth, sixth and eighth order 1-D lowpass filters, and it was verified that the such 1-D filters of different order also inhibit monotonic characteristics.

The same design and test criterias can be used for the filters of higher order with monotonic characteristics. We restricted Butterworth, Papoulis, Filanovsky and Thomson-Bessel filter implementation till fifth order because the possible number of lower order 1-D filters to extract and study increases, as there are more pole combinations. As can be readily

observed, as the orders increase, the number of combinations increases enormously and hence, a very large number will be possible. We also wanted to study different types of lowpass filters and not to be restricted to a specific type. In this Chapter, we implemented different types of 1-D analog lowpass filters with monotonic characteristics and they will be extended to 2-D lowpass filters in the subsequent chapter.

Chapter 3

Generation of Stable 2-D Butterworth, Papoulis, Filanovsky and Thomson-Bessel Lowpass Filters with monotonic characteristics, by cascade realizations

3.1 Introduction

An easier way to design a multidimensional filter is to obtain it as a product separable 1-D filter transfer function. A N-Dimensional (N-D) filter can be realized by cascading N 1-D filters, where N is a positive integer. In the case of N-D analog filters, transfer function can be expressed as product of 1-D filters in the s-domain. Similarly, in case of digital filters, transfer function can be realized as product of 1-D filters in z-domain. Depending on the type of filter it could be either a FIR or an IIR filter transfer function. We know that, FIR filter is one which has a transfer function resulting from a finite sequence and the IIR filter

is one which has a transfer function resulting from an infinite sequence [38, 39, 40].

The 2-D analog filter in the s-domain may be expressed as eqn. 1.1. The numerator, $N_a(s_1, s_2)$, and the denominator, $D_a(s_1, s_2)$, are polynomials in s_1 and s_2 with both even and odd terms. While designing IIR filters, the stability depends on the denominator polynomial, $D_a(s_1, s_2)$, of the transfer function. Hence, to simplify our analysis we can take numerator polynomial, $N_a(s_1, s_2)$, as a constant, i.e., the filter is having poles, and all zeros are located at infinity.

One of the simple methods to generate 2-D transfer function is to combine two 1-D transfer functions as a product. In other words, the resulting 2-D analog filter as product of two 1-D sequences can be expressed as

$$H_a(s_1, s_2) = H_1(s_1).H_2(s_2) \tag{3.1}$$

where, $H_1(s_1) = \frac{N_1(s_1)}{D_1(s_1)}$ and $H_2(s_2) = \frac{N_2(s_2)}{D_2(s_2)}$ are 1-D analog filters, with $N_1(s_1)$, $N_2(s_2)$ and $D_1(s_1)$, $D_2(s_2)$ as the corresponding numerator and denominator polynomials, respectively. Since the stability of the filters is governed by the denominator polynomials of the filters, to simplify our analysis of IIR filters we can take numerator polynomials to be constant, i.e., with no zeros [14, 15, 16, 17, 31].

A method of designing digital lowpass filter is to start from the analog lowpass filter transfer function, and then apply generalized bilinear transformations [19] for lowpass filters, for example,

$$s_i = k_i \frac{z_i - a_{iL}}{z_i + 1} \tag{3.2}$$

where $i = 1, 2$ for 2-D filters, to obtain the digital filter transfer function. For the resulting 2-D filter to be stable, it is required that $k_i > 0$ and $0 \leq a_{iL} \leq 1$. If the filter in analog domain is stable, then by applying bilinear transformations, and satisfying the nyquist criteria, the digital filter will also be stable. But, the complexity to define stability of filter increases as the dimensions of the multidimensional filter increases (Sec. 1.3).

All the 1-D filters realized in Chapter 2 are stable (as there poles are on the left side of the s-plane). The 1-D filters realized in Sec. 2.4, 2.5, 2.7 and 2.8, exhibit monotonic amplitude-frequency response, if the poles are further away from the origin. The 1-D filters exhibit ripples in the amplitude-frequency response of the passband if the poles are closer to the origin with magnitude of real part greater than the imaginary part (Sec. 2.7).

Multidimensional filters with monotonic amplitude-frequency response are not explored in literature till now. In this Chapter, we will realize and study 2-D lowpass filters, obtained by cascading 1-D filters, namely, Papoulis filters, Butterworth filters, Filanovsky filters, Thomson-Bessel filters and other combinational filters of the same (derived in Chapter 2), having monotonic characteristics. The monotonic characteristics, i.e., monotonic behavior of the amplitude-frequency response will be studied for the 2-D filters in both analog (s) and digital (z) domain.

We will generate fourth and fifth order Papoulis, Butterworth and Thomson-Bessel 2-D lowpass filters in both analog and digital domain in Sec. 3.2, 3.3 and 3.5. We will also generate fifth order Filanovsky analog and digital 2-D lowpass filters in Sec. 3.4. Furthermore, 2-D filters of different orders are realized by cascading lower order 1-D lowpass filters obtained from Butterworth, Papoulis, Filanovsky and Thomson-Bessel filters, with monotonic characteristics in Sec. 3.6. In Sec. 3.7, few combination 1-D lowpass filters having monotonic amplitude-frequency response are cascaded to realize 2-D lowpass filters of different orders. Our primary emphasis in this Chapter, is to implement and study different types of 2-D analog and digital lowpass filters with monotonic amplitude-frequency response and, furthermore, to study the 2-D digital lowpass filters response based on the different values of constants in the generalized bilinear transformation (eqn. 3.2).

3.2 Generation of the fourth and fifth order 2-D Papoulis lowpass filters with monotonic characteristics

The fourth and fifth order 1-D analog Papoulis lowpass filters having monotonic amplitude-frequency response were derived in Sec. 2.4.1. In this section, we will generate 2-D analog Papoulis lowpass filters by cascading the 1-D analog Papoulis lowpass filters, and study their monotonic characteristics. Furthermore, we will apply generalized bilinear transformation (eqn. 3.2) to the 2-D analog lowpass filters, to obtain 2-D digital filters having monotonic response. The 2-D digital filters will also be studied for different values of the constants, k_1, k_2, a_{1L}, a_{2L}, used in the generalized bilinear transformation.

3.2.1 Generation of fourth and fifth order 2-D analog Papoulis lowpass filters

We will generate fourth and fifth order 2-D analog Papoulis lowpass filters, by utilizing the fourth and fifth order 1-D analog Papoulis lowpass filters generated in Sec. 2.4.1 and study their monotonic characteristics.

3.2.1.1 Generation of fourth order 2-D analog Papoulis lowpass filter

The transfer function of the fourth order (i.e., $m = 4$) 1-D Papoulis filter, having flatness degree one (i.e., $i = 1$), is given by eqn. 2.41. By taking two such 1-D Papoulis lowpass filters in cascade, with denominator polynomials as function of s_1 and s_2 (with $s_1 = jw_1$ and $s_2 = jw_2$, eqn. 3.1) we get,

$$H_a(s_1, s_2) = \frac{(0.4075)^2}{\begin{matrix}(s_1^2 + 1.0994s_1 + 0.4308) & (s_1^2 + 0.4634s_1 + 0.9458) \\ (s_2^2 + 1.0994s_2 + 0.4308) & (s_2^2 + 0.4634s_2 + 0.9458)\end{matrix}} \tag{3.3}$$

Algorithm 18 The MATLAB code to plot the 3-D amplitude-frequency response and contour of the frequency response of the fourth and fifth order 2-D analog Papoulis lowpass filter

```
% Under Guidance of Prof. Dr. V. Ramachandran
% Student's name : Ajit Singh Sandhu..... ID:4841492.
clear all;
[w1,w2] = meshgrid(-1.5:0.05:1.5,-1.5:0.05:1.5);
s1=j*w1;
s2=j*w2;
ha1_1=(s1+0.2317+0.9455i).*(s1+0.2317-0.9455i).*(s1+0.5497+0.3586i).*(s1+0.5497-0.3586i);
ha1_2=(s2+0.2317+0.9455i).*(s2+0.2317-0.9455i).*(s2+0.5497+0.3586i).*(s2+0.5497-0.3586i);
h1=abs((0.4075^2)./(ha1_1.*ha1_2));
figure(1);
contour3(w1,w2,h1);
surface(w1,w2,abs(h1),'EdgeColor',[.8 .8 .8],'FaceColor','none');
grid on;
view(-15,25);
%colormap cool;
title('3-D amplitude-frequency response of the fourth order 2-D Papoulis Lowpass Filter');
xlabel(' w2 in rad/sec ');
ylabel(' w1 in rad/sec ');
zlabel(' Magnitude Response ');
figure(2);
[C,h] = contour(w1,w2,h1);
clabel(C,h);
grid on;
%colormap cool;
title('Contour response of the fourth order 2-D Papoulis Lowpass Filter');
xlabel(' w2 in rad/sec ');
ylabel(' w1 in rad/sec ');
h1_1=(s1+0.4681).*(s1+0.3881+0.5886i).*(s1+0.3881-0.5886i).*(s1+0.1536+0.9681i).*(s1+0.1536-
0.9681i);
h1_2=(s2+0.4681).*(s2+0.3881+0.5886i).*(s2+0.3881-0.5886i).*(s2+0.1536+0.9681i).*(s2+0.1536-
0.9681i);
h=abs((0.2235^2)./(h1_1.*h1_2));
figure(3);
contour3(w1,w2,h);
surface(w1,w2,abs(h),'EdgeColor',[.8 .8 .8],'FaceColor','none');
grid on;
view(-15,25);
%colormap cool;
title('3-D amplitude-frequency response of the fifth order 2-D Papoulis Lowpass Filter');
xlabel(' w2 in rad/sec ');
ylabel(' w1 in rad/sec ');
zlabel(' Magnitude Response ');
figure(4);
[C,h] = contour(w1,w2,h);
clabel(C,h);
grid on;
%colormap cool;
title('Contour response of the fifth order 2-D Papoulis Lowpass Filter');
xlabel(' w2 in rad/sec ');
ylabel(' w1 in rad/sec ');
```

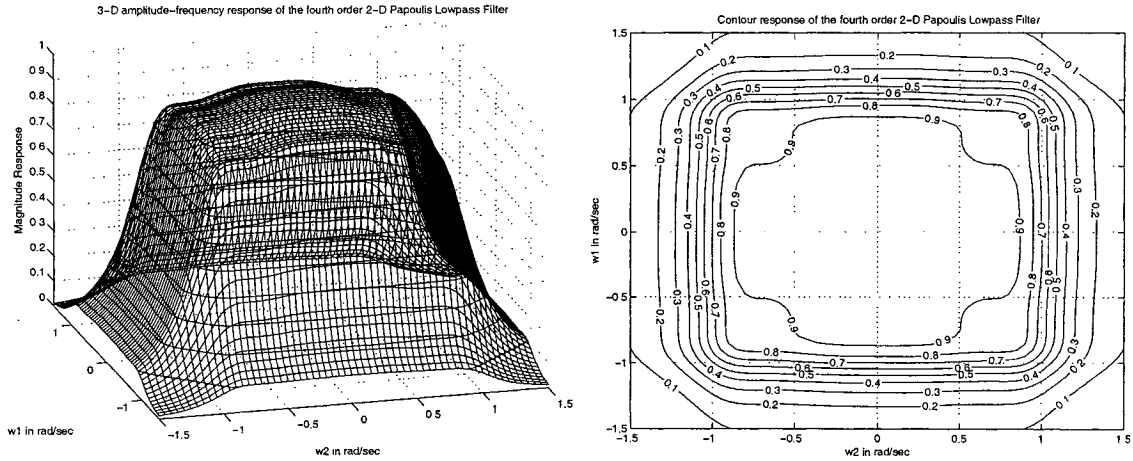

(a) 3-D amplitude-frequency response of the fourth order 2-D analog Papoulis lowpass filter

(b) Contour frequency response of the fourth order 2-D analog Papoulis lowpass filter

Figure 3.1: 3-D amplitude-frequency response and contour response of the fourth order 2-D analog Papoulis lowpass filter

The amplitude-frequency response of the fourth order 2-D analog Papoulis lowpass filter (eqn. 3.3) is shown in the fig. 3.1. We can observe that the amplitude-frequency response is monotonically decreasing. The MATLAB code to plot the 3-D amplitude-frequency response and contour of the frequency response of the fourth and fifth order 2-D analog Papoulis lowpass filter is in algorithm 18.

3.2.1.2 Generation of fifth order 2-D analog Papoulis lowpass filter

The transfer function of the fifth order (i.e., $m = 5$) 1-D Papoulis filter, having flatness degree zero (i.e., $i = 0$), is given by eqn. 2.43. By taking two such 1-D Papoulis lowpass filters in cascade, with denominator polynomials as function of s_1 and s_2 (with $s_1 = jw_1$ and $s_2 = jw_2$, eqn. 3.1) we get,

$$H_a(s_1, s_2) = \frac{(0.2235)^2}{\begin{array}{c}(s_1^2 + 0.7762s_1 + 0.4971)\,(s_1^2 + 0.3072s_1 + 0.9608) \\ (s_2^2 + 0.7762s_2 + 0.4971)\,(s_2^2 + 0.3072s_2 + 0.9608) \\ (s_1 + 0.4681)\,(s_2 + 0.4681)\end{array}} \tag{3.4}$$

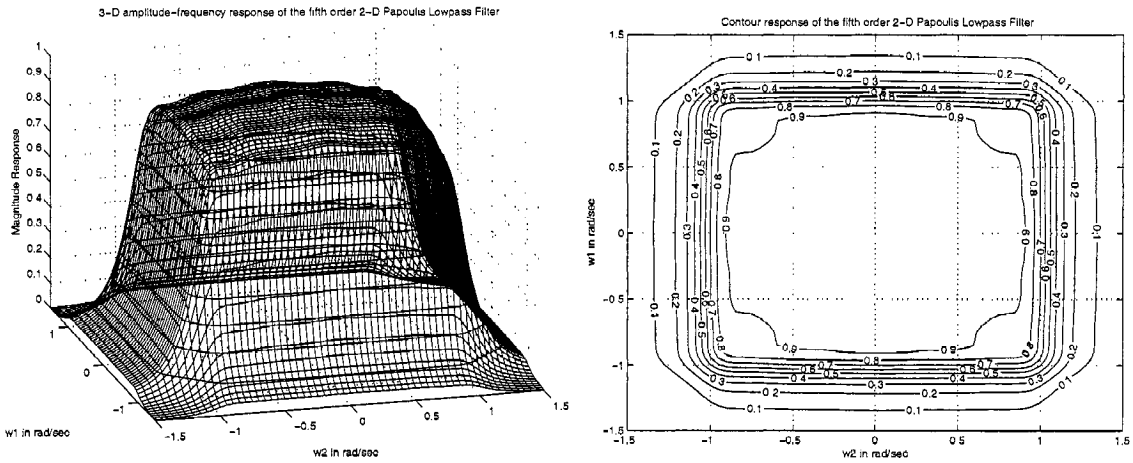

(a) 3-D amplitude-frequency response of the fifth order 2-D analog Papoulis lowpass filter

(b) Contour frequency response of the fifth order 2-D analog Papoulis lowpass filter

Figure 3.2: 3-D amplitude-frequency response and contour response of the fifth order 2-D analog Papoulis lowpass filter

The amplitude-frequency response of the fifth order 2-D analog Papoulis lowpass filter (eqn. 3.4) is shown in the fig. 3.2. We can observe that the amplitude-frequency response is monotonically decreasing. The MATLAB code to plot the 3-D amplitude-frequency response and contour of the frequency response of the fourth and fifth order 2-D analog Papoulis lowpass filter is in algorithm 18.

3.2.1.3 Discussion

The amplitude-frequency response and contour of the frequency response of the fourth and fifth order 2-D Papoulis lowpass filter is shown in fig. 3.1 and 3.2, respectively. It is observed that, though the amplitude-frequency response in the passband is not relatively flat, but still it is monotonically decreasing. The passband of the fifth order 2-D lowpass filter is much wider with steeper transition band, in comparison to the fourth order 2-D lowpass Papoulis filter. By keeping one of the frequency axes at zero as reference, if we observe the frequency response from the other frequency axes, then the cutoff frequency (i.e., frequency at 0.707 magnitude value) will exist at ± 1 rad/sec. This is in correspondence to the 1-D Papoulis filter from which the 2-D lowpass filter is derived. Hence, the 2-D lowpass

Papoulis filters have similar monotonic characteristics with cutoff frequency at ± 1 rad/sec as the equivalent 1-D Papoulis filter derived in Sec. 2.4.1. It is also observed that the 2-D frequency response is symmetrical.

3.2.2 Generation of fourth and fifth order 2-D digital Papoulis lowpass filter

Now, we will generate fourth and fifth order 2-D digital Papoulis lowpass filters. We will apply the generalized bilinear transformation (eqn. 3.2) in the fourth and fifth order 2-D analog Papoulis lowpass filters generated in Sec. 3.2.1, to obtain 2-D digital Papoulis lowpass filters. The resulting 2-D digital filter monotonic characteristics will be studied by taking different values of the constants in the bilinear transformation.

3.2.2.1 Generation of fourth order 2-D digital Papoulis lowpass filter

The transfer function of the fourth order 2-D analog Papoulis lowpass filter, is given by eqn. 3.3. By applying generalized bilinear transformation (eqn. 3.2) to eqn. 3.3, we get, transfer function of 2-D digital Papoulis lowpass filter as function of z_1 and z_2, with $z_1 = e^{jw_1}$ and $z_2 = e^{jw_2}$. Hence, we get,

$$H_d(z_1, z_2) = \frac{(0.4075)^2 (z_1+1)^4 (z_2+1)^4}{\begin{array}{l}\left[k_1^2 (z_1 - a_{1L})^2 + 1.0994 k_1 (z_1 - a_{1L})(z_1+1) + 0.4308 (z_1+1)^2\right] \\ \left[k_1^2 (z_1 - a_{1L})^2 + 0.4634 k_1 (z_1 - a_{1L})(z_1+1) + 0.9458 (z_1+1)^2\right] \\ \left[k_2^2 (z_2 - a_{2L})^2 + 1.0994 k_2 (z_2 - a_{2L})(z_2+1) + 0.4308 (z_2+1)^2\right] \\ \left[k_2^2 (z_2 - a_{2L})^2 + 0.4634 k_2 (z_2 - a_{2L})(z_2+1) + 0.9458 (z_2+1)^2\right]\end{array}} \tag{3.5}$$

The 3-D amplitude-frequency response and contour plots of the fourth order 2-D digital Papoulis lowpass filter for different combination values of the constants is shown in the fig. 3.3, 3.4, 3.5 and 3.6. We can observe that the amplitude-frequency response is monotoni-

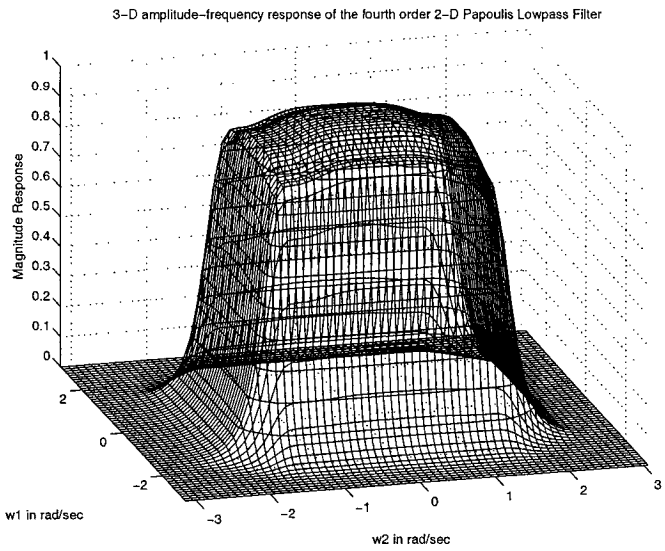

Figure 3.3: 3-D amplitude-frequency response of the fourth order 2-D digital Papoulis lowpass filter (When $k_1 = 1, k_2 = 1, a_{1L} = 1, a_{2L} = 1$)

cally decreasing when constants (k_1, k_2, a_{1L} and a_{2L}) are having non-negative values. The MATLAB code to plot the 3-D amplitude-frequency response and contour of the frequency response of the fourth order 2-D digital Papoulis lowpass filter is in algorithm 19.

3.2.2.2 Generation of fifth order 2-D digital Papoulis lowpass filter

The transfer function of the fifth order 2-D analog Papoulis lowpass filter, is given by eqn. 3.4. By applying generalized bilinear transformation (eqn. 3.2) to eqn. 3.4, we get, transfer function of 2-D digital Papoulis lowpass filter as function of z_1 and z_2, with $z_1 = e^{jw_1}$ and

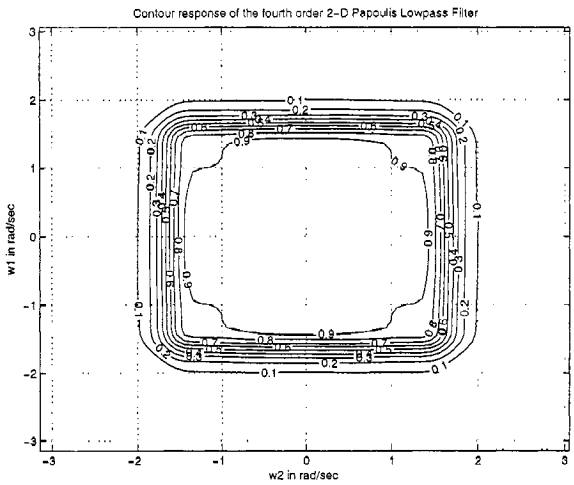

(a) When k1=1, k2=1, a1L=1 and a2L=1

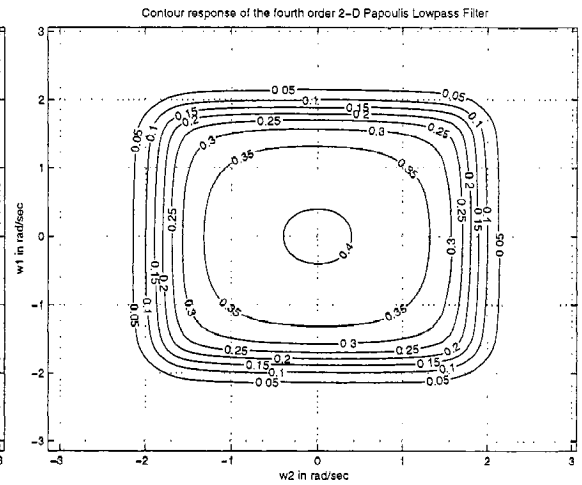

(b) When k1=1, k2=1, a1L=0.7 and a2L=0.7

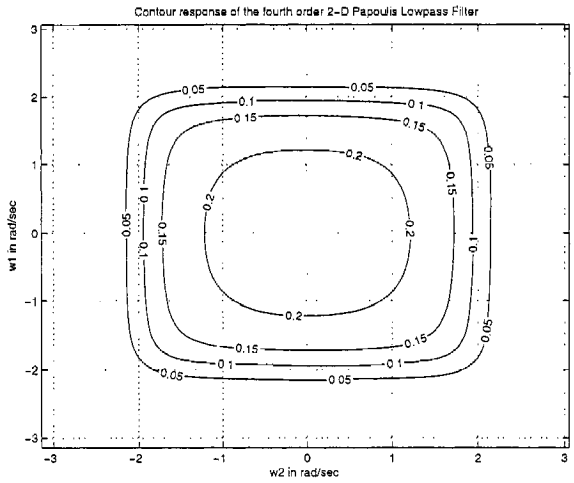

(c) When k1=1, k2=1, a1L=0.5 and a2L=0.5

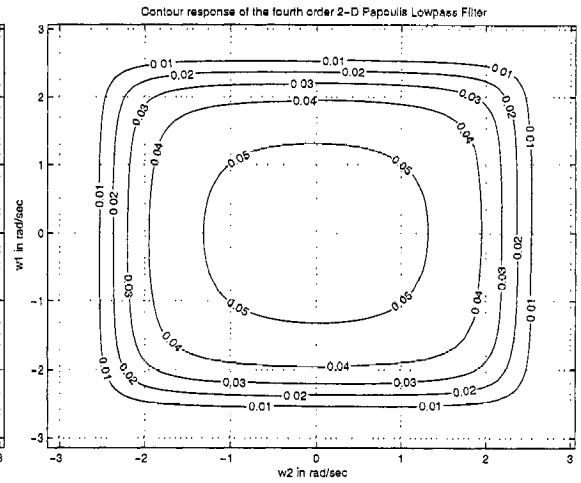

(d) When k1=1, k2=1, a1L=0 and a2L=0

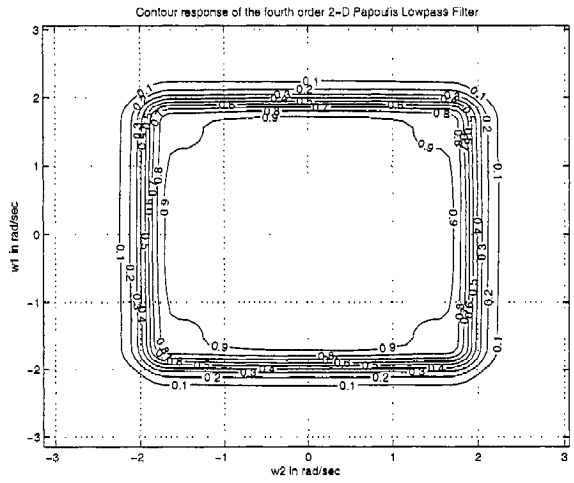

(e) When k1=0.75, k2=0.75, a1L=1 and a2L=1

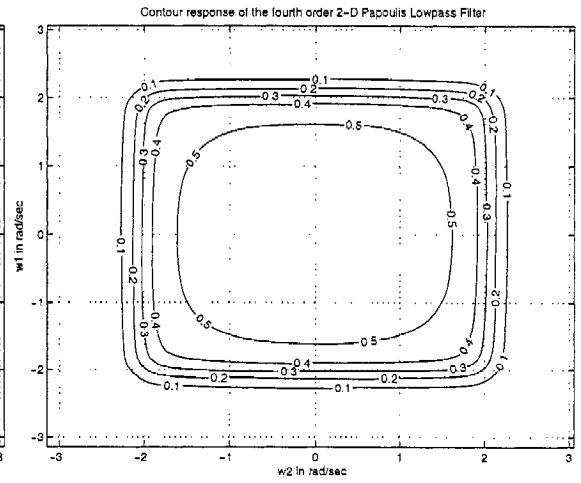

(f) When k1=0.75, k2=0.75, a1L=0.75 and a2L=0.75

Figure 3.4: Contour response of the fourth order 2-D digital Papoulis lowpass filter

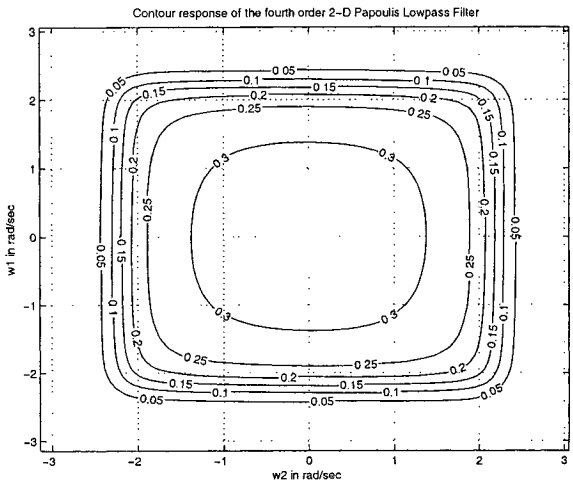

(a) When k1=0.75, k2=0.75, a1L=0.5 and a2L=0.5

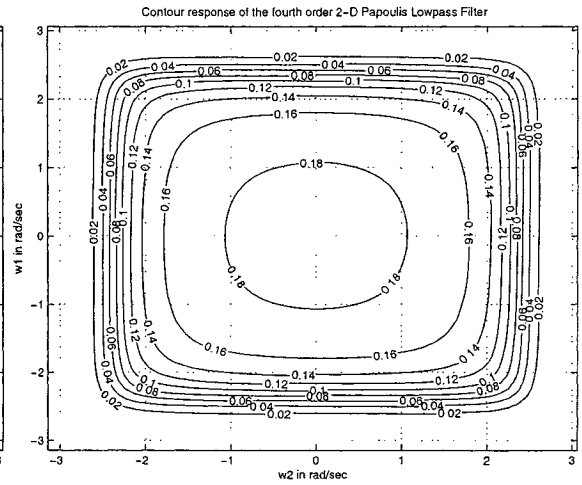

(b) When k1=0.75, k2=0.75, a1L=0.25 and a2L=0.25

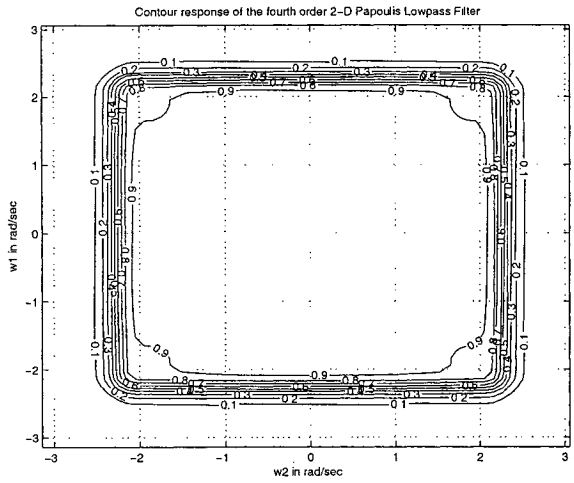

(c) When k1=0.5, k2=0.5, a1L=1 and a2L=1

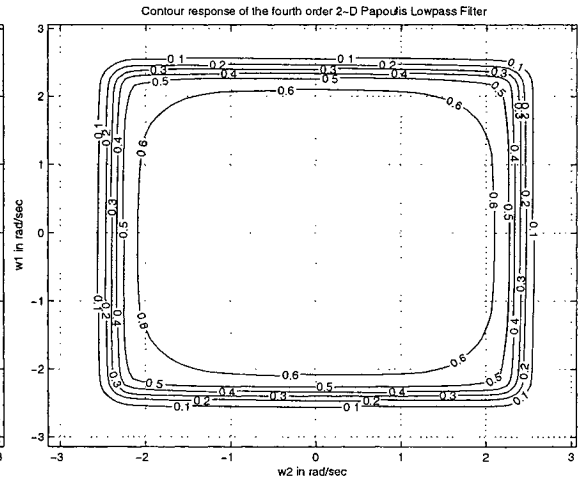

(d) When k1=0.5, k2=0.5, a1L=0.75 and a2L=0.75

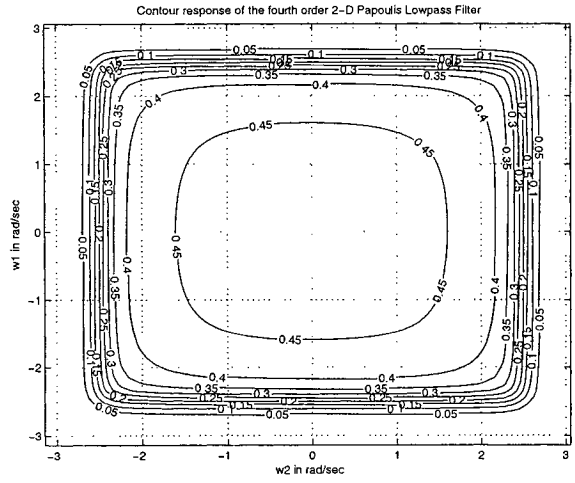

(e) When k1=0.5, k2=0.5, a1L=0.5 and a2L=0.5

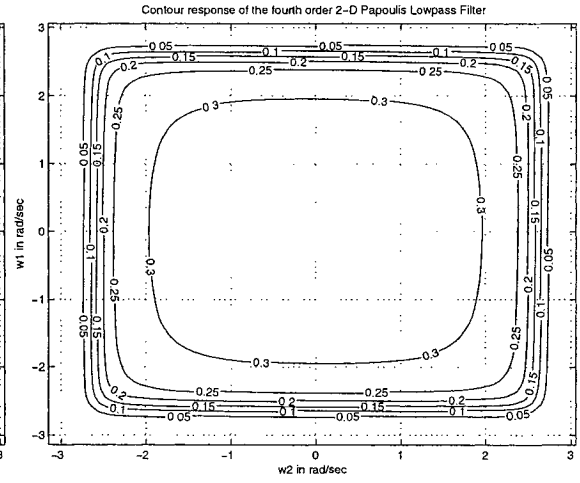

(f) When k1=0.5, k2=0.5, a1L=0.25 and a2L=0.25

Figure 3.5: Contour response of the fourth order 2-D digital Papoulis lowpass filter

Algorithm 19 The MATLAB code to plot the 3-D amplitude-frequency response and contour of the frequency response of the fourth order 2-D digital Papoulis lowpass filter

```
% Under Guidance of Prof. Dr. V. Ramachandran
% Student's name : Ajit Singh Sandhu..... ID:4841492.
clc;
clear all;
k1=input('Give the value of the constant k1 for the bilinear LP transformation => ');
k2=input('Give the value of the constant k2 for the bilinear LP transformation => ');
a1L=input('Give the value of the constant a1L for the bilinear LP transformation => ');
a2L=input('Give the value of the constant a2L for the bilinear LP transformation => ');
% Creates two dimensional square matrix (mesh grid) of angular frequency w1 and w2.
[w1,w2] = meshgrid(-pi:0.1:pi,-pi:0.1:pi);
% Apply Z1=r1*exp(jw1) and Z2=r2*exp(jw2) with r1 = r2 =1
z1=exp(j.*w1);
z2=exp(j.*w2);
% Hd is the required digital transfer function and its value is evaluated as follows.
a=z1-a1L;
b=z2-a2L;
c=z1+1;
d=z2+1;
h1_1=(((k1.^2).*(a.^2))+(k1.*1.0994.*a.*c)+(0.4308.*(c.^2))).*(((k1.^2).*(a.^2))
+(k1.*0.4634.*a.*c)+(0.9458.*(c.^2)));
h1_2=(((k2.^2).*(b.^2))+(k2.*1.0994.*b.*d)+(0.4308.*(d.^2))).*(((k2.^2).*(b.^2))
+(k2.*0.4634.*b.*d)+(0.9458.*(d.^2)));
h1=abs(((c.^4).*(d.^4).*(0.4074^2))./(h1_1.*h1_2));
figure(1);
contour3(w1,w2,h1);
surface(w1,w2,abs(h1),'EdgeColor',[.8 .8 .8],'FaceColor','none');
grid on;
view(-15,25);
%colormap cool;
title('3-D amplitude-frequency response of the fourth order 2-D Papoulis Lowpass Filter');
xlabel(' w2 in rad/sec ');
ylabel(' w1 in rad/sec ');
zlabel(' Magnitude Response ');
figure(2);
[C,h] = contour(w1,w2,h1);
clabel(C,h);
grid on;
%colormap cool;
title('Contour response of the fourth order 2-D Papoulis Lowpass Filter');
xlabel(' w2 in rad/sec ');
ylabel(' w1 in rad/sec ');
```

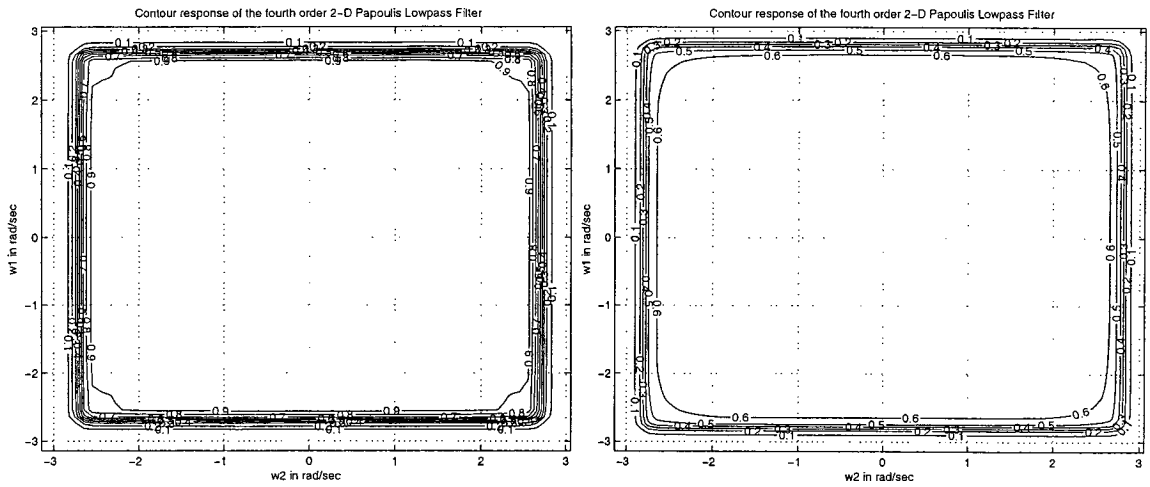

(a) When k1=0.25, k2=0.25, a1L=1 and a2L=1 (b) When k1=0.25, k2=0.25, a1L=0.5 and a2L=0.5

Figure 3.6: Contour response of the fourth order 2-D digital Papoulis lowpass filter

$z_2 = e^{jw_2}$. Hence, we get,

$$H_d(z_1, z_2) = \frac{(0.2235)^2 (z_1+1)^5 (z_2+1)^5}{\begin{array}{l}[k_1 (z_1 - a_{1L}) + 0.4681 (z_1+1)] [k_2 (z_2 - a_{2L}) + 0.4681 (z_2+1)] \\ \left[k_1^2 (z_1 - a_{1L})^2 + 0.7762 k_1 (z_1 - a_{1L}) (z_1+1) + 0.4971 (z_1+1)^2\right] \\ \left[k_1^2 (z_1 - a_{1L})^2 + 0.3072 k_1 (z_1 - a_{1L}) (z_1+1) + 0.9608 (z_1+1)^2\right] \\ \left[k_2^2 (z_2 - a_{2L})^2 + 0.7762 k_2 (z_2 - a_{2L}) (z_2+1) + 0.4971 (z_2+1)^2\right] \\ \left[k_2^2 (z_2 - a_{2L})^2 + 0.3072 k_2 (z_2 - a_{2L}) (z_2+1) + 0.9608 (z_2+1)^2\right]\end{array} \quad (3.6)$$

The 3-D amplitude-frequency response and contour plots of the fifth order 2-D digital Papoulis lowpass filter for different combination values of the constants is shown in the fig. 3.7, 3.8, 3.9 and 3.10. We can observe that the amplitude-frequency response is monotonically decreasing when constants (k_1, k_2, a_{1L} and a_{2L}) are having non-negative values. The MATLAB code to plot the 3-D amplitude-frequency response and contour of the frequency response of the fifth order 2-D digital Papoulis lowpass filter is in algorithm 20.

Algorithm 20 The MATLAB code to plot the 3-D amplitude-frequency response and contour of the frequency response of the fifth order 2-D digital Papoulis lowpass filter

```
% Under Guidance of Prof. Dr. V. Ramachandran
% Student's name : Ajit Singh Sandhu..... ID:4841492.
clc; clear all;
k1=input('Give the value of the constant k1 for the bilinear LP transformation => ');
k2=input('Give the value of the constant k2 for the bilinear LP transformation => ');
a1L=input('Give the value of the constant a1L for the bilinear LP transformation => ');
a2L=input('Give the value of the constant a2L for the bilinear LP transformation => ');
% Creates two dimensional square matrix (mesh grid) of angular frequency w1 and w2.
[w1,w2] = meshgrid(-pi:0.1:pi,-pi:0.1:pi);
% Apply Z1=r1*exp(jw1) and Z2=r2*exp(jw2) with r1 = r2 =1
z1=exp(j.*w1);
z2=exp(j.*w2);
% Hd is the required digital transfer function and its value is evaluated as follows.
a=z1-a1L;
b=z2-a2L;
c=z1+1;
d=z2+1;
h1_1=(((k1.^2).*(a.^2))+(k1.*0.7762.*a.*c)+(0.4971.*(c.^2)))
.*(((k1.^2).*(a.^2))+(k1.*0.3072.*a.*c)+(0.9608.*(c.^2))).*(a+(0.4681.*c));
h1_2=(((k2.^2).*(b.^2))+(k2.*0.7762.*b.*d)+(0.4971.*(d.^2)))
.*(((k2.^2).*(b.^2))+(k2.*0.3072.*b.*d)+(0.9608.*(d.^2))).*(b+(0.4681.*d));
h1=abs(((c.^5).*(d.^5).*(0.2235.^2))./(h1_1.*h1_2));
figure(1);
contour3(w1,w2,h1);
surface(w1,w2,abs(h1),'EdgeColor',[.8 .8 .8],'FaceColor','none');
grid on;
view(-15,25);
%colormap cool;
title('3-D amplitude-frequency response of the fifth order 2-D Papoulis Lowpass Filter');
xlabel(' w2 in rad/sec ');
ylabel(' w1 in rad/sec ');
zlabel(' Magnitude Response ');
figure(2);
[C,h] = contour(w1,w2,h1);
clabel(C,h);
grid on;
%colormap cool;
title('Contour response of the fifth order 2-D Papoulis Lowpass Filter');
xlabel(' w2 in rad/sec ');
ylabel(' w1 in rad/sec ');
```

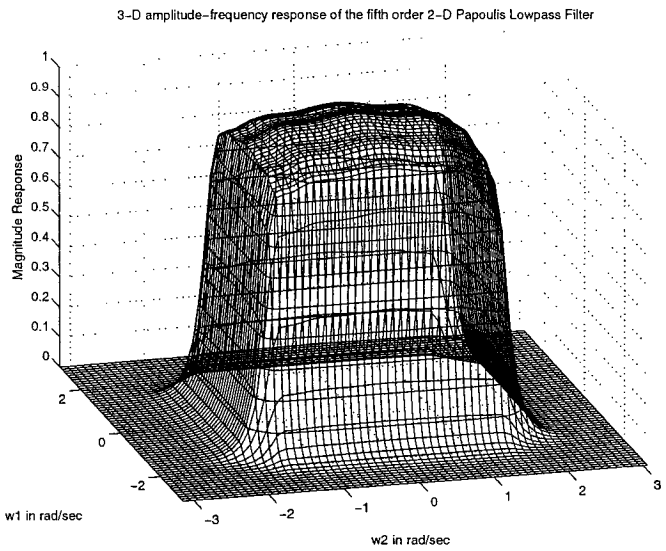

Figure 3.7: 3-D amplitude-frequency response of the fifth order 2-D digital Papoulis low-pass filter (When $k_1 = 1$, $k_2 = 1$, $a_{1L} = 1$, $a_{2L} = 1$)

3.2.2.3 Discussion

The characteristics of the 2-D digital filters proposed in Sec. 3.2.2.1 and 3.2.2.2 are studied in this sub-section. Fig. 3.3, 3.4, 3.5, 3.6, 3.7, 3.8, 3.9 and 3.10, shows amplitude-frequency response and contour plots of the 2-D Papoulis digital filters, based on the different values of the constants ,k_1, k_2, a_{1L}, a_{2L}, of the generalized bilinear transformation.

In general, the coefficients k_1, k_2 affects the passband width and a_{1L}, a_{2L} affects the gain. It is observed that for non-negative values of the constants, the 2-D digital Papoulis lowpass filters always have monotonic amplitude-frequency response with similar symmetry. The monotonic amplitude-frequency response of the fifth order 2-D digital Papoulis lowpass filters are wider in the passband and steeper in the transition band, in comparison to the fourth order 2-D Papoulis lowpass filter, for the same coefficient values (for example fig. 3.4 (a) and 3.8 (a)). It is may also be noted that as the coefficients, k_1, k_2, values are decreased, the passband of the 2-D lowpass filter increases with decrease in magnitude, and it may result in loss of signal due to aliasing, because the nyquist rate may not be satisfied for certain input signals.

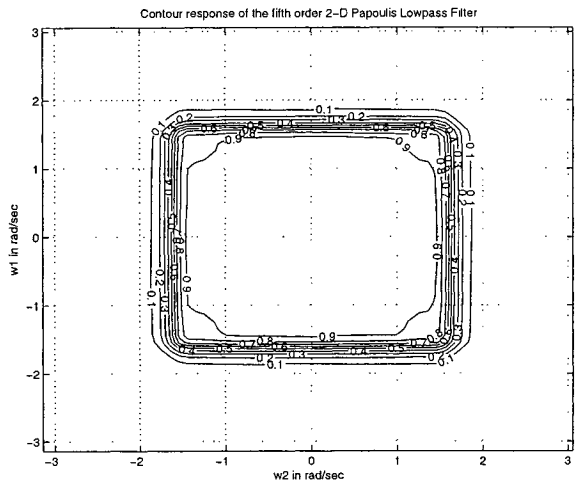

(a) When k1=1, k2=1, a1L=1 and a2L=1

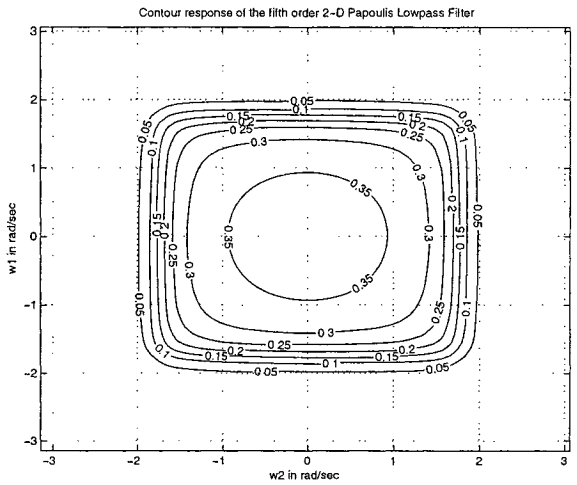

(b) When k1=1, k2=1, a1L=0.75 and a2L=0.75

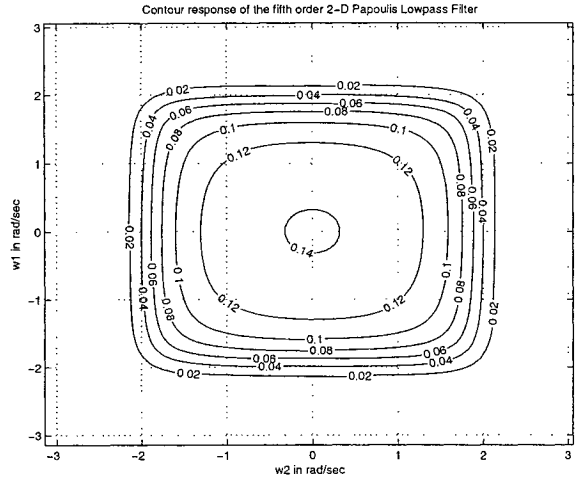

(c) When k1=1, k2=1, a1L=0.5 and a2L=0.5

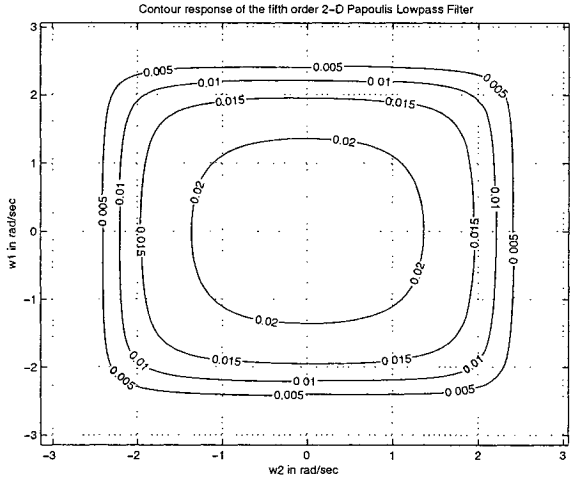

(d) When k1=1, k2=1, a1L=0 and a2L=0

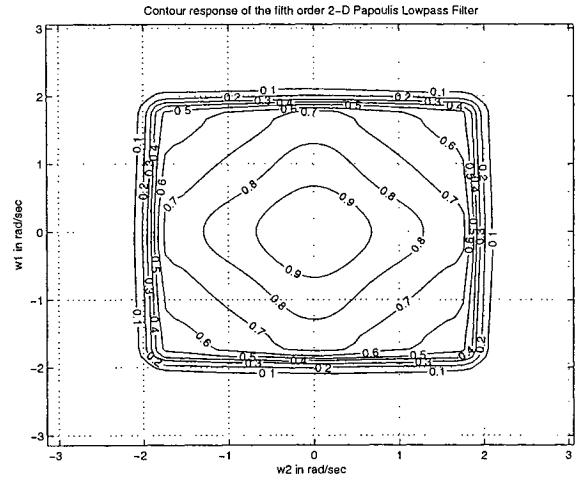

(e) When k1=0.75, k2=0.75, a1L=1 and a2L=1

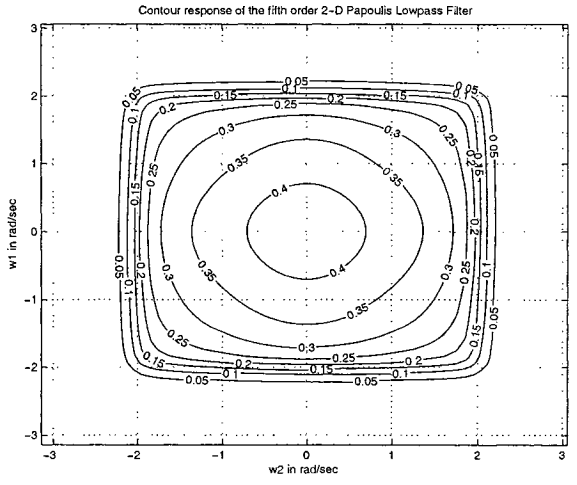

(f) When k1=0.75, k2=0.75, a1L=0.75 and a2L=0.75

Figure 3.8: Contour response of the fifth order 2-D digital Papoulis lowpass filter

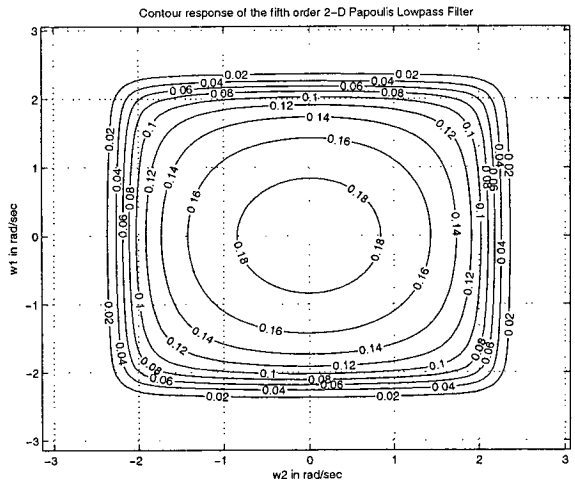

(a) When k1=0.75, k2=0.75, a1L=0.5 and a2L=0.5

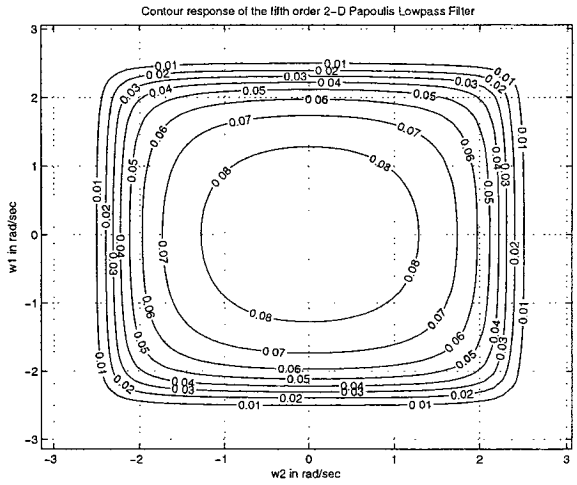

(b) When k1=0.75, k2=0.75, a1L=0.25 and a2L=0.25

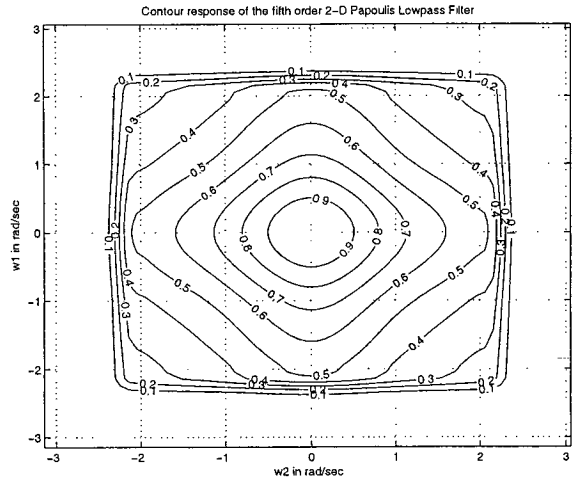

(c) When k1=0.5, k2=0.5, a1L=1 and a2L=1

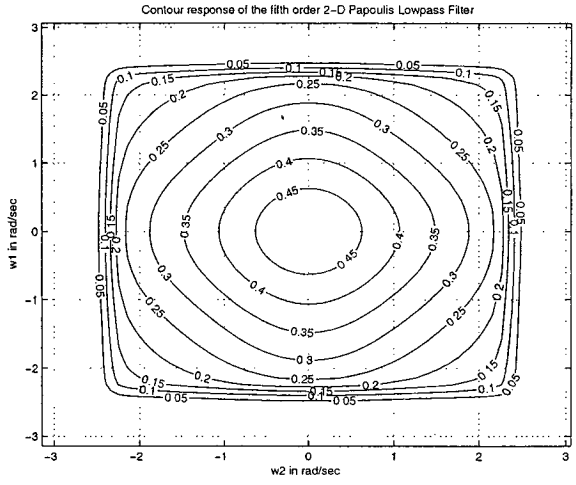

(d) When k1=0.5, k2=0.5, a1L=0.75 and a2L=0.75

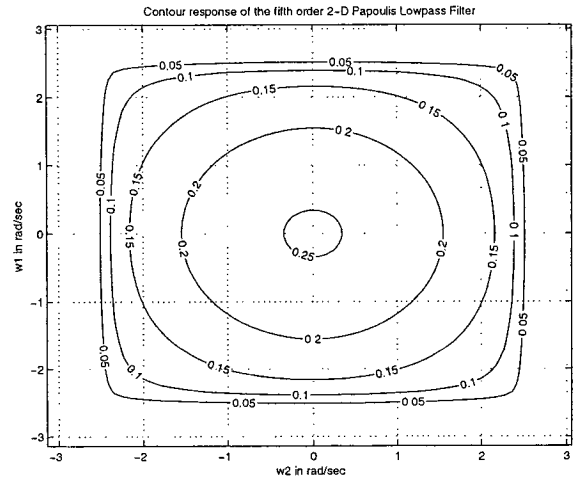

(e) When k1=0.5, k2=0.5, a1L=0.5 and a2L=0.5

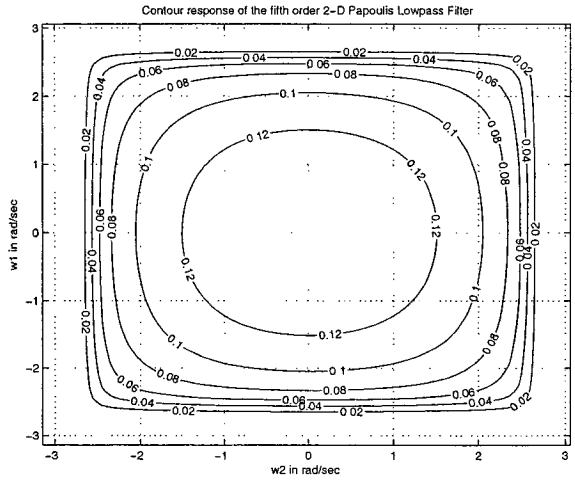

(f) When k1=0.5, k2=0.5, a1L=0.25 and a2L=0.25

Figure 3.9: Contour response of the fifth order 2-D digital Papoulis lowpass filter

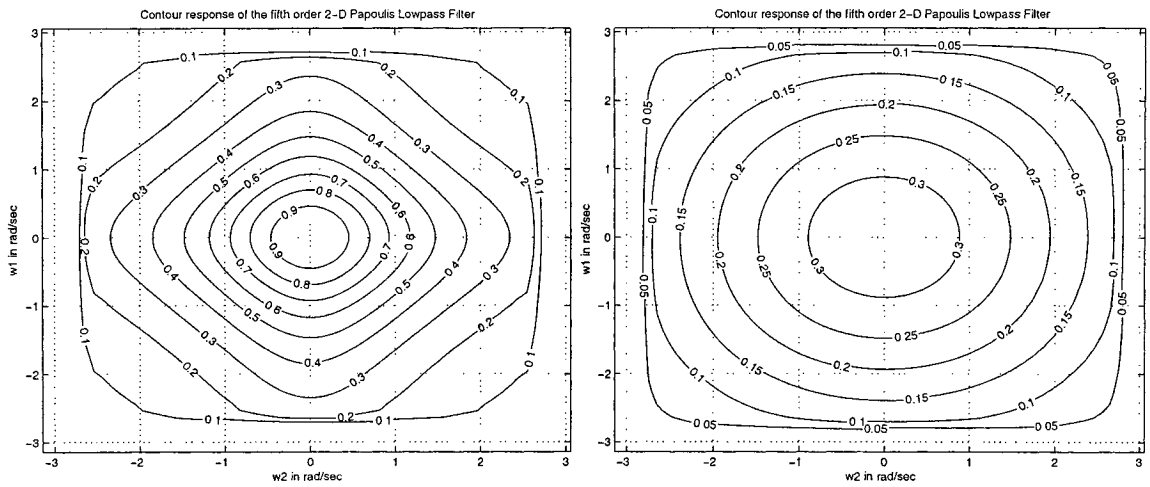

(a) When k1=0.25, k2=0.25, a1L=1 and a2L=1 (b) When k1=0.25, k2=0.25, a1L=0.5 and a2L=0.5

Figure 3.10: Contour response of the fifth order 2-D digital Papoulis lowpass filter

3.3 Generation of the fourth and fifth order 2-D Butterworth lowpass filters with monotonic characteristics

The fourth and fifth order 1-D analog Butterworth lowpass filters having monotonic amplitude-frequency response were derived in Sec. 2.4.2. In this section, we will generate 2-D analog Butterworth lowpass filters by cascading the 1-D analog Butterworth lowpass filters, and study their monotonic characteristics. Furthermore, we will apply generalized bilinear transformation (eqn. 3.2) to the 2-D analog lowpass filters to obtain 2-D digital filters having monotonic response. The 2-D digital filters will also be studied for different values of the constants, k_1, k_2, a_{1L}, a_{2L}, used in the generalized bilinear transformation.

3.3.1 Generation of fourth and fifth order 2-D analog Butterworth lowpass filter

We will generate fourth and fifth order 2-D analog Butterworth lowpass filters, by utilizing the fourth and fifth order 1-D analog Butterworth lowpass filters generated in Sec. 2.4.2 and study their monotonic characteristics.

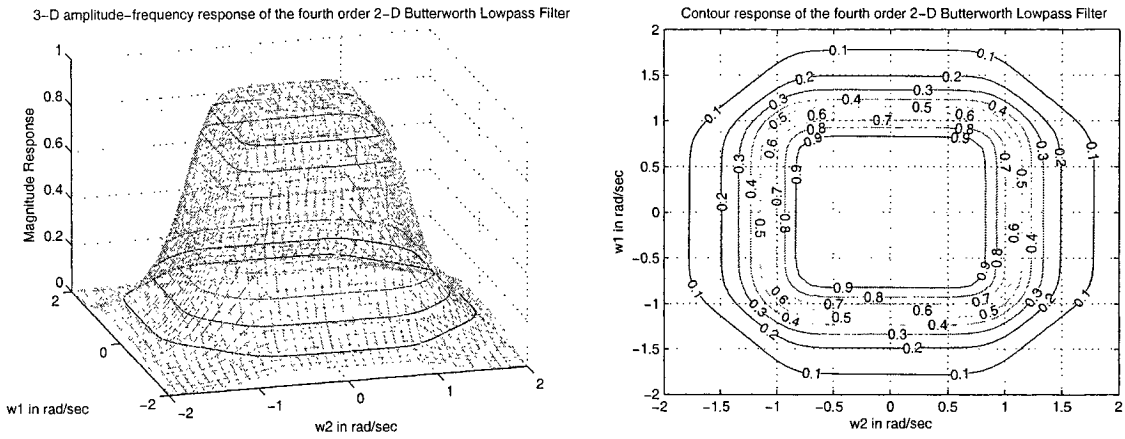

(a) 3-D amplitude-frequency response of the fourth order 2-D analog Butterworth lowpass filter

(b) Contour frequency response of the fourth order 2-D analog Butterworth lowpass filter

Figure 3.11: 3-D amplitude-frequency response and contour response of the fourth order 2-D analog Butterworth lowpass filter

3.3.1.1 Generation of fourth order 2-D analog Butterworth lowpass filter

The transfer function of the fourth order (i.e., $m = 4$) 1-D Butterworth filter, having flatness degree three (i.e., $i = 3$), is given by eqn. 2.45. By taking two such 1-D Butterworth lowpass filters in cascade, with denominator polynomials as function of s_1 and s_2 (with $s_1 = jw_1$ and $s_2 = jw_2$, eqn. 3.1) we get,

$$H_a(s_1, s_2) = \frac{1}{\begin{matrix}(s_1^2 + 1.8478s_1 + 1) & (s_1^2 + 0.7654s_1 + 1)\\ (s_2^2 + 1.8478s_2 + 1) & (s_2^2 + 0.7654s_2 + 1)\end{matrix}} \tag{3.7}$$

The amplitude-frequency response of the fourth order 2-D analog Butterworth lowpass filter (eqn. 3.7) is shown in the fig. 3.11. We can observe that the amplitude-frequency response is monotonically decreasing. The MATLAB code to plot the 3-D amplitude-frequency response and contour of the frequency response of the fourth and fifth order 2-D analog Papoulis lowpass filter is in algorithm 21.

Algorithm 21 The MATLAB code to plot the 3-D amplitude-frequency response and contour of the frequency response of the fourth and fifth order 2-D analog Butterworth lowpass filter

```
% Under Guidance of Prof. Dr. V. Ramachandran
% Student's name : Ajit Singh Sandhu..... ID:4841492.
clear all;
[w1,w2] = meshgrid(-2:0.1:2,-2:0.1:2);
s1=j*w1;
s2=j*w2;
ha1_1=(s1+0.3827+0.9239i).*(s1+0.3827-0.9239i).*(s1+0.9239+0.3827i).*(s1+0.9239-0.3827i);;
ha1_2=(s2+0.3827+0.9239i).*(s2+0.3827-0.9239i).*(s2+0.9239+0.3827i).*(s2+0.9239-0.3827i);
h1=abs(1./(ha1_1.*ha1_2));
figure(1);
contour3(w1,w2,h1);
surface(w1,w2,abs(h1),'EdgeColor',[.8 .8 .8],'FaceColor','none');
grid on;
view(-15,25);
%colormap cool;
title('3-D amplitude-frequency response of the fourth order 2-D Butterworth Lowpass Filter');
xlabel(' w2 in rad/sec ');
ylabel(' w1 in rad/sec ');
zlabel(' Magnitude Response ');
figure(2);
[C,h] = contour(w1,w2,h1);
clabel(C,h);
grid on;
%colormap cool;
title('Contour response of the fourth order 2-D Butterworth Lowpass Filter');
xlabel(' w2 in rad/sec ');
ylabel(' w1 in rad/sec ');
h1_1=(s1+1).*(s1+0.8090+0.5878i).*(s1+0.8090-0.5878i).*(s1+0.3090+0.9511i).*(s1+0.3090-0.9511i);
h1_2=(s2+1).*(s2+0.8090+0.5878i).*(s2+0.8090-0.5878i).*(s2+0.3090+0.9511i).*(s2+0.3090-0.9511i);
h=abs(1./(h1_1.*h1_2));
figure(3);
contour3(w1,w2,h);
surface(w1,w2,abs(h),'EdgeColor',[.8 .8 .8],'FaceColor','none');
grid on;
view(-15,25);
%colormap cool;
title('3-D amplitude-frequency response of the fifth order 2-D Butterworth Lowpass Filter');
xlabel(' w2 in rad/sec ');
ylabel(' w1 in rad/sec ');
zlabel(' Magnitude Response ');
figure(4);
[C,h] = contour(w1,w2,h);
clabel(C,h);
grid on;
%colormap cool;
title('Contour response of the fifth order 2-D Butterworth Lowpass Filter');
xlabel(' w2 in rad/sec ');
ylabel(' w1 in rad/sec ');
```

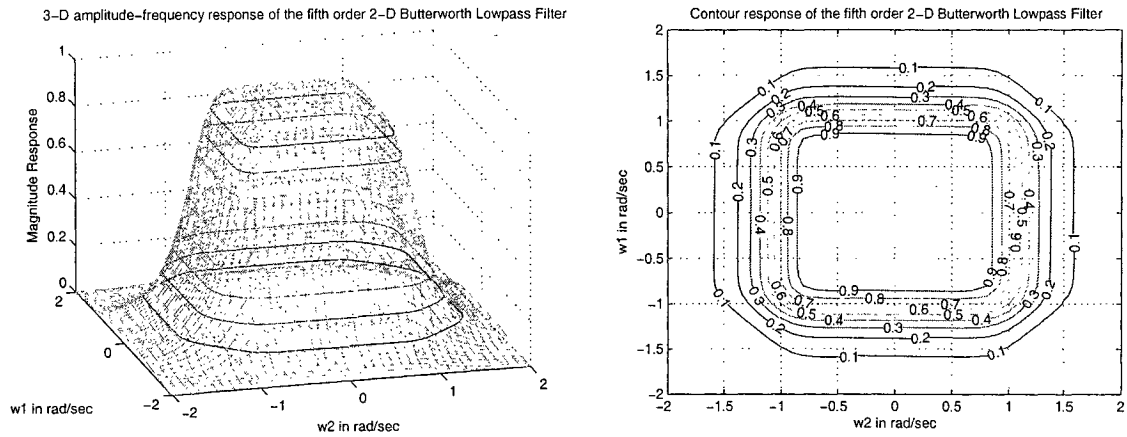

(a) 3-D amplitude-frequency response of the fifth order 2-D analog Butterworth lowpass filter

(b) Contour frequency response of the fifth order 2-D analog Butterworth lowpass filter

Figure 3.12: 3-D amplitude-frequency response and contour response of the fifth order 2-D analog Butterworth lowpass filter

3.3.1.2 Generation of fifth order 2-D analog Butterworth lowpass filter

The transfer function of the fifth order (i.e., $m = 5$) 1-D Butterworth filter, having flatness degree four (i.e., $i = 4$), is given by eqn. 2.47. By taking two such 1-D analog Butterworth lowpass filters in cascade, with denominator polynomials as function of s_1 and s_2 (with $s_1 = jw_1$ and $s_2 = jw_2$, eqn. 3.1) we get,

$$H_a(s_1, s_2) = \frac{1}{\begin{matrix}(s_1+1) & (s_1^2+1.618s_1+1) & (s_1^2+0.618s_2+1)\\ (s_2+1) & (s_2^2+1.618s_2+1) & (s_2^2+0.618s_2+1)\end{matrix}} \tag{3.8}$$

The amplitude-frequency response of the fifth order 2-D analog Butterworth lowpass filter (eqn. 3.8) is shown in the fig. 3.12. We can observe that the amplitude-frequency response is monotonically decreasing. The MATLAB code to plot the 3-D amplitude-frequency response and contour of the frequency response of the fourth and fifth order 2-D analog Papoulis lowpass filter is in algorithm 21.

3.3.1.3 Discussion

The amplitude-frequency response and contour of the frequency response of the fourth and fifth order 2-D Butterworth lowpass filter is shown in fig. 3.11 and 3.12, respectively. It is observed that, the amplitude-frequency response in the passband is flat and it is monotonically decreasing. The passband of the fifth order 2-D lowpass filter is wider with steeper transition band, in comparison to the fourth order 2-D lowpass Butterworth filter. By keeping one of the frequency axes at zero as reference, if we observe the frequency response from the other frequency axes, then the cutoff frequency (i.e., frequency at 0.707 magnitude value) will exist at ± 1 rad/sec. This is in correspondence to the 1-D Butterworth filter from which the 2-D lowpass filter is derived. Hence, the 2-D lowpass Butterworth filters have similar monotonic characteristics with cutoff frequency at ± 1 rad/sec as the equivalent 1-D Butterworth filter derived in Sec. 2.4.2. It is also observed that the 2-D frequency response is symmetrical.

3.3.2 Generation of fourth and fifth order 2-D digital Butterworth lowpass filter

Now, we will generate fourth and fifth order 2-D digital Butterworth lowpass filters. We will apply the generalized bilinear transformation (eqn. 3.2) in the fourth and fifth order 2-D analog Butterworth lowpass filters generated in Sec. 3.3.1, to obtain 2-D digital Butterworth lowpass filters. The resulting 2-D digital filter monotonic characteristics will be studied by taking different combinations of the constants in the bilinear transformation.

3.3.2.1 Generation of fourth order 2-D digital Butterworth lowpass filter

The transfer function of the fourth order 2-D analog Butterworth lowpass filter, is given by eqn. 3.7. By applying generalized bilinear transformation (eqn. 3.2) to eqn. 3.7, we get, transfer function of 2-D digital Papoulis lowpass filter as function of z_1 and z_2, with

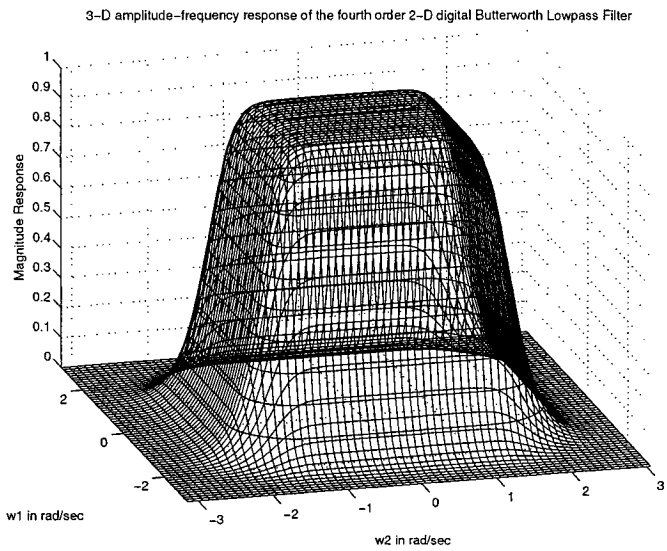

Figure 3.13: 3-D amplitude-frequency response of the fourth order 2-D digital Butterworth lowpass filter (When $k_1 = 1$, $k_2 = 1$, $a_{1L} = 1$, $a_{2L} = 1$)

$z_1 = e^{jw_1}$ and $z_2 = e^{jw_2}$. Therefore, we get,

$$H_d(z_1, z_2) = \frac{(z_1+1)^4 (z_2+1)^4}{\begin{array}{l}\left[k_1^2 (z_1 - a_{1L})^2 + 1.8478 k_1 (z_1 - a_{1L})(z_1+1) + (z_1+1)^2\right] \\ \left[k_1^2 (z_1 - a_{1L})^2 + 0.7654 k_1 (z_1 - a_{1L})(z_1+1) + (z_1+1)^2\right] \\ \left[k_2^2 (z_2 - a_{2L})^2 + 1.8478 k_2 (z_2 - a_{2L})(z_2+1) + (z_2+1)^2\right] \\ \left[k_2^2 (z_2 - a_{2L})^2 + 0.7654 k_2 (z_2 - a_{2L})(z_2+1) + (z_2+1)^2\right]\end{array}} \tag{3.9}$$

The 3-D amplitude-frequency response and contour plots of the fourth order 2-D digital Butterworth lowpass filter for different combination values of the constants is shown in the fig. 3.13, 3.14, 3.15 and 3.16. We can observe that the amplitude-frequency response is monotonically decreasing when constants (k_1, k_2, a_{1L} and a_{2L}) are having non-negative values. The MATLAB code to plot the 3-D amplitude-frequency response and contour of the frequency response of the fourth order 2-D digital Butterworth lowpass filter is in algorithm 22.

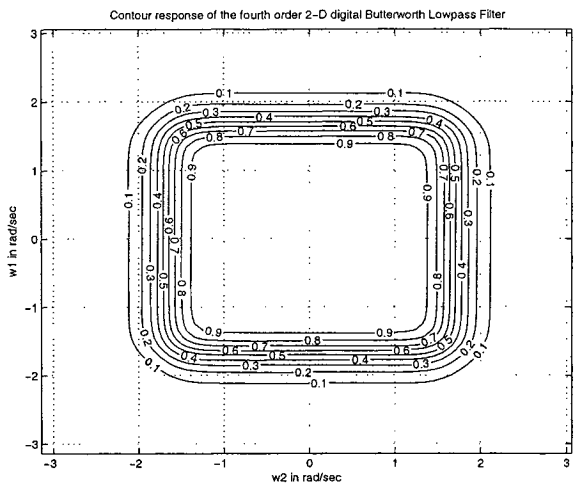

(a) When k1=1, k2=1, a1L=1 and a2L=1

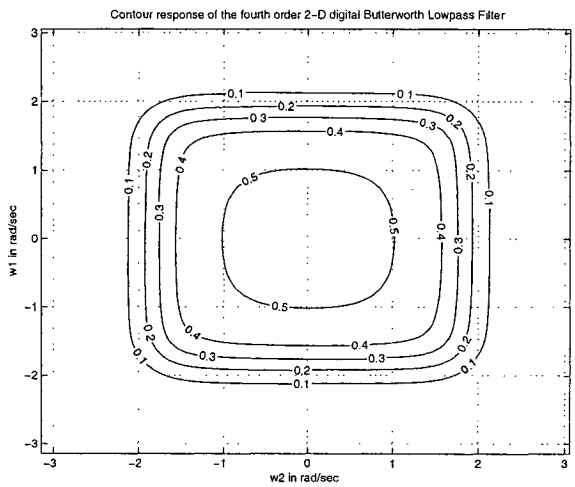

(b) When k1=1, k2=1, a1L=0.75 and a2L=0.75

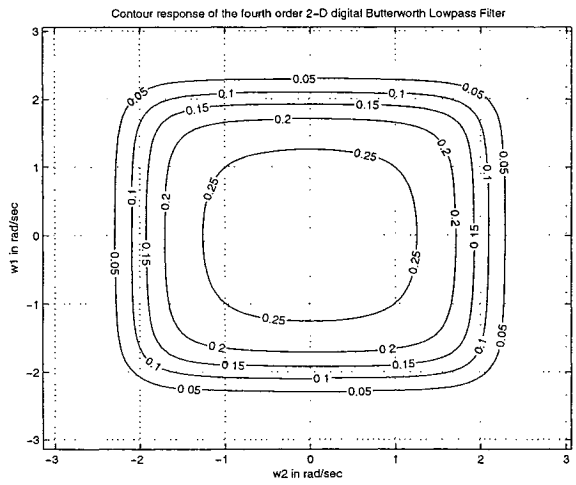

(c) When k1=1, k2=1, a1L=0.5 and a2L=0.5

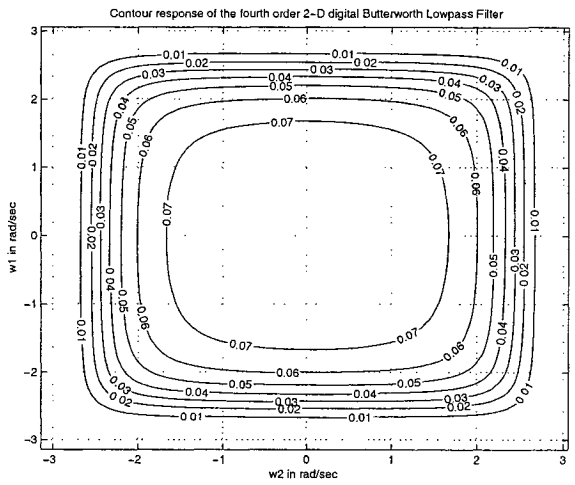

(d) When k1=1, k2=1, a1L=0 and a2L=0

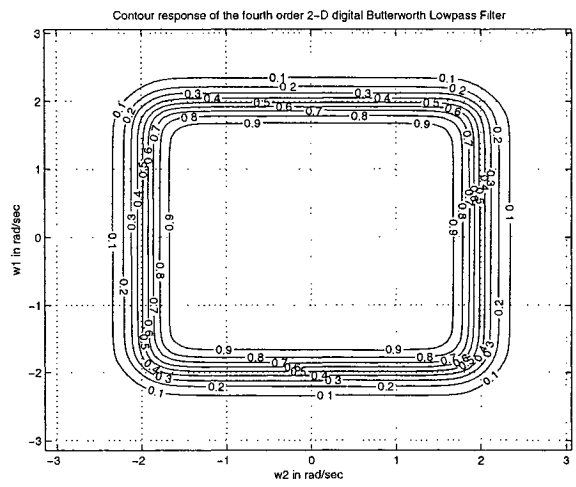

(e) When k1=0.75, k2=0.75, a1L=1 and a2L=1

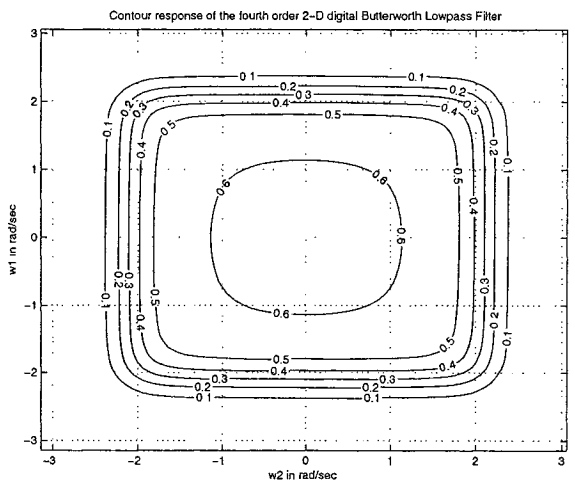

(f) When k1=0.75, k2=0.75, a1L=0.75 and a2L=0.75

Figure 3.14: Contour response of the fourth order 2-D digital Butterworth lowpass filter

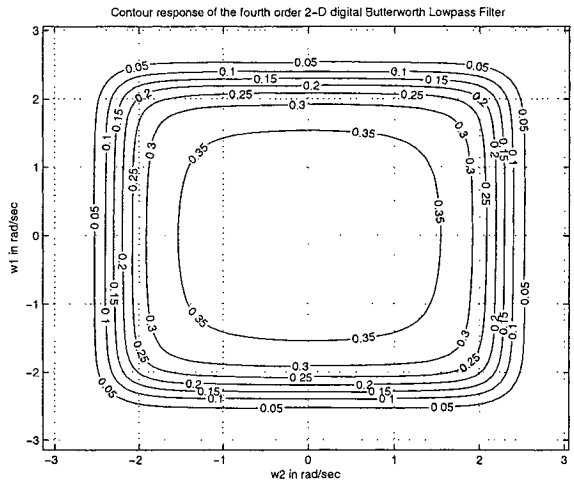

(a) When k1=0.75, k2=0.75, a1L=0.5 and a2L=0.5

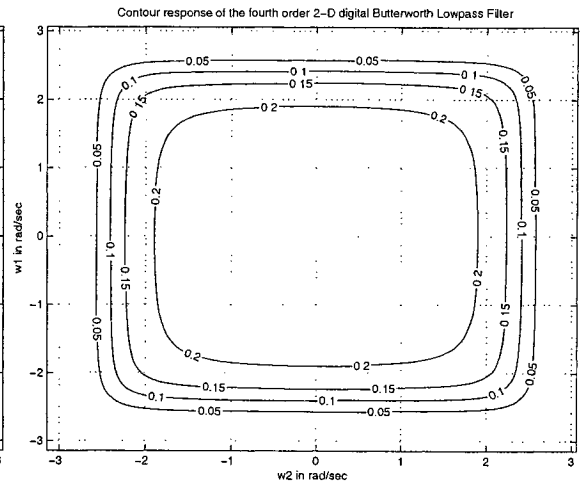

(b) When k1=0.75, k2=0.75, a1L=0.25 and a2L=0.25

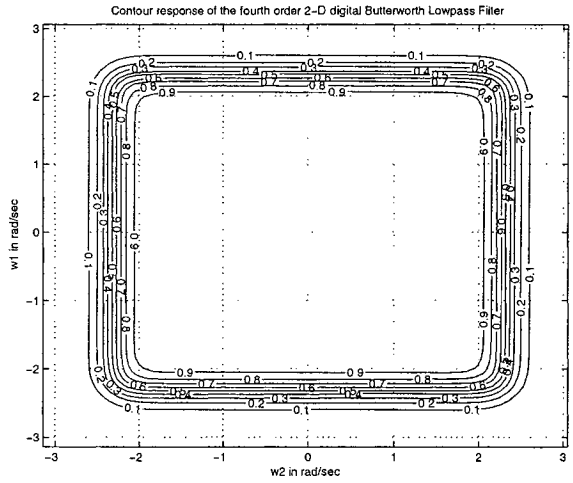

(c) When k1=0.5, k2=0.5, a1L=1 and a2L=1

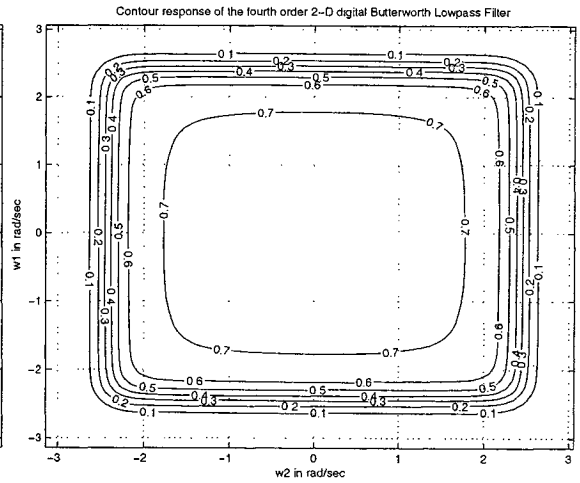

(d) When k1=0.5, k2=0.5, a1L=0.75 and a2L=0.75

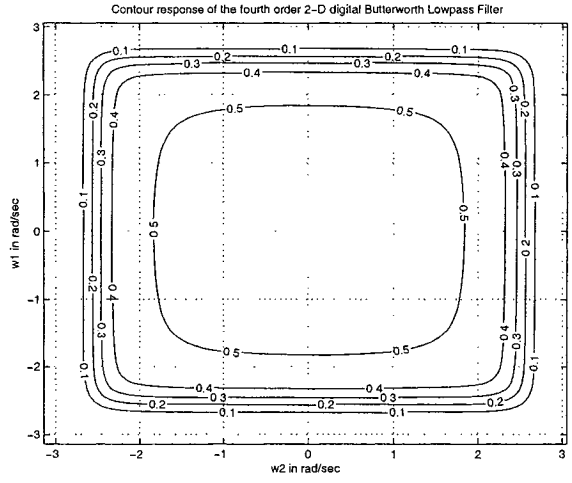

(e) When k1=0.5, k2=0.5, a1L=0.5 and a2L=0.5

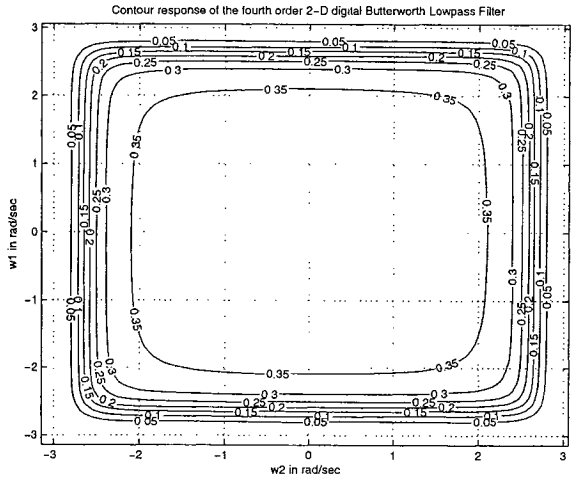

(f) When k1=0.5, k2=0.5, a1L=0.25 and a2L=0.25

Figure 3.15: Contour response of the fourth order 2-D digital Butterworth lowpass filter

Algorithm 22 The MATLAB code to plot the 3-D amplitude-frequency response and contour of the frequency response of the fourth order 2-D digital Butterworth lowpass filter

```
% Under Guidance of Prof. Dr. V. Ramachandran
% Student's name : Ajit Singh Sandhu..... ID:4841492.
clc; clear all;
k1=input('Give the value of the constant k1 for the bilinear LP transformation => ');
k2=input('Give the value of the constant k2 for the bilinear LP transformation => ');
a1L=input('Give the value of the constant a1L for the bilinear LP transformation => ');
a2L=input('Give the value of the constant a2L for the bilinear LP transformation => ');
% Creates two dimensional square matrix (mesh grid) of angular frequency w1 and w2.
[w1,w2] = meshgrid(-pi:0.1:pi,-pi:0.1:pi);
% Apply Z1=r1*exp(jw1) and Z2=r2*exp(jw2) with r1 = r2 =1
z1=exp(j.*w1);
z2=exp(j.*w2);
% Hd is the required digital transfer function and its value is evaluated as follows.
a=z1-a1L;
b=z2-a2L;
c=z1+1;
d=z2+1;
h1_1=(((k1.^2).*(a.^2))+(k1.*1.8478.*a.*c)+(c.^2))
.*(((k1.^2).*(a.^2))+(k1.*0.7654.*a.*c)+(c.^2));
h1_2=(((k2.^2).*(b.^2))+(k2.*1.8478.*b.*d)+(d.^2))
.*(((k2.^2).*(b.^2))+(k2.*0.7654.*b.*d)+(d.^2));
h1=abs(((c.^4).*(d.^4))./(h1_1.*h1_2));
figure(1);
contour3(w1,w2,h1);
surface(w1,w2,abs(h1),'EdgeColor',[.8 .8 .8],'FaceColor','none');
grid on;
view(-15,25);
%colormap cool;
title('3-D amplitude-frequency response of the fourth order 2-D digital Butterworth Lowpass Filter');
xlabel(' w2 in rad/sec ');
ylabel(' w1 in rad/sec ');
zlabel(' Magnitude Response ');
figure(2);
[C,h] = contour(w1,w2,h1);
clabel(C,h);
grid on;
%colormap cool;
title('Contour response of the fourth order 2-D digital Butterworth Lowpass Filter');
xlabel(' w2 in rad/sec ');
ylabel(' w1 in rad/sec ');
```

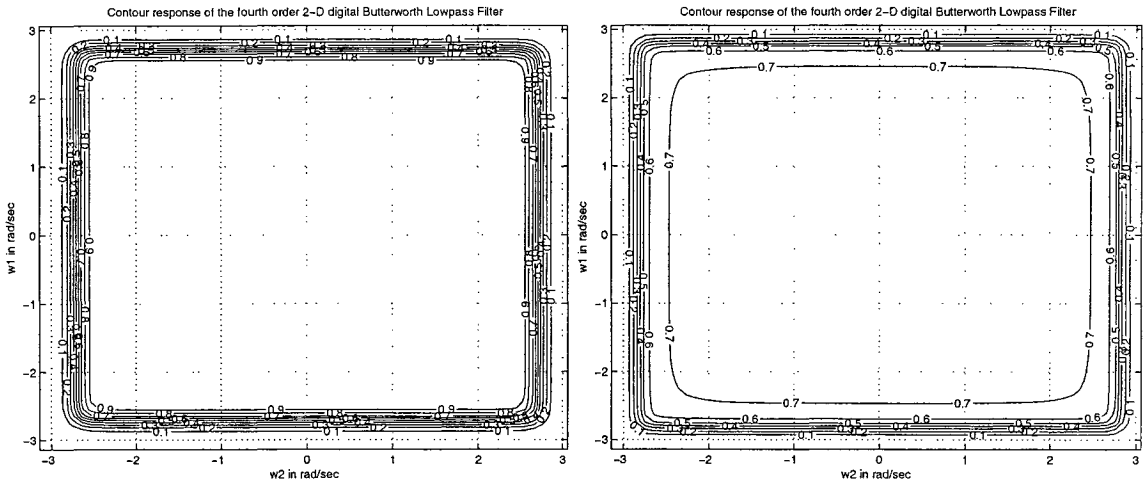

(a) When k1=0.25, k2=0.25, a1L=1 and a2L=1 (b) When k1=0.25, k2=0.25, a1L=0.5 and a2L=0.5

Figure 3.16: Contour response of the fourth order 2-D digital Butterworth lowpass filter

3.3.2.2 Generation of fifth order 2-D digital Butterworth lowpass filter

The transfer function of the fifth order 2-D analog Butterworth lowpass filter, is given by eqn. 3.8. By applying generalized bilinear transformation (eqn. 3.2) to eqn. 3.8, we get, transfer function of 2-D digital Butterworth lowpass filter as function of z_1 and z_2, with $z_1 = e^{jw_1}$ and $z_2 = e^{jw_2}$. Therefore, we get,

$$H_d(z_1, z_2) = \frac{(z_1+1)^5 (z_2+1)^5}{\begin{array}{c}[k_1 (z_1 - a_{1L}) + (z_1+1)][k_2 (z_2 - a_{2L}) + (z_2+1)] \\ \left[k_1^2 (z_1 - a_{1L})^2 + 1.618 k_1 (z_1 - a_{1L})(z_1+1) + (z_1+1)^2\right] \\ \left[k_1^2 (z_1 - a_{1L})^2 + 0.618 k_1 (z_1 - a_{1L})(z_1+1) + (z_1+1)^2\right] \\ \left[k_2^2 (z_2 - a_{2L})^2 + 1.618 k_2 (z_2 - a_{2L})(z_2+1) + (z_2+1)^2\right] \\ \left[k_2^2 (z_2 - a_{2L})^2 + 0.618 (z_2 - a_{2L})(z_2+1) + (z_2+1)^2\right]\end{array}} \quad (3.10)$$

The 3-D amplitude-frequency response and contour plots of the fifth order 2-D digital Butterworth lowpass filter for different combination values of the constants is shown in the fig. 3.17, 3.18, 3.19 and 3.20. We can observe that the amplitude-frequency response is monotonically decreasing when constants (k_1, k_2, a_{1L} and a_{2L}) are having non-negative

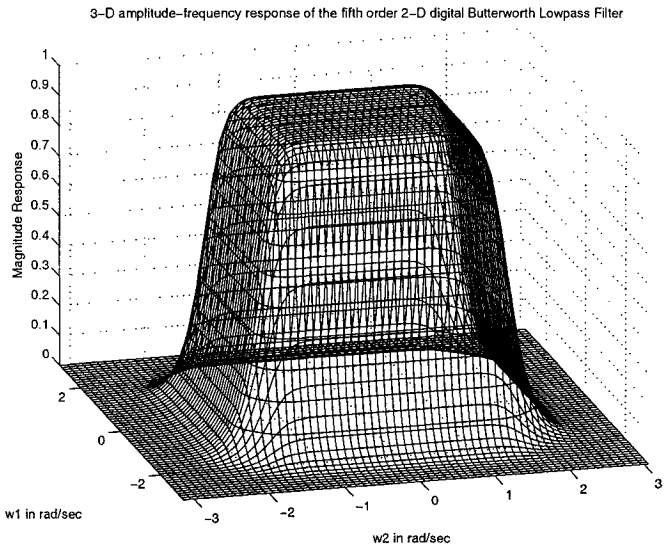

Figure 3.17: 3-D amplitude-frequency response of the fifth order 2-D digital Butterworth lowpass filter (When $k_1 = 1$, $k_2 = 1$, $a_{1L} = 1$, $a_{2L} = 1$)

values. The MATLAB code to plot the 3-D amplitude-frequency response and contour of the frequency response of the fifth order 2-D digital Papoulis lowpass filter is in algorithm 23.

3.3.2.3 Discussion

The characteristics of the 2-D digital filters proposed in Sec. 3.3.2.1 and 3.3.2.2 are studied in this sub-section. Fig. 3.13, 3.14, 3.15, 3.16, 3.17, 3.18, 3.19 and 3.20, shows amplitude-frequency response and contour plots of the 2-D Butterworth digital filters, based on the different values of the constants, k_1, k_2, a_{1L}, a_{2L}, of the generalized bilinear transformation.

In general, the coefficients, k_1, k_2, affects the passband width and a_{1L}, a_{2L} affects the gain. It is observed that for non-negative values of the constants, the 2-D digital Butterworth lowpass filters always have monotonic amplitude-frequency response with similar symmetry. The monotonic amplitude-frequency response of the fifth order 2-D digital Butterworth lowpass filters are wider in the passband and steeper in the transition band, in comparison the fourth order 2-D Butterworth lowpass filter, for the same coefficient values

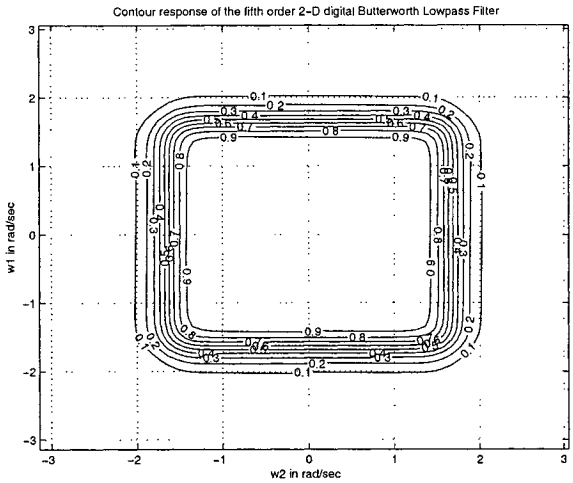

(a) When k1=1, k2=1, a1L=1 and a2L=1

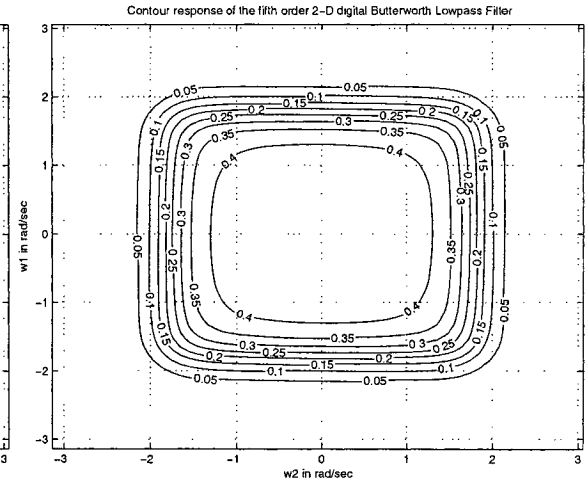

(b) When k1=1, k2=1, a1L=0.75 and a2L=0.75

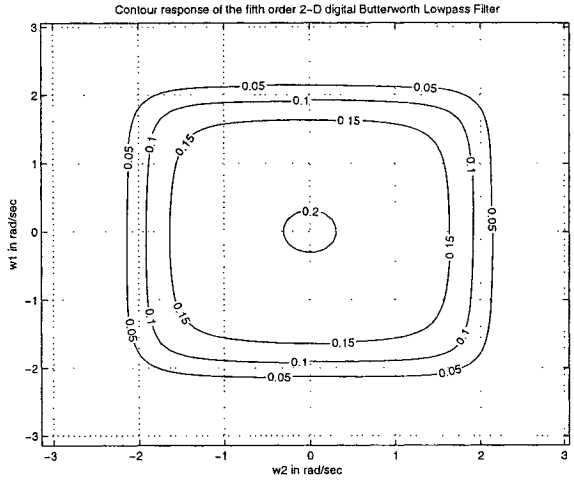

(c) When k1=1, k2=1, a1L=0.5 and a2L=0.5

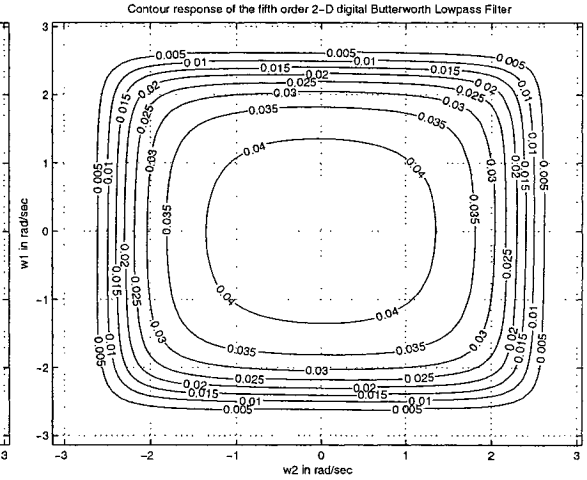

(d) When k1=1, k2=1, a1L=0 and a2L=0

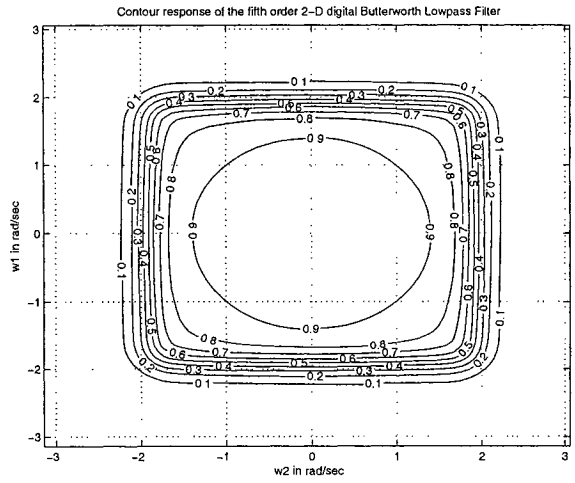

(e) When k1=0.75, k2=0.75, a1L=1 and a2L=1

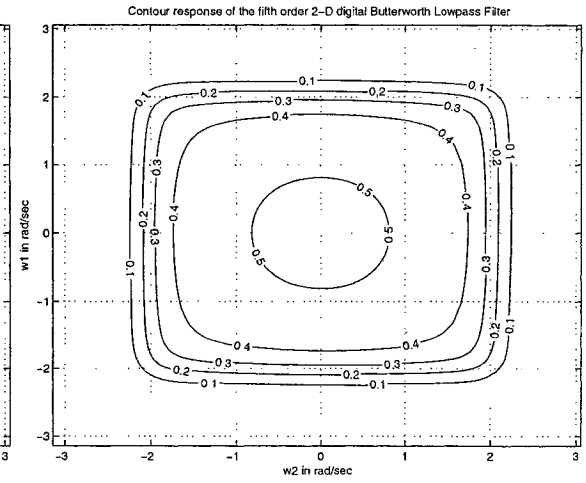

(f) When k1=0.75, k2=0.75, a1L=0.75 and a2L=0.75

Figure 3.18: Contour response of the fifth order 2-D digital Butterworth lowpass filter

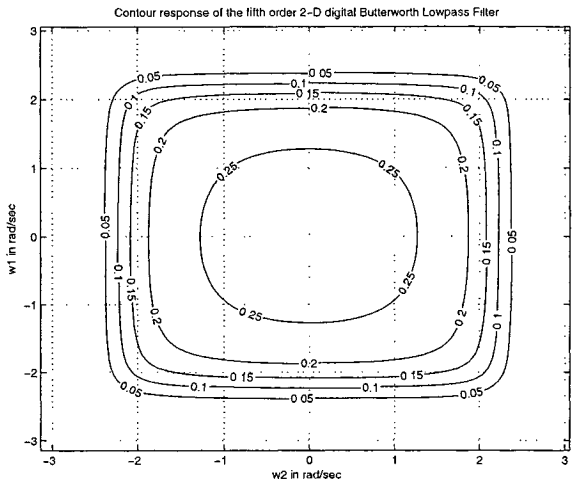

(a) When k1=0.75, k2=0.75, a1L=0.5 and a2L=0.5

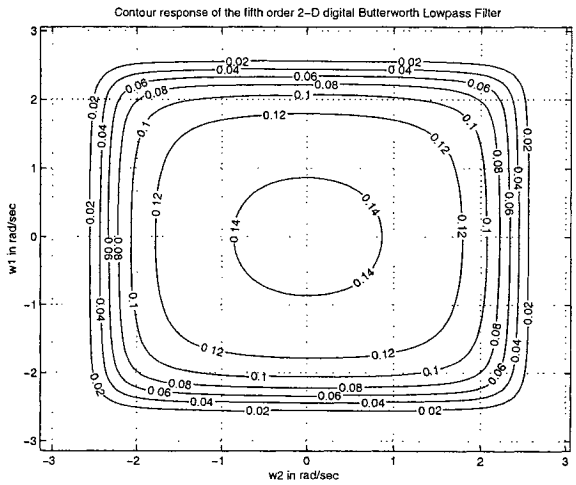

(b) When k1=0.75, k2=0.75, a1L=0.25 and a2L=0.25

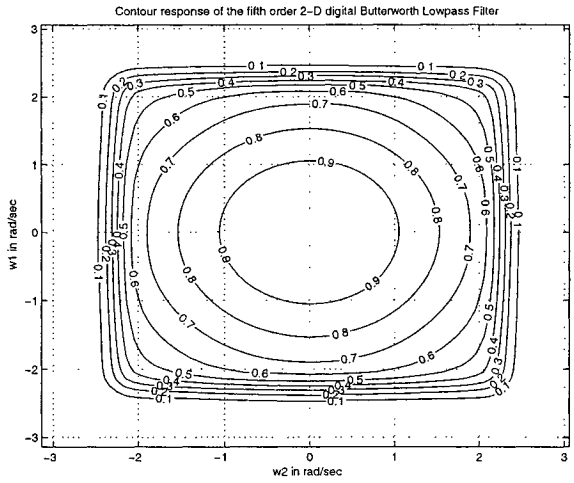

(c) When k1=0.5, k2=0.5, a1L=1 and a2L=1

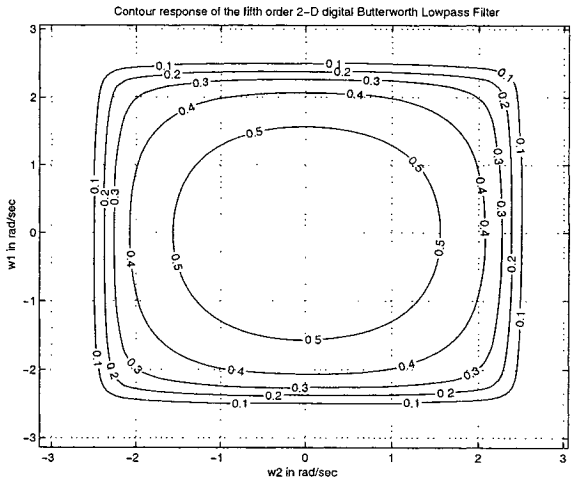

(d) When k1=0.5, k2=0.5, a1L=0.75 and a2L=0.75

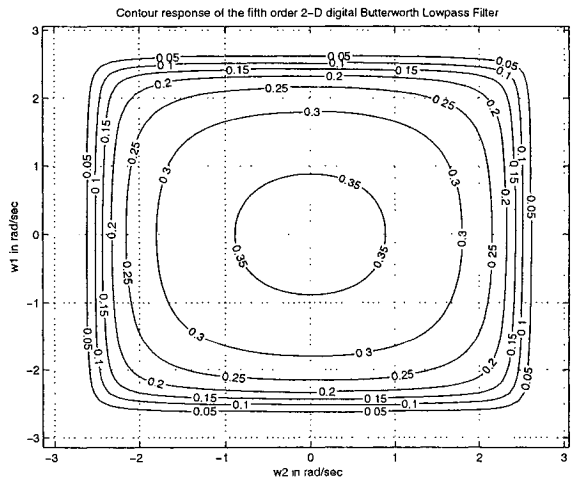

(e) When k1=0.5, k2=0.5, a1L=0.5 and a2L=0.5

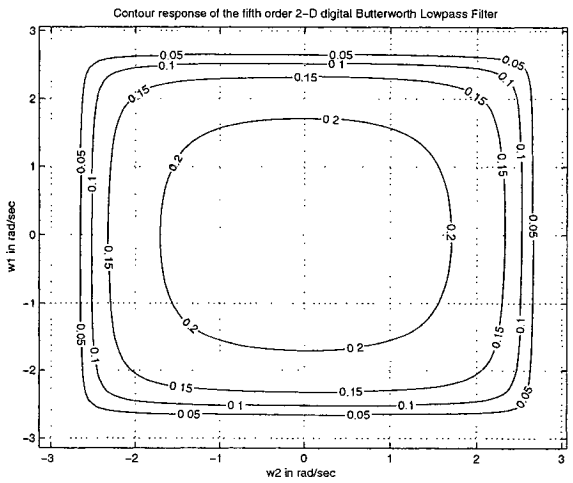

(f) When k1=0.5, k2=0.5, a1L=0.25 and a2L=0.25

Figure 3.19: Contour response of the fifth order 2-D digital Butterworth lowpass filter

Algorithm 23 The MATLAB code to plot the 3-D amplitude-frequency response and contour of the frequency response of the fifth order 2-D digital Butterworth lowpass filter

```
% Under Guidance of Prof. Dr. V. Ramachandran
% Student's name : Ajit Singh Sandhu..... ID:4841492.
clc; clear all;
k1=input('Give the value of the constant k1 for the bilinear LP transformation => ');
k2=input('Give the value of the constant k2 for the bilinear LP transformation => ');
a1L=input('Give the value of the constant a1L for the bilinear LP transformation => ');
a2L=input('Give the value of the constant a2L for the bilinear LP transformation => ');
% Creates two dimensional square matrix (mesh grid) of angular frequency w1 and w2.
[w1,w2] = meshgrid(-pi:0.1:pi,-pi:0.1:pi);
% Apply Z1=r1*exp(jw1) and Z2=r2*exp(jw2) with r1 = r2 =1
z1=exp(j.*w1);
z2=exp(j.*w2);
% Hd is the required digital transfer function and its value is evaluated as follows.
a=z1-a1L;
b=z2-a2L;
c=z1+1;
d=z2+1;
h1_1=(((k1.^2).*(a.^2))+(k1.*1.618.*a.*c)+(c.^2))
.*(((k1.^2).*(a.^2))+(k1.*0.618.*a.*c)+(c.^2)).*(a+c);
h1_2=(((k2.^2).*(b.^2))+(k2.*1.618.*b.*d)+(d.^2))
.*(((k2.^2).*(b.^2))+(k2.*0.618.*b.*d)+(d.^2)).*(b+d);
h1=abs(((c.^5).*(d.^5))./(h1_1.*h1_2));
figure(1);
contour3(w1,w2,h1);
surface(w1,w2,abs(h1),'EdgeColor',[.8 .8 .8],'FaceColor','none');
grid on;
view(-15,25);
%colormap cool;
title('3-D amplitude-frequency response of the fifth order 2-D digital Butterworth Lowpass Filter');
xlabel(' w2 in rad/sec ');
ylabel(' w1 in rad/sec ');
zlabel(' Magnitude Response ');
figure(2);
[C,h] = contour(w1,w2,h1);
clabel(C,h);
grid on;
%colormap cool;
title('Contour response of the fifth order 2-D digital Butterworth Lowpass Filter');
xlabel(' w2 in rad/sec ');
ylabel(' w1 in rad/sec ');
```

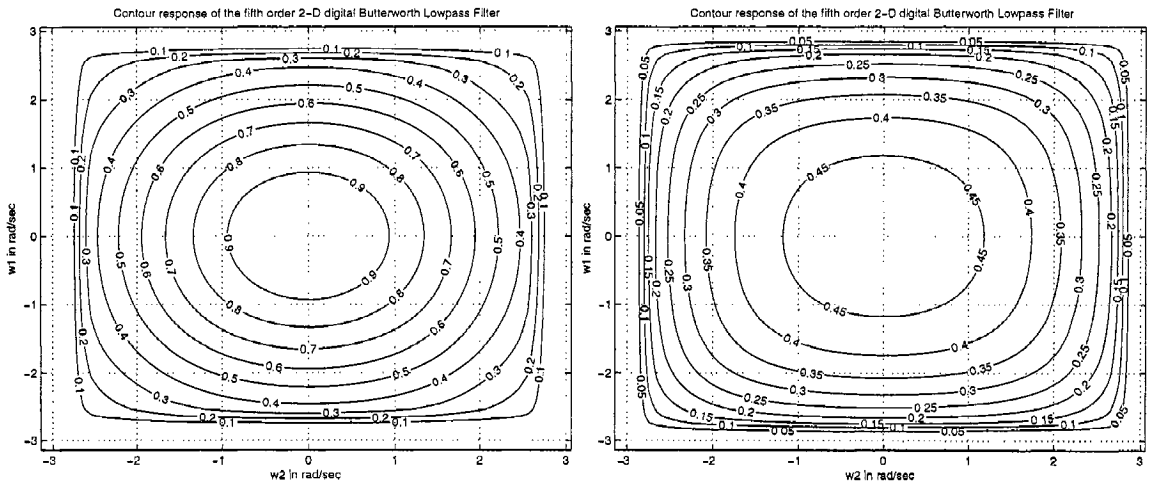

(a) When k1=0.25, k2=0.25, a1L=1 and a2L=1 (b) When k1=0.25, k2=0.25, a1L=0.5 and a2L=0.5

Figure 3.20: Contour response of the fifth order 2-D digital Butterworth lowpass filter

(for example fig. 3.14 (a) and 3.18 (a)). It is may also be noted that as the coefficients, k_1, k_2, values are decreased, the passband of the 2-D lowpass filter increases with decrease in magnitude, and it may result in loss of signal due to aliasing, because the nyguist rate may not be satisfied for certain input signals.

3.4 Generation of the fifth order 2-D Filanovsky lowpass filters with monotonic characteristics

The fifth order 1-D analog Filanovsky lowpass filters having monotonic amplitude-frequency response were derived in Sec. 2.4.3. In this section, we will generate 2-D analog Filanovsky lowpass filter by cascading the 1-D analog Filanovsky lowpass filters, and study their monotonic characteristics. Furthermore, we will apply generalized bilinear transformation (eqn. 3.2) to the 2-D analog lowpass filters to obtain 2-D digital filters having monotonic response. The 2-D digital filters will also be studied for different values of the constants, k_1, k_2, a_{1L}, a_{2L}, used in the generalized bilinear transformation.

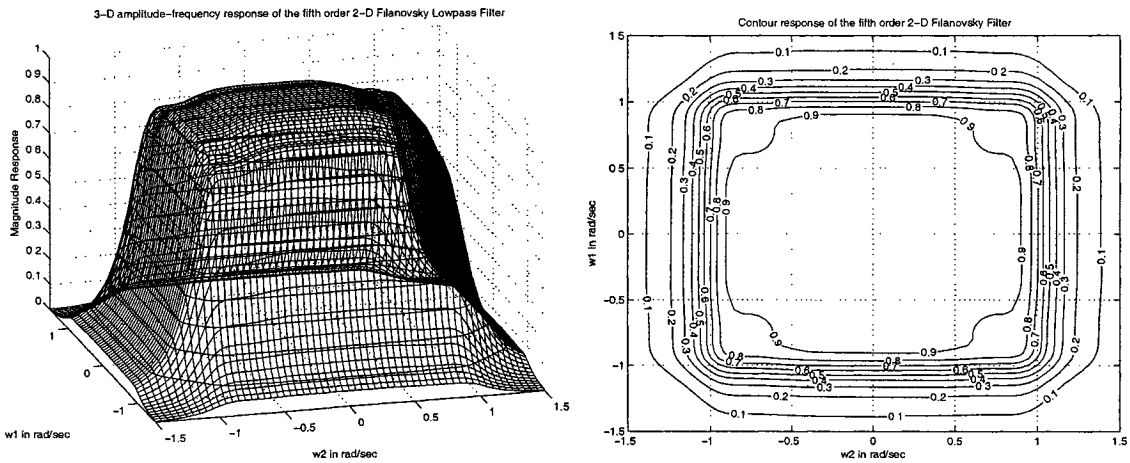

(a) 3-D amplitude-frequency response of the fifth order 2-D analog Filanovsky lowpass filter

(b) Contour frequency response of the fifth order 2-D analog Filanovsky lowpass filter

Figure 3.21: 3-D amplitude-frequency response and contour response of the fifth order 2-D analog Filanovsky lowpass filter

3.4.1 Generation of fifth order 2-D analog Filanovsky lowpass filter

We will generate fifth order 2-D analog Filanovsky lowpass filters, by utilizing the fifth order 1-D analog Filanovsky lowpass filters generated in Sec. 2.4.3 and study their monotonic characteristics. The transfer function of the fifth order (i.e., $m = 5$) 1-D Filanovsky filter, having flatness degree two (i.e., $i = 2$), is given by eqn. 2.49. By taking two such 1-D analog Filanovsky lowpass filters in cascade, with denominator polynomials as function of s_1 and s_2 (with $s_1 = jw_1$ and $s_2 = jw_2$, eqn. 3.1) we get,

$$H_a(s_1, s_2) = \frac{(0.3162)^2}{\begin{array}{l}(s_1 + 0.6445)\,(s_1^2 + 0.9508s_1 + 0.5116)\,(s_1^2 + 0.3492s_1 + 0.9592) \\ (s_2 + 0.6445)\,(s_2^2 + 0.9508s_2 + 0.5116)\,(s_2^2 + 0.3492s_2 + 0.9592)\end{array}} \tag{3.11}$$

The amplitude-frequency response of the fifth order 2-D analog Filanovsky lowpass filter (eqn. 3.11) is shown in the fig. 3.21. It is observed that, though the amplitude-frequency response in the passband is not relatively flat but still it is monotonically decreasing. By keeping one of the frequency axes at zero as reference, if we observe the frequency re-

Algorithm 24 The MATLAB code to plot the 3-D amplitude-frequency response and contour of the frequency response of the fifth order 2-D analog Filanovsky lowpass filter

```
% Under Guidance of Prof. Dr. V. Ramachandran
% Student's name : Ajit Singh Sandhu..... ID:4841492.
clear all;
[w1,w2] = meshgrid(-1.5:0.1:1.5,-1.5:0.1:1.5);
s1=j*w1;
s2=j*w2;
h1_1=(s1+0.6445).*(s1+0.4754+0.5344i).*(s1+0.4754-0.5344i).*(s1+0.1746+0.9637i).*(s1+0.1746-
0.9637i);
h1_2=(s2+0.6445).*(s2+0.4754+0.5344i).*(s2+0.4754-0.5344i).*(s2+0.1746+0.9637i).*(s2+0.1746-
0.9637i);
h=abs((0.3162^2)./(h1_1.*h1_2));
figure(1);
contour3(w1,w2,h);
surface(w1,w2,abs(h),'EdgeColor',[.8 .8 .8],'FaceColor','none');
grid on;
view(-15,25);
%colormap cool;
title('3-D amplitude-frequency response of the fifth order 2-D Filanovsky Lowpass Filter');
xlabel(' w2 in rad/sec ');
ylabel(' w1 in rad/sec ');
zlabel(' Magnitude Response ');
figure(2);
[C,h] = contour(w1,w2,h);
clabel(C,h);
grid on;
%colormap cool;
title('Contour response of the fifth order 2-D Filanovsky Lowpass Filter');
xlabel(' w2 in rad/sec ');
ylabel(' w1 in rad/sec ');
```

sponse from the other frequency axes, then the cutoff frequency (i.e., frequency at 0.707 magnitude value) will exist at ± 1 rad/sec. This is in correspondence to the 1-D Filanovsky filter from which the 2-D lowpass filter is derived. Hence, the 2-D lowpass Filanovsky filters have similar monotonic characteristics with cutoff frequency at ± 1 rad/sec as the equivalent 1-D Filanovsky filter derived in Sec. 2.4.3. It is also observed that the 2-D frequency response is symmetrical. The MATLAB code to plot the 3-D amplitude-frequency response and contour of the frequency response of the fifth order 2-D analog Filanovsky lowpass filter is in algorithm 24.

3.4.2 Generation of fifth order 2-D digital Filanovsky lowpass filter

The transfer function of the fifth order 2-D analog Filanovsky lowpass filter, is given by eqn. 3.11. By applying generalized bilinear transformation (eqn. 3.2) to eqn. 3.11, we get, transfer function of 2-D digital Filanovsky lowpass filter as function of z_1 and z_2, with $z_1 = e^{jw_1}$ and $z_2 = e^{jw_2}$. Therefore, we get,

$$H_d(z_1, z_2) = \frac{(0.3162)^2 (z_1+1)^5 (z_2+1)^5}{\begin{array}{l}[k_1 (z_1 - a_{1L}) + 0.6445 (z_1+1)]\,[k_2 (z_2 - a_{2L}) + 0.6445 (z_2+1)] \\ \left[k_1^2 (z_1 - a_{1L})^2 + 0.9508 k_1 (z_1 - a_{1L})(z_1+1) + 0.5116 (z_1+1)^2\right] \\ \left[k_1^2 (z_1 - a_{1L})^2 + 0.3492 k_1 (z_1 - a_{1L})(z_1+1) + 0.9592 (z_1+1)^2\right] \\ \left[k_2^2 (z_2 - a_{2L})^2 + 0.9508 k_2 (z_2 - a_{2L})(z_2+1) + 0.5116 (z_2+1)^2\right] \\ \left[k_2^2 (z_2 - a_{2L})^2 + 0.3492 (z_2 - a_{2L})(z_2+1) + 0.9592 (z_2+1)^2\right]\end{array}} \tag{3.12}$$

The 3-D amplitude-frequency response and contour plots of the fifth order 2-D digital Filanovsky lowpass filter for different combination values of the constants is shown in the fig. 3.22, 3.23, 3.24 and 3.25. The coefficients, k_1, k_2, affects the passband width and a_{1L}, a_{2L} affects the gain. We can observe that the amplitude-frequency response is monotonically decreasing with similar symmetry when constants (k_1, k_2, a_{1L} and a_{2L}) are having non-negative values. It is may also be noted that as the coefficients, k_1, k_2, values

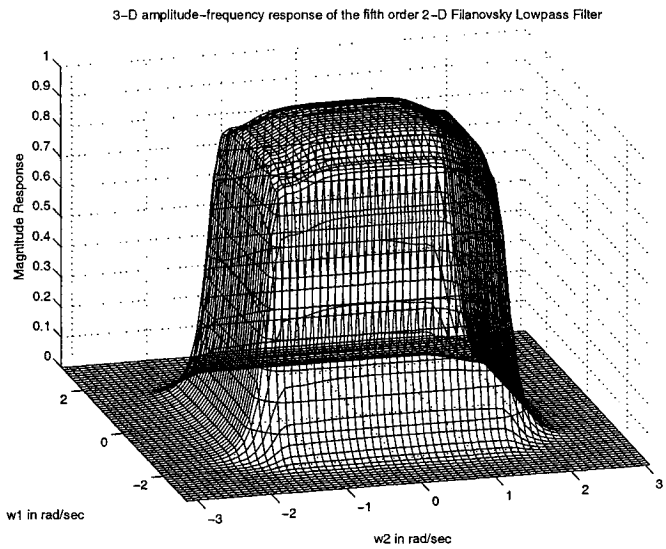

Figure 3.22: 3-D amplitude-frequency response of the fifth order 2-D digital Filanovsky lowpass filter (When $k_1 = 1, k_2 = 1, a_{1L} = 1, a_{2L} = 1$)

are decreased, the passband of the 2-D lowpass filter increases with decrease in magnitude, and it may result in loss of signal due to aliasing, because the nyguist rate may not be satisfied for certain input signals. The MATLAB code to plot the 3-D amplitude-frequency response and contour of the frequency response of the fifth order 2-D digital Filanovsky lowpass filter is in algorithm 25.

3.5 Generation of the fourth and fifth order 2-D Thomson-Bessel lowpass filters with monotonic characteristics

The fourth and fifth order 1-D analog Thomson-Bessel lowpass filters having monotonic amplitude-frequency response were derived in Sec. 2.5. In this section, we will generate 2-D analog Thomson-Bessel lowpass filters by cascading the 1-D analog Thomson-Bessel lowpass filters, and study their monotonic characteristics. Furthermore, we will apply generalized bilinear transformation (eqn. 3.2) to the 2-D analog lowpass filters, to obtain 2-D digital filters having monotonic response. The 2-D digital filters will also be studied for

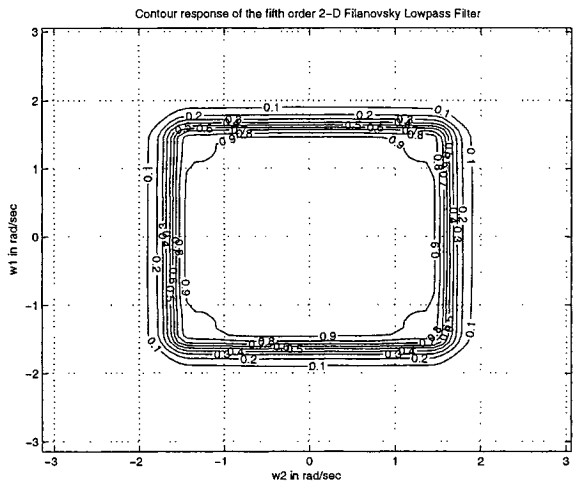

(a) When k1=1, k2=1, a1L=1 and a2L=1

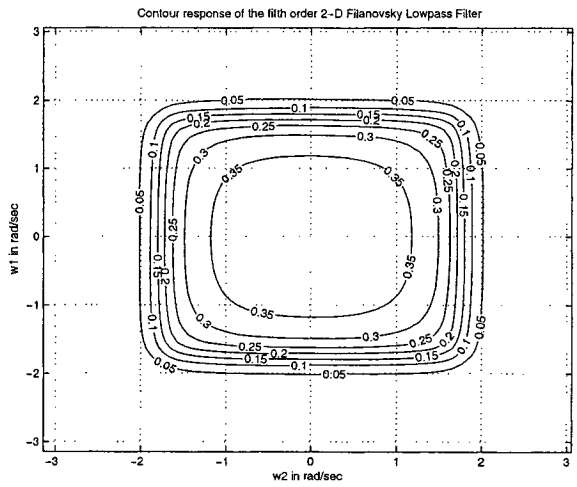

(b) When k1=1, k2=1, a1L=0.75 and a2L=0.75

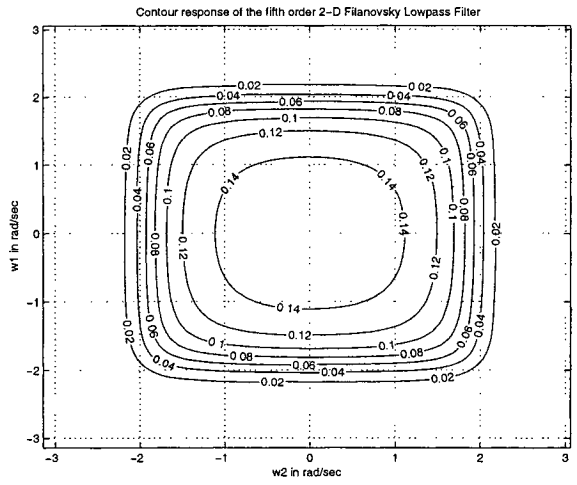

(c) When k1=1, k2=1, a1L=0.5 and a2L=0.5

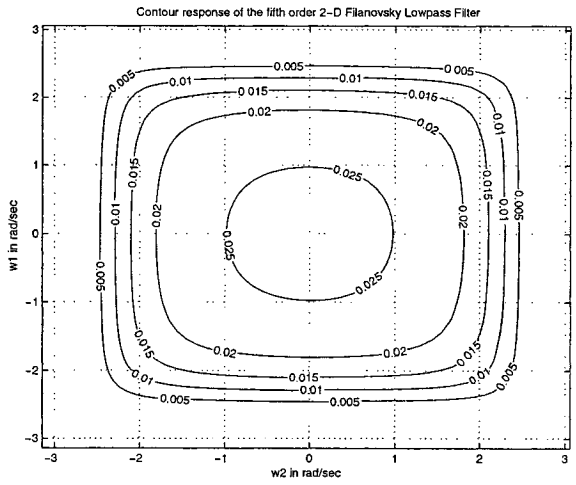

(d) When k1=1, k2=1, a1L=0 and a2L=0

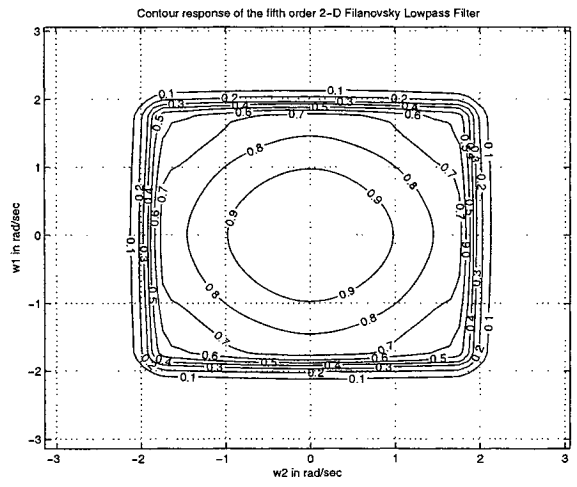

(e) When k1=0.75, k2=0.75, a1L=1 and a2L=1

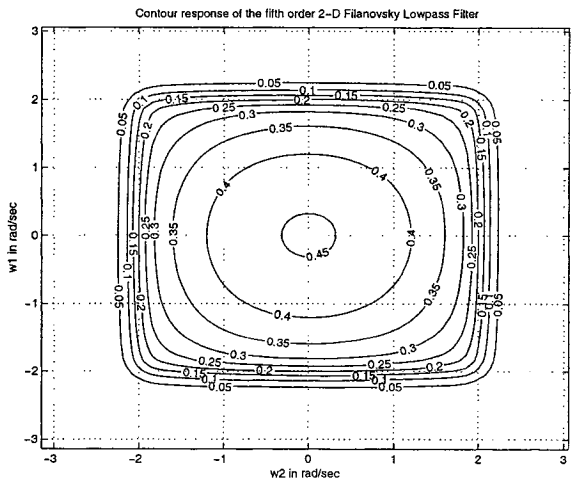

(f) When k1=0.75, k2=0.75, a1L=0.75 and a2L=0.75

Figure 3.23: Contour response of the fifth order 2-D digital Filanovsky lowpass filter

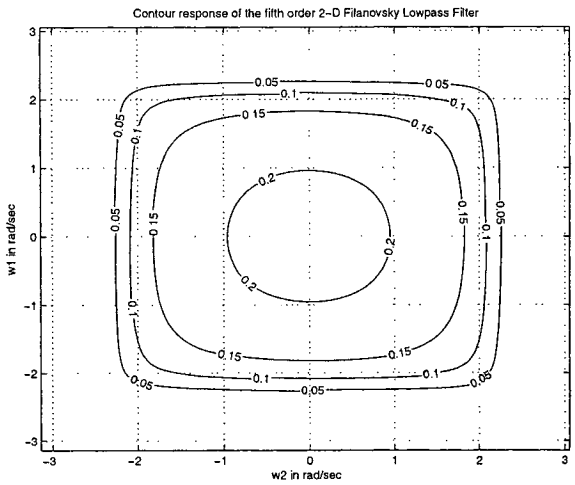

(a) When k1=0.75, k2=0.75, a1L=0.5 and a2L=0.5

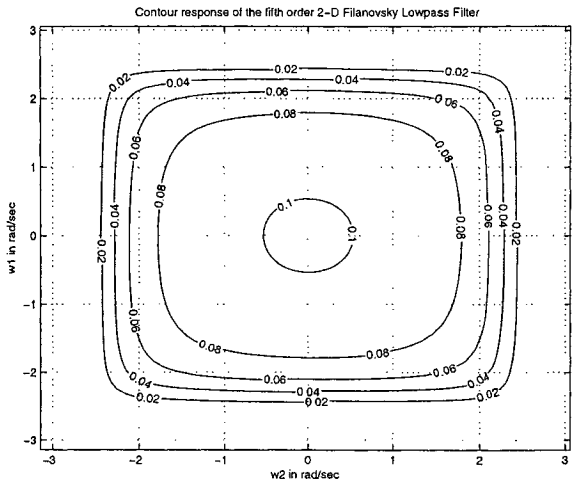

(b) When k1=0.75, k2=0.75, a1L=0.25 and a2L=0.25

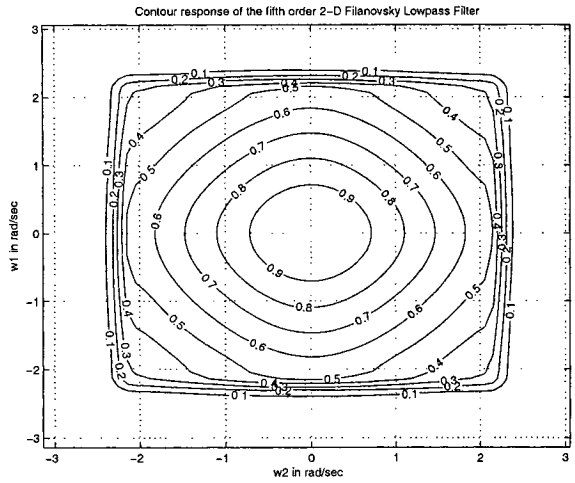

(c) When k1=0.5, k2=0.5, a1L=1 and a2L=1

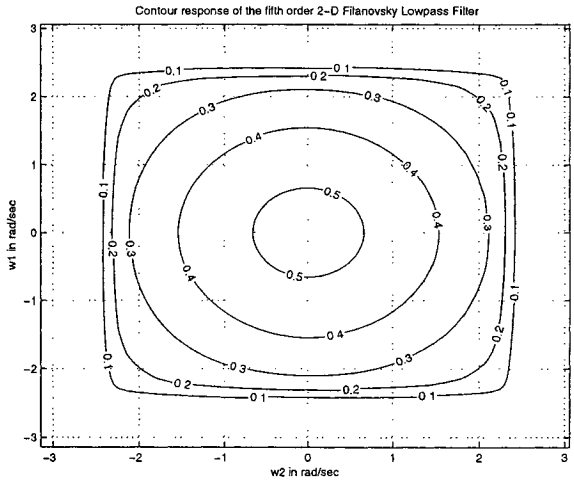

(d) When k1=0.5, k2=0.5, a1L=0.75 and a2L=0.75

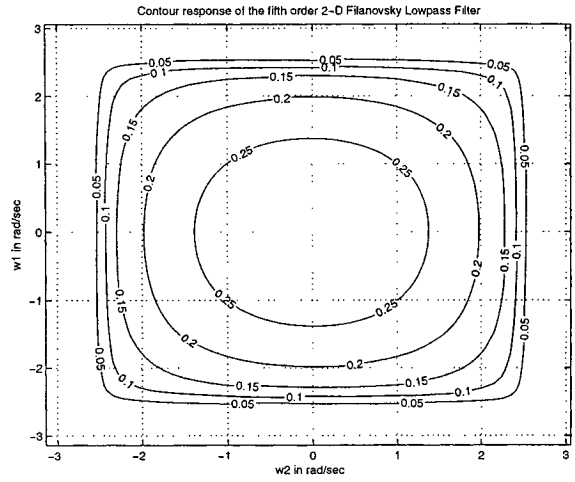

(e) When k1=0.5, k2=0.5, a1L=0.5 and a2L=0.5

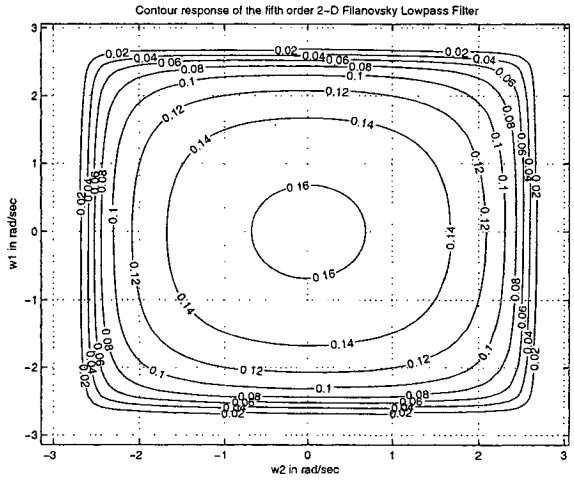

(f) When k1=0.5, k2=0.5, a1L=0.25 and a2L=0.25

Figure 3.24: Contour response of the fifth order 2-D digital Filanovsky lowpass filter

Algorithm 25 The MATLAB code to plot the 3-D amplitude-frequency response and contour of the frequency response of the fifth order 2-D digital Filanovsky lowpass filter

```
% Under Guidance of Prof. Dr. V. Ramachandran
% Student's name : Ajit Singh Sandhu..... ID:4841492.
clc; clear all;
k1=input('Give the value of the constant k1 for the bilinear LP transformation => ');
k2=input('Give the value of the constant k2 for the bilinear LP transformation => ');
a1L=input('Give the value of the constant a1L for the bilinear LP transformation => ');
a2L=input('Give the value of the constant a2L for the bilinear LP transformation => ');
% Creates two dimensional square matrix (mesh grid) of angular frequency w1 and w2.
[w1,w2] = meshgrid(-pi:0.1:pi,-pi:0.1:pi);
% Apply Z1=r1*exp(jw1) and Z2=r2*exp(jw2) with r1 = r2 =1
z1=exp(j.*w1);
z2=exp(j.*w2);
% Hd is the required digital transfer function and its value is evaluated as follows.
a=z1-a1L;
b=z2-a2L;
c=z1+1;
d=z2+1;
h1_1=(((k1.^2).*(a.^2))+(k1.*0.9508.*a.*c)+(0.5116.*(c.^2)))
.*(((k1.^2).*(a.^2))+(k1.*0.3492.*a.*c)+(0.9592.*(c.^2))).*(a+(0.6445.*c));
h1_2=(((k2.^2).*(b.^2))+(k2.*0.9508.*b.*d)+(0.5116.*(d.^2)))
.*(((k2.^2).*(b.^2))+(k2.*0.3492.*b.*d)+(0.9592.*(d.^2))).*(b+(0.6445.*d));
h1=abs(((c.^5).*(d.^5).*(0.3162.^2))./(h1_1.*h1_2));
figure(1);
contour3(w1,w2,h1);
surface(w1,w2,abs(h1),'EdgeColor',[.8 .8 .8],'FaceColor','none');
grid on;
view(-15,25);
%colormap cool;
title('3-D amplitude-frequency response of the fifth order 2-D Filanovsky Lowpass Filter');
xlabel(' w2 in rad/sec ');
ylabel(' w1 in rad/sec ');
zlabel(' Magnitude Response ');
figure(2);
[C,h] = contour(w1,w2,h1);
clabel(C,h);
grid on;
%colormap cool;
title('Contour response of the fifth order 2-D Filanovsky Lowpass Filter');
xlabel(' w2 in rad/sec ');
ylabel(' w1 in rad/sec ');
```

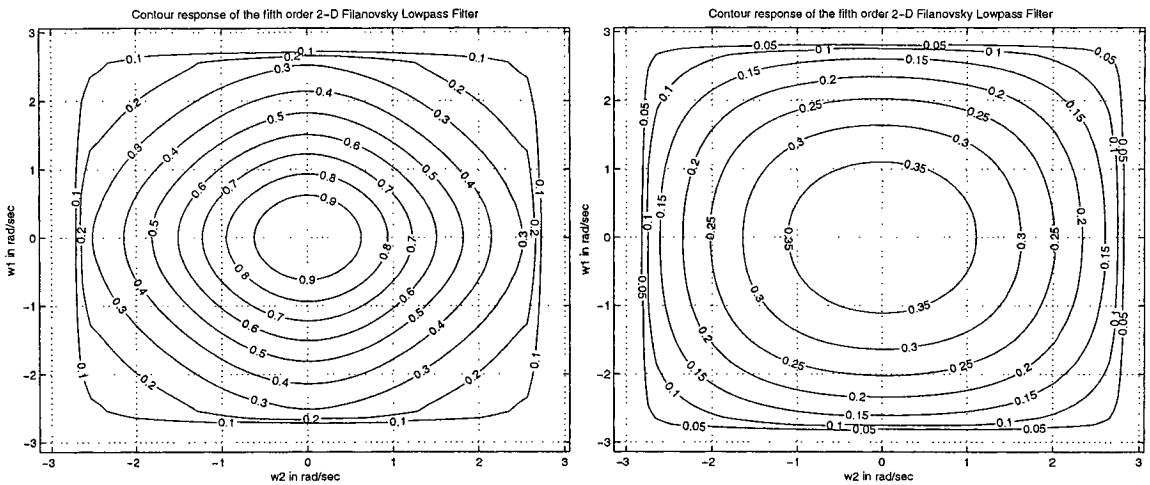

(a) When k1=0.25, k2=0.25, a1L=1 and a2L=1 (b) When k1=0.25, k2=0.25, a1L=0.5 and a2L=0.5

Figure 3.25: Contour response of the fifth order 2-D digital Filanovsky lowpass filter

different values of the constants, k_1, k_2, a_{1L}, a_{2L}, used in the generalized bilinear transformation.

3.5.1 Generation of fourth and fifth order 2-D analog Thomson-Bessel lowpass filters

We will generate fourth and fifth order 2-D analog Thomson-Bessel lowpass filters, by utilizing the fourth and fifth order 1-D analog Thomson-Bessel lowpass filters generated in Sec. 2.5 and study their monotonic characteristics.

3.5.1.1 Generation of fourth order 2-D analog Thomson-Bessel lowpass filter

The transfer function of the fourth order 1-D Thomson-Bessel filter, is given by eqn. 2.51. By taking two such 1-D Thomson-Bessel lowpass filters in cascade, with denominator polynomials as function of s_1 and s_2 (with $s_1 = jw_1$ and $s_2 = jw_2$, eqn. 3.1) we get,

$$H_a(s_1, s_2) = \frac{(105)^2}{(s_1^4 + 10s_1^3 + 45s_1^2 + 105s_1 + 105)} \\ (s_2^4 + 10s_2^3 + 45s_2^2 + 105s_2 + 105) \tag{3.13}$$

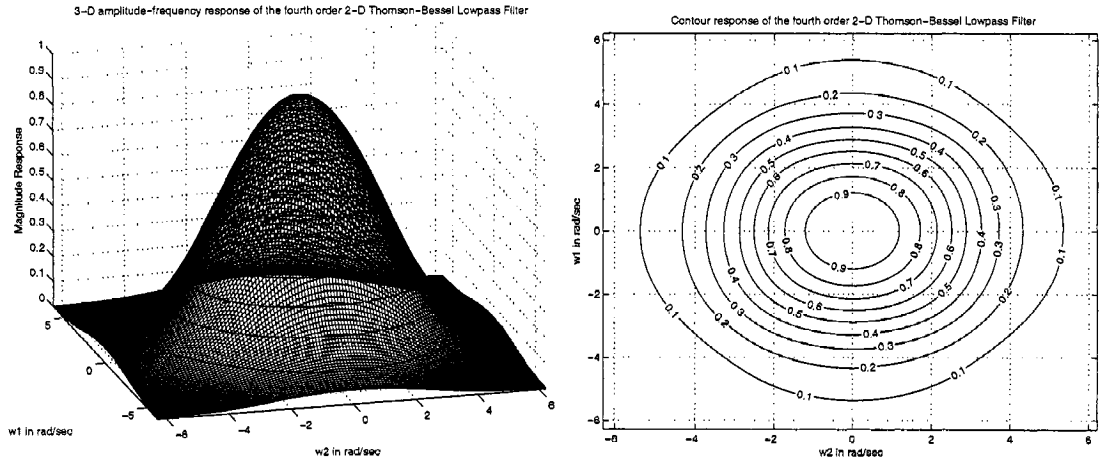

(a) 3-D amplitude-frequency response of the fourth order 2-D analog Thomson-Bessel lowpass filter

(b) Contour frequency response of the fourth order 2-D analog Thomson-Bessel lowpass filter

Figure 3.26: 3-D amplitude-frequency response and contour response of the fourth order 2-D analog Thomson-Bessel lowpass filter

The amplitude-frequency response of the fourth order 2-D analog Thomson-Bessel lowpass filter (eqn. 3.13) is shown in the fig. 3.26. We can observe that the amplitude-frequency response is monotonically decreasing. The MATLAB code to plot the 3-D amplitude-frequency response and contour of the frequency response of the fourth and fifth order 2-D analog Thomson-Bessel lowpass filter is in algorithm 26.

3.5.1.2 Generation of fifth order 2-D analog Thomson-Bessel lowpass filter

The transfer function of the fifth order 1-D Thomson-Bessel filter, is given by eqn. 2.53. By taking two such 1-D Thomson-Bessel lowpass filters in cascade, with denominator polynomials as function of s_1 and s_2 (with $s_1 = jw_1$ and $s_2 = jw_2$, eqn. 3.1) we get,

$$H_a(s_1, s_2) = \frac{(945)^2}{(s_1^5 + 15s_1^4 + 105s_1^3 + 420s_1^2 + 945s_1 + 945)} \\ (s_2^5 + 15s_2^4 + 105s_2^3 + 420s_2^2 + 945s_2 + 945) \tag{3.14}$$

The amplitude-frequency response of the fifth order 2-D analog Thomson-Bessel low-

Algorithm 26 The MATLAB code to plot the 3-D amplitude-frequency response and contour of the frequency response of the fourth and fifth order 2-D analog Thomson-Bessel lowpass filter

```
% Under Guidance of Prof. Dr. V. Ramachandran
% Student's name : Ajit Singh Sandhu..... ID:4841492.
clear all;
[w1,w2] = meshgrid(-2*pi:0.1:2*pi,-2*pi:0.1:2*pi);
s1=j*w1;
s2=j*w2;
ha1_1=s1.^4+10.*s1.^3+45.*s1.^2+105.*s1+105;
ha1_2=s2.^4+10.*s2.^3+45.*s2.^2+105.*s2+105;
h1=abs((105^2)./(ha1_1.*ha1_2));
figure(1);
contour3(w1,w2,h1);
surface(w1,w2,abs(h1),'EdgeColor',[.8 .8 .8],'FaceColor','none');
grid on;
view(-15,25);
%colormap cool;
title('3-D amplitude-frequency response of the fourth order 2-D Thomson-Bessel Lowpass Filter');
xlabel(' w2 in rad/sec ');
ylabel(' w1 in rad/sec ');
zlabel(' Magnitude Response ');
figure(2);
[C,h] = contour(w1,w2,h1);
clabel(C,h);
grid on;
%colormap cool;
title('Contour response of the fourth order 2-D Thomson-Bessel Lowpass Filter');
xlabel(' w2 in rad/sec ');
ylabel(' w1 in rad/sec ');
h1_1=(s1.^5+15.*s1.^4+105.*s1.^3+420.*s1.^2+945.*s1+945);
h1_2=(s2.^5+15.*s2.^4+105.*s2.^3+420.*s2.^2+945.*s2+945);
h=abs((945^2)./(h1_1.*h1_2));
figure(3);
contour3(w1,w2,h);
surface(w1,w2,abs(h),'EdgeColor',[.8 .8 .8],'FaceColor','none');
grid on;
view(-15,25);
%colormap cool;
title('3-D amplitude-frequency response of the fifth order 2-D Thomson-Bessel Lowpass Filter');
xlabel(' w2 in rad/sec ');
ylabel(' w1 in rad/sec ');
zlabel(' Magnitude Response ');
figure(4);
[C,h] = contour(w1,w2,h);
clabel(C,h);
grid on;
%colormap cool;
title('Contour response of the fifth order 2-D Thomson-Bessel Lowpass Filter');
xlabel(' w2 in rad/sec ');
ylabel(' w1 in rad/sec ');
```

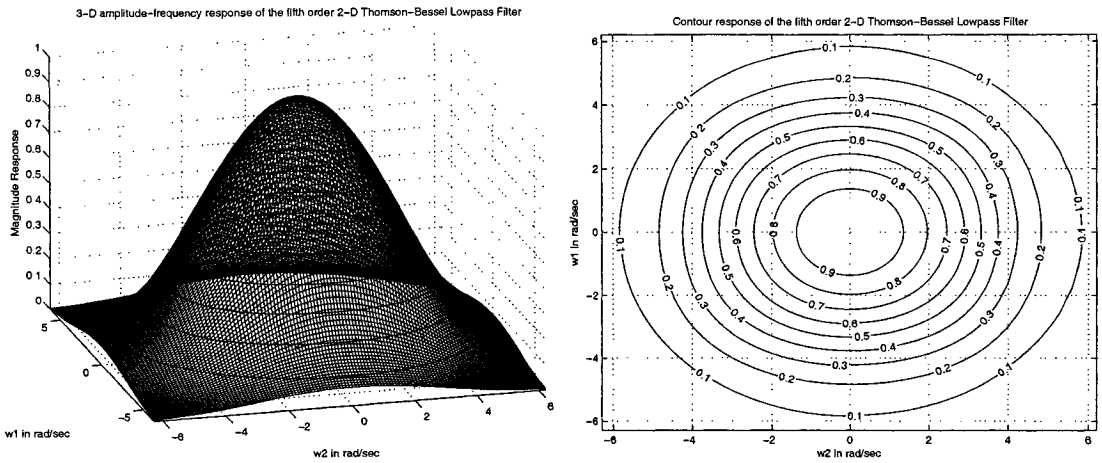

(a) 3-D amplitude-frequency response of the fifth order 2-D analog Thomson-Bessel lowpass filter

(b) Contour frequency response of the fifth order 2-D analog Thomson-Bessel lowpass filter

Figure 3.27: 3-D amplitude-frequency response and contour response of the fifth order 2-D analog Thomson-Bessel lowpass filter

pass filter (eqn. 3.14) is shown in the fig. 3.27. We can observe that the amplitude-frequency response is monotonically decreasing. The MATLAB code to plot the 3-D amplitude-frequency response and contour of the frequency response of the fourth and fifth order 2-D analog Thomson-Bessel lowpass filter is in algorithm 26.

3.5.1.3 Discussion

The amplitude-frequency response and contour of the frequency response of the Thomson-Bessel fourth and fifth order 2-D Thomson-Bessel lowpass filter is shown in fig. 3.26 and 3.27, respectively. It is observed that the amplitude-frequency response in the passband is flat, and it is monotonically decreasing. The passband of the fifth order 2-D lowpass filter is much wider with steeper transition band, in comparison to the fourth order 2-D lowpass Thomson-Bessel filter. The 2-D lowpass Thomson-Bessel filters have similar monotonic characteristics as the equivalent 1-D Thomson-Bessel filter derived in Sec. 2.5. It is also observed that the 2-D frequency response is symmetrical.

3.5.2 Generation of fourth and fifth order 2-D digital Thomson-Bessel lowpass filter

Now, we will generate fourth and fifth order 2-D digital Thomson-Bessel lowpass filters. We will apply the generalized bilinear transformation (eqn. 3.2) in the fourth and fifth order 2-D analog Thomson-Bessel lowpass filters generated in Sec. 3.5.1, to obtain 2-D digital Thomson-Bessel lowpass filters. The resulting 2-D digital filter monotonic characteristics will be studied by taking different values of the constants in the bilinear transformation.

3.5.2.1 Generation of fourth order 2-D digital Thomson-Bessel lowpass filter

The transfer function of the fourth order 2-D analog Thomson-Bessel lowpass filter, is given by eqn. 3.13. By applying generalized bilinear transformation (eqn. 3.2) to eqn. 3.13, we get, transfer function of 2-D digital Thomson-Bessel lowpass filter as function of z_1 and z_2, with $z_1 = e^{jw_1}$ and $z_2 = e^{jw_2}$. Hence, we get,

$$H_d(z_1, z_2) = \frac{(105)^2 (z_1+1)^4 (z_2+1)^4}{\left[k_1^4 (z_1 - a_{1L})^4 + 10k_1^3 (z_1 - a_{1L})^3 (z_1+1) + 45k_1^2 (z_1 - a_{1L})^2 (z_1+1)^2 + 105k_1 (z_1 - a_{1L}) (z_1+1)^3 + 105 (z_1+1)^4\right] \left[k_2^4 (z_2 - a_{2L})^4 + 10k_2^3 (z_2 - a_{2L})^3 (z_2+1) + 45k_2^2 (z_2 - a_{2L})^2 (z_2+1)^2 + 105k_2 (z_2 - a_{2L}) (z_2+1)^3 + 105 (z_2+1)^4\right]} \tag{3.15}$$

The 3-D amplitude-frequency response and contour plots of the fourth order 2-D digital Thomson-Bessel lowpass filter for different combination values of the constants is shown in the fig. 3.28, 3.29, 3.30 and 3.31. We can observe that the amplitude-frequency response is monotonically decreasing when constants (k_1, k_2, a_{1L} and a_{2L}) are having non-negative values. The MATLAB code to plot the 3-D amplitude-frequency response and contour of the frequency response of the fourth order 2-D digital Thomson-Bessel lowpass filter is in

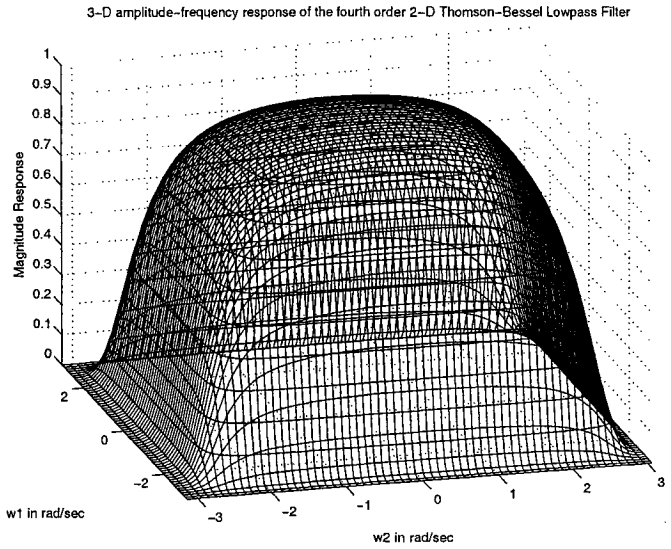

Figure 3.28: 3-D amplitude-frequency response of the fourth order 2-D digital Thomson-Bessel lowpass filter (When $k_1 = 1, k_2 = 1, a_{1L} = 1, a_{2L} = 1$)

algorithm 27.

3.5.2.2 Generation of fifth order 2-D digital Thomson-Bessel lowpass filter

The transfer function of the fifth order 2-D analog Thomson-Bessel lowpass filter, is given by eqn. 3.14. By applying generalized bilinear transformation (eqn. 3.2) to eqn. 3.14, we get, transfer function of 2-D digital Thomson-Bessel lowpass filter as function of z_1 and z_2, with $z_1 = e^{jw_1}$ and $z_2 = e^{jw_2}$. Hence, we get,

$$H_d(z_1, z_2) = \frac{(945)^2 (z_1+1)^5 (z_2+1)^5}{\left[k_1^5 (z_1 - a_{1L})^5 + 15k_1^4 (z_1 - a_{1L})^4 (z_1+1) + 105k_1^3 (z_1 - a_{1L})^3 (z_1+1)^2 + 420k_1^2 (z_1 - a_{1L})^2 (z_1+1)^3 + 945k_1 (z_1 - a_{1L}) (z_1+1)^4 + 945 (z_1+1)^5\right] \left[k_2^5 (z_2 - a_{2L})^5 + 15k_2^4 (z_2 - a_{2L})^4 (z_2+1) + 105k_2^3 (z_2 - a_{2L})^3 (z_2+1)^2 + 420k_2^2 (z_2 - a_{2L})^2 (z_2+1)^3 + 945k_2 (z_2 - a_{2L}) (z_2+1)^4 + 945 (z_2+1)^5\right]} \quad (3.16)$$

The 3-D amplitude-frequency response and contour plots of the fifth order 2-D digital Thomson-Bessel lowpass filter for different combination values of the constants is shown

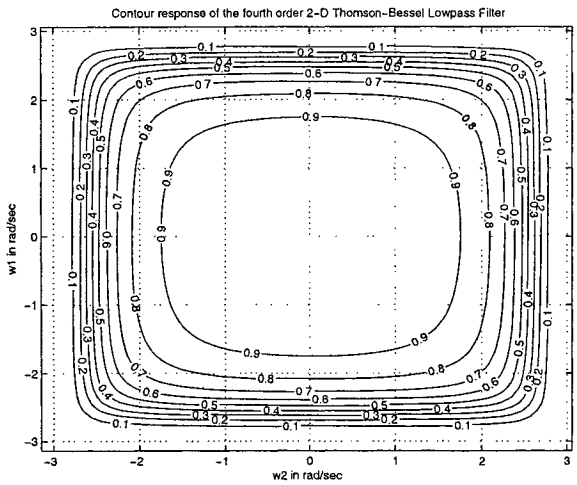

(a) When k1=1, k2=1, a1L=1 and a2L=1

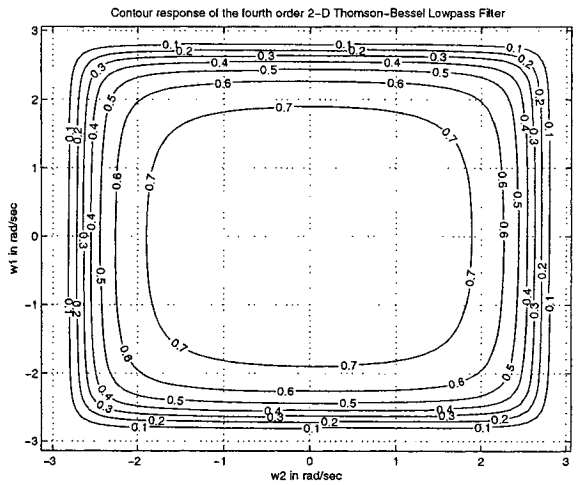

(b) When k1=1, k2=1, a1L=0.75 and a2L=0.75

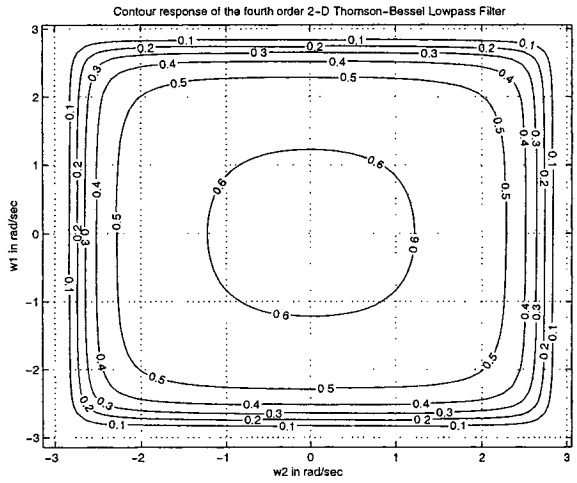

(c) When k1=1, k2=1, a1L=0.5 and a2L=0.5

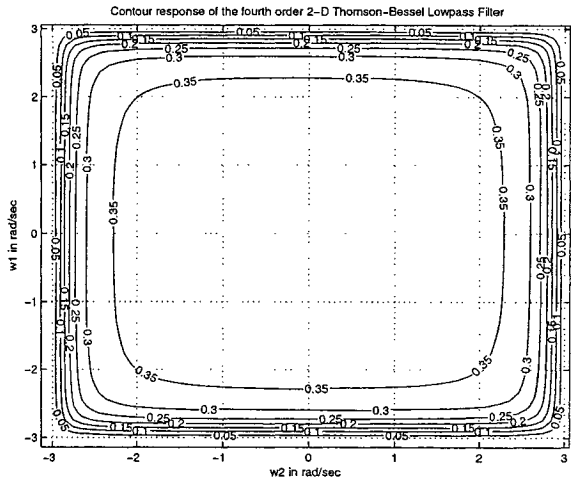

(d) When k1=1, k2=1, a1L=0 and a2L=0

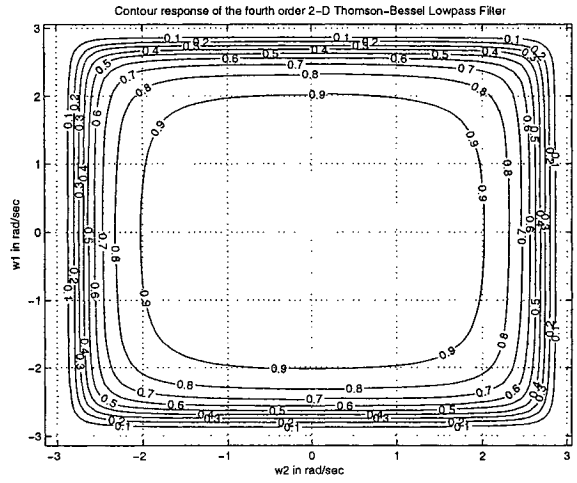

(e) When k1=0.75, k2=0.75, a1L=1 and a2L=1

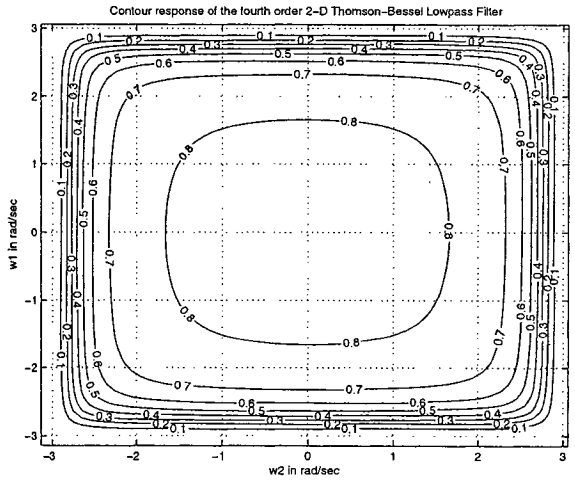

(f) When k1=0.75, k2=0.75, a1L=0.75 and a2L=0.75

Figure 3.29: Contour response of the fourth order 2-D digital Thomson-Bessel lowpass filter

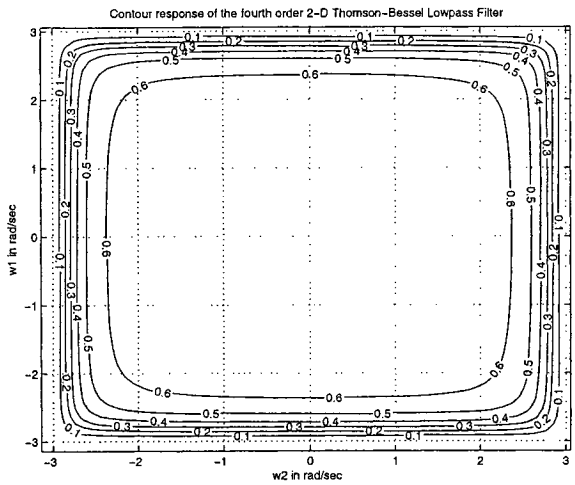

(a) When k1=0.75, k2=0.75, a1L=0.5 and a2L=0.5

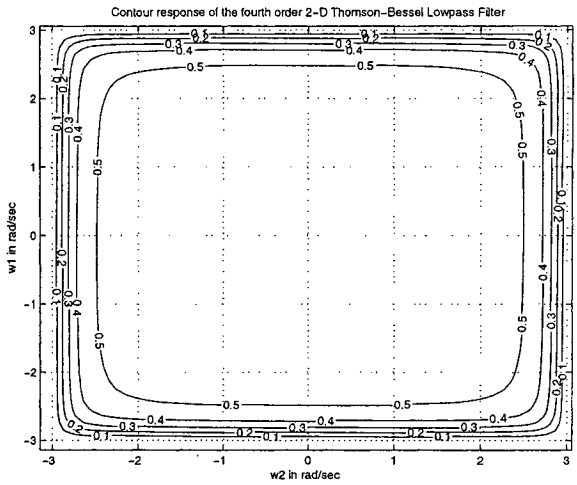

(b) When k1=0.75, k2=0.75, a1L=0.25 and a2L=0.25

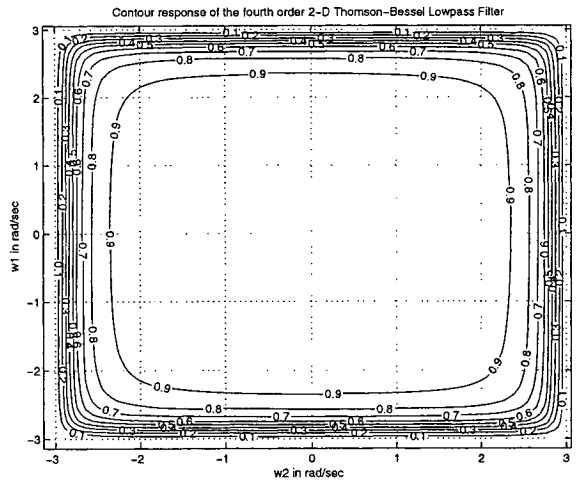

(c) When k1=0.5, k2=0.5, a1L=1 and a2L=1

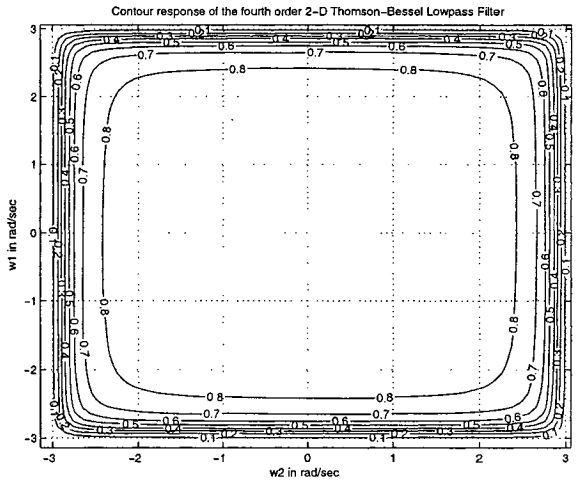

(d) When k1=0.5, k2=0.5, a1L=0.75 and a2L=0.75

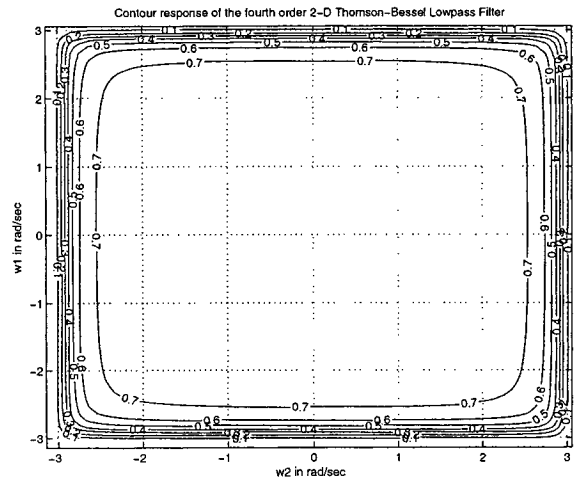

(e) When k1=0.5, k2=0.5, a1L=0.5 and a2L=0.5

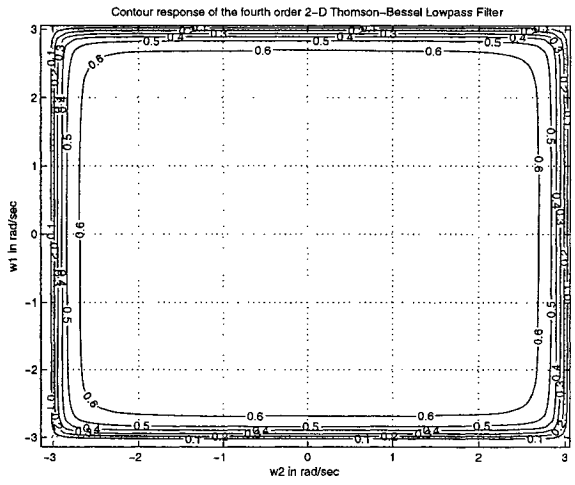

(f) When k1=0.5, k2=0.5, a1L=0.25 and a2L=0.25

Figure 3.30: Contour response of the fourth order 2-D digital Thomson-Bessel lowpass filter

Algorithm 27 The MATLAB code to plot the 3-D amplitude-frequency response and contour of the frequency response of the fourth order 2-D digital Thomson-Bessel lowpass filter

```
% Under Guidance of Prof. Dr. V. Ramachandran
% Student's name : Ajit Singh Sandhu..... ID:4841492.
clc; clear all;
k1=input('Give the value of the constant k1 for the bilinear LP transformation => ');
k2=input('Give the value of the constant k2 for the bilinear LP transformation => ');
a1L=input('Give the value of the constant a1L for the bilinear LP transformation => ');
a2L=input('Give the value of the constant a2L for the bilinear LP transformation => ');
% Creates two dimensional square matrix (mesh grid) of angular frequency w1 and w2.
[w1,w2] = meshgrid(-pi:0.1:pi,-pi:0.1:pi);
% Apply Z1=r1*exp(jw1) and Z2=r2*exp(jw2) with r1 = r2 =1
z1=exp(j.*w1);
z2=exp(j.*w2);
% Hd is the required digital transfer function and its value is evaluated as follows.
a=z1-a1L;
b=z2-a2L;
c=z1+1;
d=z2+1;
h1_1=((k1.^4).*(a.^4))+((k1.^3).*10.*(a.^3).*c)+((k1.^2).*45.*(a.^2).*(c.^2))+(k1.*105.*a.*(c.^3))
+(105.*(c.^4));
h1_2=((k1.^4).*(b.^4))+((k1.^3).*10.*(b.^3).*d)+((k1.^2).*45.*(b.^2).*(d.^2))+(k1.*105.*b.*(d.^3))
+(105.*(d.^4));
h1=abs(((c.^4).*(d.^4).*(105^2))./(h1_1.*h1_2));
figure(1);
contour3(w1,w2,h1);
surface(w1,w2,abs(h1),'EdgeColor',[.8 .8 .8],'FaceColor','none');
grid on;
view(-15,25);
%colormap cool;
title('3-D amplitude-frequency response of the fourth order 2-D Thomson-Bessel Lowpass Filter');
xlabel(' w2 in rad/sec ');
ylabel(' w1 in rad/sec ');
zlabel(' Magnitude Response ');
figure(2);
[C,h] = contour(w1,w2,h1);
clabel(C,h);
grid on;
%colormap cool;
title('Contour response of the fourth order 2-D Thomson-Bessel Lowpass Filter');
xlabel(' w2 in rad/sec ');
ylabel(' w1 in rad/sec ');
```

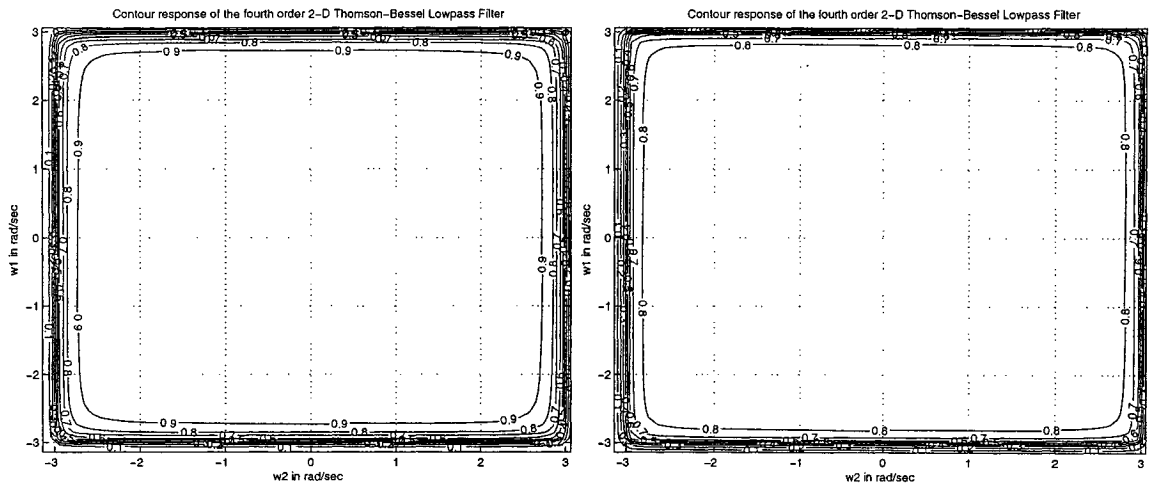

(a) When k1=0.25, k2=0.25, a1L=1 and a2L=1 (b) When k1=0.25, k2=0.25, a1L=0.5 and a2L=0.5

Figure 3.31: Contour response of the fourth order 2-D digital Thomson-Bessel lowpass filter

in the fig. 3.32, 3.33, 3.34 and 3.35. We can observe that the amplitude-frequency response is monotonically decreasing when constants (k_1, k_2, a_{1L} and a_{2L}) are having non-negative values. The MATLAB code to plot the 3-D amplitude-frequency response and contour of the frequency response of the fifth order 2-D digital Thomson-Bessel lowpass filter is in algorithm 28.

3.5.2.3 Discussion

The characteristics of the 2-D digital filters proposed in Sec. 3.5.2.1 and 3.5.2.2 are studied in this sub-section. Fig. 3.28, 3.29, 3.30, 3.31, 3.32, 3.33, 3.34 and 3.35, shows amplitude-frequency response and contour plots of the 2-D Thomson-Bessel digital filters, based on the different values of the constants ,k_1, k_2, a_{1L}, a_{2L}, of the generalized bilinear transformation.

In general, the coefficients k_1, k_2 affects the passband width and a_{1L}, a_{2L} affects the gain. It is observed that for non-negative values of the constants, the 2-D digital Thomson-Bessel lowpass filters always have monotonic amplitude-frequency response with similar symmetry. The monotonic amplitude-frequency response of the fifth order 2-D digital

Algorithm 28 The MATLAB code to plot the 3-D amplitude-frequency response and contour of the frequency response of the fifth order 2-D digital Thomson-Bessel lowpass filter

```
% Under Guidance of Prof. Dr. V. Ramachandran
% Student's name : Ajit Singh Sandhu..... ID:4841492.
clc; clear all;
k1=input('Give the value of the constant k1 for the bilinear LP transformation => ');
k2=input('Give the value of the constant k2 for the bilinear LP transformation => ');
a1L=input('Give the value of the constant a1L for the bilinear LP transformation => ');
a2L=input('Give the value of the constant a2L for the bilinear LP transformation => ');
% Creates two dimensional square matrix (mesh grid) of angular frequency w1 and w2.
[w1,w2] = meshgrid(-pi:0.1:pi,-pi:0.1:pi);
% Apply Z1=r1*exp(jw1) and Z2=r2*exp(jw2) with r1 = r2 =1
z1=exp(j.*w1);
z2=exp(j.*w2);
% Hd is the required digital transfer function and its value is evaluated as follows.
a=z1-a1L;
b=z2-a2L;
c=z1+1;
d=z2+1;
h1_1=((k1.^5).*(a.^5))+((k1.^4).*15.*(a.^4).*c)+((k1.^3).*105.*(a.^3).*(c.^2))+((k1.^2).*420.*(a.^2).*(c.^3))
+(k1.*945.*a.*(c.^4))+(945.*(c.^5));
h1_2=((k2.^5).*(b.^5))+((k2.^4).*15.*(b.^4).*d)+((k2.^3).*105.*(b.^3).*(d.^2))+((k2.^2).*420.*(b.^2).*(d.^3))
+(k2.*945.*b.*(d.^4))+(945.*(d.^5));
h1=abs(((c.^5).*(d.^5).*(945^2))./(h1_1.*h1_2));
figure(1);
contour3(w1,w2,h1);
surface(w1,w2,abs(h1),'EdgeColor',[.8 .8 .8],'FaceColor','none');
grid on;
view(-15,25);
%colormap cool;
title('3-D amplitude-frequency response of the fifth order 2-D Thomson-Bessel Lowpass Filter');
xlabel(' w2 in rad/sec ');
ylabel(' w1 in rad/sec ');
zlabel(' Magnitude Response ');
figure(2);
[C,h] = contour(w1,w2,h1);
clabel(C,h);
grid on;
%colormap cool;
title('Contour response of the fifth order 2-D Thomson-Bessel Lowpass Filter');
xlabel(' w2 in rad/sec ');
ylabel(' w1 in rad/sec ');
```

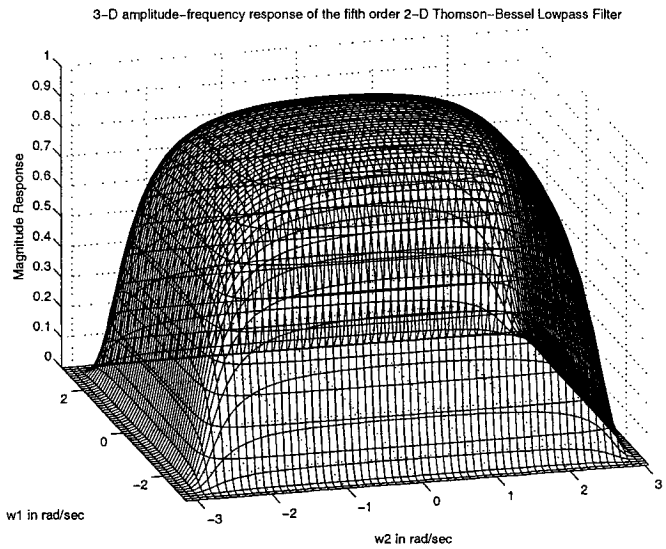

Figure 3.32: 3-D amplitude-frequency response of the fifth order 2-D digital Thomson-Bessel lowpass filter (When $k_1 = 1$, $k_2 = 1$, $a_{1L} = 1$, $a_{2L} = 1$)

Thomson-Bessel lowpass filters are wider in the passband and steeper in the transition band, in comparison to the fourth order 2-D Thomson-Bessel lowpass filter, for the same coefficient values (for example fig. 3.29 (a) and 3.33 (a)). It is may also be noted that as the coefficients, k_1, k_2, values are decreased, the passband of the 2-D lowpass filter increases with decrease in magnitude, and it may result in loss of signal due to aliasing, because the Nyquist rate may not be satisfied for certain input signals.

3.6 Cascading lower order monotonic 1-D lowpass filters obtained from Butterworth, Papoulis, Filanovsky and Thomson-Bessel filters, to generate 2-D lowpass filters with monotonic characteristics

In Sec. 2.7, we segregated lower order 1-D filters, derived from the Butterworth, Filanovsky, Papoulis and Thomson-Bessel filters, having monotonic amplitude-frequency

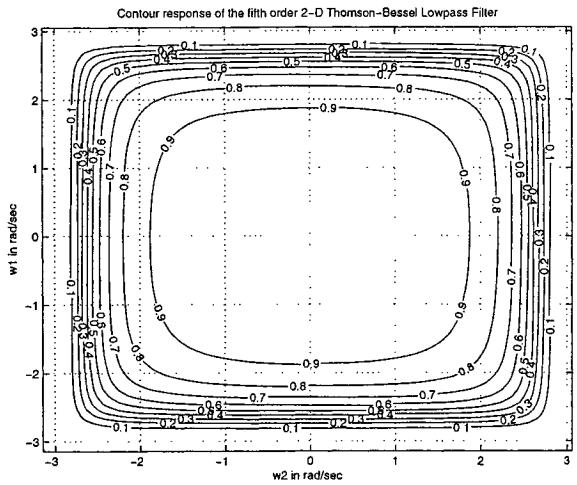

(a) When k1=1, k2=1, a1L=1 and a2L=1

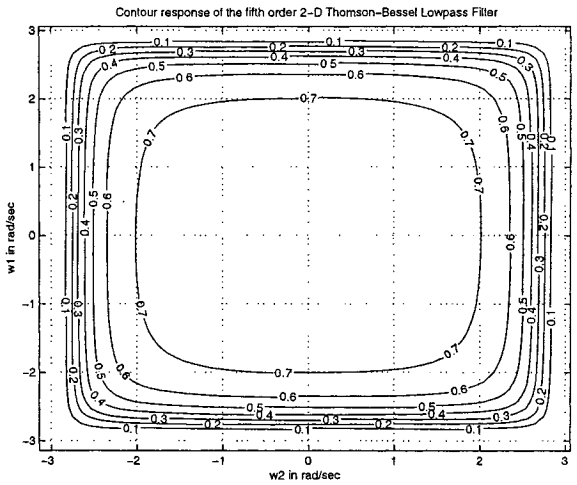

(b) When k1=1, k2=1, a1L=0.75 and a2L=0.75

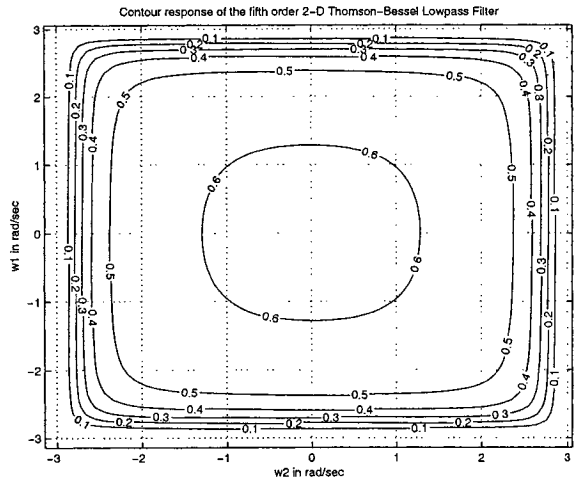

(c) When k1=1, k2=1, a1L=0.5 and a2L=0.5

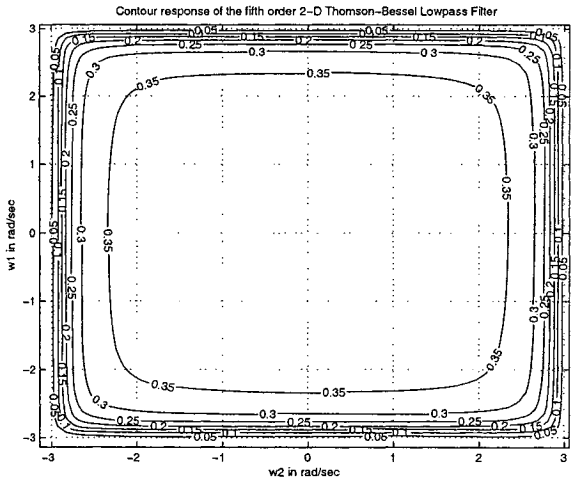

(d) When k1=1, k2=1, a1L=0 and a2L=0

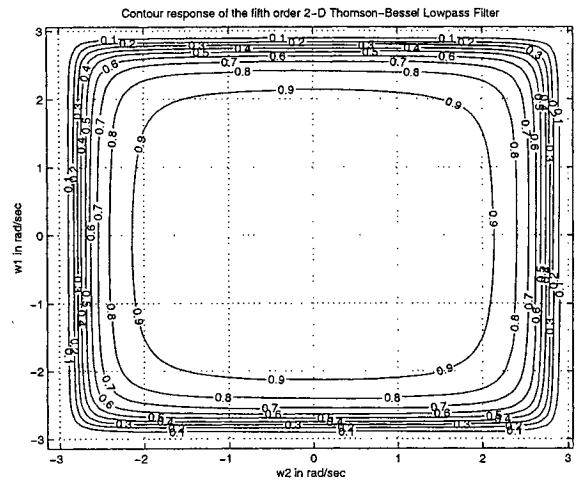

(e) When k1=0.75, k2=0.75, a1L=1 and a2L=1

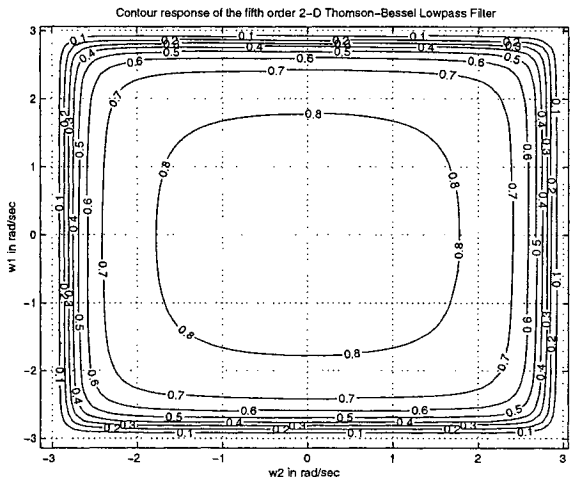

(f) When k1=0.75, k2=0.75, a1L=0.75 and a2L=0.75

Figure 3.33: Contour response of the fifth order 2-D digital Thomson-Bessel lowpass filter

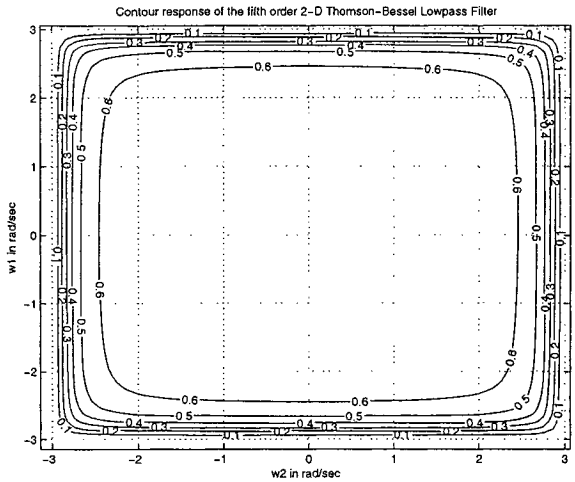

(a) When k1=0.75, k2=0.75, a1L=0.5 and a2L=0.5

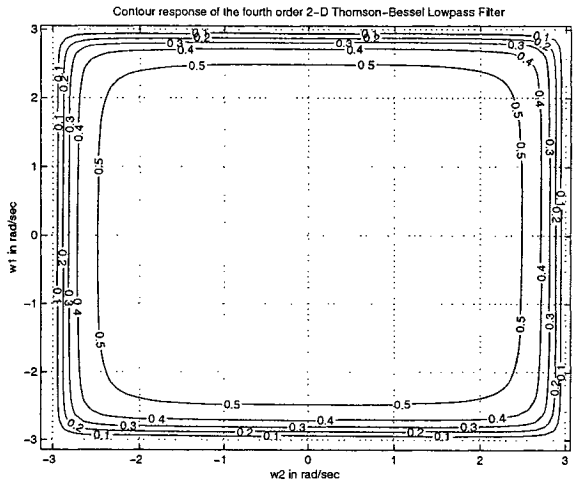

(b) When k1=0.75, k2=0.75, a1L=0.25 and a2L=0.25

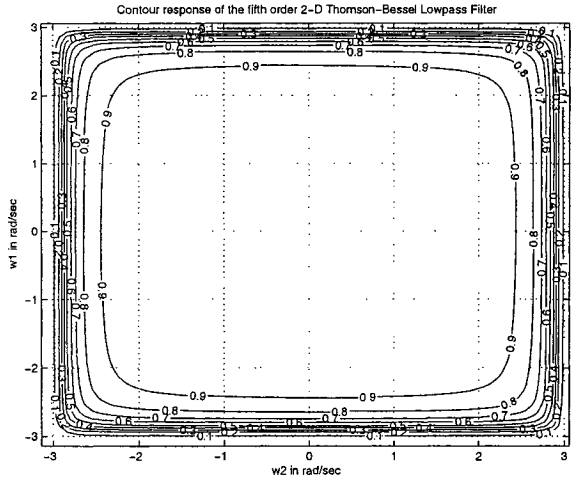

(c) When k1=0.5, k2=0.5, a1L=1 and a2L=1

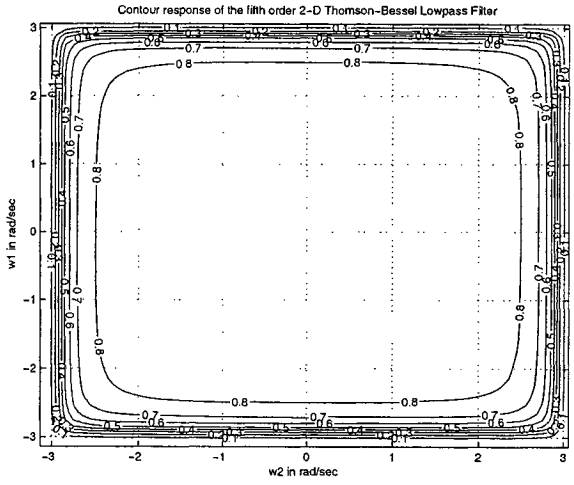

(d) When k1=0.5, k2=0.5, a1L=0.75 and a2L=0.75

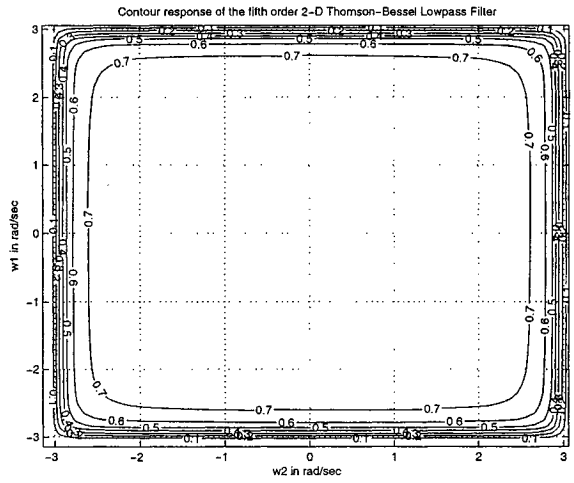

(e) When k1=0.5, k2=0.5, a1L=0.5 and a2L=0.5

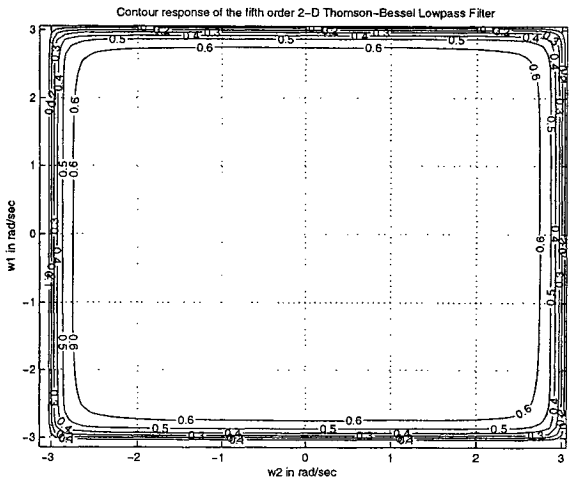

(f) When k1=0.5, k2=0.5, a1L=0.25 and a2L=0.25

Figure 3.34: Contour response of the fifth order 2-D digital Thomson-Bessel lowpass filter

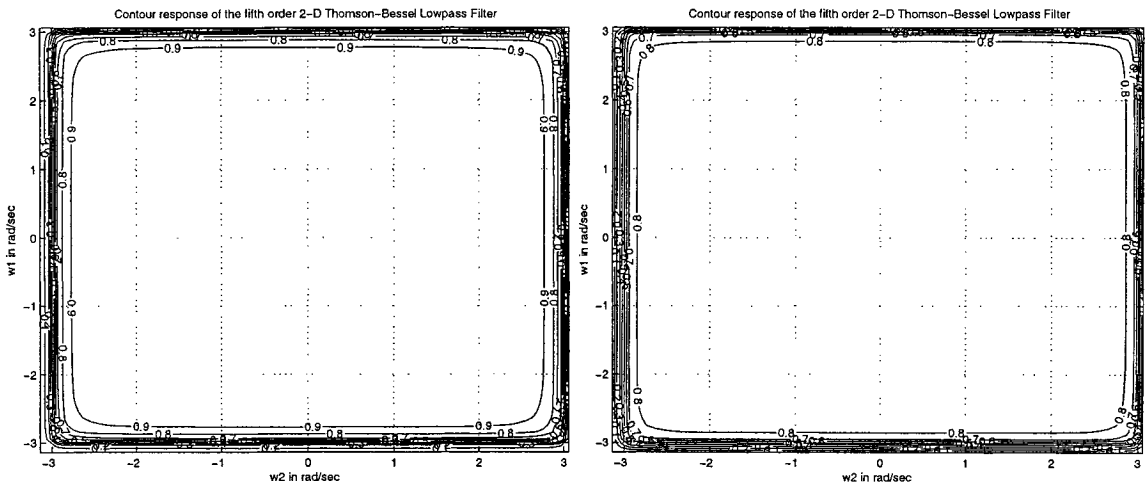

(a) When k1=0.25, k2=0.25, a1L=1 and a2L=1 (b) When k1=0.25, k2=0.25, a1L=0.5 and a2L=0.5

Figure 3.35: Contour response of the fifth order 2-D digital Thomson-Bessel lowpass filter

response. We know that, a simple approach to obtain multidimensional filters is by cascading 1-D filters in the frequency domain. Hence, we will utilize the derived 1-D analog lowpass filters, namely, P2, P3, P6, B1, B3, B4, B7, F1, F5, TB1, TB3, TB4, TB6, TB7 and TB8 (Sec. 2.7), with monotonic behavior, and cascade them to realize 2-D analog lowpass filters. We will study the amplitude-frequency response of the mentioned filters in 2-D respectively, to obtain 2-D lowpass filters of different order with monotonic amplitude-frequency response.

Table: 3.1 shows, few cascaded analog 1-D lowpass filters resulting in the 2-D transfer function, $H_a(s_1, s_2)$, of the 2-D lowpass filter having monotonic amplitude-frequency response, with the filter combination (*F. Combination*), order of the 2-D filter (o), and the filter number, *F.No* (FLi, with i as integer varying from 1 to 13). The MATLAB code to plot the 3-D amplitude-frequency response and contour response of the 2-D analog lowpass filters (refer table: 3.1), having monotonic characteristics is in algorithm 29. The amplitude-frequency response and contour of the frequency response of the 2-D lowpass filters proposed in table: 3.1 are shown in fig. 3.36, 3.37, 3.38, 3.39 and 3.40. All the 2-D lowpass filters exhibit monotonic amplitude-frequency response.

F.No.	*O*	*F. Combination*	*Transfer Func.* $H_a(s_1, s_2)$
FL1	1	B3.B3	$\frac{1}{(s_1+1)(s_2+1)}$
FL2	1	TB3.TB3	$\frac{(3.6467)^2}{(s_1+3.6467)(s_2+3.6467)}$
FL3	2	P2.P2	$\frac{(0.4308)^2}{(s_1^2+1.0994s_1+0.4308)(s_2^2+1.0994s_2+0.4308)}$
FL4	2	B1.B1	$\frac{1}{(s_1^2+1.8478s_1+1)(s_2^2+1.8478s_2+1)}$
FL5	2	B4.B4	$\frac{1}{(s_1^2+1.618s_1+1)(s_2^2+1.618s_2+1)}$
FL6	2	TB1.TB1	$\frac{(9.14)^2}{(s_1^2+5.7924s_1+9.14)(s_2^2+5.7924s_2+9.14)}$
FL7	2	TB4.TB4	$\frac{(14.2729)^2}{(s_1^2+6.704s_1+14.2729)(s_2^2+6.704s_2+14.2729)}$
FL8	3	B7.B7	$\frac{1}{(s_1^3+2.618s_1^2+2.618s_1+1)(s_2^3+2.618s_2^2+2.618s_2+1)}$
FL9	3	P6.P6	$\frac{(0.2327)^2}{(s_1^3+1.2443s_1^2+0.8604s_1+0.2327)(s_2^3+1.2443s_2^2+0.8604s_2+0.2327)}$
FL10	3	F5.F5	$\frac{(0.3297)^2}{(s_1^3+1.5953s_1^2+1.1244s_1+0.3297)(s_2^3+1.5953s_2^2+1.1244s_2+0.3297)}$
FL11	3	TB6.TB6	$\frac{(52.049)^2}{(s_1^3+10.3507s_1^2+38.7204s_1+52.049)(s_2^3+10.3507s_2^2+38.7204s_2+52.049)}$
FL12	3	TB7.TB7	$\frac{(66.2106)^2}{(s_1^3+8.2961s_1^2+35.1113s_1+66.2106)(s_2^3+8.2961s_2^2+35.1113s_2+66.2106)}$
FL13	4	TB8.TB8	$\frac{(259.1431)^2}{(s_1^4+11.3534s_1^3+63.5988s_1^2+188.0802s_1+259.1431)(s_2^4+11.3534s_2^3+63.5988s_2^2+188.0802s_2+259.1431)}$

Table 3.1: Cascading 1-D lowpass filters obtained from 1-D Papoulis, Butterworth, Filanovsky and Thomson-Bessel lowpass filters, respectively, to obtain 2-D analog lowpass filters with monotonic characteristics.

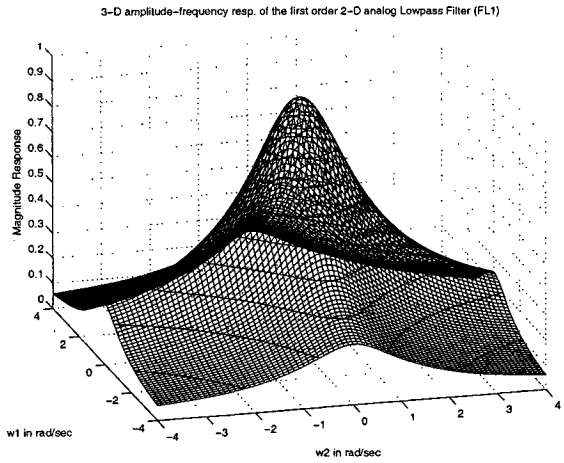

(a) 3-D amplitude-frequency response (FL1)

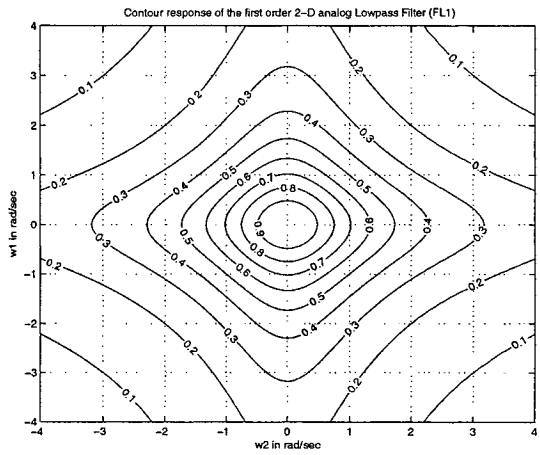

(b) Contour of the frequency response (FL1)

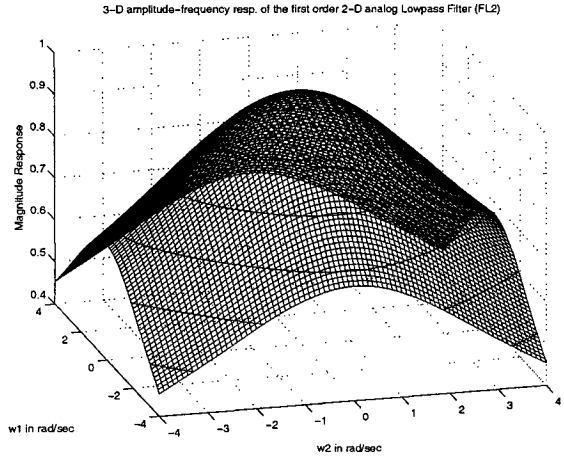

(c) 3-D amplitude-frequency response (FL2)

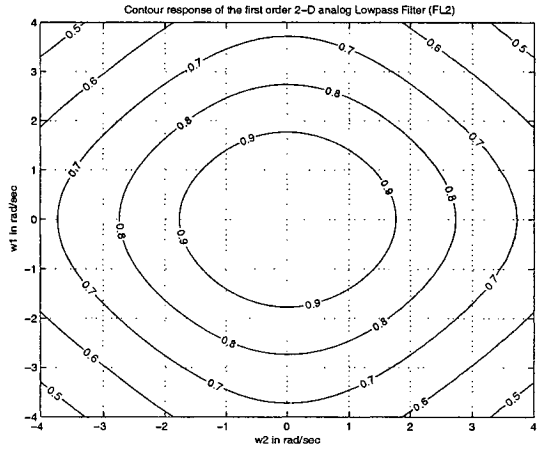

(d) Contour of the frequency response (FL2)

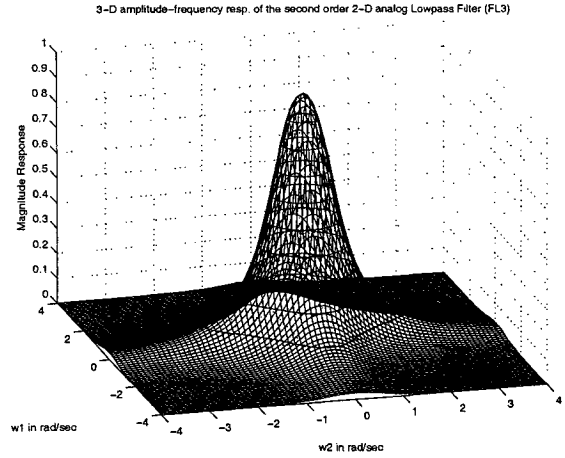

(e) 3-D amplitude-frequency response (FL3)

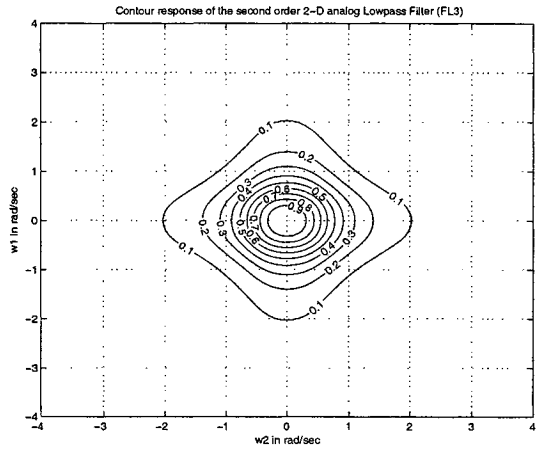

(f) Contour of the frequency response (FL3)

Figure 3.36: Frequency response of 2-D analog lowpass filter, FL1, FL2, FL3, having monotonic characteristics, obtained from cascaded 1-D lowpass filters (Refer Table: 3.1).

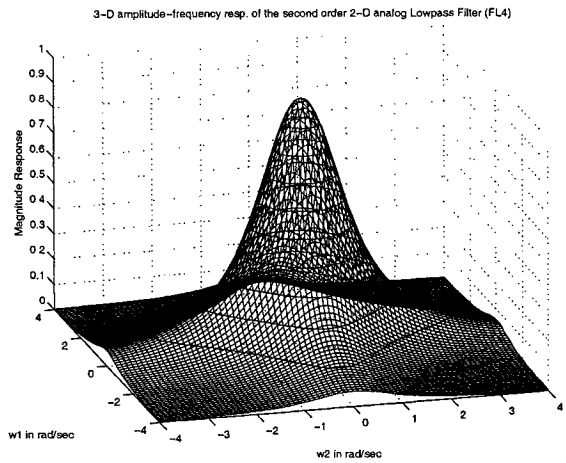

(a) 3-D amplitude-frequency response (FL4)

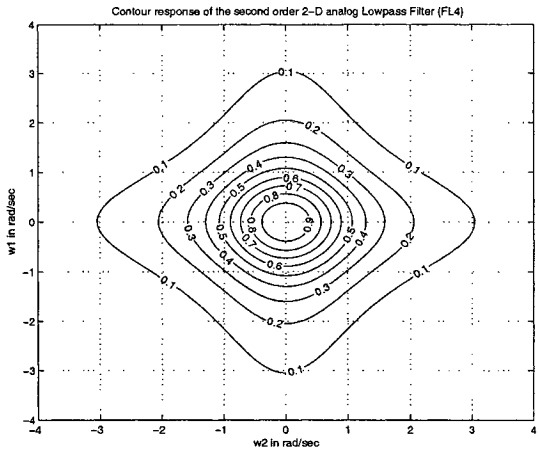

(b) Contour of the frequency response (FL4)

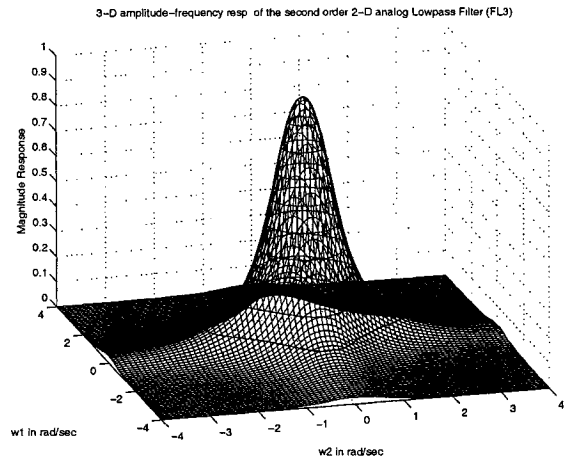

(c) 3-D amplitude-frequency response (FL5)

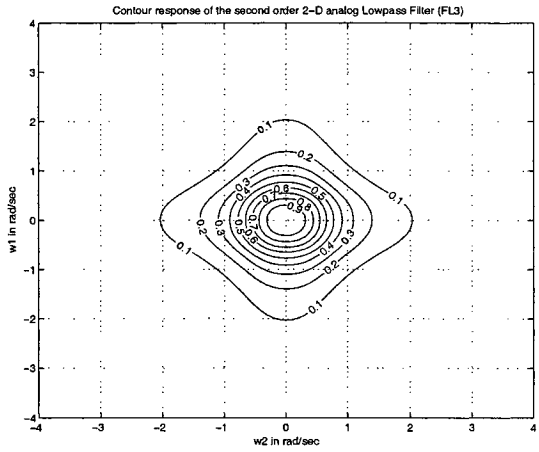

(d) Contour of the frequency response (FL5)

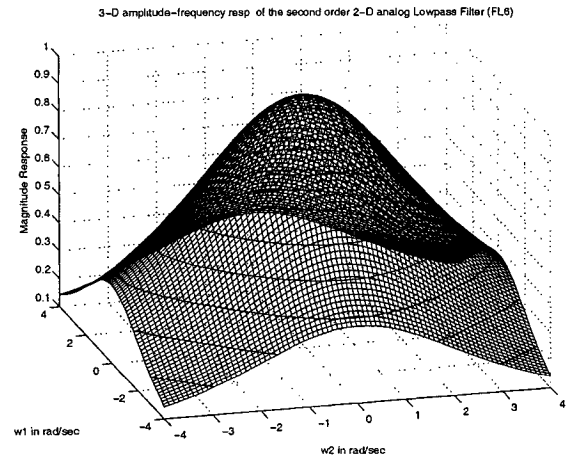

(e) 3-D amplitude-frequency response (FL6)

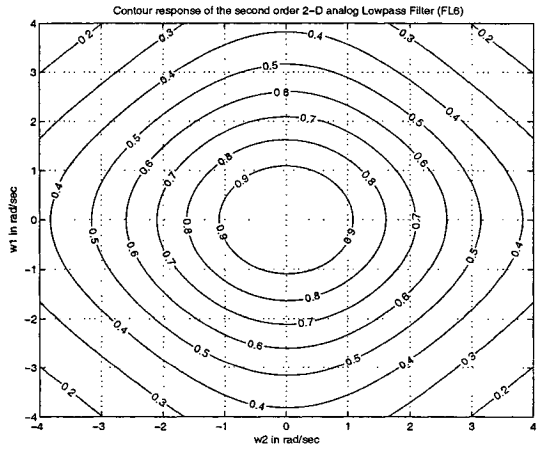

(f) Contour of the frequency response (FL6)

Figure 3.37: Frequency response of 2-D analog lowpass filter, FL4, FL5, FL6, having monotonic characteristics, obtained from cascaded 1-D lowpass filters (Refer Table: 3.1).

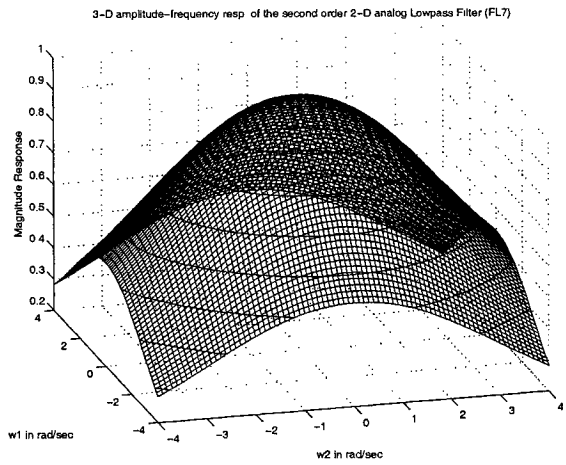

(a) 3-D amplitude-frequency response (FL7)

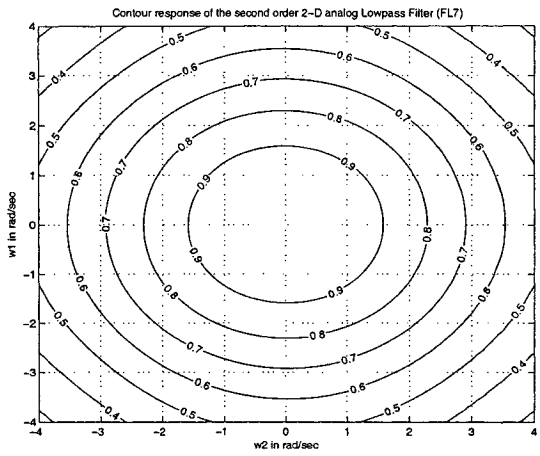

(b) Contour of the frequency response (FL7)

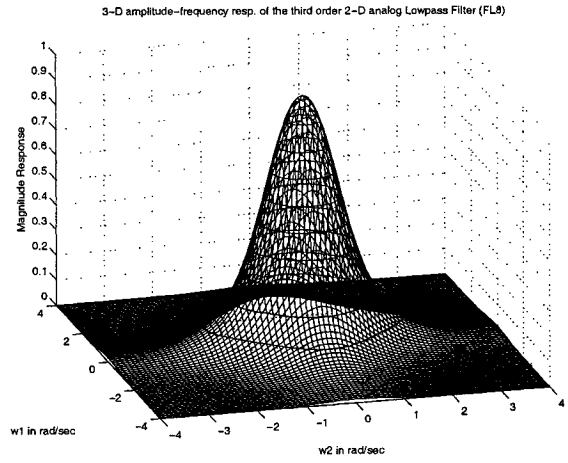

(c) 3-D amplitude-frequency response (FL8)

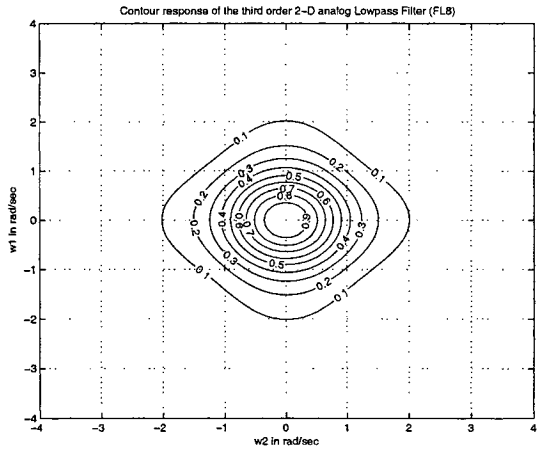

(d) Contour of the frequency response (FL8)

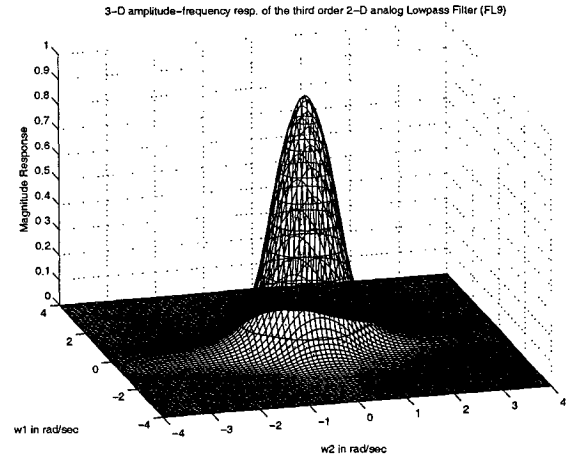

(e) 3-D amplitude-frequency response (FL9)

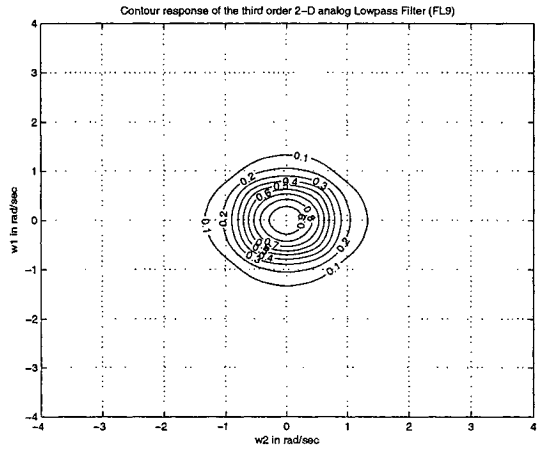

(f) Contour of the frequency response (FL9)

Figure 3.38: Frequency response of 2-D analog lowpass filter, FL7, FL8, FL9, having monotonic characteristics, obtained from cascaded 1-D lowpass filters (Refer Table: 3.1).

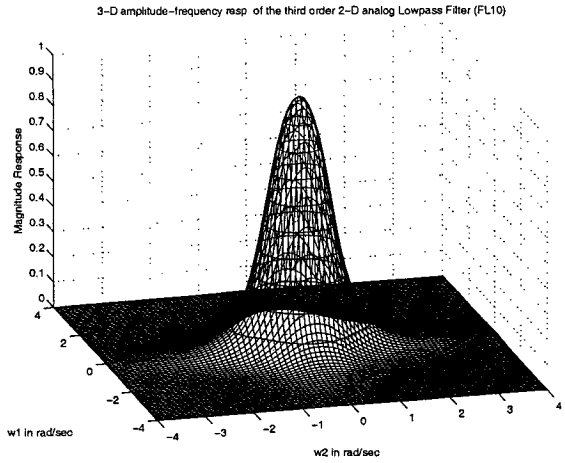

(a) 3-D amplitude-frequency response (FL10)

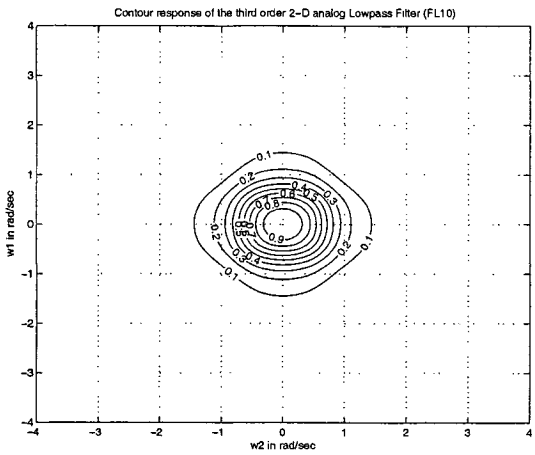

(b) Contour of the frequency response (FL10)

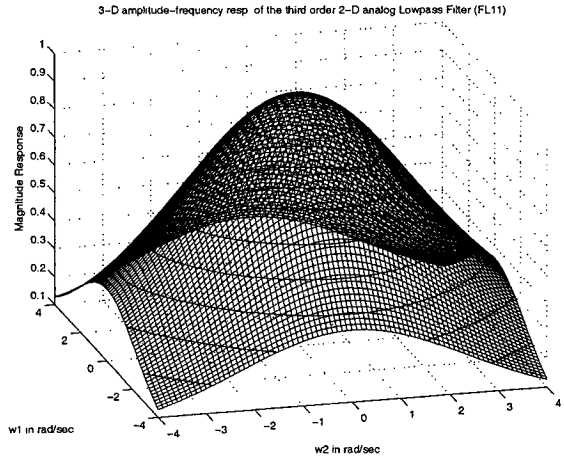

(c) 3-D amplitude-frequency response (FL11)

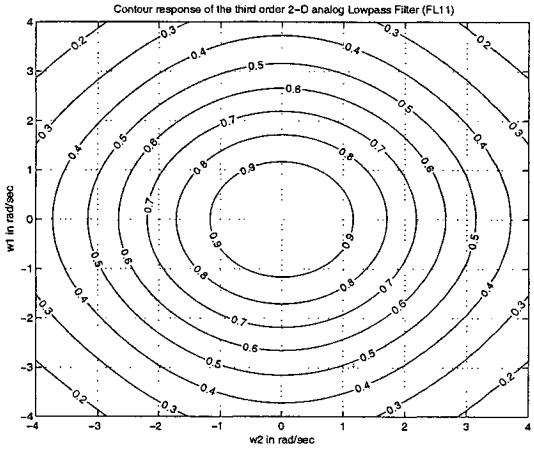

(d) Contour of the frequency response (FL11)

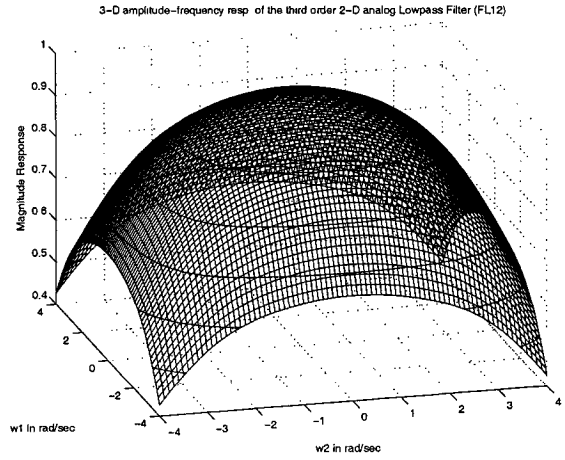

(e) 3-D amplitude-frequency response (FL12)

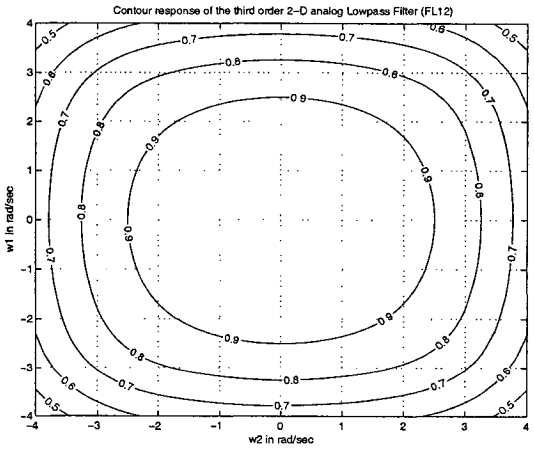

(f) Contour of the frequency response (FL12)

Figure 3.39: Frequency response of 2-D analog lowpass filter, FL10, FL11, FL12, having monotonic characteristics, obtained from cascaded 1-D lowpass filters (Refer Table: 3.1).

Algorithm 29 The MATLAB code to plot the 3-D amplitude-frequency response and contour response of the 2-D analog lowpass filters (refer table: 3.1), having monotonic characteristics.

```
% Under Guidance of Prof. Dr. V. Ramachandran
% Student's name : Ajit Singh Sandhu..... ID:4841492.
clear all;
[w1,w2] = meshgrid(-4:0.1:4,-4:0.1:4);
s1=j*w1; s2=j*w2;
%Transfer function of the 2-D analog Filter - FL1
h1_1=(s1+1);
h1_2=(s2+1);
h1=abs(1./(h1_1.*h1_2));
figure(1);
contour3(w1,w2,h1);
surface(w1,w2,abs(h1),'EdgeColor',[.8 .8 .8],'FaceColor','none');
grid on; view(-15,25);
title('3-D amplitude-frequency resp. of the first order 2-D analog Lowpass Filter (FL1)');
xlabel(' w2 in rad/sec ');
ylabel(' w1 in rad/sec ');
zlabel(' Magnitude Response ');
figure(2);
[C,h] = contour(w1,w2,h1);
clabel(C,h); grid on;
title('Contour response of the first order 2-D analog Lowpass Filter (FL1)');
xlabel(' w2 in rad/sec ');
ylabel(' w1 in rad/sec ');
%Transfer function of the 2-D analog Filter - FL2
h1_1=(s1+3.6467);
h1_2=(s2+3.6467);
h1=abs((3.6467^2)./(h1_1.*h1_2));
figure(3);
contour3(w1,w2,h1);
surface(w1,w2,abs(h1),'EdgeColor',[.8 .8 .8],'FaceColor','none');
grid on; view(-15,25);
title('3-D amplitude-frequency resp. of the first order 2-D analog Lowpass Filter (FL2)');
xlabel(' w2 in rad/sec ');
ylabel(' w1 in rad/sec ');
zlabel(' Magnitude Response ');
figure(4);
[C,h] = contour(w1,w2,h1);
clabel(C,h); grid on;
title('Contour response of the first order 2-D analog Lowpass Filter (FL2)');
xlabel(' w2 in rad/sec ');
ylabel(' w1 in rad/sec ');
%Transfer function of the 2-D analog Filter - FL3
h1_1=(s1.^2+1.0994.*s1+0.4308);
h1_2=(s2.^2+1.0994.*s2+0.4308);
h1=abs((0.4308^2)./(h1_1.*h1_2));
```

To be Continued...

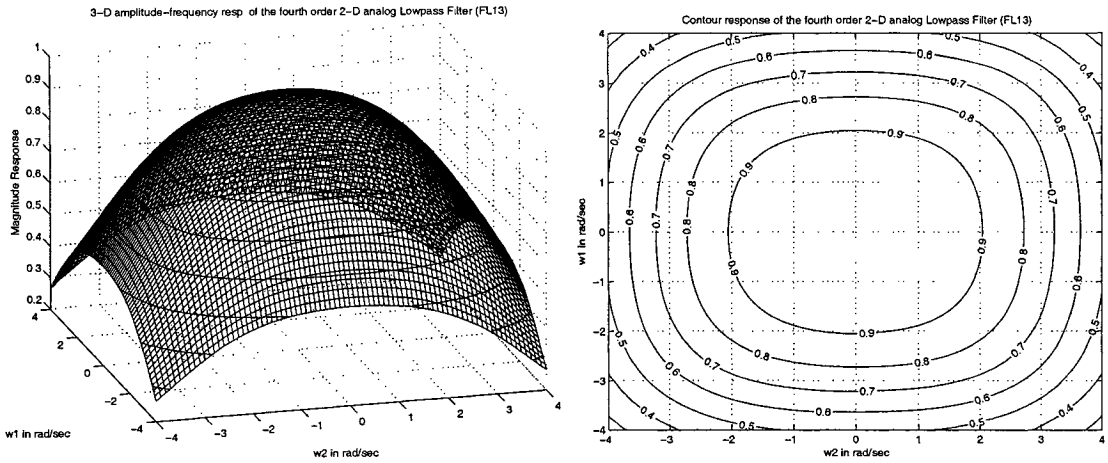

(a) 3-D amplitude-frequency response (b) Contour of the frequency response

Figure 3.40: Frequency response of 2-D analog lowpass filter, FL13, having monotonic characteristics, obtained from cascaded 1-D lowpass filters (Refer Table: 3.1).

Algorithm 29 (Contd...)

```
figure(5);
contour3(w1,w2,h1);
surface(w1,w2,abs(h1),'EdgeColor',[.8 .8 .8],'FaceColor','none');
grid on; view(-15,25);
title('3-D amplitude-frequency resp. of the second order 2-D analog Lowpass Filter (FL3)');
xlabel(' w2 in rad/sec ');
ylabel(' w1 in rad/sec ');
zlabel(' Magnitude Response ');
figure(6);
[C,h] = contour(w1,w2,h1);
clabel(C,h); grid on;
title('Contour response of the second order 2-D analog Lowpass Filter (FL3)');
xlabel(' w2 in rad/sec ');
ylabel(' w1 in rad/sec ');
%Transfer function of the 2-D analog Filter - FL4
h2_1=(s1.^2+1.8478.*s1+1);
h2_2=(s2.^2+1.8478.*s2+1);
h2=abs(1./(h2_1.*h2_2));
figure(7);
```

```
contour3(w1,w2,h2);
surface(w1,w2,abs(h2),'EdgeColor',[.8 .8 .8],'FaceColor','none');
grid on; view(-15,25);
title('3-D amplitude-frequency resp. of the second order 2-D analog Lowpass Filter (FL4)');
xlabel(' w2 in rad/sec ');
ylabel(' w1 in rad/sec ');
zlabel(' Magnitude Response ');
figure(8);
[C,h] = contour(w1,w2,h2);
clabel(C,h); grid on;
title('Contour response of the second order 2-D analog Lowpass Filter (FL4)');
xlabel(' w2 in rad/sec ');
ylabel(' w1 in rad/sec ');
%Transfer function of the 2-D analog Filter - FL5
h3_1=(s1.^2+1.618.*s1+1);
h3_2=(s2.^2+1.618.*s2+1);
h3=abs(1./(h3_1.*h3_2));
figure(9);
contour3(w1,w2,h3);
surface(w1,w2,abs(h3),'EdgeColor',[.8 .8 .8],'FaceColor','none');
grid on; view(-15,25);
title('3-D amplitude-frequency resp. of the second order 2-D analog Lowpass Filter (FL5)');
xlabel(' w2 in rad/sec ');
ylabel(' w1 in rad/sec ');
zlabel(' Magnitude Response ');
figure(10);
[C,h] = contour(w1,w2,h3);
clabel(C,h); grid on;
title('Contour response of the second order 2-D analog Lowpass Filter (FL5)');
xlabel(' w2 in rad/sec ');
ylabel(' w1 in rad/sec ');
%Transfer function of the 2-D analog Filter - FL6
h1_1=(s1.^2+5.7924.*s1+9.14);
```

```
h1_2=(s2.^2+5.7924.*s2+9.14);
h1=abs((9.14^2)./(h1_1.*h1_2));
figure(11);
contour3(w1,w2,h1);
surface(w1,w2,abs(h1),'EdgeColor',[.8 .8 .8],'FaceColor','none');
grid on; view(-15,25);
title('3-D amplitude-frequency resp. of the second order 2-D analog Lowpass Filter (FL6)');
xlabel(' w2 in rad/sec ');
ylabel(' w1 in rad/sec ');
zlabel(' Magnitude Response ');
figure(12);
[C,h] = contour(w1,w2,h1);
clabel(C,h); grid on;
title('Contour response of the second order 2-D analog Lowpass Filter (FL6)');
xlabel(' w2 in rad/sec ');
ylabel(' w1 in rad/sec ');
%Transfer function of the 2-D analog Filter - FL7
h1_1=(s1.^2+6.704.*s1+14.2729);
h1_2=(s2.^2+6.704.*s2+14.2729);
h1=abs((14.2729^2)./(h1_1.*h1_2));
figure(13);
contour3(w1,w2,h1);
surface(w1,w2,abs(h1),'EdgeColor',[.8 .8 .8],'FaceColor','none');
grid on; view(-15,25);
title('3-D amplitude-frequency resp. of the second order 2-D analog Lowpass Filter (FL7)');
xlabel(' w2 in rad/sec ');
ylabel(' w1 in rad/sec ');
zlabel(' Magnitude Response ');
figure(14);
[C,h] = contour(w1,w2,h1);
clabel(C,h); grid on;
title('Contour response of the second order 2-D analog Lowpass Filter (FL7)');
xlabel(' w2 in rad/sec ');
```

```
ylabel(' w1 in rad/sec ');
%Transfer function of the 2-D analog Filter - FL8
h4_1=(s1.^3+2.618.*(s1.^2)+2.618.*s1+1);
h4_2=(s2.^3+2.618.*(s2.^2)+2.618.*s2+1);
h4=abs(1./(h4_1.*h4_2));
figure(15);
contour3(w1,w2,h4);
surface(w1,w2,abs(h4),'EdgeColor',[.8 .8 .8],'FaceColor','none');
grid on; view(-15,25);
title('3-D amplitude-frequency resp. of the third order 2-D analog Lowpass Filter (FL8)');
xlabel(' w2 in rad/sec ');
ylabel(' w1 in rad/sec ');
zlabel(' Magnitude Response ');
figure(16);
[C,h] = contour(w1,w2,h4);
clabel(C,h); grid on;
title('Contour response of the third order 2-D analog Lowpass Filter (FL8)');
xlabel(' w2 in rad/sec ');
ylabel(' w1 in rad/sec ');
%Transfer function of the 2-D analog Filter - FL9
h5_1=(s1.^3+1.2446.*(s1.^2)+0.8604.*s1+0.2327);
h5_2=(s2.^3+1.2446.*(s2.^2)+0.8604.*s2+0.2327);
h5=abs((0.2327^2)./(h5_1.*h5_2));
figure(17);
contour3(w1,w2,h5);
surface(w1,w2,abs(h5),'EdgeColor',[.8 .8 .8],'FaceColor','none');
grid on; view(-15,25);
title('3-D amplitude-frequency resp. of the third order 2-D analog Lowpass Filter (FL9)');
xlabel(' w2 in rad/sec ');
ylabel(' w1 in rad/sec ');
zlabel(' Magnitude Response ');
figure(18);
[C,h] = contour(w1,w2,h5);
```

```
clabel(C,h); grid on;
title('Contour response of the third order 2-D analog Lowpass Filter (FL9)');
xlabel(' w2 in rad/sec ');
ylabel(' w1 in rad/sec ');
%Transfer function of the 2-D analog Filter - FL10
h6_1=(s1.^3+1.5953.*(s1.^2)+1.1244.*s1+0.3297);
h6_2=(s2.^3+1.5953.*(s2.^2)+1.1244.*s2+0.3297);
h6=abs((0.3297^2)./(h6_1.*h6_2));
figure(19);
contour3(w1,w2,h6);
surface(w1,w2,abs(h6),'EdgeColor',[.8 .8 .8],'FaceColor','none');
grid on; view(-15,25);
title('3-D amplitude-frequency resp. of the third order 2-D analog Lowpass Filter (FL10)');
xlabel(' w2 in rad/sec ');
ylabel(' w1 in rad/sec ');
zlabel(' Magnitude Response ');
figure(20);
[C,h] = contour(w1,w2,h6);
clabel(C,h); grid on;
title('Contour response of the third order 2-D analog Lowpass Filter (FL10)');
xlabel(' w2 in rad/sec ');
ylabel(' w1 in rad/sec ');
%Transfer function of the 2-D analog Filter - FL11
h6_1=(s1.^3+10.3507.*(s1.^2)+38.7204.*s1+52.0490);
h6_2=(s2.^3+10.3507.*(s2.^2)+38.7204.*s2+52.0490);
h6=abs((52.0490^2)./(h6_1.*h6_2));
figure(21);
contour3(w1,w2,h6);
surface(w1,w2,abs(h6),'EdgeColor',[.8 .8 .8],'FaceColor','none');
grid on; view(-15,25);
title('3-D amplitude-frequency resp. of the third order 2-D analog Lowpass Filter (FL11)');
xlabel(' w2 in rad/sec ');
ylabel(' w1 in rad/sec ');
```

```
zlabel(' Magnitude Response ');
figure(22);
[C,h] = contour(w1,w2,h6);
clabel(C,h); grid on;
title('Contour response of the third order 2-D analog Lowpass Filter (FL11)');
xlabel(' w2 in rad/sec ');
ylabel(' w1 in rad/sec ');
%Transfer function of the 2-D analog Filter - FL12
h6_1=(s1.^3+8.2961.*(s1.^2)+35.1113.*s1+66.2106);
h6_2=(s2.^3+8.2961.*(s2.^2)+35.1113.*s2+66.2106);
h6=abs((66.2106^2)./(h6_1.*h6_2));
figure(23);
contour3(w1,w2,h6);
surface(w1,w2,abs(h6),'EdgeColor',[.8 .8 .8],'FaceColor','none');
grid on; view(-15,25);
title('3-D amplitude-frequency resp. of the third order 2-D analog Lowpass Filter (FL12)');
xlabel(' w2 in rad/sec ');
ylabel(' w1 in rad/sec ');
zlabel(' Magnitude Response ');
figure(24);
[C,h] = contour(w1,w2,h6);
clabel(C,h); grid on;
title('Contour response of the third order 2-D analog Lowpass Filter (FL12)');
xlabel(' w2 in rad/sec ');
ylabel(' w1 in rad/sec ');
%Transfer function of the 2-D analog Filter - FL13
h6_1=s1.^4+11.3534.*(s1.^3)+63.5988.*(s1.^2)+188.0802.*s1+259.1431;
h6_2=s2.^4+11.3534.*(s2.^3)+63.5988.*(s2.^2)+188.0802.*s2+259.1431;
h6=abs((259.1431^2)./(h6_1.*h6_2));
figure(25);
contour3(w1,w2,h6);
surface(w1,w2,abs(h6),'EdgeColor',[.8 .8 .8],'FaceColor','none');
grid on; view(-15,25);
```

```
title('3-D amplitude-frequency resp. of the fourth order 2-D analog Lowpass Filter (FL13)');
xlabel(' w2 in rad/sec ');
ylabel(' w1 in rad/sec ');
zlabel(' Magnitude Response ');
figure(26);
[C,h] = contour(w1,w2,h6);
clabel(C,h); grid on;
title('Contour response of the fourth order 2-D analog Lowpass Filter (FL13)');
xlabel(' w2 in rad/sec ');
ylabel(' w1 in rad/sec ');
```

3.7 Cascading combination 1-D lowpass filters having monotonic characteristics, to generate 2-D lowpass filters with monotonic amplitude-frequency response

In Sec. 2.8, we generated cascaded combination 1-D filters, derived from the Butterworth, Filanovsky, Papoulis and Thomson-Bessel filters, having monotonic amplitude-frequency response. We will utilize the derived cascaded 1-D analog lowpass filters having monotonic amplitude-frequency response (Sec. 2.8), and cascade few of these 1-D filters to realize 2-D analog lowpass filters.

Table: 3.2 shows, few cascaded analog 1-D lowpass filters resulting in the 2-D transfer function, $H_a(s_1, s_2)$, of the 2-D lowpass filter having monotonic amplitude-frequency response, filter combination (*F. Combination*), order of the 2-D filter (O) and the filter number, *F.No* (FLi, with i as integer varying from 14 to 22). The MATLAB code to plot the 3-D amplitude-frequency response and contour response of the 2-D analog lowpass filters (refer table: 3.2), having monotonic characteristics, and obtained cascaded 1-D lowpass filters is in algorithm 30. The amplitude-frequency response and contour plots of the 2-D lowpass filters proposed in table: 3.2 are shown in fig. 3.41, 3.42 and 3.43.

F.No.	*O*	*F. Combination*	*Transfer Func.* $H_a(s_1, s_2)$
FL14	4	C1.C1	$\frac{(0.4308)^4}{(s_1^2+1.0994s_1+0.4308)(s_1^2+1.0994s_1+0.4308)(s_2^2+1.0994s_2+0.4308)(s_2^2+1.0994s_2+0.4308)}$
FL15	4	C7.C7	$\frac{1}{(s_1^2+1.8478s_1+1)(s_1^2+1.618s_1+1)(s_2^2+1.8478s_2+1)(s_2^2+1.618s_2+1)}$
FL16	4	C17.C17	$\frac{(9.14)^4}{(s_1^2+5.7924s_1+9.14)(s_1^2+5.7924s_1+9.14)(s_2^2+5.7924s_2+9.14)(s_2^2+5.7924s_2+9.14)}$
FL17	6	C10.C10	$\frac{1}{(s_1^2+1.8478s_1+1)(s_1+1)(s_1^3+2.618s_1^2+2.618s_1+1)(s_2^2+1.8478s_2+1)(s_2+1)(s_2^3+2.618s_2^2+2.618s_2+1)}$
FL18	6	C14.C14	$\frac{(0.3297)^4}{(s_1^3+1.5953s_1^2+1.1244s_1+0.3297)(s_1^3+1.5953s_1^2+1.1244s_1+0.3297)(s_2^3+1.5953s_2^2+1.1244s_2+0.3297)(s_2^3+1.5953s_2^2+1.1244s_2+0.3297)}$
FL19	6	C19.C19	$\frac{(9.14)^6}{(s_1^2+5.7924s_1+9.14)(s_1^2+5.7924s_1+9.14)(s_1^2+5.7924s_1+9.14)(s_2^2+5.7924s_2+9.14)(s_2^2+5.7924s_2+9.14)(s_2^2+5.7924s_2+9.14)}$
FL20	8	C6.C6	$\frac{(0.4308)^8}{(s_1^2+1.0994s_1+0.4308)(s_1^2+1.0994s_1+0.4308)(s_1^2+1.0994s_1+0.4308)(s_1^2+1.0994s_1+0.4308)(s_2^2+1.0994s_2+0.4308)(s_2^2+1.0994s_2+0.4308)(s_2^2+1.0994s_2+0.4308)(s_2^2+1.0994s_2+0.4308)}$
FL21	8	C12.C12	$\frac{1}{(s_1^2+1.8478s_1+1)(s_1^2+1.618s_1+1)(s_1^2+1.8478s_1+1)(s_1^2+1.618s_1+1)(s_2^2+1.8478s_2+1)(s_2^2+1.618s_2+1)(s_2^2+1.8478s_2+1)(s_2^2+1.618s_2+1)}$
FL22	8	C22.C22	$\frac{(259.1431)^4}{(s_1^4+11.3534s_1^3+63.5988s_1^2+188.0802s_1+259.1431)(s_1^4+11.3534s_1^3+63.5988s_1^2+188.0802s_1+259.1431)(s_2^4+11.3534s_2^3+63.5988s_2^2+188.0802s_2+259.1431)(s_2^4+11.3534s_2^3+63.5988s_2^2+188.0802s_2+259.1431)}$

Table 3.2: Cascading combination 1-D lowpass filters having monotonic characteristics, to obtain 2-D analog lowpass filters with monotonic frequency response.

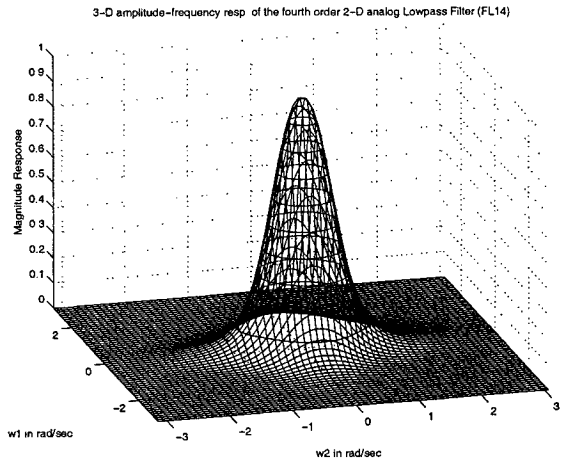

(a) 3-D amplitude-frequency response (FL14)

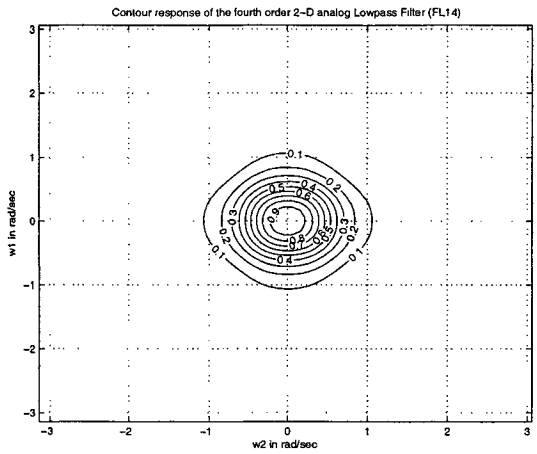

(b) Contour of the frequency response (FL14)

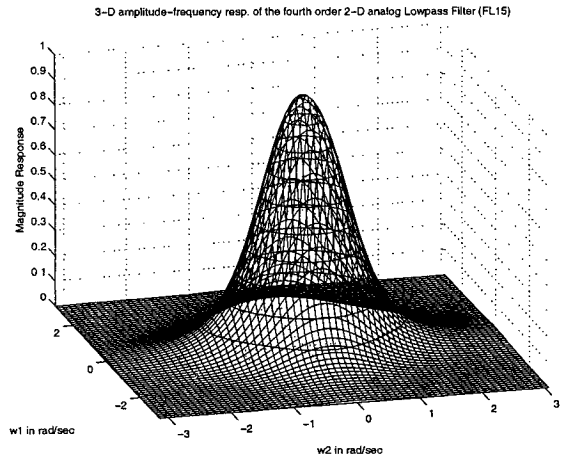

(c) 3-D amplitude-frequency response (FL15)

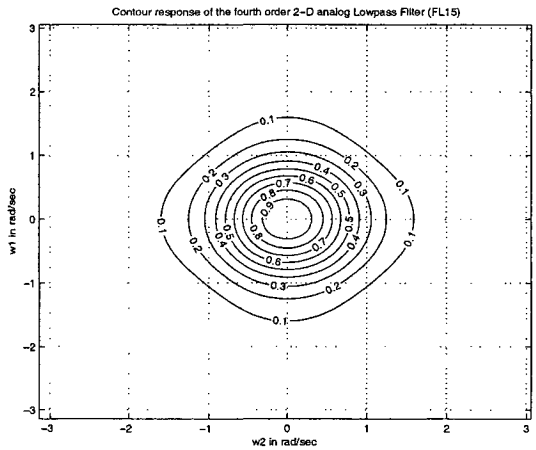

(d) Contour of the frequency response (FL15)

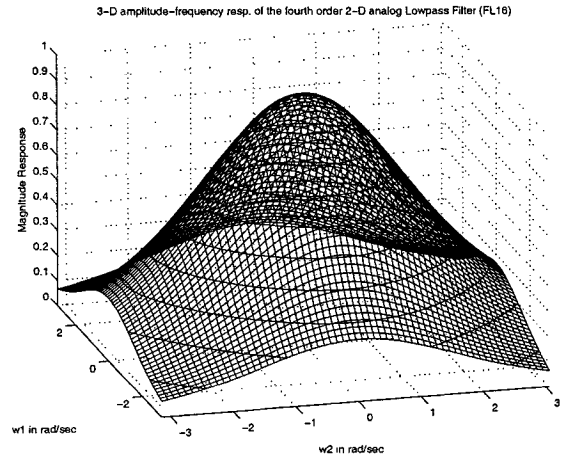

(e) 3-D amplitude-frequency response (FL16)

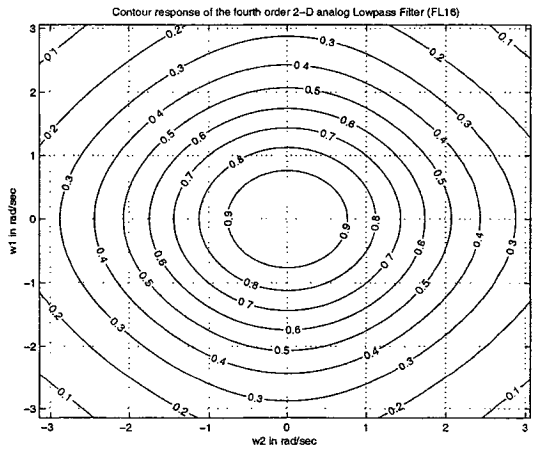

(f) Contour of the frequency response (FL16)

Figure 3.41: Frequency response of 2-D analog lowpass filter, FL14, FL15, FL16, having monotonic characteristics, obtained from cascaded 1-D lowpass filters (Refer Table: 3.2).

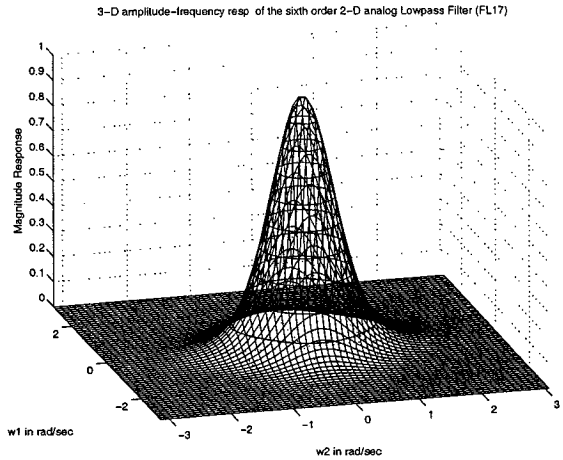

(a) 3-D amplitude-frequency response (FL17)

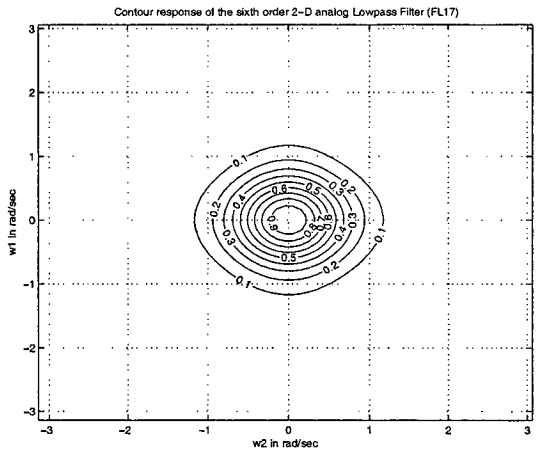

(b) Contour of the frequency response (FL17)

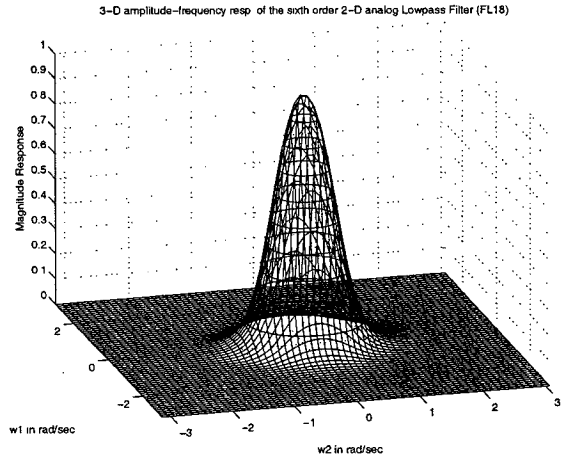

(c) 3-D amplitude-frequency response (FL18)

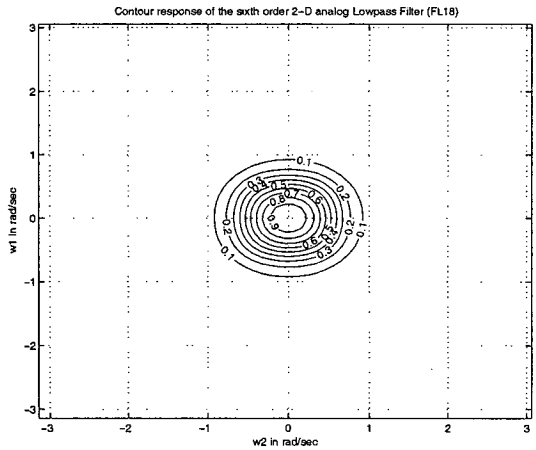

(d) Contour of the frequency response (FL18)

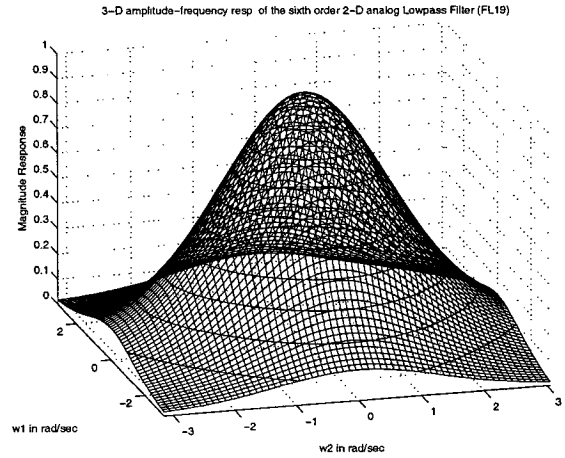

(e) 3-D amplitude-frequency response (FL19)

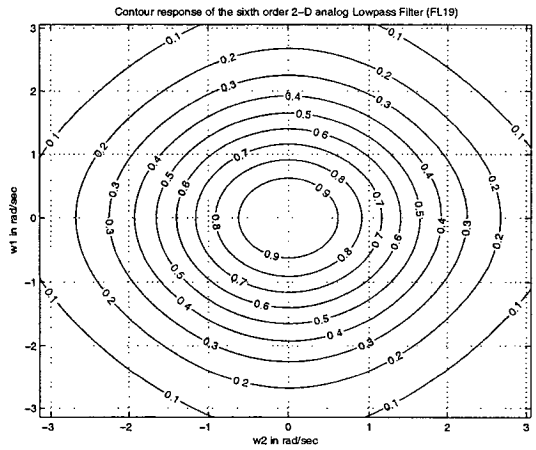

(f) Contour of the frequency response (FL19)

Figure 3.42: Frequency response of 2-D analog lowpass filter, FL17, FL18, FL19, having monotonic characteristics, obtained from cascaded 1-D lowpass filters (Refer Table: 3.2).

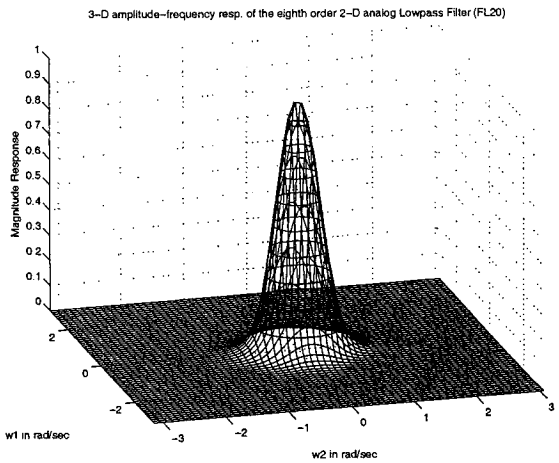

(a) 3-D amplitude-frequency response (FL20)

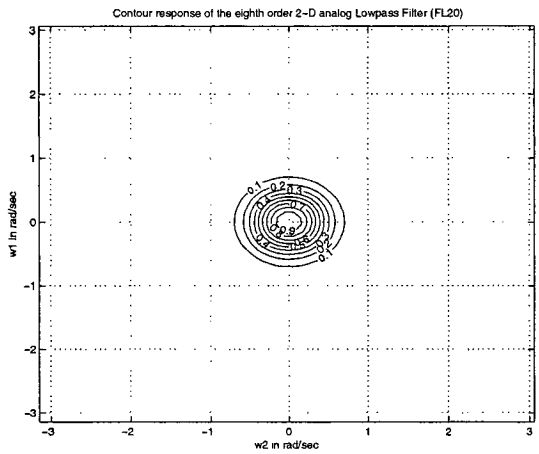

(b) Contour of the frequency response (FL20)

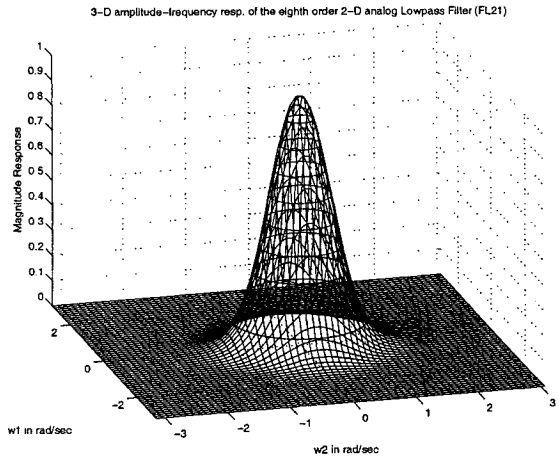

(c) 3-D amplitude-frequency response (FL21)

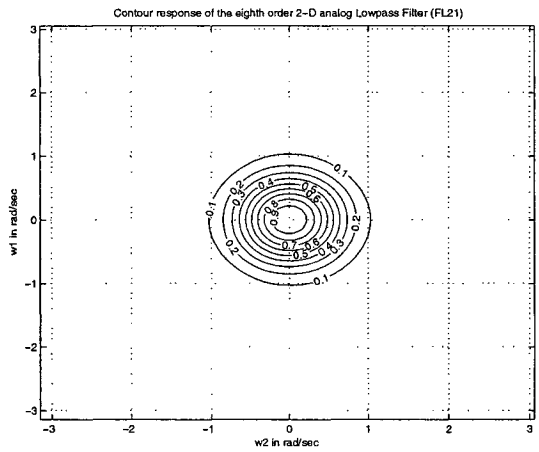

(d) Contour of the frequency response (FL21)

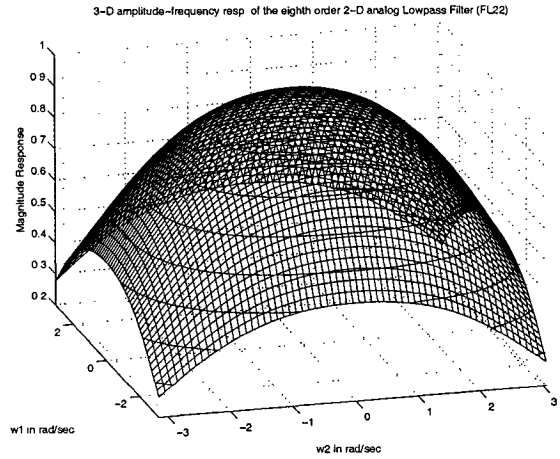

(e) 3-D amplitude-frequency response (FL22)

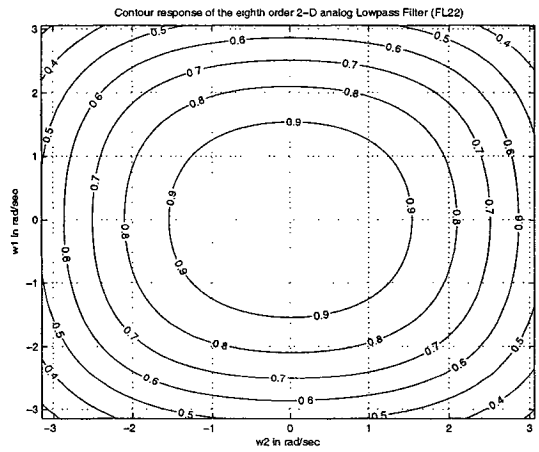

(f) Contour of the frequency response (FL22)

Figure 3.43: Frequency response of 2-D analog lowpass filter, FL20, FL21, FL22, having monotonic characteristics, obtained from cascaded 1-D lowpass filters (Refer Table: 3.2).

Algorithm 30 The MATLAB code to plot the 3-D amplitude-frequency response and contour response of the 2-D analog lowpass filters (refer table: 3.2), having monotonic characteristics and obtained from cascaded 1-D lowpass filters.

```
% Under Guidance of Prof. Dr. V. Ramachandran
% Student's name : Ajit Singh Sandhu..... ID:4841492.
clear all;
[w1,w2] = meshgrid(-pi:0.1:pi,-pi:0.1:pi);
s1=j*w1; s2=j*w2;
%Transfer function of the 2-D analog Filter - FL14
h1_1=(s1.^2+1.0994.*s1+0.4308).*(s1.^2+1.0994.*s1+0.4308);
h1_2=(s2.^2+1.0994.*s2+0.4308).*(s2.^2+1.0994.*s2+0.4308);
h1=abs((0.4308^4)./(h1_1.*h1_2));
figure(1);
contour3(w1,w2,h1);
surface(w1,w2,abs(h1),'EdgeColor',[.8 .8 .8],'FaceColor','none');
grid on;
view(-15,25);
title('3-D amplitude-frequency resp. of the fourth order 2-D analog Lowpass Filter (FL14)');
xlabel(' w2 in rad/sec ');
ylabel(' w1 in rad/sec ');
zlabel(' Magnitude Response ');
figure(2);
[C,h] = contour(w1,w2,h1);
clabel(C,h);
grid on;
title('Contour response of the fourth order 2-D analog Lowpass Filter (FL14)');
xlabel(' w2 in rad/sec ');
ylabel(' w1 in rad/sec ');
%Transfer function of the 2-D analog Filter - FL15
h2_1=(s1.^2+1.8478.*s1+1).*(s1.^2+1.618.*s1+1);
h2_2=(s2.^2+1.8478.*s2+1).*(s2.^2+1.618.*s2+1);
h2=abs(1./(h2_1.*h2_2));
figure(3);
contour3(w1,w2,h2);
surface(w1,w2,abs(h2),'EdgeColor',[.8 .8 .8],'FaceColor','none');
grid on;
view(-15,25);
title('3-D amplitude-frequency resp. of the fourth order 2-D analog Lowpass Filter (FL15)');
xlabel(' w2 in rad/sec ');
ylabel(' w1 in rad/sec ');
zlabel(' Magnitude Response ');
figure(4);
[C,h] = contour(w1,w2,h2);
clabel(C,h);
grid on;
title('Contour response of the fourth order 2-D analog Lowpass Filter (FL15)');
xlabel(' w2 in rad/sec ');
ylabel(' w1 in rad/sec ');
```

(To be continued...)

Algorithm 30 (Contd...)

```
%Transfer function of the 2-D analog Filter - FL16
h2_1=(s1.^2+5.7924.*s1+9.14).*(s1.^2+5.7924.*s1+9.14);
h2_2=(s2.^2+5.7924.*s2+9.14).*(s2.^2+5.7924.*s2+9.14);
h2=abs((9.14^4)./(h2_1.*h2_2));
figure(5);
contour3(w1,w2,h2);
surface(w1,w2,abs(h2),'EdgeColor',[.8 .8 .8],'FaceColor','none');
grid on; view(-15,25);
title('3-D amplitude-frequency resp. of the fourth order 2-D analog Lowpass Filter (FL16)');
xlabel(' w2 in rad/sec ');
ylabel(' w1 in rad/sec ');
zlabel(' Magnitude Response ');
figure(6);
[C,h] = contour(w1,w2,h2);
clabel(C,h); grid on;
title('Contour response of the fourth order 2-D analog Lowpass Filter (FL16)');
xlabel(' w2 in rad/sec ');
ylabel(' w1 in rad/sec ');
%Transfer function of the 2-D analog Filter - FL17
h3_1=(s1.^2+1.8478.*s1+1).*(s1+1).*(s1.^3+2.618.*(s1.^2)+2.618.*s1+1);
h3_2=(s2.^2+1.8478.*s2+1).*(s2+1).*(s2.^3+2.618.*(s2.^2)+2.618.*s2+1);
h3=abs(1./(h3_1.*h3_2));
figure(7);
contour3(w1,w2,h3);
surface(w1,w2,abs(h3),'EdgeColor',[.8 .8 .8],'FaceColor','none');
grid on; view(-15,25);
title('3-D amplitude-frequency resp. of the sixth order 2-D analog Lowpass Filter (FL17)');
xlabel(' w2 in rad/sec ');
ylabel(' w1 in rad/sec ');
zlabel(' Magnitude Response ');
figure(8);
[C,h] = contour(w1,w2,h3);
```

```
clabel(C,h); grid on;
title('Contour response of the sixth order 2-D analog Lowpass Filter (FL17)');
xlabel(' w2 in rad/sec ');
ylabel(' w1 in rad/sec ');
%Transfer function of the 2-D analog Filter - FL18
h4_1=(s1.^3+1.5953.*(s1.^2)+1.1244.*s1+0.3297).*(s1.^3+1.5953.*(s1.^2)+1.1244.*s1+0.3297);
h4_2=(s2.^3+1.5953.*(s2.^2)+1.1244.*s2+0.3297).*(s2.^3+1.5953.*(s2.^2)+1.1244.*s2+0.3297);
h4=abs((0.3297^4)./(h4_1.*h4_2));
figure(9);
contour3(w1,w2,h4);
surface(w1,w2,abs(h4),'EdgeColor',[.8 .8 .8],'FaceColor','none');
grid on; view(-15,25);
title('3-D amplitude-frequency resp. of the sixth order 2-D analog Lowpass Filter (FL18)');
xlabel(' w2 in rad/sec ');
ylabel(' w1 in rad/sec ');
zlabel(' Magnitude Response ');
figure(10);
[C,h] = contour(w1,w2,h4);
clabel(C,h); grid on;
title('Contour response of the sixth order 2-D analog Lowpass Filter (FL18)');
xlabel(' w2 in rad/sec ');
ylabel(' w1 in rad/sec ');
%Transfer function of the 2-D analog Filter - FL19
h2_1=(s1.^2+5.7924.*s1+9.14).*(s1.^2+5.7924.*s1+9.14).*(s1.^2+5.7924.*s1+9.14);
h2_2=(s2.^2+5.7924.*s2+9.14).*(s2.^2+5.7924.*s2+9.14).*(s2.^2+5.7924.*s2+9.14);
h2=abs((9.14^6)./(h2_1.*h2_2));
figure(11);
contour3(w1,w2,h2);
surface(w1,w2,abs(h2),'EdgeColor',[.8 .8 .8],'FaceColor','none');
grid on; view(-15,25);
title('3-D amplitude-frequency resp. of the sixth order 2-D analog Lowpass Filter (FL19)');
xlabel(' w2 in rad/sec ');
ylabel(' w1 in rad/sec ');
```

```
zlabel(' Magnitude Response ');
figure(12);
[C,h] = contour(w1,w2,h2);
clabel(C,h); grid on;
title('Contour response of the sixth order 2-D analog Lowpass Filter (FL19)');
xlabel(' w2 in rad/sec ');
ylabel(' w1 in rad/sec ');
%Transfer function of the 2-D analog Filter - FL20
h5_1=(s1.^2+1.0994.*s1+0.4308).*(s1.^2+1.0994.*s1+0.4308)
.*(s1.^2+1.0994.*s1+0.4308).*(s1.^2+1.0994.*s1+0.4308);
h5_2=(s2.^2+1.0994.*s2+0.4308).*(s2.^2+1.0994.*s2+0.4308)
.*(s2.^2+1.0994.*s2+0.4308).*(s2.^2+1.0994.*s2+0.4308);
h5=abs((0.4308^8)./(h5_1.*h5_2));
figure(13);
contour3(w1,w2,h5);
surface(w1,w2,abs(h5),'EdgeColor',[.8 .8 .8],'FaceColor','none');
grid on; view(-15,25);
title('3-D amplitude-frequency resp. of the eighth order 2-D analog Lowpass Filter (FL20)');
xlabel(' w2 in rad/sec ');
ylabel(' w1 in rad/sec ');
zlabel(' Magnitude Response ');
figure(14);
[C,h] = contour(w1,w2,h5);
clabel(C,h); grid on;
title('Contour response of the eighth order 2-D analog Lowpass Filter (FL20)');
xlabel(' w2 in rad/sec ');
ylabel(' w1 in rad/sec ');
%Transfer function of the 2-D analog Filter - FL21
h6_1=(s1.^2+1.8478.*s1+1).*(s1.^2+1.618.*s1+1).*(s1.^2+1.8478.*s1+1).*(s1.^2+1.618.*s1+1);
h6_2=(s2.^2+1.8478.*s2+1).*(s2.^2+1.618.*s2+1).*(s2.^2+1.8478.*s2+1).*(s2.^2+1.618.*s2+1);
h6=abs(1./(h6_1.*h6_2));
figure(15);
contour3(w1,w2,h6);
```

```
surface(w1,w2,abs(h6),'EdgeColor',[.8 .8 .8],'FaceColor','none');
grid on; view(-15,25);
title('3-D amplitude-frequency resp. of the eighth order 2-D analog Lowpass Filter (FL21)');
xlabel(' w2 in rad/sec ');
ylabel(' w1 in rad/sec ');
zlabel(' Magnitude Response ');
figure(16);
[C,h] = contour(w1,w2,h6);
clabel(C,h); grid on;
title('Contour response of the eighth order 2-D analog Lowpass Filter (FL21)');
xlabel(' w2 in rad/sec ');
ylabel(' w1 in rad/sec ');
%Transfer function of the 2-D analog Filter - FL22
h6_1=(s1.^4+11.3534.*(s1.^3)+63.5988.*(s1.^2)+188.0802.*s1+259.1431)
.*(s1.^4+11.3534.*(s1.^3)+63.5988.*(s1.^2)+188.0802.*s1+259.1431);
h6_2=(s2.^4+11.3534.*(s2.^3)+63.5988.*(s2.^2)+188.0802.*s2+259.1431)
.*(s2.^4+11.3534.*(s2.^3)+63.5988.*(s2.^2)+188.0802.*s2+259.1431);
h6=abs((259.1431^4)./(h6_1.*h6_2));
figure(17);
contour3(w1,w2,h6);
surface(w1,w2,abs(h6),'EdgeColor',[.8 .8 .8],'FaceColor','none');
grid on; view(-15,25);
title('3-D amplitude-frequency resp. of the eighth order 2-D analog Lowpass Filter (FL22)');
xlabel(' w2 in rad/sec ');
ylabel(' w1 in rad/sec ');
zlabel(' Magnitude Response ');
figure(18);
[C,h] = contour(w1,w2,h6);
clabel(C,h); grid on;
title('Contour response of the eighth order 2-D analog Lowpass Filter (FL22)');
xlabel(' w2 in rad/sec ');
ylabel(' w1 in rad/sec ');
```

3.8 Summary

In this Chapter, we proposed generation of analog and digital 2-D lowpass filters by utilizing the 1-D lowpass filters, with monotonic amplitude frequency response and studied their characteristics.

The filters discussed and proposed in Chapter 2, namely, Butterworth, Papoulis, Thomson-Bessel and Filanovsky filters, their extracted lower order monotonic 1-D filters, and their cascaded combinational monotonic higher order 1-D filters, were extended as 2-D analog and digital lowpass filters with monotonic characteristics. The 2-D analog lowpass filters with monotonic characteristics were derived by cascade realization of the corresponding 1-D lowpass filters. The 2-D digital lowpass filters were generated by applying generalized lowpass filter bilinear transformation to the corresponding 2-D analog lowpass filters.

We have generated fourth and fifth order Papoulis, Butterworth and Thomson-Bessel 2-D analog lowpass filters with monotonic characteristics by cascading the corresponding 1-D lowpass filters derived in Chapter 2, and their results were discussed. The 2-D lowpass filters were also realized in digital (z) domain, and the properties of the digital lowpass filters based on different values of coefficients of the generalized bilinear transformation were studied. Similarly, fifth order 2-D Filanovsky lowpass analog and digital filters were generated and their properties were studied.

We also generated all possible first to fourth order 2-D analog lowpass filters with monotonic characteristics, by cascade combination of the corresponding extracted lower order 1-D lowpass filters with monotonic amplitude-frequency response (derived in Chapter 2).

Furthermore, we also realized few fourth, sixth and eighth order 2-D analog lowpass filters, by cascading combination 1-D lowpass filters derived in Chapter 2, with monotonic amplitude-frequency response.

Chapter 4

Generation of 2-D lowpass filter by considering a stable generalized doubly terminated network with monotonic amplitude-frequency response

4.1 Introduction

In Chapter 2, we generated different types of stable 1-D lowpass filters of different order with monotonic amplitude-frequency response. They were furthermore, extended to 2-D analog and digital lowpass filters of different types and order with monotonic amplitude-frequency response (Chapter 3). Therefore, the work proposed till now is primarily concentrated on generation of stable 1-D lowpass filters and their extension to different types of stable 2-D lowpass filters of different order and types, with monotonic characteristics.

In various applications, we already have an existing network, or have to implement a multidimensional stable filter not from its 1-D equivalents. In multidimensional domain, filter design and analysis becomes a tedious process. Often design of such filters are based

on various conditions and assumptions, which will still make the solutions practically feasible. Hence, if we consider a generalized 2-D network, its implementation as a stable 2-D filter with monotonic amplitude-frequency response require certain conditions to be satisfied. But, in a 2-D network, specifying necessary and sufficient conditions for the coefficients of the filter is often a tedious task. Our emphasis in this Chapter will be to find simple possible ways to specify conditions to achieve monotonic amplitude response in 2-D analog and digital filters.

In this Chapter, we will design 2-D lowpass filters in analog and digital domain, by considering a doubly terminated network obtained from a Continued Fraction Expansion (CFE), and ensure its stability by verifying it to be a VSHP in Sec. 4.2. Since, the main motive of the thesis is to design monotonic filters, in Sec. 4.3, we will derive condition for monotonicity to be satisfied for design of 2-D filter with monotonic amplitude-frequency response. In Sec. 4.4, we will generate 2-D analog lowpass filters from the considered 2-D network, and study the affect of coefficients of filter to obtain monotonic characteristics. In Sec. 4.5, we will generate 2-D digital lowpass filters and study the affects of coefficients to achieve monotonic amplitude-frequency response. We shall also propose that how the coefficients of the generalized bilinear transformation be adjusted to get 2-D digital lowpass filter with monotonic amplitude-frequency response from a 2-D analog lowpass filter with ripple in passband. In Sec. 4.6, firstly we will find the value of the filter coefficients to realize 2-D analog Butterworth filter from the considered doubly terminated network. Then, we will generate 2-D analog and digital Butterworth lowpass filters, and show the affect of coefficients of generalized bilinear transformation to achieve monotonic amplitude-frequency response in digital domain. We will also derive relationship between cutoff frequency and gain for the 2-D analog Butterworth lowpass filter.

4.2 Considering a doubly terminated network and defining its stability

Let us consider a doubly terminated network, and the generalized expression of the Continued Fraction Expansion (CFE) [47] can be expressed as

$$1+\frac{a_{11}s_1s_2+a_{00}}{a_{10}s_1+a_{01}s_2}+\frac{1}{\frac{b_{11}s_1s_2+b_{00}}{b_{10}s_1+b_{01}s_2}+1} \tag{4.1}$$

If invert the CFE, and simplify it further, we get,

$$H_a(s_1,s_2)=\frac{N_a(s_1,s_2)}{D_a(s_1,s_2)}$$

$$=\frac{(a_{10}s_1+a_{01}s_2)(b_{11}s_1s_2+b_{00}+b_{10}s_1+b_{01}s_2)}{\begin{array}{c}(a_{11}s_1s_2+a_{00}+a_{10}s_1+a_{01}s_2)(b_{11}s_1s_2+b_{00}+b_{10}s_1+b_{01}s_2)\\+(a_{10}s_1+a_{01}s_2)(b_{10}s_1+b_{01}s_2)\end{array}} \tag{4.2}$$

To define the stability of the filter, we have to make the filter's transfer function free from singularities of the first and second kind (Sec. 1.2). Therefore, we should define and/or prove the denominator polynomial to be VSHP [6, 7]. If we simplify the numerator and denominator (eqn. 4.2), it can be easily seen that they are Stable Hurwitz Polynomial (SHP) [7], respectively. Based on the test methodology to check for VSHP [7], we get,

$$N_a(s_1,s_2)=N_a\left(\frac{1}{s_1},s_2\right)=N_a\left(s_1,\frac{1}{s_2}\right)=N_a\left(\frac{1}{s_1},\frac{1}{s_2}\right)\neq\frac{0}{0}$$

$$D(s_1,s_2)=D_a\left(\frac{1}{s_1},s_2\right)=D_a\left(s_1,\frac{1}{s_2}\right)=D_a\left(\frac{1}{s_1},\frac{1}{s_2}\right)\neq\frac{0}{0}$$

where, $s_1=0$ and $s_2=0$.

Since the non-essential singularities of the first and second kind are ruled out, we can conclude that the numerator polynomial, $N_a(s_1,s_2)$, and denominator polynomial, $D_a(s_1,s_2)$, are VSHPs. If we go into digital (z) domain (by applying analog to digital

transformation, for example, bilinear transformation), the polynomials will still remain VSHP.

Since the stability of the filter is defined by the denominator of the transfer function, let us take numerator of the transfer function in eqn. 4.2 as a constant (A_0). Therefore, the transfer function can be represented as,

$$H_a(s_1, s_2) = \frac{A_0}{D_a(s_1, s_2)} \tag{4.3}$$

where, $D_a(s_1, s_2)$ is the denominator polynomial of the eqn. 4.2, $s_1 = jw_1$ and $s_2 = jw_2$. Similar to Chapter 2, we want the magnitude response of the 2-D filter, at $w_1 = 0$, $w_2 = 0$, to be unity, i.e.,

$$|H_a(0,0)| = \left| \frac{A_0}{D_a(0,0)} \right| = 1 \tag{4.4}$$

Therefore, the value of A_0 after simplifying eqn. 4.4 will be the numerator constant value for the 2-D analog filter.

4.3 Condition for monotonicity in amplitude-frequency response of the 2-D analog lowpass filter

In this section, we will define condition for monotonic behavior of the 2-D analog filter obtained from the doubly terminated network transfer function (eqn. 4.2). According to the definition of monotonicity in the amplitude-frequency response, the 2-D analog filter should satisfy the following conditions,

$$\left\{ \begin{array}{l} \frac{\partial |H_a(w_1.w_2)|}{\partial w_1} \leq 0, w_2 = 0 \\ \frac{\partial |H_a(w_1.w_2)|}{\partial w_2} \leq 0, w_1 = 0 \end{array} \right\} \tag{4.5}$$

where, $s_1 = jw_1$ and $s_2 = jw_2$. By substituting eqn. 4.3 in eqn. 4.5 we get,

$$\left\{ \begin{array}{l} \frac{\partial |D_a(w_1.w_2)|}{\partial w_1} \geq 0, w_2 = 0 \\ \frac{\partial |D_a(w_1.w_2)|}{\partial w_2} \geq 0, w_1 = 0 \end{array} \right\} \tag{4.6}$$

as the condition for monotonic amplitude-frequency response of the 2-D analog filter. Therefore, from eqn. 4.2 and 4.3, with $s_1 = jw_1$ and $s_2 = jw_2$, the denominator polynomial can be represented as,

$$\begin{aligned} D_a(w_1, w_2) = & \{(-a_{11}w_1w_2 + a_{00}) + j(a_{10}w_1 + a_{01}w_2)\} \\ & \{(-b_{11}w_1w_2 + b_{00}) + j(b_{10}w_1 + b_{01}w_2)\} \\ & -(a_{10}w_1 + a_{01}w_2)(b_{10}w_1 + b_{01}w_2) \end{aligned} \tag{4.7}$$

Case I: When $w_2 = 0$ in eqn. 4.7, we get

$$D_a(w_1, 0) = (a_{00} + ja_{10}w_1)(b_{00} + jb_{10}w_1) - a_{10}b_{10}w_1^2$$

$$|D_a(w_1, 0)| = \sqrt{(a_{00}b_{00} - 2a_{10}b_{10}w_1^2)^2 + (a_{00}b_{10} + a_{10}b_{00})^2 w_1^2}$$

$$\frac{\partial |D_a(w_1, 0)|}{\partial w_1} = w_1 \left[-4a_{10}b_{10}(a_{00}b_{00} - 2a_{10}b_{10}w_1^2) + (a_{00}b_{10} + a_{10}b_{00})^2 \right] \geq 0$$

$$w_1 \geq 0, w_1 \geq \left| \frac{a_{00}b_{10} - a_{10}b_{00}}{2\sqrt{2}a_{10}b_{10}} \right| \tag{4.8}$$

Case II: When $w_1 = 0$ in eqn. 4.7, we get

$$D_a(0, w_2) = (a_{00} + ja_{01}w_2)(b_{00} + jb_{01}w_2) - a_{01}b_{01}w_2^2$$

$$|D_a(0, w_2)| = \sqrt{(a_{00}b_{00} - 2a_{01}b_{01}w_2^2)^2 + (a_{00}b_{01} + a_{01}b_{00})^2 w_2^2}$$

$$\frac{\partial |D_a(0,w_2)|}{\partial w_2} = w_2 \left[-4a_{01}b_{01}\left(a_{00}b_{00} - 2a_{01}b_{01}w_2^2\right) + \left(a_{00}b_{01} + a_{01}b_{00}\right)^2 \right] \geq 0$$

$$w_2 \geq 0, w_2 \geq \left| \frac{a_{00}b_{01} - a_{01}b_{00}}{2\sqrt{2}a_{01}b_{01}} \right| \tag{4.9}$$

Hence, the conditions 4.8 and 4.9, in terms of the filter coefficients and frequency, have to be satisfied for monotonic behavior in the amplitude-frequency response of the 2-D analog filter considered. But, these may not be sufficient conditions to be satisfied for defining monotonicity in amplitude-frequency response of the 2-D analog filter.

4.4 Generation of 2-D analog lowpass filter obtained from the doubly terminated network considered, with monotonic amplitude-frequency response

The transfer function of the 2-D analog generalized lowpass filter obtained from CFE (eqn. 4.2 and 4.3), with $s_1 = jw_1$ and $s_2 = jw_2$, can be given by eqn. 4.10,

$$H_a(s_1,s_2) = \frac{a_{00}b_{00}}{\begin{array}{r}\left(a_{11}s_1s_2 + a_{00} + a_{10}s_1 + a_{01}s_2\right)\left(b_{11}s_1s_2 + b_{00} + b_{10}s_1 + b_{01}s_2\right) \\ + \left(a_{10}s_1 + a_{01}s_2\right)\left(b_{10}s_1 + b_{01}s_2\right)\end{array}} \tag{4.10}$$

where, $A_0 = a_{00}b_{00}$, obtained by simplifying eqn. 4.4.

In the design of 2-D analog lowpass filter, the filter coefficients (a_{00}, a_{01}, a_{10}, a_{11}, b_{00}, b_{01}, b_{10} and b_{11}) of the 2-D transfer function can be determined by various approaches. But in the design, certain condition have to be satisfied and/or constraints have to be imposed. Let us consider the filter coefficients such that they satisfy condition for monotonicity (eqn. 4.8 and 4.9).

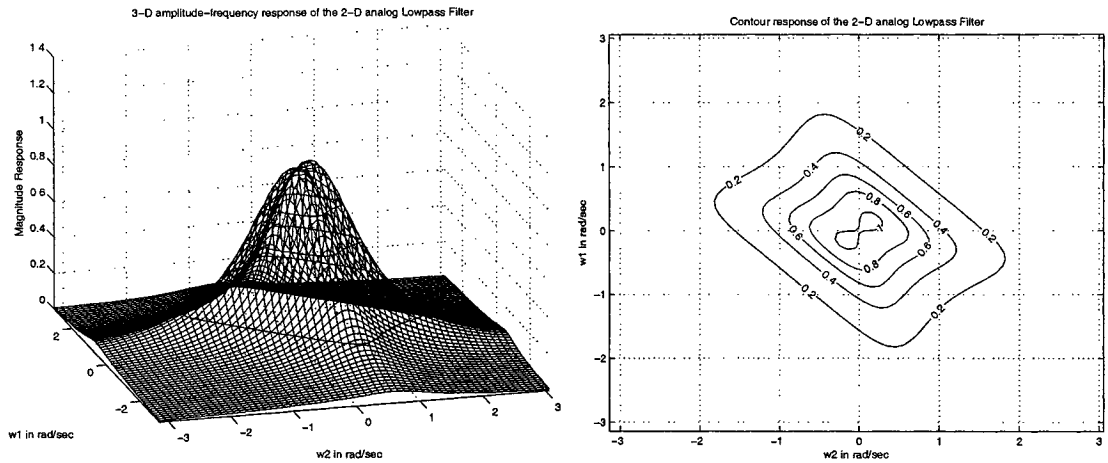

(a) 3-D amplitude-frequency response of the 2-D analog lowpass filter

(b) Contour frequency response of the 2-D analog lowpass filter

Figure 4.1: 3-D amplitude-frequency response and contour response of the 2-D analog lowpass filter with $a_{00} = a_{01} = a_{10} = a_{11} = b_{00} = b_{01} = b_{10} = b_{11} = 1$

Let us assume all the coefficients to be unity, i.e., $a_{00} = 1$, $a_{01} = 1$, $a_{10} = 1$, $a_{11} = 1$, $b_{00} = 1$, $b_{01} = 1$, $b_{10} = 1$, $b_{11} = 1$, and 3-D amplitude-frequency response and contour plot for the corresponding 2-D analog lowpass filter is as shown in fig. 4.1. It is observed that there is a ripple in the passband at lower frequency range. This is primarily because of coefficients a_{11} and b_{11} which were not taken into consideration while defining the monotonicity condition in Sec. 4.3. The simulation results indicate that smaller the value of coefficients a_{11} and b_{11}(i.e. as a_{11}, b_{11} tends to zero), the more the 2-D filter will approach towards monotonic characteristics. It can be seen in fig. 4.1, 4.2, 4.3 and 4.4 that as a_{11} and b_{11} decreases from 1 to 0.05, the ripple in the passband decreases and it shows monotonic amplitude-frequency response in fig. 4.4. But, this results in expansion of the contour plot along the frequency axis. Hence, the cutoff frequencies increases and they should satisfy the nyquist criterion (in digital domain) to avoid loss of signal. The MATLAB code to plot the 3-D amplitude-frequency response and contour response of the 2-D analog lowpass filters having monotonic characteristics, based on different combinations of filter coefficients is in algorithm 31.

Furthermore, after simplifying eqn. 4.10, we get

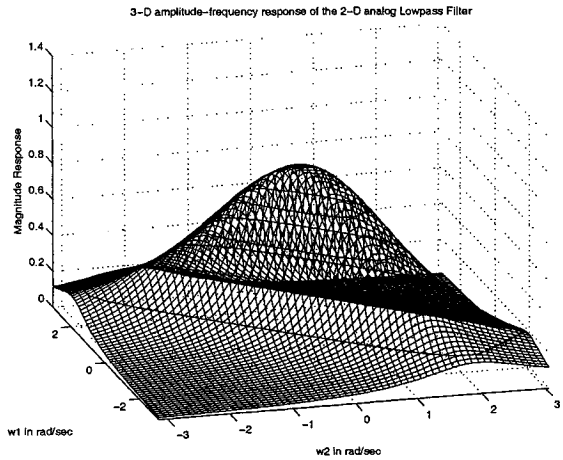

(a) 3-D amplitude-frequency response of the 2-D analog lowpass filter

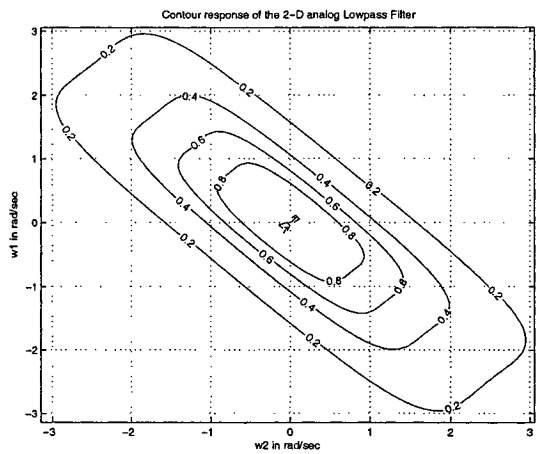

(b) Contour frequency response of the 2-D analog lowpass filter

Figure 4.2: 3-D amplitude-frequency response and contour response of the 2-D analog lowpass filter with $a_{00} = a_{01} = a_{10} = b_{00} = b_{01} = b_{10} = 1$ and $a_{11} = b_{11} = 0.2$

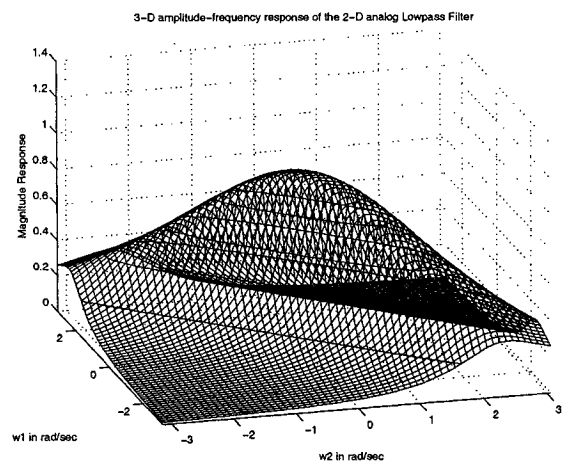

(a) 3-D amplitude-frequency response of the 2-D analog lowpass filter

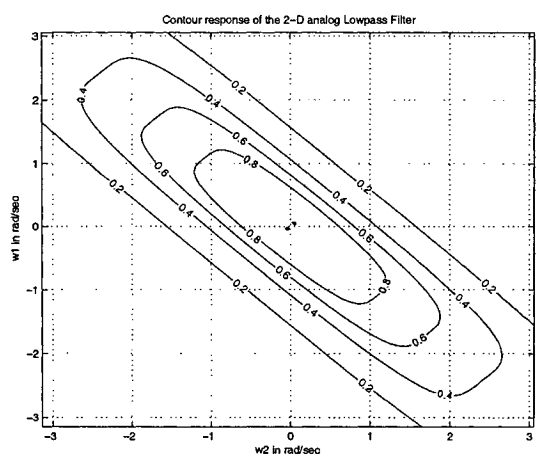

(b) Contour frequency response of the 2-D analog lowpass filter

Figure 4.3: 3-D amplitude-frequency response and contour response of the 2-D analog lowpass filter with $a_{00} = a_{01} = a_{10} = b_{00} = b_{01} = b_{10} = 1$ and $a_{11} = b_{11} = 0.1$

Algorithm 31 The MATLAB code to plot the 3-D amplitude-frequency response and contour response of the 2-D analog lowpass filters having monotonic characteristics, based on different combination of filter coefficients.

```
% Under Guidance of Prof. Dr. V. Ramachandran
% Student's name : Ajit Singh Sandhu..... ID:4841492.
clear all; clc;
% Input the values of the constants in the LP bilinear transformation.
a00=input('Give the value of the a00 => ');
a10=input('Give the value of the a10 => ');
a01=input('Give the value of the a01 => ');
a11=input('Give the value of the a11 => ');
b00=input('Give the value of the b00 => ');
b10=input('Give the value of the b10 => ');
b01=input('Give the value of the b01 => ');
b11=input('Give the value of the b11 => ');
% Create two dimensional square matrix (mesh grid) of angular frequency w1 and w2.
[w1,w2] = meshgrid(-pi:0.1:pi,-pi:0.1:pi);
s1=j.*w1;
s2=j.*w2;
d=((a11.*s1.*s2+a10.*s1+a01.*s2+a00).*(b11.*s1.*s2+b10.*s1+b01.*s2+b00))
+((a10.*s1+a01.*s2).*(b10.*s1+b01.*s2));
h=abs((a00.*b00)./d);
% Figure 1 represents a 3D contour plot of hd in accordance to values of w1 and w2 in the meshgrid
figure(1);
contour3(w1,w2,h);
surface(w1,w2,abs(h),'EdgeColor',[.8 .8 .8],'FaceColor','none');
grid on;
view(-15,25);
%colormap cool;
title('3-D amplitude-frequency response of the 2-D analog Lowpass Filter');
xlabel(' w2 in rad/sec ');
ylabel(' w1 in rad/sec ');
zlabel(' Magnitude Response ');
% Figure 2 represents the top view of the 3d contour observed in figure 1. We can observe the contour
position
% with the corresponding values of the h in the meshgrid representing w1 and w2 in X and Y axes resp.
figure(2);
[C,hh] = contour(w1,w2,h);
clabel(C,hh);
%colormap cool;
grid on;
title('Contour response of the 2-D analog Lowpass Filter');
xlabel(' w2 in rad/sec ');
ylabel(' w1 in rad/sec ');
```

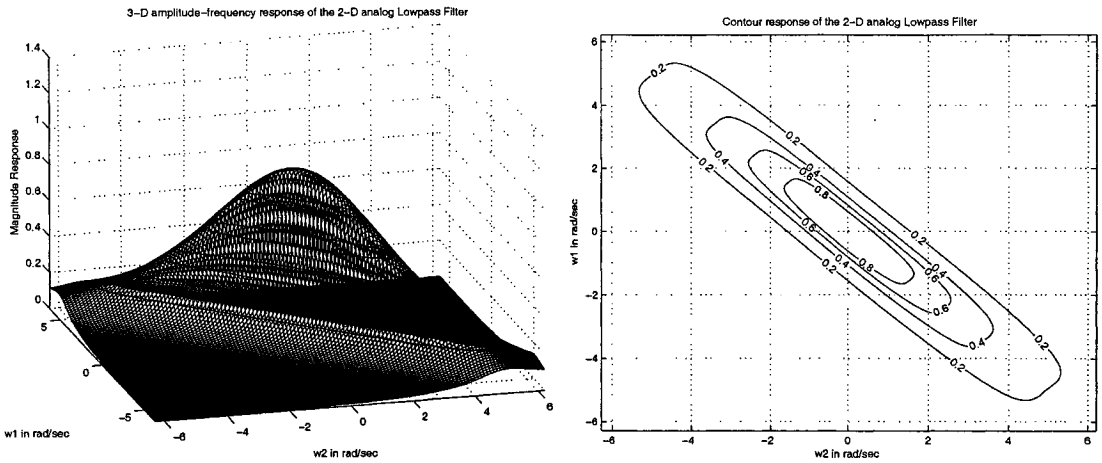

(a) 3-D amplitude-frequency response of the 2-D analog lowpass filter

(b) Contour frequency response of the 2-D analog lowpass filter

Figure 4.4: 3-D amplitude-frequency response and contour response of the 2-D analog lowpass filter with $a_{00} = a_{01} = a_{10} = b_{00} = b_{01} = b_{10} = 1$ and $a_{11} = b_{11} = 0.05$

$$H_a(s_1, s_2) = \frac{a_{00}b_{00}}{\begin{aligned} &a_{11}b_{11}s_1^2s_2^2 + (a_{11}b_{10} + a_{10}b_{11})\, s_1^2 s_2 + (a_{11}b_{01} + a_{01}b_{11})\, s_1 s_2^2 \\ &+ (a_{11}b_{00} + a_{00}b_{11} + 2a_{10}b_{01} + 2a_{01}b_{10})\, s_1 s_2 + 2a_{10}b_{10}s_1^2 + 2a_{01}b_{01}s_2^2 \\ &+ (a_{00}b_{10} + a_{10}b_{00})\, s_1 + (a_{00}b_{01} + a_{01}b_{00})\, s_2 + a_{00}b_{00} \end{aligned}} \tag{4.11}$$

If we can expand the second order 2-D analog filters derived in Sec. 3.6, the transfer functions will be having denominator polynomials similar to that of eqn. 4.11. Hence, by comparing the transfer functions in eqn. 4.11 and table: 3.1, we can associate the coefficients of the 2-D analog lowpass filter considered (eqn. 4.11) to that derived in Sec. 3.6.

4.5 Generation of 2-D digital lowpass filter obtained from the doubly terminated network considered, with monotonic amplitude-frequency response

By applying the generalized bilinear transformation for lowpass filters (eqn. 3.2) to eqn. 4.10 we get, transfer function of 2-D digital lowpass filter as function of z_1 and z_2, with $z_1 = e^{jw_1}$ and $z_2 = e^{jw_2}$. Therefore, we get,

$$
\begin{aligned}
H_d(z_1, z_2) = \frac{a_{00}b_{00}(z_1+1)^2(z_2+1)^2}{\Big[\Big\{a_{11}k_1k_2(z_1-a_{1L})(z_2-a_{2L}) + a_{00}(z_1+1)(z_2+1) \\
+a_{10}k_1(z_1-a_{1L})(z_2+1) + a_{01}k_2(z_2-a_{2L})(z_1+1)\Big\} \\
\Big\{b_{11}k_1k_2(z_1-a_{1L})(z_2-a_{2L}) + b_{00}(z_1+1)(z_2+1) \\
+b_{10}k_1(z_1-a_{1L})(z_2+1) + b_{01}k_2(z_2-a_{2L})(z_1+1)\Big\}\Big] \\
+\Big[\Big\{a_{10}k_1(z_1-a_{1L})(z_2+1) + a_{01}k_2(z_2-a_{2L})(z_1+1)\Big\} \\
\Big\{b_{10}k_1(z_1-a_{1L})(z_2+1) + b_{01}k_2(z_2-a_{2L})(z_1+1)\Big\}\Big]}
\end{aligned}
\tag{4.12}
$$

Let us consider the filter coefficients to be unity i.e. $a_{00} = a_{01} = a_{10} = a_{11} = b_{00} = b_{01} = b_{10} = b_{11} = 1$ (corresponding to the 2-D analog lowpass filter in fig. 4.1). Under this condition, the 3-D amplitude-frequency response and contour plots of the 2-D digital filter for different combinations of the bilinear transformation coefficients are as shown in fig. 4.5, 4.6, 4.7 and 4.8. The MATLAB code to plot the 3-D amplitude-frequency response and contour of the frequency response of the 2-D digital lowpass filter is in algorithm 32.

It is observed that the coefficients, k_1, k_2, affects the passband width and a_{1L}, a_{2L} affects the gain. As k_1 and k_2 values are decreased the passband increases and vice versa. For example, in fig. 4.6 (c), 4.7 (c) and 4.8 (a), (d), the passband increases with decrease in values of k_1, k_2 from 1 to 0.2, for same values of $a_{1L} = a_{2L} = 0.7$. As a_{1L} and a_{2L} values are decreased the amplitude of the magnitude response decreases and vice versa.

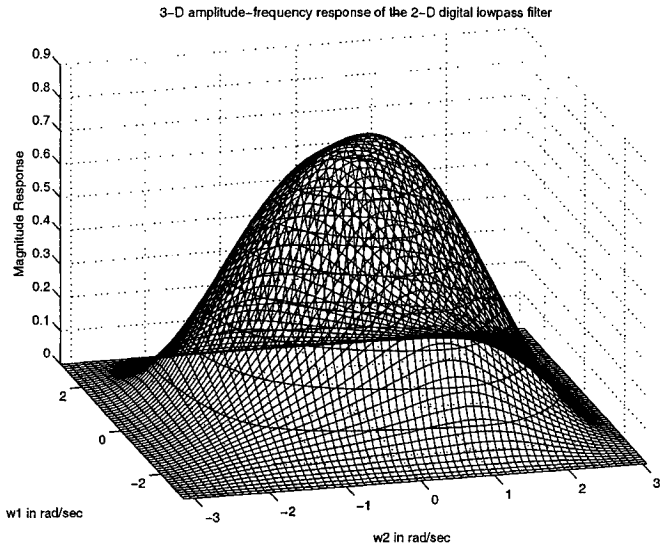

Figure 4.5: 3-D amplitude-frequency response of the 2-D digital lowpass filter obtained from the doubly terminated network considered (When $k_1 = 1$, $k_2 = 1$, $a_{1L} = 0.9$, $a_{2L} = 0.9$)

For example, in fig. 4.6 (a), (b), (c), (d), (e) and (f), amplitude of the magnitude response decreases with decrease in values of a_{1L}, a_{2L}, from 1 to 0, for same values of $k_1 = k_2 = 1$.

To achieve monotonic characteristics we should get rid of the ripple present in the equivalent 2-D analog lowpass filter in Sec. 4.4 (fig. 4.1). This is achieved by decreasing the coefficients a_{1L} and a_{2L} by a small fraction. It is observed in fig. 4.6 (a), (b) and 4.7 (a), (b), that as the value of a_{1L}, a_{2L} is decreased from 1 to 0.9, the ripple in the passband vanishes. Similarly, as the value of a_{1L}, a_{2L} is decreased from 1 to 0.7, the ripple in the passband is removed from fig. 4.7 (f) to 4.8 (a), and we get monotonic amplitude-frequency response. The MATLAB code to plot the 3-D amplitude-frequency response and contour response of the 2-D digital lowpass filters having monotonic characteristics, based on different combinations of coefficients of bilinear transformation is in algorithm 32.

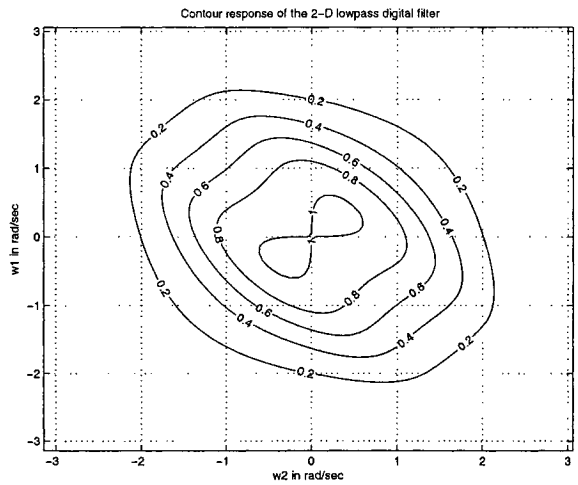

(a) When k1=1, k2=1, a1L=1 and a2L=1

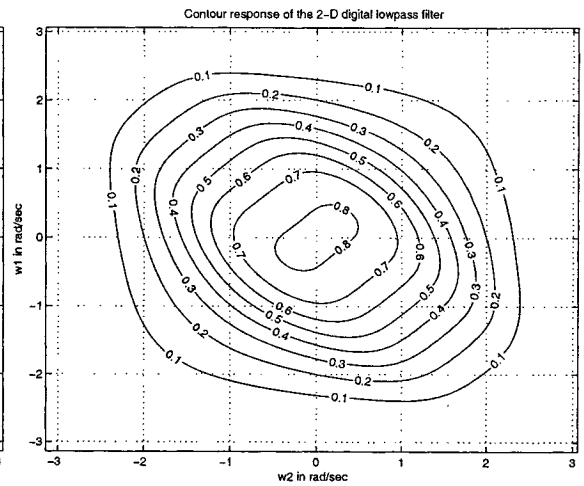

(b) When k1=1, k2=1, a1L=0.9 and a2L=0.9

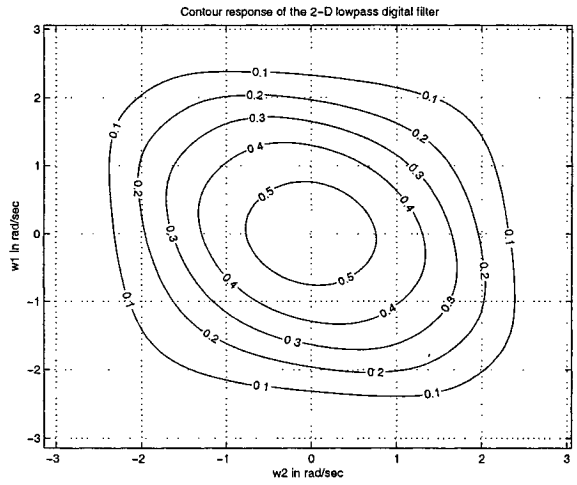

(c) When k1=1, k2=1, a1L=0.7 and a2L=0.7

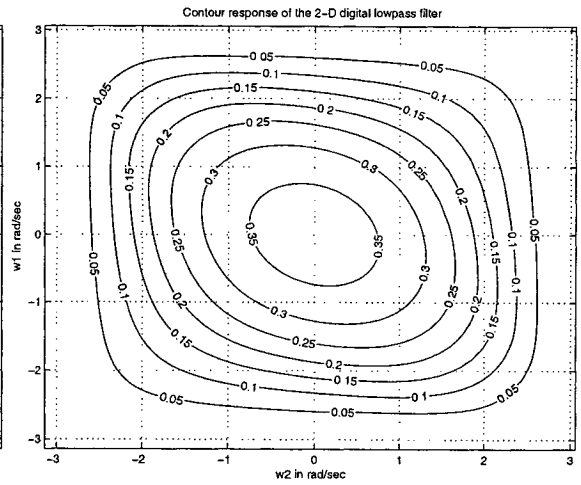

(d) When k1=1, k2=1, a1L=0.5 and a2L=0.5

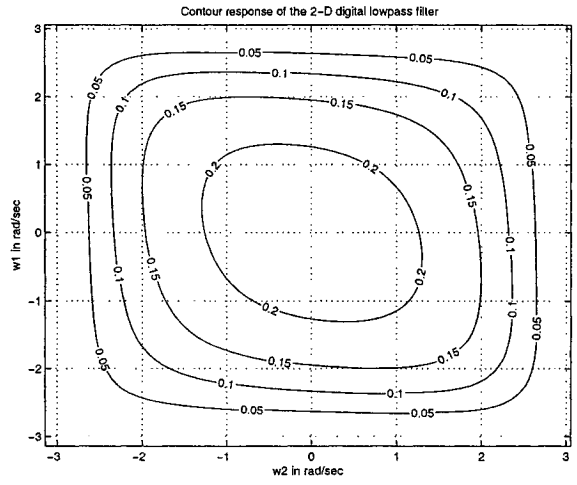

(e) When k1=1, k2=1, a1L=0.2 and a2L=0.2

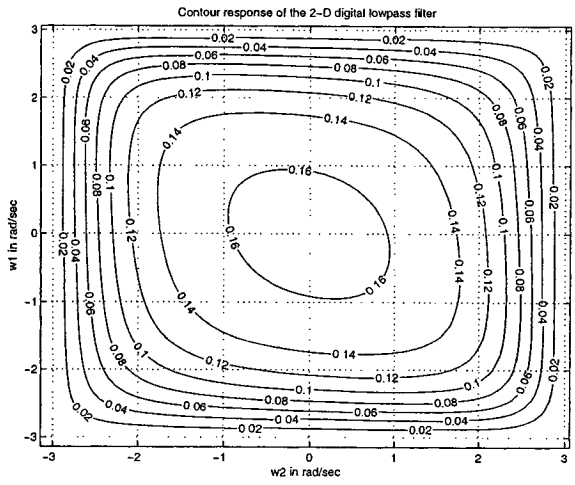

(f) When k1=1, k2=1, a1L=0 and a2L=0

Figure 4.6: Contour response of the 2-D digital lowpass filter obtained from the doubly terminated network considered

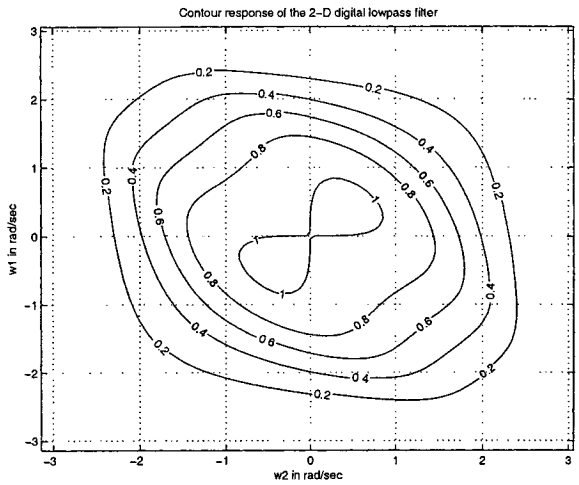

(a) When k1=0.7, k2=0.7, a1L=1 and a2L=1

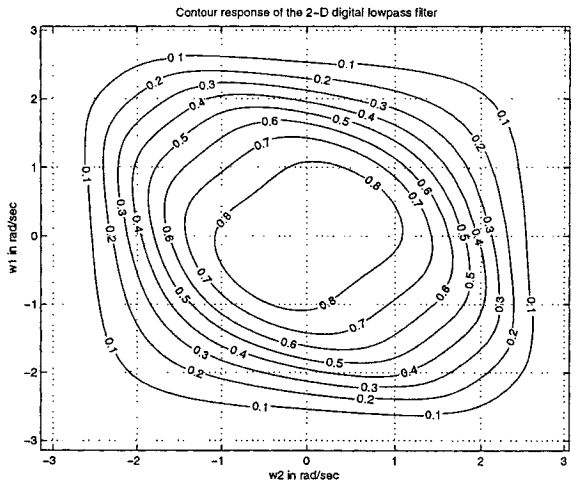

(b) When k1=0.7, k2=0.7, a1L=0.9 and a2L=0.9

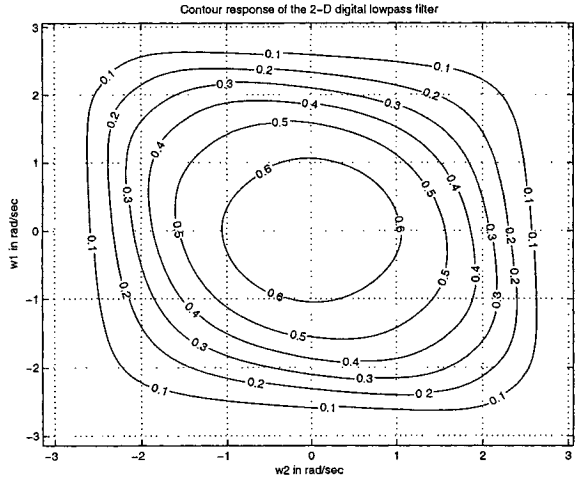

(c) When k1=0.7, k2=0.7, a1L=0.7 and a2L=0.7

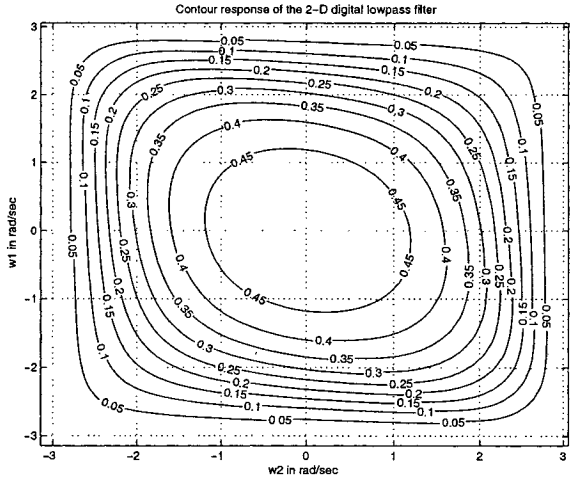

(d) When k1=0.7, k2=0.7, a1L=0.5 and a2L=0.5

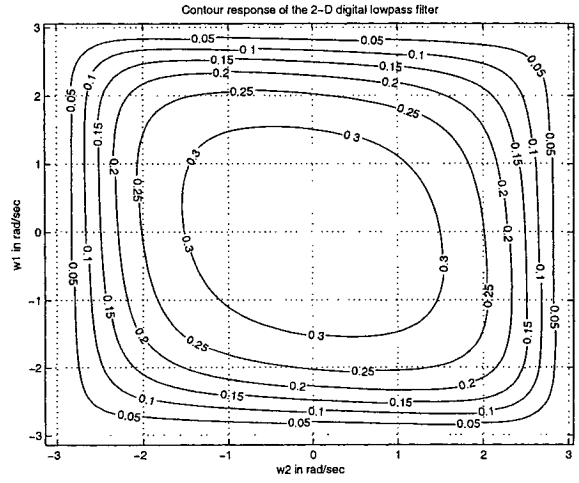

(e) When k1=0.7, k2=0.7, a1L=0.2 and a2L=0.2

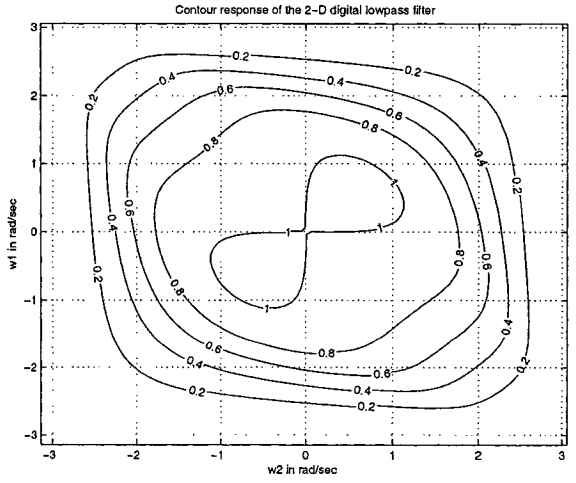

(f) When k1=0.5, k2=0.5, a1L=1 and a2L=1

Figure 4.7: Contour response of the 2-D digital lowpass filter obtained from the doubly terminated network considered

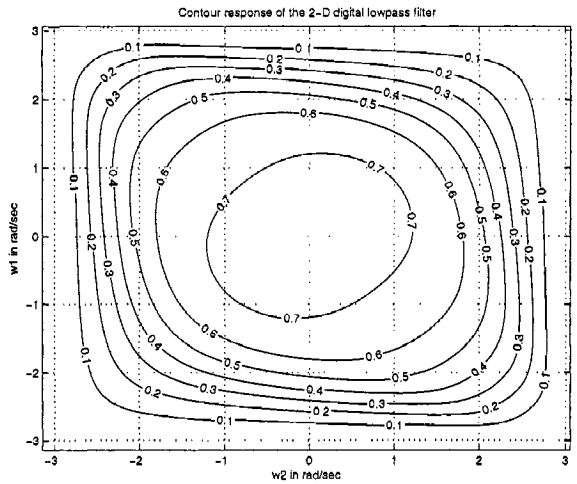

(a) When k1=0.5, k2=0.5, a1L=0.7 and a2L=0.7

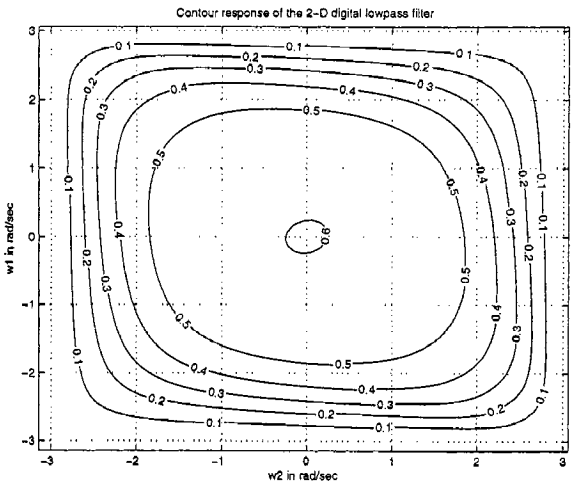

(b) When k1=0.5, k2=0.5, a1L=0.5 and a2L=0.5

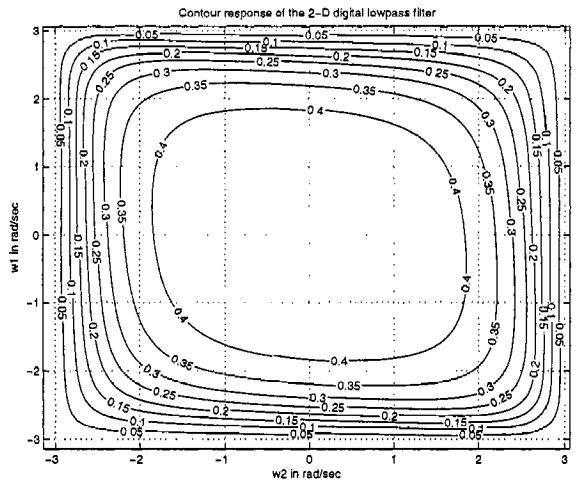

(c) When k1=0.5, k2=0.5, a1L=0.2 and a2L=0.2

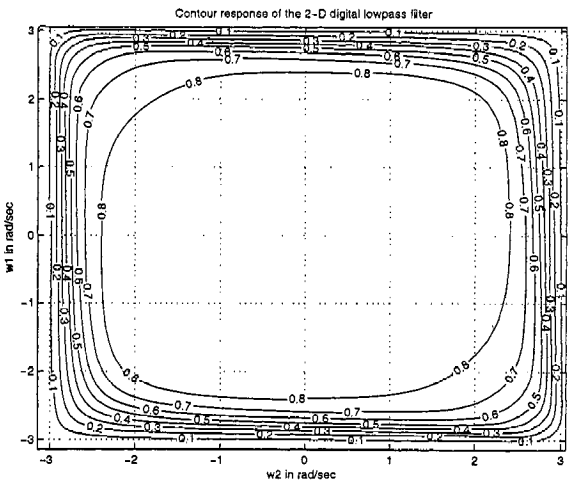

(d) When k1=0.2, k2=0.2, a1L=0.7 and a2L=0.7

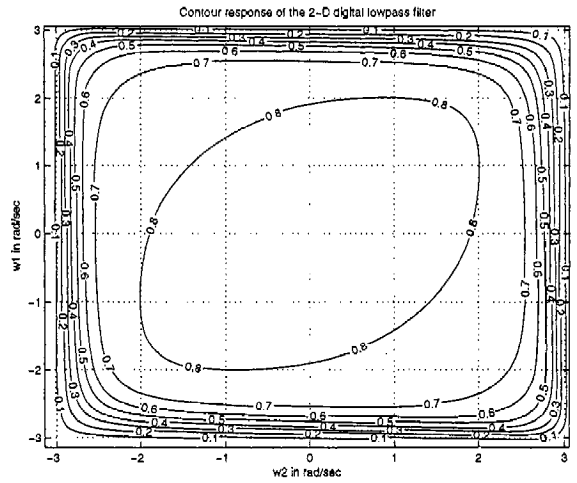

(e) When k1=0.2, k2=0.2, a1L=0.5 and a2L=0.5

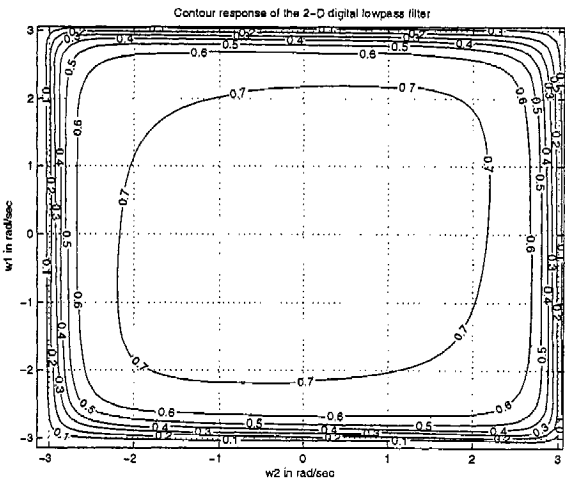

(f) When k1=0.2, k2=0.2, a1L=0.2 and a2L=0.2

Figure 4.8: Contour response of the 2-D digital lowpass filter obtained from the doubly terminated network considered

Algorithm 32 The MATLAB code to plot the 3-D amplitude-frequency response and contour response of the 2-D digital lowpass filters having monotonic characteristics, based on different combination of coefficients of the bilinear transformation.

```
% Under Guidance of Prof. Dr. V. Ramachandran
% Student's name : Ajit Singh Sandhu..... ID:4841492.
% This is a general program with all the variables as input parameters for the 2-D lowpass digital filter
clear all; clc;
a11=input('Give the value of the constant a11 => ');
a10=input('Give the value of the constant a10 => ');
a01=input('Give the value of the constant a01 => ');
a00=input('Give the value of the constant a00 => ');
b11=input('Give the value of the constant b11 => ');
b10=input('Give the value of the constant b10 => ');
b01=input('Give the value of the constant b01 => ');
b00=input('Give the value of the constant b00 => ');
% Input the values of the constants in the LP bilinear transformation.
k1=input('Give the value of the constant k1 for the bilinear LP transformation => ');
k2=input('Give the value of the constant k2 for the bilinear LP transformation => ');
a1L=input('Give the value of the constant a1L for the bilinear LP transformation => ');
a2L=input('Give the value of the constant a2L for the bilinear LP transformation => ');
% Create two dimensional square matrix (mesh grid) of angular frequency w1 and w2.
[w1,w2] = meshgrid(-pi:0.1:pi,-pi:0.1:pi);
z1=exp(j.*w1); z2=exp(j.*w2);
% Hd is the required digital transfer function and its value is evaluated as follows.....
a=z1-a1L; b=z2-a2L;
c=z1+1; d=z2+1;
hd1=((a11.*k1.*k2.*a.*b)+(a10.*k1.*a.*d)+(a01.*k2.*b.*c)+(a00.*c.*d))
.*((b11.*k1.*k2.*a.*b)+(b10.*k1.*a.*d)+(b01.*k2.*b.*c)+(b00.*c.*d));
hd2=((a10.*k1.*a.*d)+(a01.*k2.*b.*c)).*((b10.*k1.*a.*d)+(b01.*k2.*b.*c));
hd=abs(((c.^2).*(d.^2).*(a00.*b00))./(hd1+hd2));
% Figure 1 represents a 3D contour plot of hd in accordance to values of w1 and w2 in the meshgrid
figure(1);
contour3(w1,w2,hd);
surface(w1,w2,abs(hd),'EdgeColor',[.8 .8 .8],'FaceColor','none');
grid on; view(-15,25);
title('3-D amplitude-fequency response of the 2-D lowpass digital filter');
xlabel(' w2 in rad/sec ');
ylabel(' w1 in rad/sec ');
zlabel(' Magnitude Response ');
% Figure 2 represents the top view of the 3D contour observed in figure 1. We can observe the contour
position
% with the corresponding values of the hd in the meshgrid representing w1 and w2 in X and Y axes resp.
figure(2);
[C,h] = contour(w1,w2,hd);
clabel(C,h); grid on;
title('Contour response of the 2-D lowpass digital filter');
xlabel(' w2 in rad/sec ');
ylabel(' w1 in rad/sec ');
```

4.6 Generation of 2-D Butterworth lowpass filter by utilizing the considered doubly terminated network

After discussing the monotonic characteristics of the doubly terminated network considered, we can attempt to realize the same to standard filters, e.g. Butterworth filter with monotonic characteristics. In process to generate the 2-D analog lowpass filter as Butterworth filter, we have to find the values of its constant parameters/coefficients (a_{00}, a_{01}, a_{10}, a_{11}, b_{00}, b_{01}, b_{10}, b_{11}).

4.6.1 Finding the coefficients of 2-D Butterworth filter

In case of 1-D analog lowpass filter, the second order Butterworth polynomial [29] is given by $B_2 = s^2 + \sqrt{2}s + 1$. Also,

$$\frac{B_2}{\frac{dB_2}{ds}} = \frac{s^2 + \sqrt{2}s + 1}{2s + \sqrt{2}} = \frac{s}{2} + \frac{\frac{\sqrt{2}}{2}s + 1}{2s + \sqrt{2}}$$

Hence, by using Koga's Technique [29], B_2 can be rewritten for a 2-D network as follows,

$$B_2(s_1, s_2) = \frac{s_2}{2}\left(2s_1 + \sqrt{2}\right) + \frac{\sqrt{2}}{2}s_1 + 1$$

$$= s_1 s_2 + \frac{s_1}{\sqrt{2}} + \frac{s_2}{\sqrt{2}} + 1 \tag{4.13}$$

By comparing the reactance function in eqn. 4.13 with $\frac{a_{10}s_1 + a_{01}s_2}{a_{11}s_1 s_2 + a_{00}}$ and $\frac{b_{10}s_1 + b_{01}s_2}{b_{11}s_1 s_2 + b_{00}}$ (from eqn. 4.1 and 4.2), we get the coefficient of the 2-D analog Butterworth lowpass filter as $a_{00} = a_{11} = b_{00} = b_{11} = 1$ and $a_{01} = a_{10} = b_{01} = b_{10} = \frac{1}{\sqrt{2}}$.

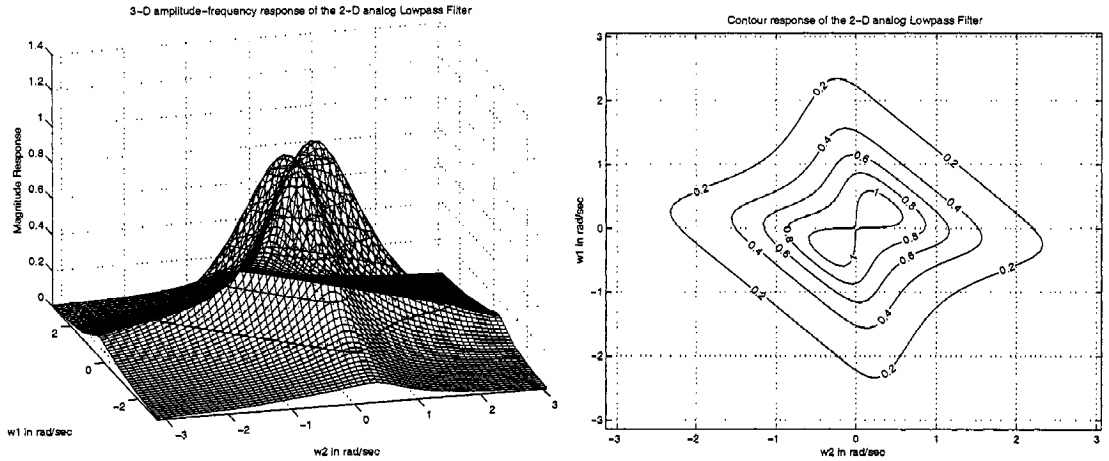

(a) 3-D amplitude-frequency response of the 2-D analog lowpass filter

(b) Contour frequency response of the 2-D analog lowpass filter

Figure 4.9: 3-D amplitude-frequency response and contour response of the 2-D Butterworth analog lowpass filter

4.6.2 Generation of 2-D analog and digital Butterworth lowpass filters and study their characteristics

After substituting the Butterworth filter coefficients (Sec. 4.6.1) in eqn. 4.10, we get the transfer function as,

$$H_a(s_1, s_2) = \frac{1}{\left[s_1 s_2 + \frac{1}{\sqrt{2}}(s_1 + s_2) + 1\right]^2 + \frac{1}{2}(s_1 + s_2)^2} \tag{4.14}$$

The 3-D amplitude frequency response and contour frequency response of the 2-D Butterworth lowpass filter is shown in fig. 4.9. It is observed that there is ripple in the passband of the 2-D analog lowpass filter. This ripple can be removed in the digital domain based on the technique proposed in Sec. 4.5.

The filter in digital domain can be obtained by applying generalized bilinear transformation for lowpass filters. By applying the generalized bilinear transformation for lowpass filters (eqn. 3.2) to eqn. 4.14 we get, transfer function of 2-D digital lowpass filter as

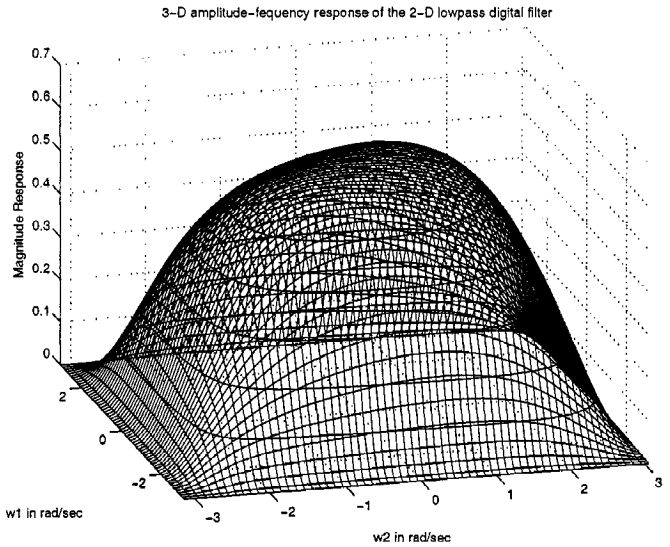

Figure 4.10: 3-D amplitude-frequency response of the 2-D digital Butterworth lowpass filter obtained from the doubly terminated network considered (When $k_1 = 0.7$, $k_2 = 0.7$, $a_{1L} = 0.5$, $a_{2L} = 0.5$)

function of z_1 and z_2, with $z_1 = e^{jw_1}$ and $z_2 = e^{jw_2}$. Therefore, we get,

$$H_d(z_1, z_2) = \frac{(z_1+1)^2 (z_2+1)^2}{\left[\left\{k_1 k_2 (z_1 - a_{1L})(z_2 - a_{2L}) + (z_1+1)(z_2+1)\right\} + \frac{1}{\sqrt{2}}\left\{k_1 (z_1 - a_{1L})(z_2+1) + k_2 (z_2 - a_{2L})(z_1+1)\right\}\right]^2 + \frac{1}{2}\left[k_1 (z_1 - a_{1L})(z_2+1) + k_2 (z_2 - a_{2L})(z_1+1)\right]^2} \quad (4.15)$$

The 3-D amplitude-frequency response and contour response of the 2-D digital Butterworth lowpass filter for different combination values of coefficients are as shown in fig. 4.10, 4.11 and 4.12. The MATLAB code to plot the 3-D amplitude-frequency response and contour of the frequency response of the 2-D digital Butterworth lowpass filter is in algorithm 32.

As k_1 and k_2 values are decreased the passband increases and vice versa. For example, in fig. 4.11 (c), (f) and fig. 4.12 (b), as k_1 and k_2 values decreases from 1 to 0.5, the passband increases, for $a_{1L} = a_{2L} = 0.5$. With decrease in value of a_{1L} and a_{2L} the

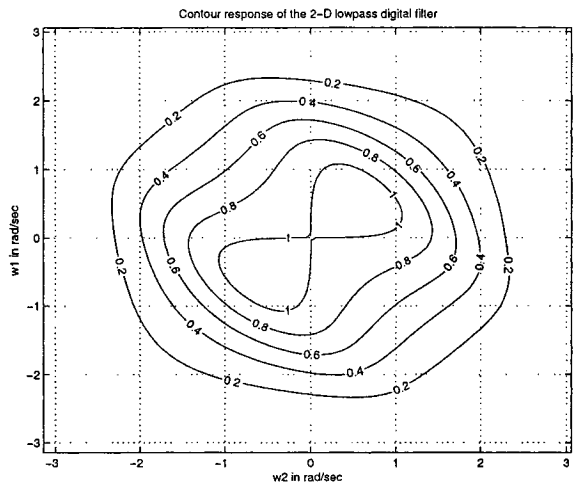

(a) When k1=1, k2=1, a1L=1 and a2L=1

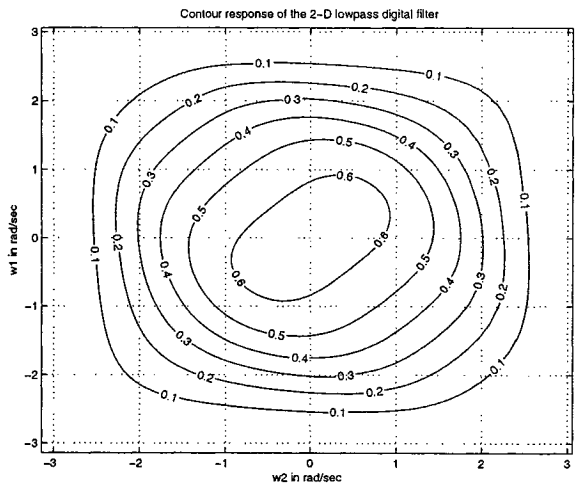

(b) When k1=1, k2=1, a1L=0.7 and a2L=0.7

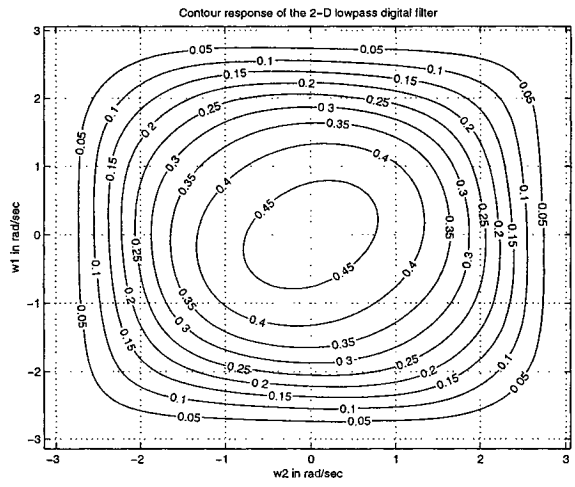

(c) When k1=1, k2=1, a1L=0.5 and a2L=0.5

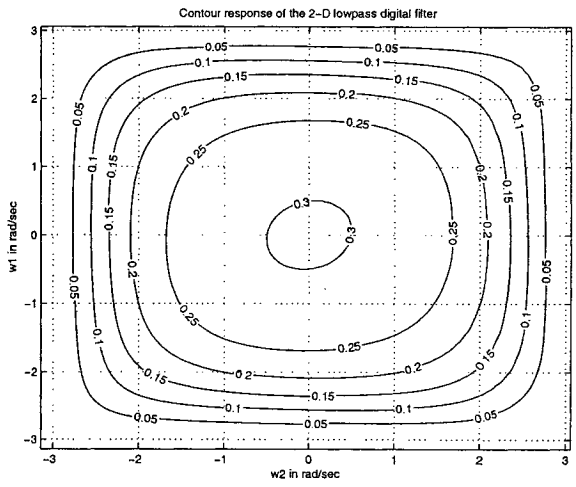

(d) When k1=1, k2=1, a1L=0.2 and a2L=0.2

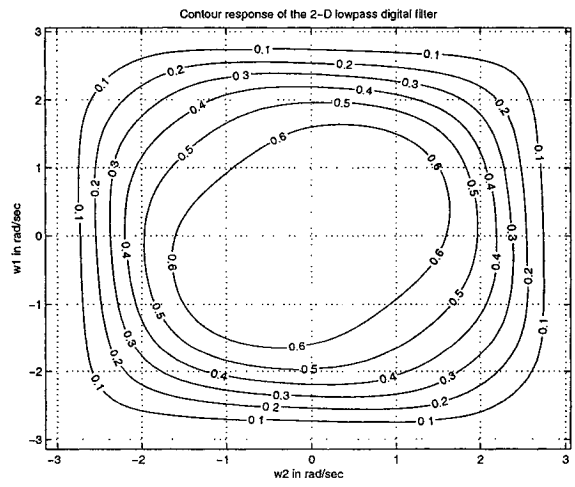

(e) When k1=0.7, k2=0.7, a1L=0.65 and a2L=0.65

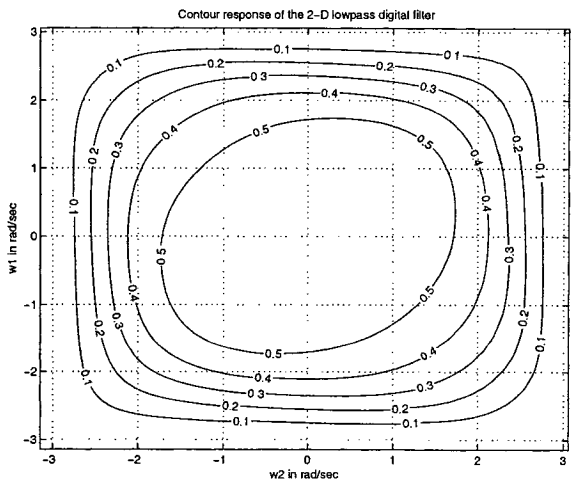

(f) When k1=0.7, k2=0.7, a1L=0.5 and a2L=0.5

Figure 4.11: Contour response of the 2-D digital Butterworth lowpass filter obtained from the doubly terminated network considered

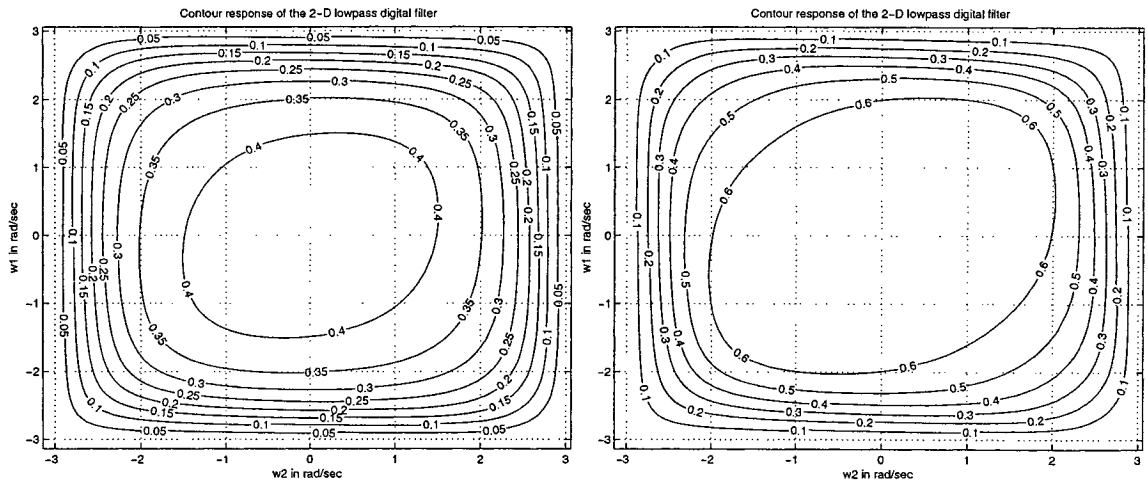

(a) When k1=0.7, k2=0.7, a1L=0.2 and a2L=0.2

(b) When k1=0.5, k2=0.5, a1L=0.5 and a2L=0.5

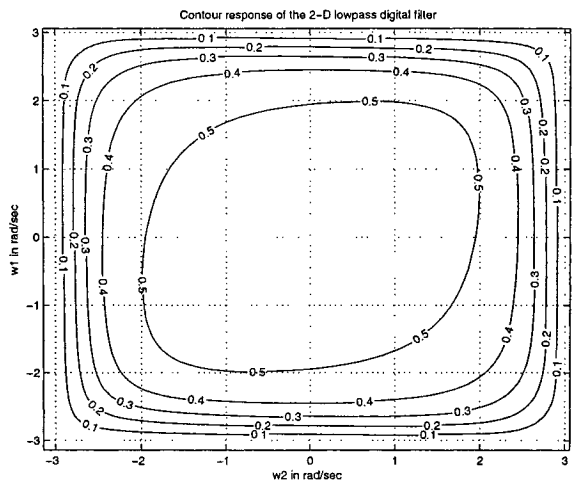

(c) When k1=0.5, k2=0.5, a1L=0.2 and a2L=0.2

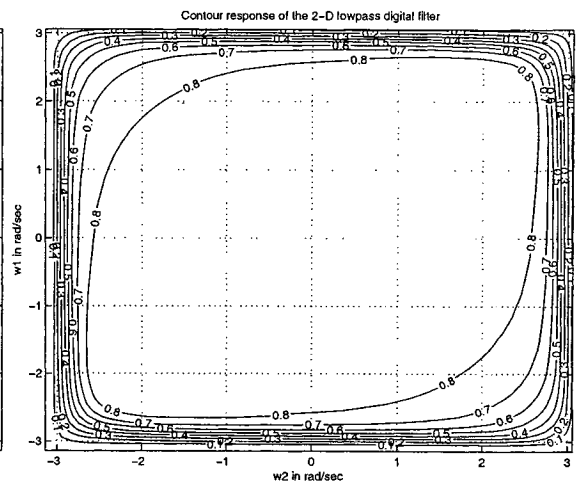

(d) When k1=0.2, k2=0.2, a1L=0.5 and a2L=0.5

Figure 4.12: Contour response of the 2-D digital Butterworth lowpass filter obtained from the doubly terminated network considered

magnitude of the amplitude-frequency response decreases and vice versa. For example, in fig. 4.11(e), (f) and fig. 4.12 (a), as a_{1L} and a_{2L} values decreases from 0.65 to 0.2, the amplitude of the magnitude response decreases, for $k_1 = k_2 = 0.7$.

To achieve monotonic characteristics we should get rid of the ripple present in the equivalent 2-D analog lowpass filter (fig. 4.9), which will be reflected in digital domain too. As proposed in Sec. 4.5, this can be achieved by decreasing the value of coefficients a_{1L} and a_{2L} by a small fraction. For example, it is observed in fig. 4.11 (a), (b), that by decreasing the values of a_{1L} and a_{2L} from 1 to 0.7, for same values of $k_1 = k_2 = 1$, we are able to attain monotonic amplitude-frequency response for 2-D digital Butterworth lowpass filter.

4.6.3 Relationship between cutoff frequencies and gain for 2-D Butterworth filter

To determine the relationship between cutoff frequencies and gain, let us use the definition that modulus of the 2-D analog Butterworth lowpass filter transfer function is equal to gain. Therefore, relationship between cutoff frequencies for transfer function of 2-D Butterworth analog lowpass filter (eqn. 4.14), with $s_1 = jw_{1c}$ and $s_2 = jw_{2c}$, and gain is given by,

$$|H_a(w_{1c}, w_{2c})| = G \tag{4.16}$$

where, G is the gain and w_{1c}, w_{2c} are the cutoff frequencies. After simplification we get,

$$|H_a(w_{1c}, w_{2c})| = \frac{1}{\sqrt{\left[(1 - w_{1c}w_{2c})^2 - (w_{1c} + w_{2c})^2\right]^2 + 2(w_{1c} + w_{2c})^2 (1 - w_{1c}w_{2c})^2}} = G$$

$$= (1 - w_{1c}w_{2c})^4 + (w_{1c} + w_{2c})^4 = \frac{1}{G^2} \tag{4.17}$$

This is the relationship between the cutoff frequencies and gain of the 2-D Butterworth analog lowpass filter, which can be very useful while designing and testing performance of the 2-D filter. For example, when gain is -3db, i.e., $G = 1/\sqrt{2}$, we get the relationship,

$$(1 - w_{1c}w_{2c})^4 + (w_{1c} + w_{2c})^4 = 2 \tag{4.18}$$

Similarly, we can find such relationships for any 2-D filter.

4.7 Summary

In this Chapter, starting from a generalized doubly terminated network, we generated 2-D analog and digital lowpass filters, with monotonic amplitude-frequency response and studied their characteristics. We defined conditions to be satisfied and constraints on the coefficients to be considered in both analog and digital domain, while designing the 2-D lowpass filters. We also generated and studied 2-D Butterworth analog and digital lowpass filters based on the proposed approach.

We considered a doubly terminated network by using a Continued Fraction Expansion (CFE). The stability of the 2-D analog lowpass filter was defined and proved by checking the transfer function polynomial to be a Very Stable Hurwitz Polynomial (VSHP). Some conditions for monotonicity in the amplitude-frequency response were derived.

The generalized 2-D analog filter was implemented, and constraints on the coefficients to be considered for attaining monotonic characteristics were defined, and verified by simulation results. The 2-D digital lowpass filter was generated by applying generalized bilinear transformation. The affect of the coefficients were studied, and their impact to achieve monotonic amplitude-frequency response were discussed.

Furthermore, the coefficients of the generalized 2-D analog lowpass filter required to generate 2-D Butterworth analog lowpass filter were derived. The corresponding 2-D Butterworth analog lowpass filter was implemented. The 2-D Butterworth lowpass filter was

implemented in digital domain by applying generalized bilinear transformation. The effect of the coefficients to achieve monotonic amplitude-frequency response were discussed. Also, a simplified relationship between cutoff frequencies and gain of the 2-D Butterworth filter was established.

Chapter 5

Generation of stable 2-D digital highpass and bandpass filters with monotonic amplitude-frequency response

5.1 Introduction

In Chapter 2, 3 and 4, we restricted our discussions to implementation of lowpass filters. We know that other types of filters, e.g. highpass and bandpass filters can be obtained from the equivalent lowpass pass filters, or combinations of the same.

Therefore, in this Chapter, we will implement 2-D digital Butterworth, Papoulis, Filanovsky and Thomson-Bessel highpass and bandpass filters from their equivalent 2-D lowpass filters proposed in Chapter 3. Also, 2-D digital Butterworth highpass and bandpass filters shall be implemented from the 2-D Butterworth lowpass filter proposed in Chapter 4. The 2-D highpass and bandpass digital filters are possible from all the 2-D lowpass filters discussed in Chapter 3, 4, and we will be implementing and discussing one example of each type of filter. Our primary emphasis will be to generate 2-D digital highpass and bandpass filters with monotonic amplitude-frequency response.

5.2 Generation of 2-D digital highpass filters with monotonic amplitude-frequency response

A method of designing digital highpass filter is to start from the analog lowpass filter transfer function, and then apply generalized bilinear transformations [19], i.e.,

$$s_i = k_i \frac{z_i + a_i}{z_i + b_i} \tag{5.1}$$

where $i = 1, 2$ for 2-D filter, to obtain the digital filter transfer function. For the resulting 2-D filter to be stable and highpass, it is required that $k_i > 0$ and $0 \leq a_i \leq 1$ and $-1 \leq b_i \leq 0$.

In this section, we will propose some examples of implementation of 2-D digital Butterworth, Papoulis, Filanovsky and Thomson-Bessel highpass filters, from their equivalent 2-D analog lowpass filters, having monotonic characteristics. We will implement fifth order 2-D digital Papoulis, Butterworth, Filanovsky and Thomson-Bessel highpass filters by using the transfer functions proposed in Chapter 3. Furthermore, we will also implement 2-D digital Butterworth highpass filter by utilizing the lowpass filter transfer function proposed in Chapter 4.

5.2.1 Generation of fifth order 2-D digital Papoulis highpass filter with monotonic characteristics

The transfer function of the fifth order 2-D analog Papoulis lowpass filter, is given by eqn. 3.4. By applying generalized bilinear transformation (eqn. 5.1) to eqn. 3.4, we get, the transfer function of 2-D digital Papoulis highpass filter as function of z_1 and z_2, with

$z_1 = e^{jw_1}$ and $z_2 = e^{jw_2}$. Hence, we get,

$$H_d(z_1, z_2) = \frac{(0.2235)^2 (z_1 + b_1)^5 (z_2 + b_2)^5}{[k_1 (z_1 + a_1) + 0.4681 (z_1 + b_1)] [k_2 (z_2 + a_2) + 0.4681 (z_2 + b_2)] \left[k_1^2 (z_1 + a_1)^2 + 0.7762 k_1 (z_1 + a_1) (z_1 + b_1) + 0.4971 (z_1 + b_1)^2\right] \left[k_1^2 (z_1 + a_1)^2 + 0.3072 k_1 (z_1 + a_1) (z_1 + b_1) + 0.9608 (z_1 + b_1)^2\right] \left[k_2^2 (z_2 + a_2)^2 + 0.7762 k_2 (z_2 + a_2) (z_2 + b_2) + 0.4971 (z_2 + b_2)^2\right] \left[k_2^2 (z_2 + a_2)^2 + 0.3072 k_2 (z_2 + a_2) (z_2 + b_2) + 0.9608 (z_2 + b_2)^2\right]} \quad (5.2)$$

The 3-D amplitude-frequency response and contour plots of the fifth order 2-D digital Papoulis highpass filter for different combination values of the coefficients of generalized bilinear transformation are shown in the fig. 5.1, 5.2, 5.3 and 5.4. The MATLAB code to plot the 3-D amplitude-frequency response and contour of the frequency response of the fifth order 2-D digital Papoulis lowpass filter is in algorithm 33.

The coefficients k_1, k_2, affects passband width and a_1, a_2, affects gain of the amplitude-frequency response in fig. 5.2, 5.3 and 5.4 (a), for $b_1 = b_2 = -1$. It may be noted that as the coefficients k_1, k_2, values are decreased, the passband width of the 2-D highpass filter increases. For example, in fig. 5.2 (b), (f) and fig. 5.3 (c), (f), as k_1, k_2, are decreased from 1 to 0.2, for same values of $a_1 = a_2 = 0.7$ and $b_1 = b_2 = -1$, the passband width of 2-D highpass filter increases. Similarly, in fig. 5.2 (a), (e) and fig. 5.3 (b), (e), as k_1, k_2, are decreased from 1 to 0.2, for same values of $a_1 = a_2 = 1$ and $b_1 = b_2 = -1$, the passband width of 2-D highpass filter increases. As the coefficients a_1, a_2, values are decreased, the magnitude of the amplitude-frequency response of the 2-D highpass filter decreases. For example, in fig. 5.2 (a), (b), (c) and (d), as a_1, a_2, are decreased from 1 to 0.2, for same values of $k_1 = k_2 = 1$ and $b_1 = b_2 = -1$, the magnitude of the passband decreases. Similarly, in fig. 5.3 (b), (c) and (d), as a_1, a_2, are decreased from 1 to 0.5, for same values of $k_1 = k_2 = 0.5$ and $b_1 = b_2 = -1$, the magnitude of the passband decreases. As b_1, b_2, are decreased to -0.7 and -0.5 in fig. 5.4 from -1 in fig. 5.2 and 5.3, the polarity

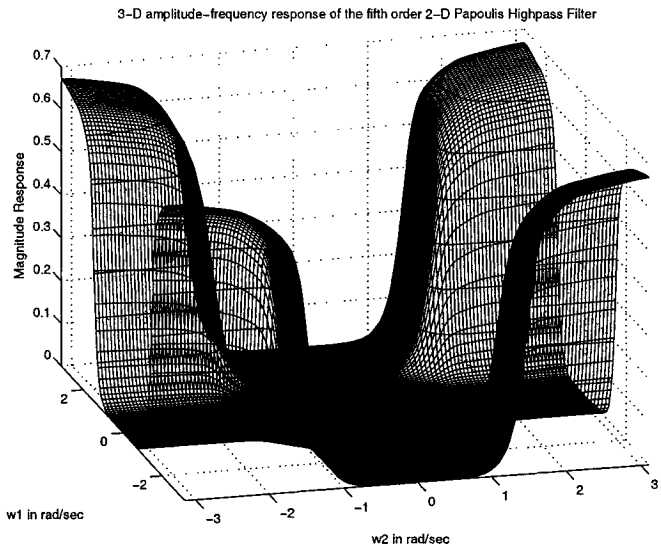

Figure 5.1: 3-D amplitude-frequency response of the fifth order 2-D digital Papoulis highpass filter (When $k_1 = k_2 = 1$, $a_1 = a_2 = 0.9$ and $b_1 = b_2 = -1$)

of the amplitude-frequency response changes, and there is rounding of contour edges with decrease in passband. In all the cases discussed, the 2-D Papoulis highpass filter inhibits monotonic amplitude-frequency response.

5.2.2 Generation of 2-D digital Butterworth highpass filter with monotonic characteristics

In this section, we will generate 2-D digital Butterworth highpass filters by utilizing, *(i)* the fifth order 2-D Butterworth lowpass filter proposed in Sec. 3.3.1.2, and *(ii)* second order 2-D Butterworth lowpass filter proposed in Sec. 4.6.2.

5.2.2.1 Generation of fifth order 2-D digital Butterworth highpass filters with monotonic characteristics

The transfer function of the fifth order 2-D analog Butterworth lowpass filter, is given by eqn. 3.8. By applying generalized bilinear transformation (eqn. 5.1) to eqn. 3.8, we get, transfer function of 2-D digital Butterworth highpass filter as function of z_1 and z_2, with

Algorithm 33 The MATLAB code to plot the 3-D amplitude-frequency response and contour response of the fifth order 2-D digital Papoulis highpass filters having monotonic characteristics.

```
% Under Guidance of Prof. Dr. V. Ramachandran
% Student's name : Ajit Singh Sandhu..... ID:4841492.
clc; clear all;
%————————Lowpass filter————————
k1=input('Give the value of the constant k1 for the bilinear LP transformation => ');
k2=input('Give the value of the constant k2 for the bilinear LP transformation => ');
a1L=input('Give the value of the constant a1L for the bilinear LP transformation => ');
a2L=input('Give the value of the constant a2L for the bilinear LP transformation => ');
% Creates two dimensional square matrix (mesh grid) of angular frequency w1 and w2.
[w1,w2] = meshgrid(-pi:0.05:pi,-pi:0.05:pi);
% Apply Z1=r1*exp(jw1) and Z2=r2*exp(jw2) with r1 = r2 =1
z1=exp(j.*w1);
z2=exp(j.*w2);
% h1 is the required digital transfer function and its value is evaluated as follows.
a=z1-a1L; b=z2-a2L; c=z1+1; d=z2+1;
h1_1=(((k1.^2).*(a.^2))+(k1.*0.7762.*a.*c)+(0.4971.*(c.^2))).*(((k1.^2).*(a.^2))
+(k1.*0.3072.*a.*c)+(0.9608.*(c.^2))).*(a+(0.4681.*c));
h1_2=(((k2.^2).*(b.^2))+(k2.*0.7762.*b.*d)+(0.4971.*(d.^2))).*(((k2.^2).*(b.^2))
+(k2.*0.3072.*b.*d)+(0.9608.*(d.^2))).*(b+(0.4681.*d));
h_lpf=((c.^5).*(d.^5).*(0.2235.^2))./(h1_1.*h1_2); h1=abs(h_lpf);
% ——— High Pass filter————————
k1=input('Give the value of the constant k1 for the bilinear LP transformation => ');
k2=input('Give the value of the constant k2 for the bilinear LP transformation => ');
a1=input('Give the value of the constant a1 for the bilinear LP transformation => ');
a2=input('Give the value of the constant a2 for the bilinear LP transformation => ');
b1=input('Give the value of the constant b1 for the bilinear LP transformation => ');
b2=input('Give the value of the constant b2 for the bilinear LP transformation => ');
% hh1 is the required digital transfer function and its value is evaluated as follows.
a=z1+a1; b=z2+a2; c=z1+b1; d=z2+b2;
hh1_1=(((k1.^2).*(a.^2))+(k1.*0.7762.*a.*c)+(0.4971.*(c.^2))).*(((k1.^2).*(a.^2))
+(k1.*0.3072.*a.*c)+(0.9608.*(c.^2))).*(a+(0.4681.*c));
hh1_2=(((k2.^2).*(b.^2))+(k2.*0.7762.*b.*d)+(0.4971.*(d.^2))).*(((k2.^2).*(b.^2))
+(k2.*0.3072.*b.*d)+(0.9608.*(d.^2))).*(b+(0.4681.*d));
h_hpf=((c.^5).*(d.^5).*(0.2235.^2))./(hh1_1.*hh1_2); hh1=abs(h_hpf);
figure(1);
contour3(w1,w2,hh1);
surface(w1,w2,abs(hh1),'EdgeColor',[.8 .8 .8],'FaceColor','none');
grid on; view(-15,25);
title('3-D amplitude-frequency response of the fifth order 2-D Papoulis Highpass Filter');
xlabel(' w2 in rad/sec ');
ylabel(' w1 in rad/sec ');
zlabel(' Magnitude Response ');
figure(2);
[C,h] = contour(w1,w2,hh1);
clabel(C,h); grid on;
title('Contour response of the fifth order 2-D Papoulis Highpass Filter');
xlabel(' w2 in rad/sec ');
ylabel(' w1 in rad/sec ');
```

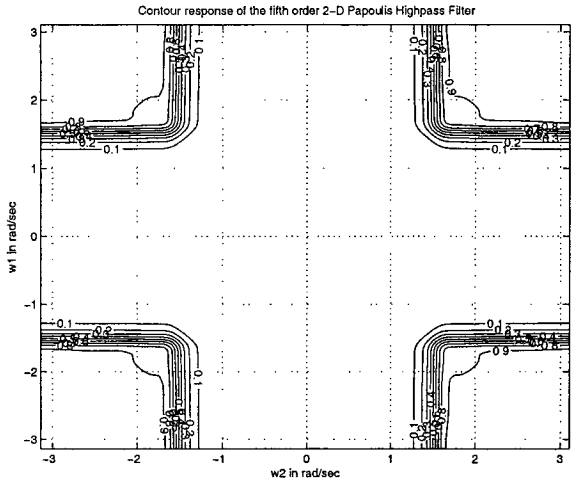

(a) When k1=k2=1, a1=a2=1 and b1=b2=-1

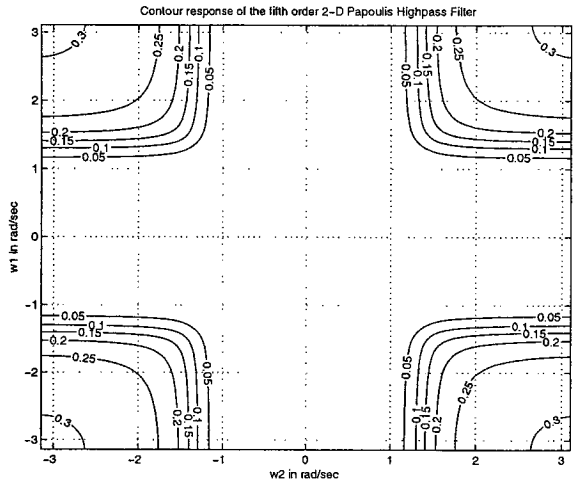

(b) When k1=k2=1, a1=a2=0.7 and b1=b2=-1

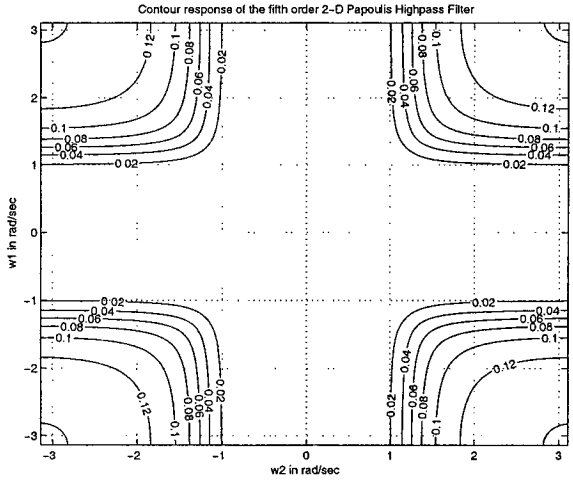

(c) When k1=k2=1, a1=a2=0.5 and b1=b2=-1

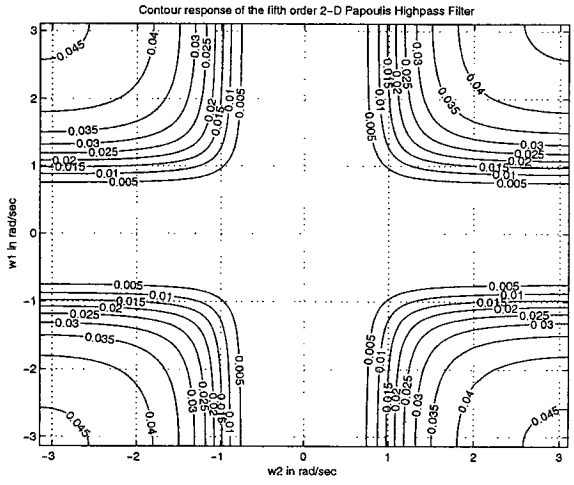

(d) When k1=k2=1, a1=a2=0.2 and b1=b2=-1

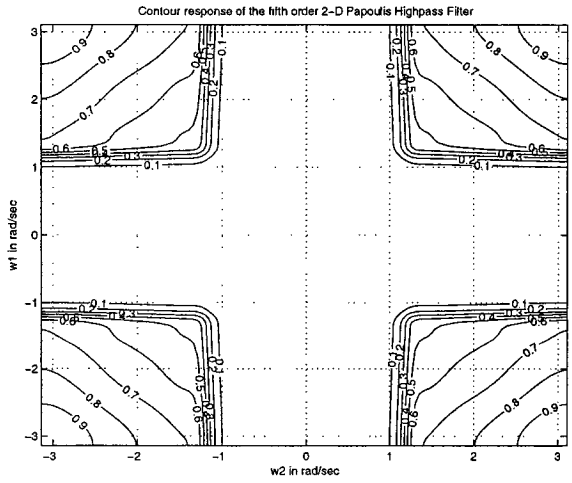

(e) When k1=k2=0.7, a1=a2=1 and b1=b2=-1

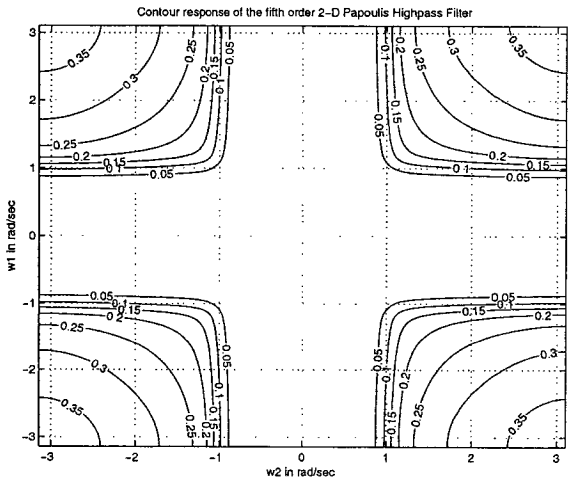

(f) When k1=k2=0.7, a1=a2=0.7 and b1=b2=-1

Figure 5.2: Contour response of the fifth order 2-D digital Papoulis highpass filter

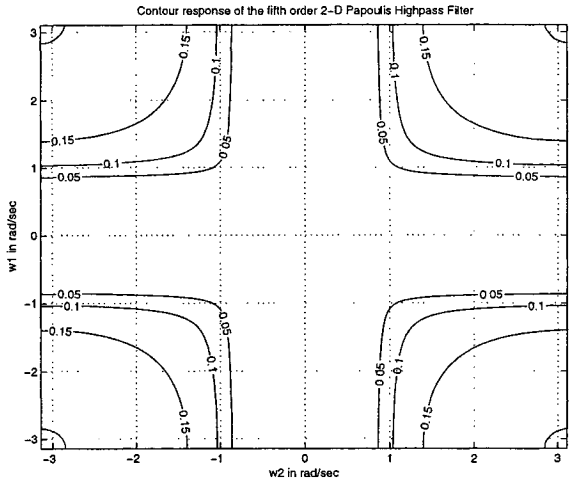

(a) When k1=k2=0.7, a1=a2=0.5 and b1=b2=-1

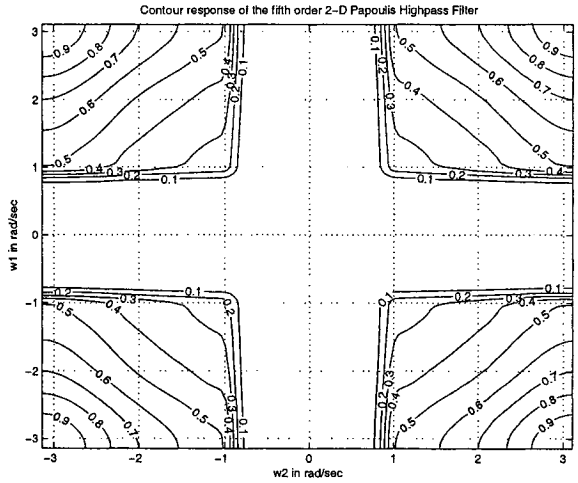

(b) When k1=k2=0.5, a1=a2=1 and b1=b2=-1

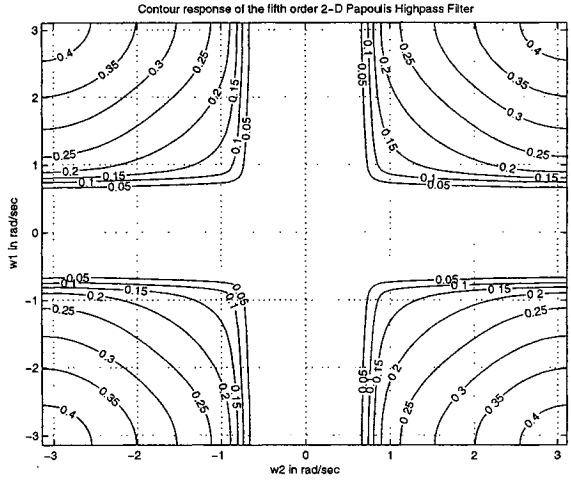

(c) When k1=k2=0.5, a1=a2=0.7 and b1=b2=-1

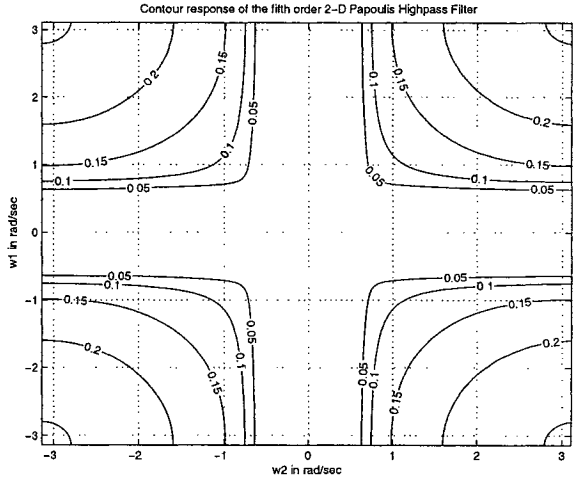

(d) When k1=k2=0.5, a1=a2=0.5 and b1=b2=-1

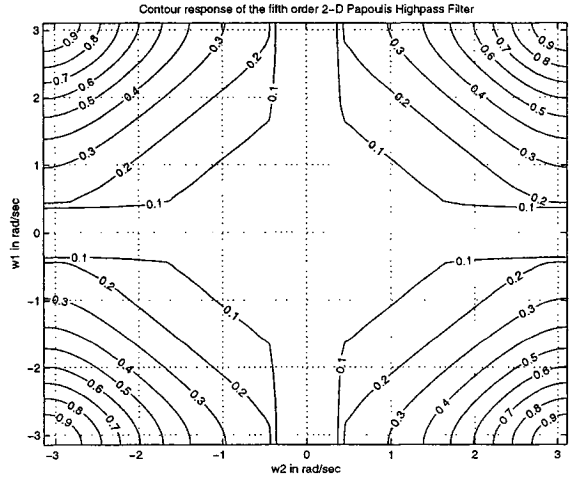

(e) When k1=k2=0.2, a1=a2=1 and b1=b2=-1

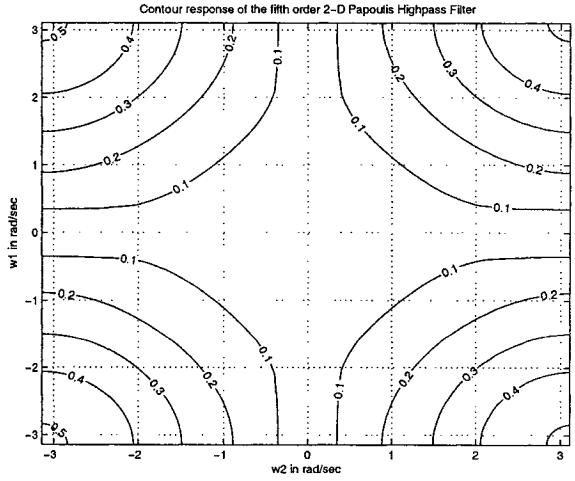

(f) When k1=k2=0.2, a1=a2=0.7 and b1=b2=-1

Figure 5.3: Contour response of the fifth order 2-D digital Papoulis highpass filter

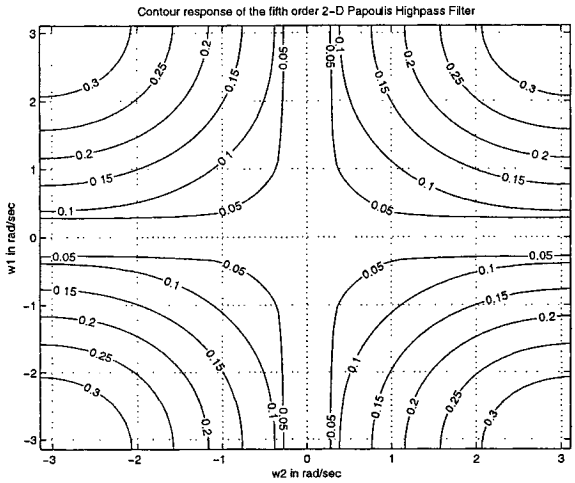

(a) When k1=k2=0.2, a1=a2=0.5 and b1=b2=-1

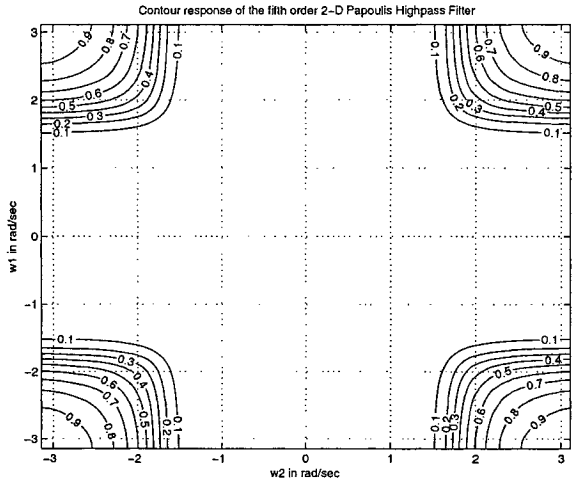

(b) When k1=k2=1, a1=a2=1 and b1=b2=-0.7

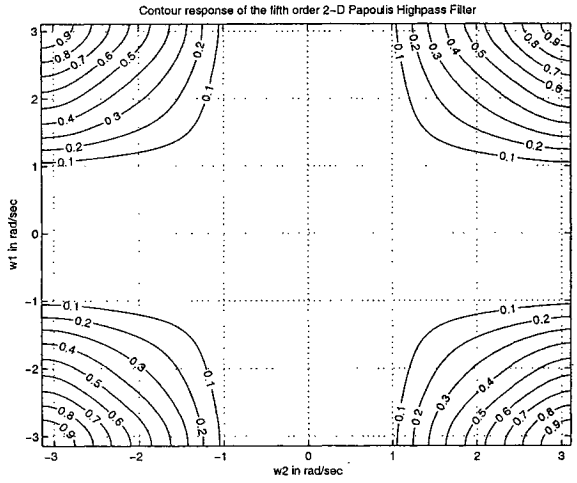

(c) When k1=k2=0.5, a1=a2=1 and b1=b2=-0.7

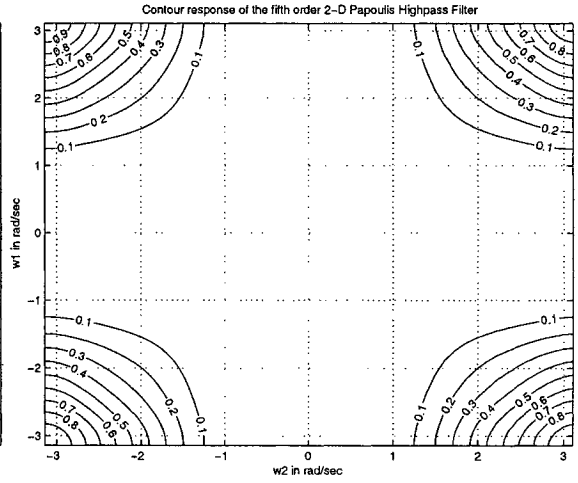

(d) When k1=k2=0.5, a1=a2=1 and b1=b2=-0.5

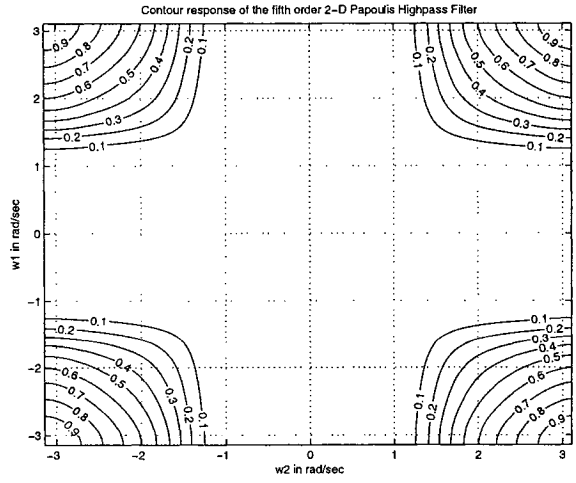

(e) When k1=k2=0.7, a1=a2=1 and b1=b2=-0.7

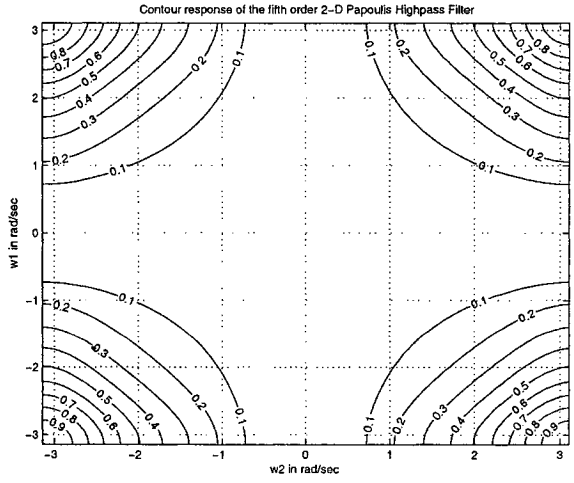

(f) When k1=k2=0.2, a1=a2=1 and b1=b2=-0.7

Figure 5.4: Contour response of the fifth order 2-D digital Papoulis highpass filter

$z_1 = e^{jw_1}$ and $z_2 = e^{jw_2}$. Hence, we get,

$$H_d(z_1, z_2) = \frac{(z_1 + b_1)^5 (z_2 + b_2)^5}{[k_1 (z_1 + a_1) + (z_1 + b_1)] [k_2 (z_2 + a_2) + (z_2 + b_2)]} \\ \left[k_1^2 (z_1 + a_1)^2 + 1.618 k_1 (z_1 + a_1)(z_1 + b_1) + (z_1 + b_1)^2\right] \\ \left[k_1^2 (z_1 + a_1)^2 + 0.618 k_1 (z_1 + a_1)(z_1 + b_1) + (z_1 + b_1)^2\right] \\ \left[k_2^2 (z_2 + a_2)^2 + 1.618 k_2 (z_2 + a_2)(z_2 + b_2) + (z_2 + b_2)^2\right] \\ \left[k_2^2 (z_2 + a_2)^2 + 0.618 (z_2 + a_2)(z_2 + b_2) + (z_2 + b_2)^2\right] \tag{5.3}$$

The 3-D amplitude-frequency response and contour plots of the fifth order 2-D digital Butterworth highpass filter for different combination values of the coefficients of generalized bilinear transformation are shown in the fig. 5.5, 5.6, 5.7 and 5.8. The MATLAB code to plot the 3-D amplitude-frequency response and contour of the frequency response of the fifth order 2-D digital Butterworth lowpass filter is in algorithm 34.

The coefficients k_1, k_2, affects passband width and a_1, a_2, affects gain of the amplitude-frequency response in fig. 5.6, 5.7 and 5.8 (a), for $b_1 = b_2 = -1$. It may be noted that as the coefficients k_1, k_2, values are decreased, the passband width of the 2-D highpass filter increases. For example, in fig. 5.6 (b), (f) and fig. 5.7 (c), (f), as k_1, k_2, are decreased from 1 to 0.2, for same values of $a_1 = a_2 = 0.7$ and $b_1 = b_2 = -1$, the passband width of 2-D highpass filter increases. Similarly, in fig. 5.6 (a), (e) and fig. 5.7 (b), (e), as k_1, k_2, are decreased from 1 to 0.2, for same values of $a_1 = a_2 = 1$ and $b_1 = b_2 = -1$, the passband width of 2-D highpass filter increases. As the coefficients a_1, a_2, values are decreased, the magnitude of the amplitude-frequency response of the 2-D highpass filter decreases. For example, in fig. 5.6 (a), (b), (c) and (d), as a_1, a_2, are decreased from 1 to 0.2, for same values of $k_1 = k_2 = 1$ and $b_1 = b_2 = -1$, the magnitude of the passband decreases. Similarly, in fig. 5.7 (b), (c) and (d), as a_1, a_2, are decreased from 1 to 0.5, for same values of $k_1 = k_2 = 0.5$ and $b_1 = b_2 = -1$, the magnitude of the passband decreases. As b_1, b_2, are decreased to -0.7 and -0.5 in fig. 5.8 from -1 in fig. 5.6 and 5.7, the polarity

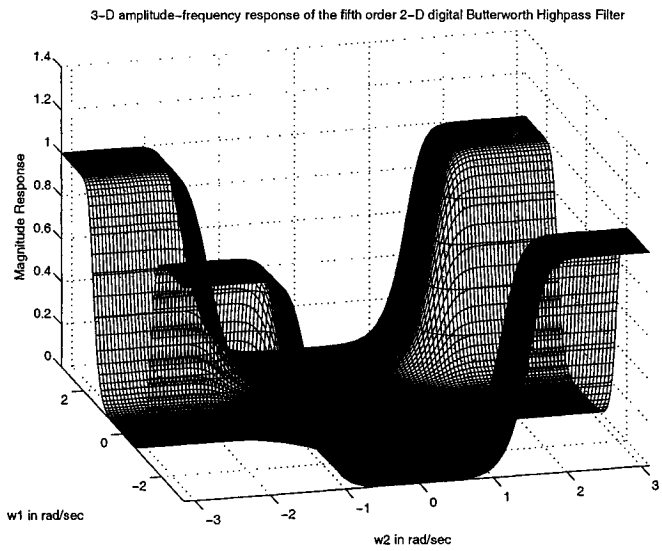

Figure 5.5: 3-D amplitude-frequency response of the fifth order 2-D digital Butterworth highpass filter (When $k_1 = k_2 = a_1 = a_2 = 1$ and $b_1 = b_2 = -1$)

of the amplitude-frequency response changes, and there is rounding of contour edges with decrease in passband. In all the cases discussed, the fifth order 2-D Butterworth highpass filter inhibits monotonic amplitude-frequency response.

5.2.2.2 Generation of second order 2-D digital Butterworth highpass filters with monotonic characteristics

The transfer function of the second order 2-D analog Butterworth lowpass filter, is given by eqn. 4.14. By applying generalized bilinear transformation (eqn. 5.1) to eqn. 4.14, we get, transfer function of 2-D digital Butterworth highpass filter as function of z_1 and z_2, with $z_1 = e^{jw_1}$ and $z_2 = e^{jw_2}$. Hence, we get,

$$H_d(z_1, z_2) = \frac{(z_1 + b_1)^2 (z_2 + b_2)^2}{\left[\left\{k_1 k_2 (z_1 + a_1)(z_2 + a_2) + (z_1 + b_1)(z_2 + b_2)\right\} + \frac{1}{\sqrt{2}}\left\{k_1 (z_1 + a_1)(z_2 + b_2) + k_2 (z_2 + a_2)(z_1 + b_1)\right\}\right]^2 + \frac{1}{2}\left[k_1 (z_1 + a_1)(z_2 + b_2) + k_2 (z_2 + a_2)(z_1 + b_1)\right]^2} \quad (5.4)$$

Algorithm 34 The MATLAB code to plot the 3-D amplitude-frequency response and contour response of the fifth order 2-D digital Butterworth highpass filters having monotonic characteristics.

```
% Under Guidance of Prof. Dr. V. Ramachandran
% Student's name : Ajit Singh Sandhu..... ID:4841492.
clc; clear all;
% ————Lowpass Filter————
k1=input('Give the value of the constant k1 for the bilinear LP transformation => ');
k2=input('Give the value of the constant k2 for the bilinear LP transformation => ');
a1L=input('Give the value of the constant a1L for the bilinear LP transformation => ');
a2L=input('Give the value of the constant a2L for the bilinear LP transformation => ');
% Creates two dimensional square matrix (mesh grid) of angular frequency w1 and w2.
[w1,w2] = meshgrid(-pi:0.05:pi,-pi:0.05:pi);
% Apply Z1=r1*exp(jw1) and Z2=r2*exp(jw2) with r1 = r2 =1
z1=exp(j.*w1); z2=exp(j.*w2);
% h1 is the required digital transfer function and its value is evaluated as follows.
a=z1-a1L; b=z2-a2L; c=z1+1; d=z2+1;
h1_1=(((k1.^2).*(a.^2))+(k1.*1.618.*a.*c)+(c.^2)).*(((k1.^2).*(a.^2))+(k1.*0.618.*a.*c)+(c.^2)).*(a+c);
h1_2=(((k2.^2).*(b.^2))+(k2.*1.618.*b.*d)+(d.^2)).*(((k2.^2).*(b.^2))+(k2.*0.618.*b.*d)+(d.^2)).*(b+d);
h_lpf=((c.^5).*(d.^5))./(h1_1.*h1_2);
h1=abs(h_lpf);
%————————Highpass filter————————
k1=input('Give the value of the constant k1 for the bilinear LP transformation => ');
k2=input('Give the value of the constant k2 for the bilinear LP transformation => ');
a1=input('Give the value of the constant a1 for the bilinear LP transformation => ');
a2=input('Give the value of the constant a2 for the bilinear LP transformation => ');
b1=input('Give the value of the constant b1 for the bilinear LP transformation => ');
b2=input('Give the value of the constant b2 for the bilinear LP transformation => ');
% hh1 is the required digital transfer function and its value is evaluated as follows.
a=z1+a1; b=z2+a2; c=z1+b1; d=z2+b2;
hh1_1=(((k1.^2).*(a.^2))+(k1.*1.618.*a.*c)+(c.^2)).*(((k1.^2).*(a.^2))+(k1.*0.618.*a.*c)+(c.^2)).*(a+c);
hh1_2=(((k2.^2).*(b.^2))+(k2.*1.618.*b.*d)+(d.^2)).*(((k2.^2).*(b.^2))+(k2.*0.618.*b.*d)+(d.^2)).*(b+d);
h_hpf=((c.^5).*(d.^5))./(hh1_1.*hh1_2);
hh1=abs(h_hpf);
figure(1);
contour3(w1,w2,hh1);
surface(w1,w2,abs(hh1),'EdgeColor',[.8 .8 .8],'FaceColor','none');
grid on; view(-15,25);
title('3-D amplitude-frequency response of the fifth order 2-D digital Butterworth Highpass Filter');
xlabel(' w2 in rad/sec ');
ylabel(' w1 in rad/sec ');
zlabel(' Magnitude Response ');
figure(2);
[C,h] = contour(w1,w2,hh1);
clabel(C,h); grid on;
title('Contour response of the fifth order 2-D digital Butterworth Highpass Filter');
xlabel(' w2 in rad/sec ');
ylabel(' w1 in rad/sec ');
```

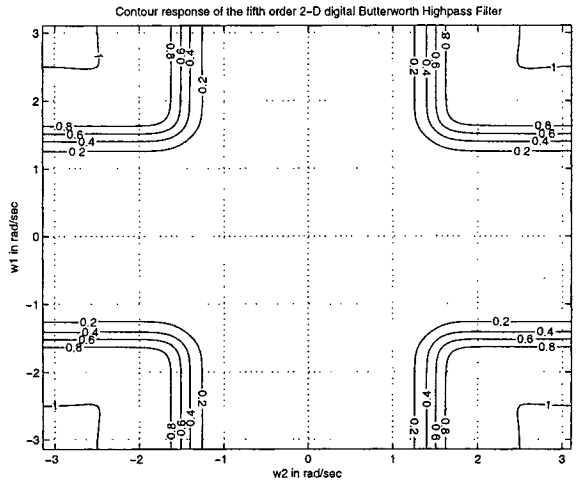

(a) When k1=k2=1, a1=a2=1 and b1=b2=-1

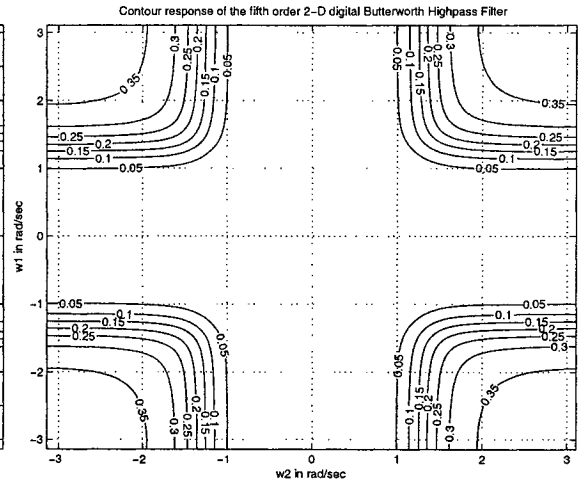

(b) When k1=k2=1, a1=a2=0.7 and b1=b2=-1

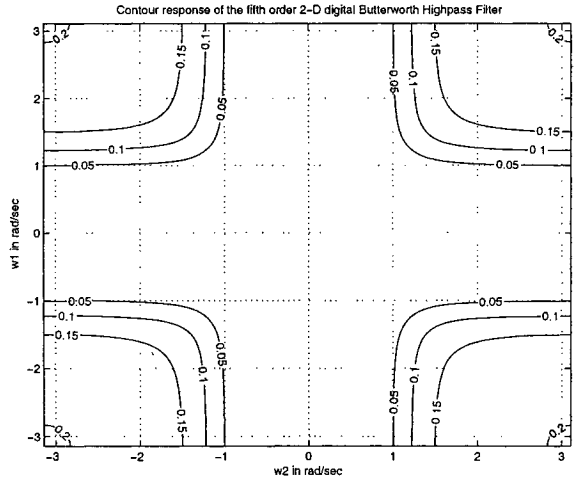

(c) When k1=k2=1, a1=a2=0.5 and b1=b2=-1

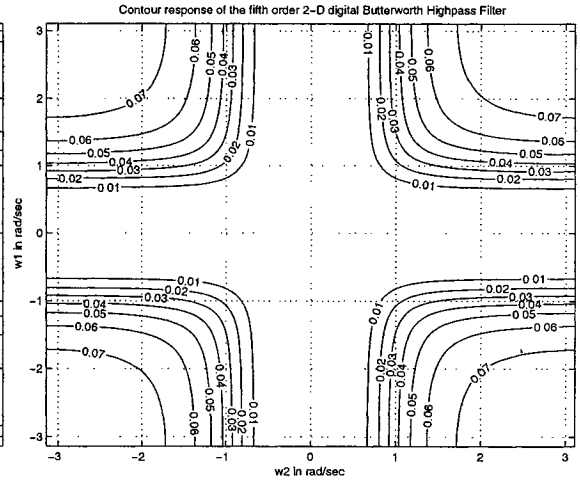

(d) When k1=k2=1, a1=a2=0.2 and b1=b2=-1

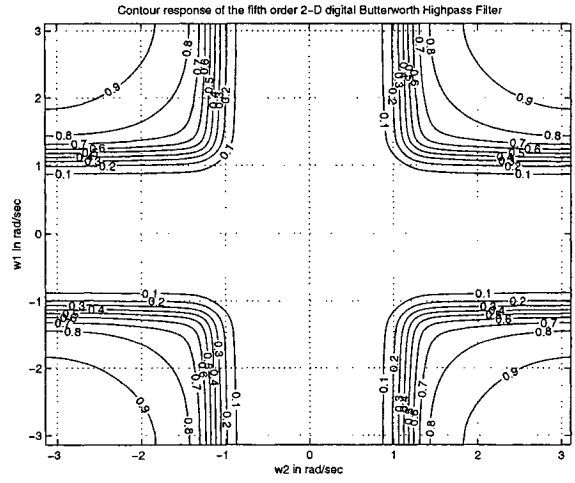

(e) When k1=k2=0.7, a1=a2=1 and b1=b2=-1

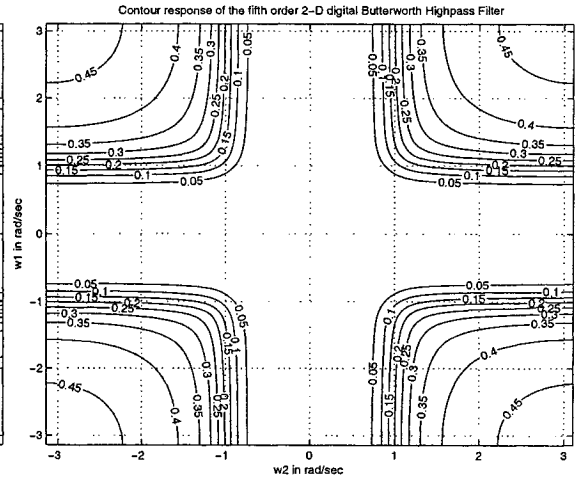

(f) When k1=k2=0.7, a1=a2=0.7 and b1=b2=-1

Figure 5.6: Contour response of the fifth order 2-D digital Butterworth highpass filter

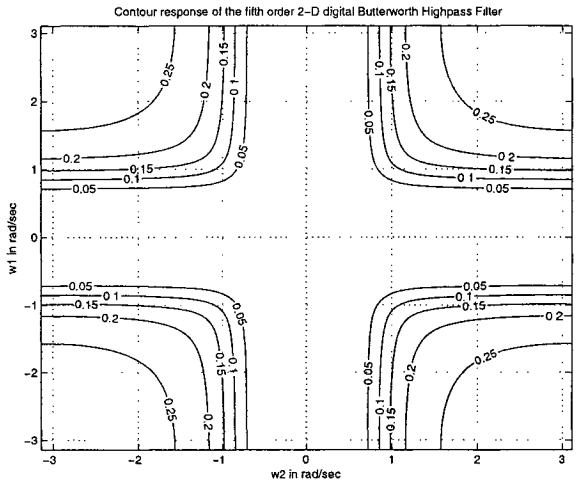

(a) When k1=k2=0.7, a1=a2=0.5 and b1=b2=-1

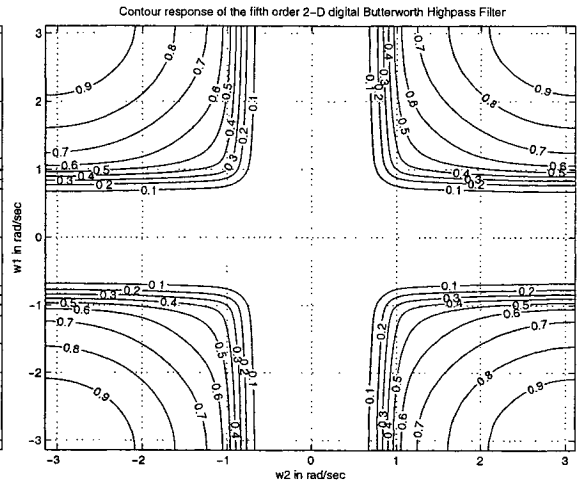

(b) When k1=k2=0.5, a1=a2=1 and b1=b2=-1

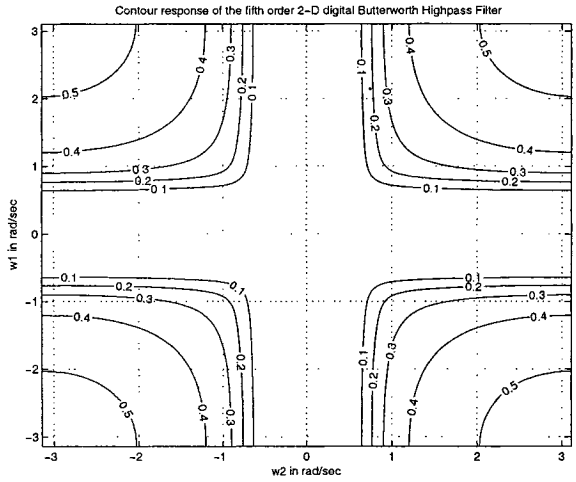

(c) When k1=k2=0.5, a1=a2=0.7 and b1=b2=-1

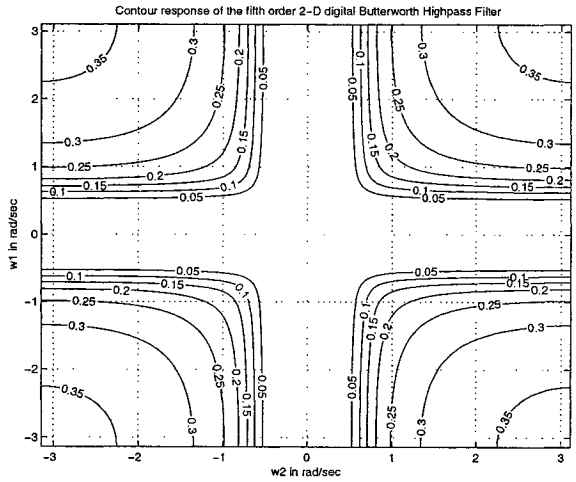

(d) When k1=k2=0.5, a1=a2=0.5 and b1=b2=-1

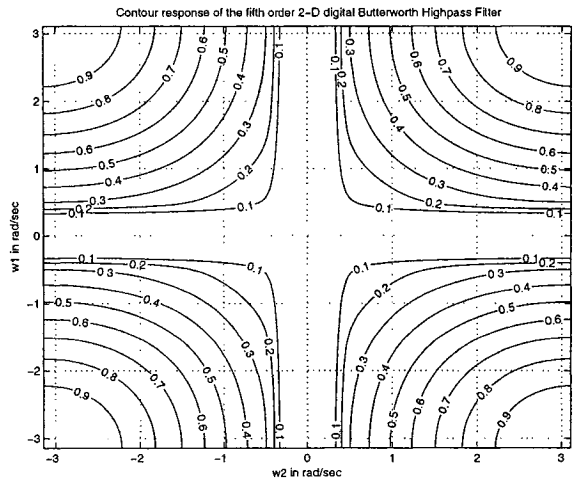

(e) When k1=k2=0.2, a1=a2=1 and b1=b2=-1

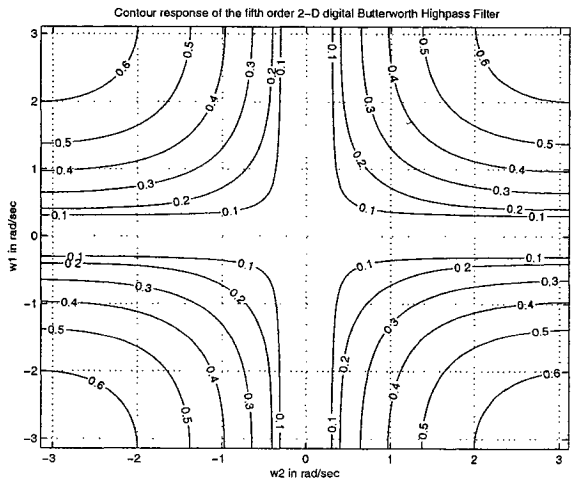

(f) When k1=k2=0.2, a1=a2=0.7 and b1=b2=-1

Figure 5.7: Contour response of the fifth order 2-D digital Butterworth highpass filter

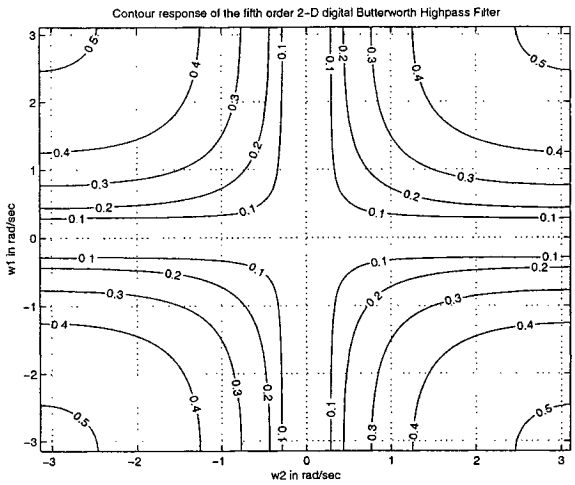

(a) When k1=k2=0.2, a1=a2=0.5 and b1=b2=-1

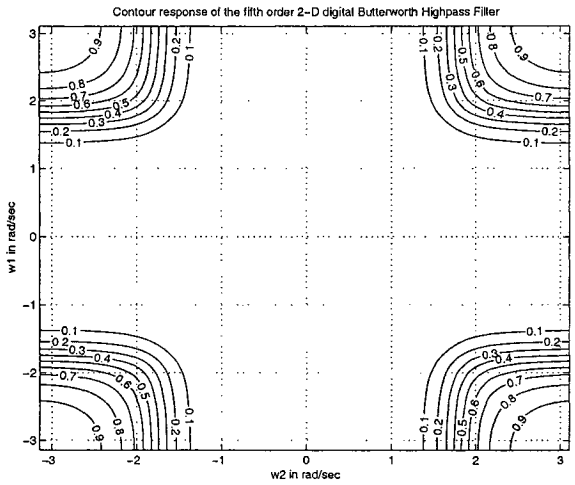

(b) When k1=k2=1, a1=a2=1 and b1=b2=-0.7

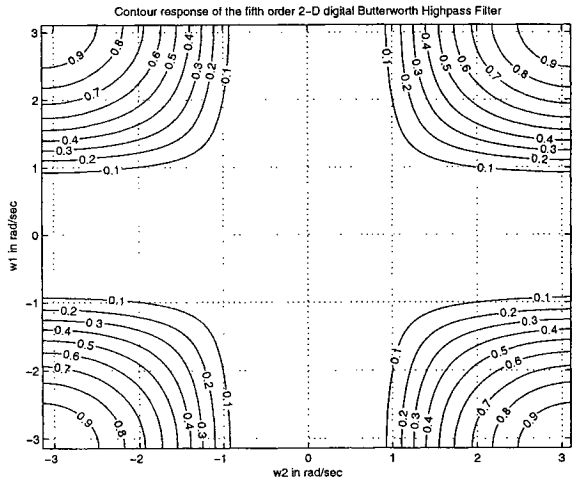

(c) When k1=k2=0.5, a1=a2=1 and b1=b2=-0.7

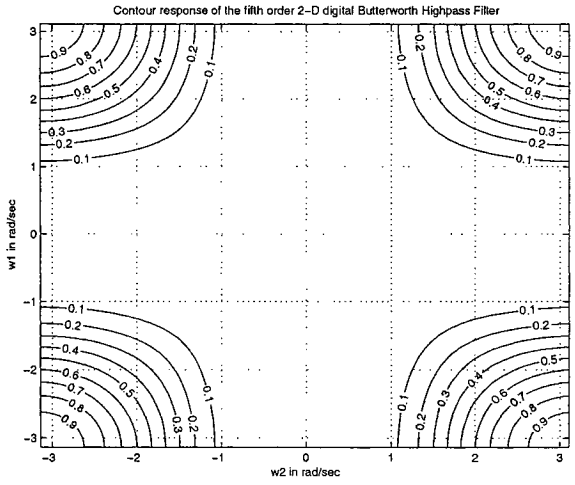

(d) When k1=k2=0.5, a1=a2=1 and b1=b2=-0.5

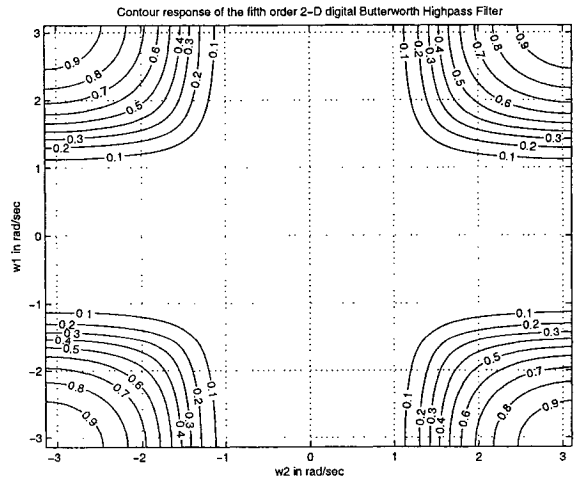

(e) When k1=k2=0.7, a1=a2=1 and b1=b2=-0.7

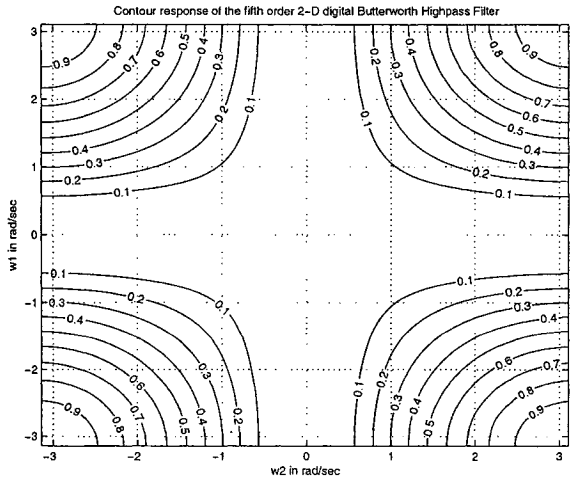

(f) When k1=k2=0.2, a1=a2=1 and b1=b2=-0.7

Figure 5.8: Contour response of the fifth order 2-D digital Butterworth highpass filter

The 3-D amplitude-frequency response and contour plots of the second order 2-D digital Butterworth highpass filter for different combination values of the coefficients of generalized bilinear transformation are shown in the fig. 5.9, 5.10 and 5.11. The MATLAB code to plot the 3-D amplitude-frequency response and contour of the frequency response of the second order 2-D digital Butterworth lowpass filter is in algorithm 35.

The coefficients k_1, k_2, affects passband width and a_1, a_2, affects gain of the amplitude-frequency response in fig. 5.10 and 5.11 (a), (b), (c), for $b_1 = b_2 = -1$. It may be noted that as the coefficients k_1, k_2, values are decreased, the passband width of the 2-D highpass filter increases. For example, in fig. 5.10 (b), (e) and fig. 5.11 (a), (c), as k_1, k_2, are decreased from 1 to 0.2, for same values of $a_1 = a_2 = 0.5$ and $b_1 = b_2 = -1$, the passband width of 2-D highpass filter increases. Similarly, in fig. 5.10 (c), (f) and fig. 5.11 (b), as k_1, k_2, are decreased from 1 to 0.5, for same values of $a_1 = a_2 = 0.2$ and $b_1 = b_2 = -1$, the passband width of 2-D highpass filter increases. As the coefficients a_1, a_2, values are decreased, the magnitude of the amplitude-frequency response of the 2-D highpass filter decreases. For example, in fig. 5.10 (a), (b) and (c), as a_1, a_2, are decreased from 0.7 to 0.2, for same values of $k_1 = k_2 = 1$ and $b_1 = b_2 = -1$, the magnitude of the passband decreases. Similarly, in fig. 5.10 (d), (e) and (f), as a_1, a_2, are decreased from 0.65 to 0.2, for same values of $k_1 = k_2 = 0.7$ and $b_1 = b_2 = -1$, the magnitude of the passband decreases. As b_1, b_2, are decreased to -0.7 and -0.5 in fig. 5.10 (d), (e), (f) from -1 in fig. 5.10 and 5.11 (a), (b), (c), the polarity of the amplitude-frequency response changes, and there is rounding of contour edges with decrease in passband. In all the cases discussed, the second order 2-D Butterworth highpass filter inhibits monotonic amplitude-frequency response.

Algorithm 35 The MATLAB code to plot the 3-D amplitude-frequency response and contour response of the second order 2-D digital Butterworth highpass filters having monotonic characteristics.

```
% Under Guidance of Prof. Dr. V. Ramachandran
% Student's name : Ajit Singh Sandhu..... ID:4841492.
clear all; clc;
a11=1; a10=1/sqrt(2); a01=1/sqrt(2); a00=1;
b11=1; b10=1/sqrt(2); b01=1/sqrt(2); b00=1;
%----------Lowpass Filter----------
% Input the values of the constants in the LP bilinear transformation.
k1=input('Give the value of the constant k1 for the bilinear LP transformation => ');
k2=input('Give the value of the constant k2 for the bilinear LP transformation => ');
a1L=input('Give the value of the constant a1L for the bilinear LP transformation => ');
a2L=input('Give the value of the constant a2L for the bilinear LP transformation => ');
% Create two dimensional square matrix (mesh grid) of angular frequency w1 and w2.
[w1,w2] = meshgrid(-pi:0.05:pi,-pi:0.05:pi);
% Apply Z1=r1*exp(jw1) and Z2=r2*exp(jw2) with r1 = r2 =1
z1=exp(j.*w1); z2=exp(j.*w2);
% h1 is the required digital transfer function and its value is evaluated as follows.....
a=z1-a1L; b=z2-a2L; c=z1+1; d=z2+1;
hd1=((a11.*k1.*k2.*a.*b)+(a10.*k1.*a.*d)+(a01.*k2.*b.*c)+(a00.*c.*d))
.*((b11.*k1.*k2.*a.*b)+(b10.*k1.*a.*d)+(b01.*k2.*b.*c)+(b00.*c.*d));
hd2=((a10.*k1.*a.*d)+(a01.*k2.*b.*c)).*((b10.*k1.*a.*d)+(b01.*k2.*b.*c));
h_lpf=((c.^2).*(d.^2).*(a00.*b00))./(hd1+hd2);
hd=abs(h_lpf);
%----------Highpass Filter----------
k1=input('Give the value of the constant k1 for the bilinear LP transformation => ');
k2=input('Give the value of the constant k2 for the bilinear LP transformation => ');
a1=input('Give the value of the constant a1 for the bilinear LP transformation => ');
a2=input('Give the value of the constant a2 for the bilinear LP transformation => ');
b1=input('Give the value of the constant b1 for the bilinear LP transformation => ');
b2=input('Give the value of the constant b2 for the bilinear LP transformation => ');
% hh1 is the required digital transfer function and its value is evaluated as follows.
a=z1+a1; b=z2+a2; c=z1+b1; d=z2+b2;
hhd1=((a11.*k1.*k2.*a.*b)+(a10.*k1.*a.*d)+(a01.*k2.*b.*c)+(a00.*c.*d))
.*((b11.*k1.*k2.*a.*b)+(b10.*k1.*a.*d)+(b01.*k2.*b.*c)+(b00.*c.*d));
hhd2=((a10.*k1.*a.*d)+(a01.*k2.*b.*c)).*((b10.*k1.*a.*d)+(b01.*k2.*b.*c));
h_hpf=((c.^2).*(d.^2).*(a00.*b00))./(hhd1+hhd2);
hhd=abs(h_hpf);
figure(1);
contour3(w1,w2,hhd);
surface(w1,w2,abs(hhd),'EdgeColor',[.8 .8 .8],'FaceColor','none');
grid on; view(-15,25);
title('3-D amplitude-frequency response of the 2-D digital Butterworth Highpass filter');
xlabel(' w2 in rad/sec ');
ylabel(' w1 in rad/sec ');
zlabel(' Magnitude Response ');
figure(2);
[C,h] = contour(w1,w2,hhd);
clabel(C,h); grid on;
title('Contour response of the 2-D digital Butterworth Highpass filter');
xlabel(' w2 in rad/sec ');
ylabel(' w1 in rad/sec ');
```

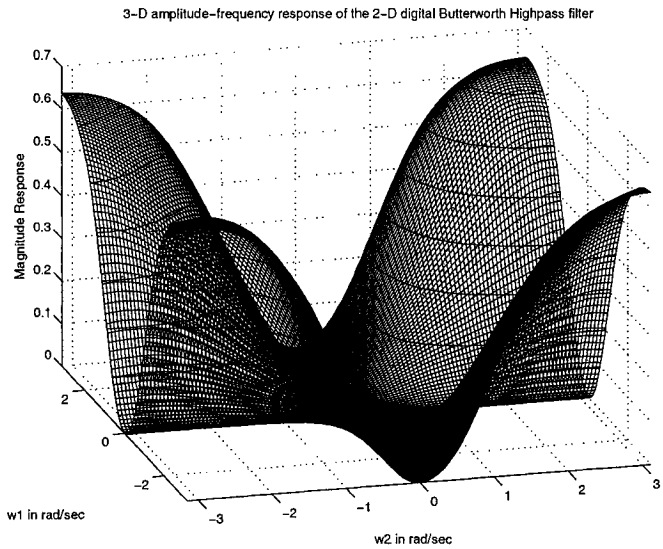

Figure 5.9: 3-D amplitude-frequency response of the second order 2-D digital Butterworth highpass filter (When $k_1 = k_2 = 1$, $a_1 = a_2 = 0.7$ and $b_1 = b_2 = -1$)

5.2.3 Generation of fifth order 2-D digital Filanovsky highpass filter with monotonic characteristics

The transfer function of the fifth order 2-D analog Filanovsky lowpass filter, is given by eqn. 3.11. By applying generalized bilinear transformation (eqn. 5.1) to eqn. 3.11, we get, transfer function of 2-D digital Filanovsky highpass filter as function of z_1 and z_2, with $z_1 = e^{jw_1}$ and $z_2 = e^{jw_2}$. Hence, we get,

$$H_d(z_1, z_2) = \frac{(0.3162)^2 (z_1 + b_1)^5 (z_2 + b_2)^5}{\begin{array}{l}[k_1 (z_1 + a_1) + 0.6445 (z_1 + b_1)] [k_2 (z_2 + a_2) + 0.6445 (z_2 + b_2)] \\ \left[k_1^2 (z_1 + a_1)^2 + 0.9508 k_1 (z_1 + a_1) (z_1 + b_1) + 0.5116 (z_1 + b_1)^2\right] \\ \left[k_1^2 (z_1 + a_1)^2 + 0.3492 k_1 (z_1 + a_1) (z_1 + b_1) + 0.9592 (z_1 + b_1)^2\right] \\ \left[k_2^2 (z_2 + a_2)^2 + 0.9508 k_2 (z_2 + a_2) (z_2 + b_2) + 0.5116 (z_2 + b_2)^2\right] \\ \left[k_2^2 (z_2 + a_2)^2 + 0.3492 (z_2 + a_2) (z_2 + b_2) + 0.9592 (z_2 + b_2)^2\right]\end{array}} \quad (5.5)$$

The 3-D amplitude-frequency response and contour plots of the fifth order 2-D digital Filanovsky highpass filter for different combination values of the coefficients of generalized

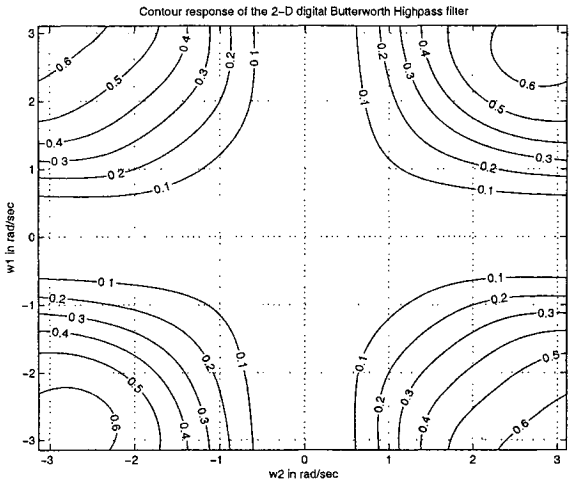

(a) When k1=k2=1, a1=a2=0.7 and b1=b2=-1

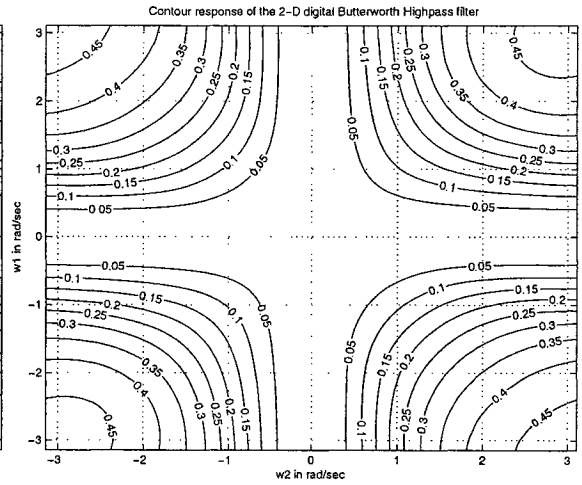

(b) When k1=k2=1, a1=a2=0.5 and b1=b2=-1

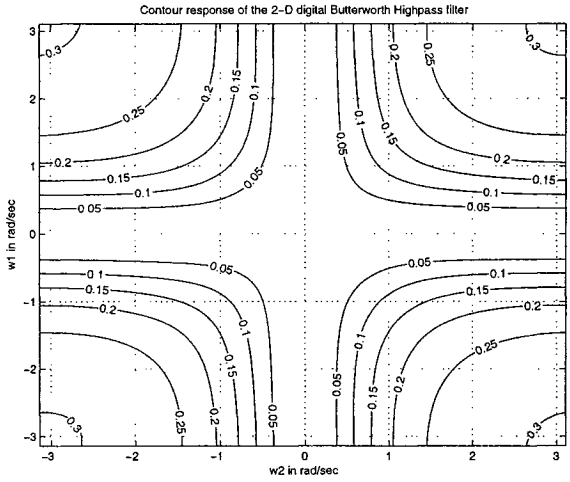

(c) When k1=k2=1, a1=a2=0.2 and b1=b2=-1

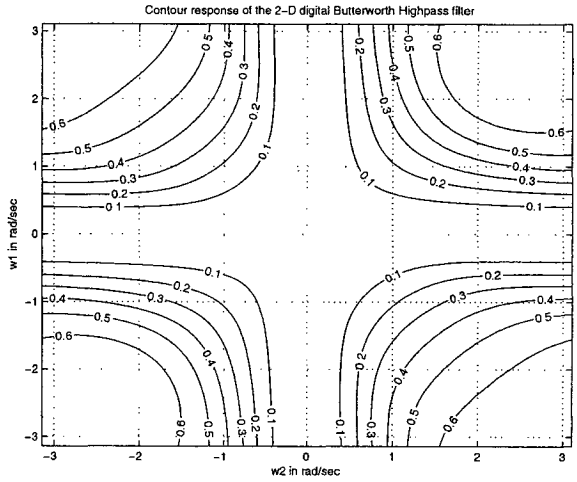

(d) When k1=k2=0.7, a1=a2=0.65 and b1=b2=-1

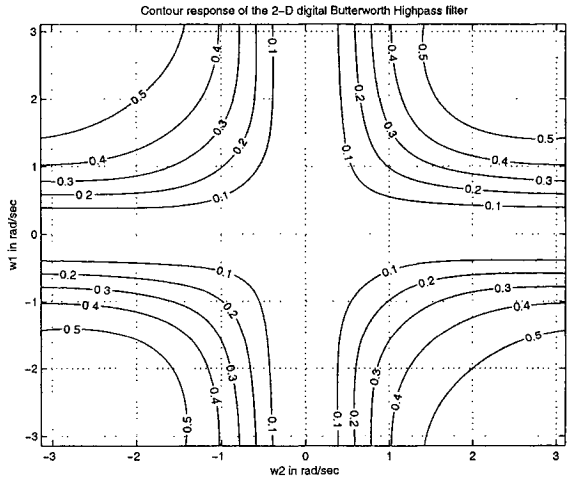

(e) When k1=k2=0.7, a1=a2=0.5 and b1=b2=-1

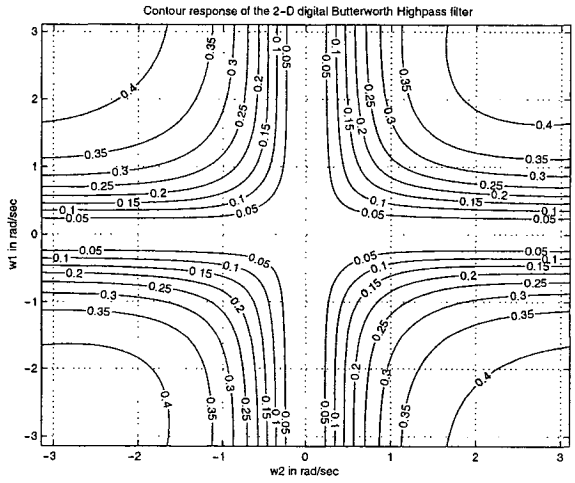

(f) When k1=k2=0.7, a1=a2=0.2 and b1=b2=-1

Figure 5.10: Contour response of the second order 2-D digital Butterworth highpass filter

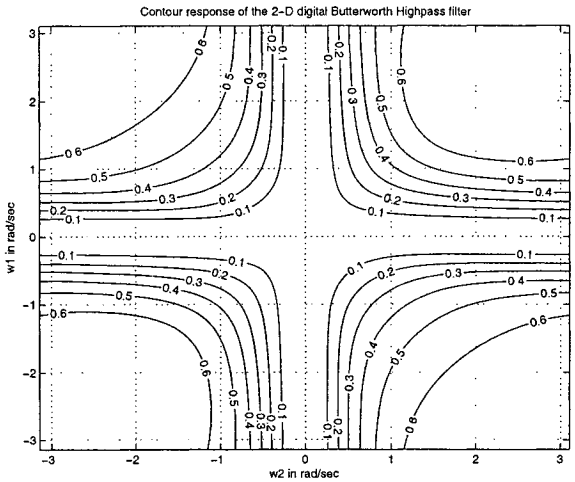

(a) When k1=k2=0.5, a1=a2=0.5 and b1=b2=-1

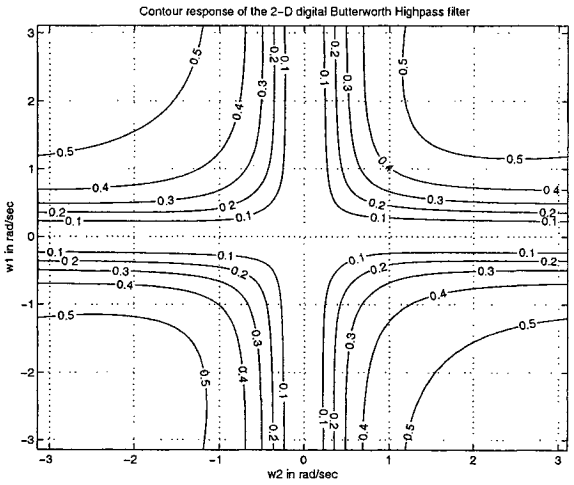

(b) When k1=k2=0.5, a1=a2=0.2 and b1=b2=-1

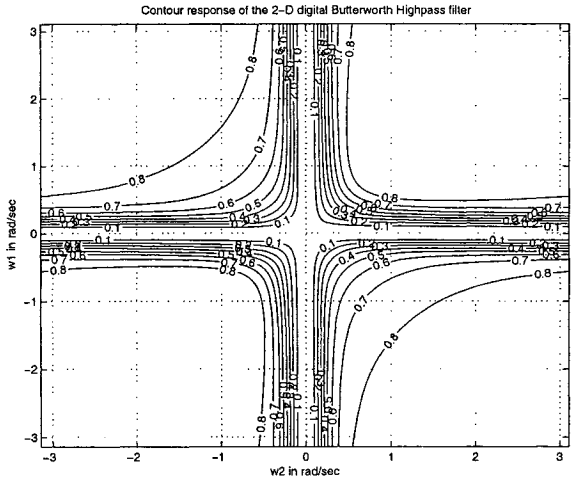

(c) When k1=k2=0.2, a1=a2=0.5 and b1=b2=-1

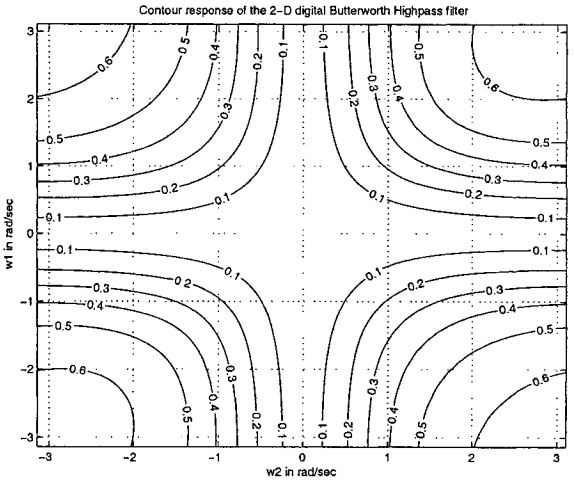

(d) When k1=k2=0.5, a1=a2=0.5 and b1=b2=-0.7

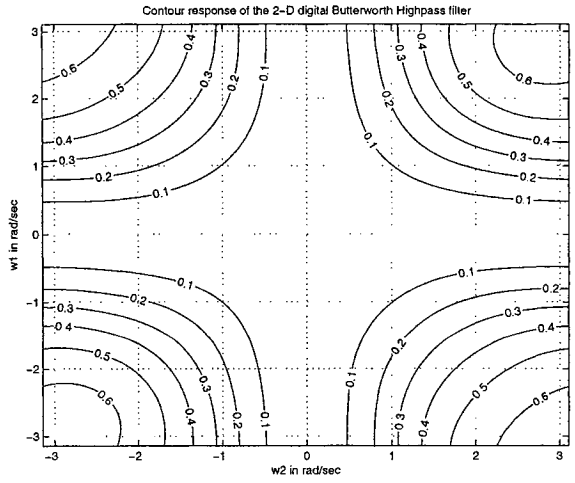

(e) When k1=k2=0.7, a1=a2=0.65 and b1=b2=-0.7

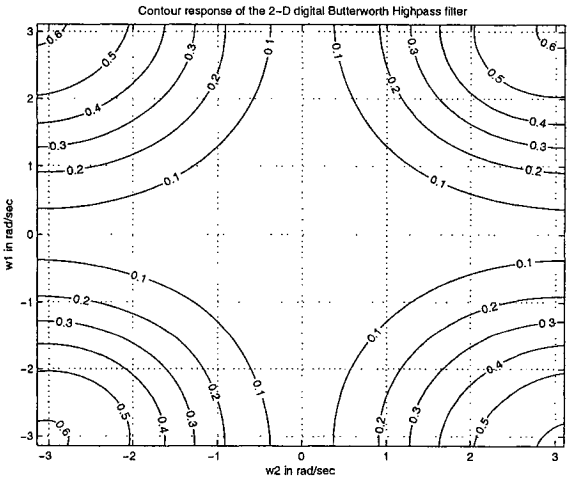

(f) When k1=k2=0.7, a1=a2=0.65 and b1=b2=-0.5

Figure 5.11: Contour response of the second order 2-D digital Butterworth highpass filter

bilinear transformation are shown in the fig. 5.12, 5.13, 5.14 and 5.15. The MATLAB code to plot the 3-D amplitude-frequency response and contour of the frequency response of the fifth order 2-D digital Filanovsky lowpass filter is in algorithm 36.

The coefficients k_1, k_2, affects passband width and a_1, a_2, affects gain of the amplitude-frequency response in fig. 5.13, 5.14 and 5.15 (a), for $b_1 = b_2 = -1$. It may be noted that as the coefficients k_1, k_2, values are decreased, the passband width of the 2-D highpass filter increases. For example, in fig. 5.13 (b), (f) and fig. 5.14 (c), (f), as k_1, k_2, are decreased from 1 to 0.2, for same values of $a_1 = a_2 = 0.7$ and $b_1 = b_2 = -1$, the passband width of 2-D highpass filter increases. Similarly, in fig. 5.13 (a), (e) and fig. 5.14 (b), (e), as k_1, k_2, are decreased from 1 to 0.2, for same values of $a_1 = a_2 = 1$ and $b_1 = b_2 = -1$, the passband width of 2-D highpass filter increases. As the coefficients a_1, a_2, values are decreased, the magnitude of the amplitude-frequency response of the 2-D highpass filter decreases. For example, in fig. 5.13 (a), (b), (c) and (d), as a_1, a_2, are decreased from 1 to 0.2, for same values of $k_1 = k_2 = 1$ and $b_1 = b_2 = -1$, the magnitude of the passband decreases. Similarly, in fig. 5.14 (b), (c) and (d), as a_1, a_2, are decreased from 1 to 0.5, for same values of $k_1 = k_2 = 0.5$ and $b_1 = b_2 = -1$, the magnitude of the passband decreases. As b_1, b_2, are decreased to -0.7 and -0.5 in fig. 5.15 from -1 in fig. 5.13 and 5.14, the polarity of the amplitude-frequency response changes, and there is rounding of contour edges with decrease in passband. In all the cases discussed, the fifth order 2-D digital Filanovsky highpass filter inhibits monotonic amplitude-frequency response.

5.2.4 Generation of fifth order 2-D digital Thomson-Bessel highpass filter with monotonic characteristics

The transfer function of the fifth order 2-D analog Thomson-Bessel lowpass filter, is given by eqn. 3.14. By applying generalized bilinear transformation (eqn. 5.1) to eqn. 3.14, we get, transfer function of 2-D digital Thomson-Bessel highpass filter as function of z_1 and

Algorithm 36 The MATLAB code to plot the 3-D amplitude-frequency response and contour response of the fifth order 2-D digital Filanovsky highpass filters having monotonic characteristics.

```
% Under Guidance of Prof. Dr. V. Ramachandran
% Student's name : Ajit Singh Sandhu..... ID:4841492.
clc; clear all;
%————Lowpass filter————
k1=input('Give the value of the constant k1 for the bilinear LP transformation => ');
k2=input('Give the value of the constant k2 for the bilinear LP transformation => ');
a1L=input('Give the value of the constant a1L for the bilinear LP transformation => ');
a2L=input('Give the value of the constant a2L for the bilinear LP transformation => ');
% Creates two dimensional square matrix (mesh grid) of angular frequency w1 and w2.
[w1,w2] = meshgrid(-pi:0.05:pi,-pi:0.05:pi);
% Apply Z1=r1*exp(jw1) and Z2=r2*exp(jw2) with r1 = r2 =1
z1=exp(j.*w1); z2=exp(j.*w2);
% h1 is the required digital transfer function and its value is evaluated as follows.
a=z1-a1L; b=z2-a2L; c=z1+1; d=z2+1;
h1_1=(((k1.^2).*(a.^2))+(k1.*0.9508.*a.*c)+(0.5116.*(c.^2))).*(((k1.^2)
.*(a.^2))+(k1.*0.3492.*a.*c)+(0.9592.*(c.^2))).*(a+(0.6445.*c));
h1_2=(((k2.^2).*(b.^2))+(k2.*0.9508.*b.*d)+(0.5116.*(d.^2))).*(((k2.^2)
.*(b.^2))+(k2.*0.3492.*b.*d)+(0.9592.*(d.^2))).*(b+(0.6445.*d));
h_lpf=((c.^5).*(d.^5).*(0.3162^2))./(h1_1.*h1_2);
h1=abs(h_lpf);
%————————Highpass filter————————
k1=input('Give the value of the constant k1 for the bilinear LP transformation => ');
k2=input('Give the value of the constant k2 for the bilinear LP transformation => ');
a1=input('Give the value of the constant a1 for the bilinear LP transformation => ');
a2=input('Give the value of the constant a2 for the bilinear LP transformation => ');
b1=input('Give the value of the constant b1 for the bilinear LP transformation => ');
b2=input('Give the value of the constant b2 for the bilinear LP transformation => ');
% hh1 is the required digital transfer function and its value is evaluated as follows.
a=z1+a1; b=z2+a2; c=z1+b1; d=z2+b2;
hh1_1=(((k1.^2).*(a.^2))+(k1.*0.9508.*a.*c)+(0.5116.*(c.^2))).*(((k1.^2)
.*(a.^2))+(k1.*0.3492.*a.*c)+(0.9592.*(c.^2))).*(a+(0.6445.*c));
hh1_2=(((k2.^2).*(b.^2))+(k2.*0.9508.*b.*d)+(0.5116.*(d.^2))).*(((k2.^2)
.*(b.^2))+(k2.*0.3492.*b.*d)+(0.9592.*(d.^2))).*(b+(0.6445.*d));
h_hpf=((c.^5).*(d.^5).*(0.3162^2))./(hh1_1.*hh1_2);
hh1=abs(h_hpf);
figure(3);
contour3(w1,w2,hh1);
surface(w1,w2,abs(hh1),'EdgeColor',[.8 .8 .8],'FaceColor','none');
grid on; view(-15,25);
title('3-D amplitude-frequency response of the fifth order 2-D Filanovsky Highpass Filter');
xlabel(' w2 in rad/sec ');
ylabel(' w1 in rad/sec ');
zlabel(' Magnitude Response ');
figure(4);
[C,h] = contour(w1,w2,hh1);
clabel(C,h); grid on;
title('Contour response of the fifth order 2-D Filanovsky Highpass Filter');
xlabel(' w2 in rad/sec ');
ylabel(' w1 in rad/sec ');
```

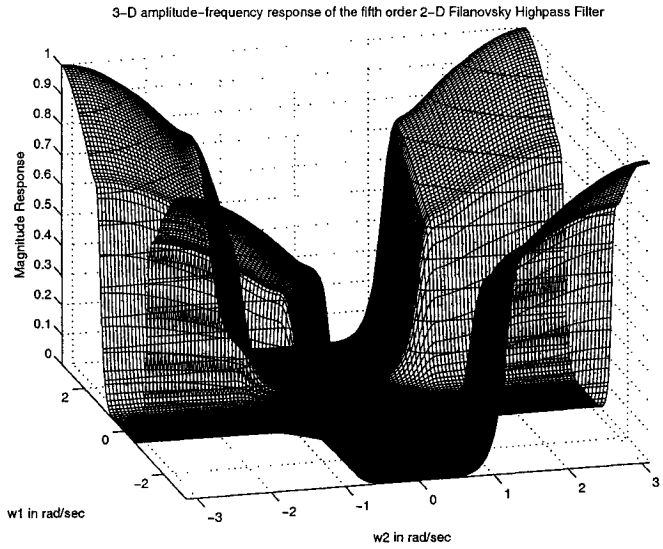

Figure 5.12: 3-D amplitude-frequency response of the fifth order 2-D digital Filanovsky highpass filter (When $k_1 = k_2 = 0.7$, $a_1 = a_2 = 1$ and $b_1 = b_2 = -1$)

z_2, with $z_1 = e^{jw_1}$ and $z_2 = e^{jw_2}$. Hence, we get,

$$H_d(z_1, z_2) = \frac{(945)^2 (z_1 + b_1)^5 (z_2 + b_2)^5}{\left[k_1^5 (z_1 + a_1)^5 + 15k_1^4 (z_1 + a_1)^4 (z_1 + b_1) + 105k_1^3 (z_1 + a_1)^3 (z_1 + b_1)^2 + 420k_1^2 (z_1 + a_1)^2 (z_1 + b_1)^3 + 945k_1 (z_1 + a_1) (z_1 + b_1)^4 + 945 (z_1 + b_1)^5\right] \left[k_2^5 (z_2 + a_2)^5 + 15k_2^4 (z_2 + a_2)^4 (z_2 + b_2) + 105k_2^3 (z_2 + a_2)^3 (z_2 + b_2)^2 + 420k_2^2 (z_2 + a_2)^2 (z_2 + b_2)^3 + 945k_2 (z_2 + a_2) (z_2 + b_2)^4 + 945 (z_2 + b_2)^5\right]} \quad (5.6)$$

The 3-D amplitude-frequency response and contour plots of the fifth order 2-D digital Thomson-Bessel highpass filter for different combination values of the coefficients of generalized bilinear transformation are shown in the fig. 5.16, 5.17, 5.18 and 5.19. The MATLAB code to plot the 3-D amplitude-frequency response and contour of the frequency response of the fifth order 2-D digital Thomson-Bessel lowpass filter is in algorithm 37.

The coefficients k_1, k_2, affects passband width and a_1, a_2, affects gain of the amplitude-frequency response in fig. 5.17, 5.18 and 5.19 (a), for $b_1 = b_2 = -1$. It may be noted that as the coefficients k_1, k_2, values are decreased, the passband width of the 2-D highpass filter

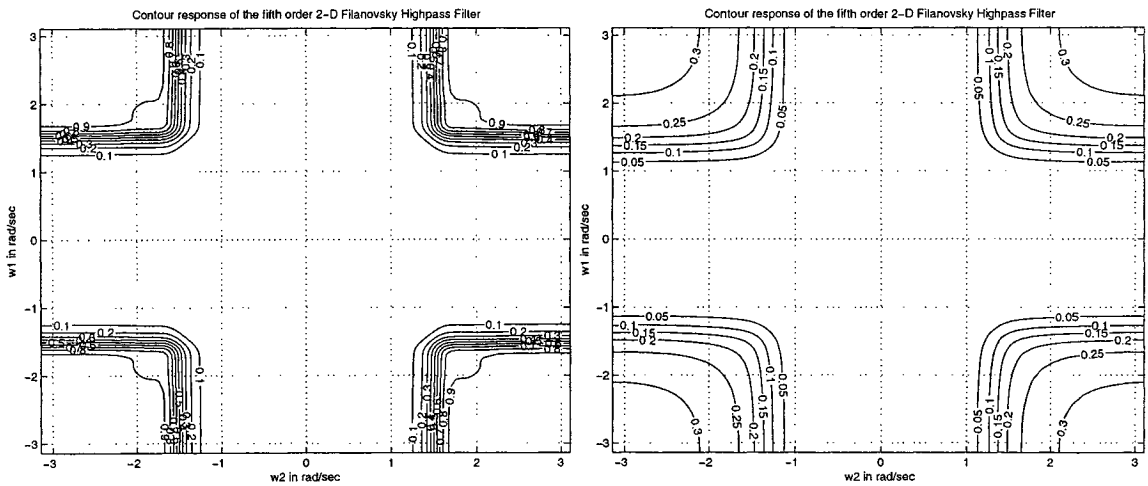

(a) When k1=k2=1, a1=a2=1 and b1=b2=-1

(b) When k1=k2=1, a1=a2=0.7 and b1=b2=-1

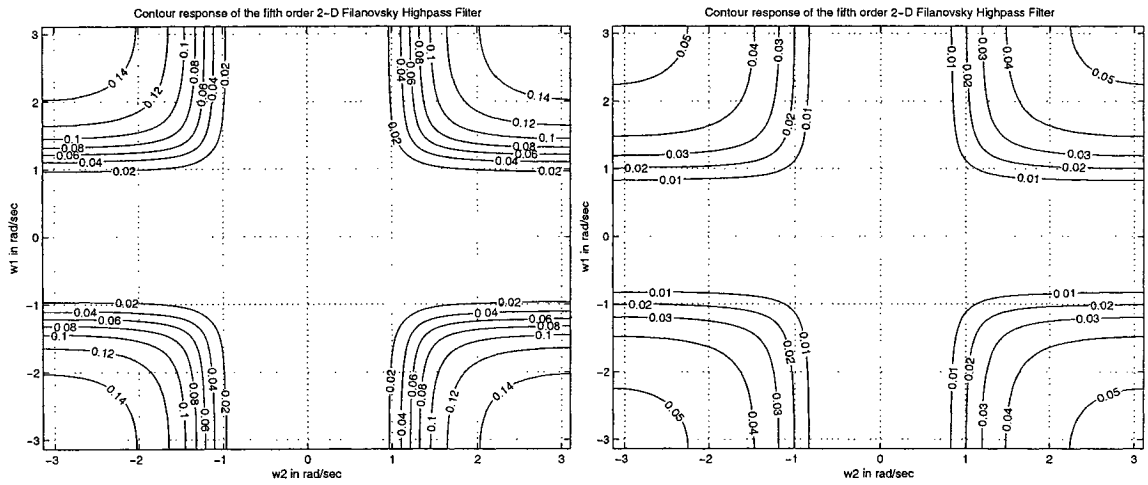

(c) When k1=k2=1, a1=a2=0.5 and b1=b2=-1

(d) When k1=k2=1, a1=a2=0.2 and b1=b2=-1

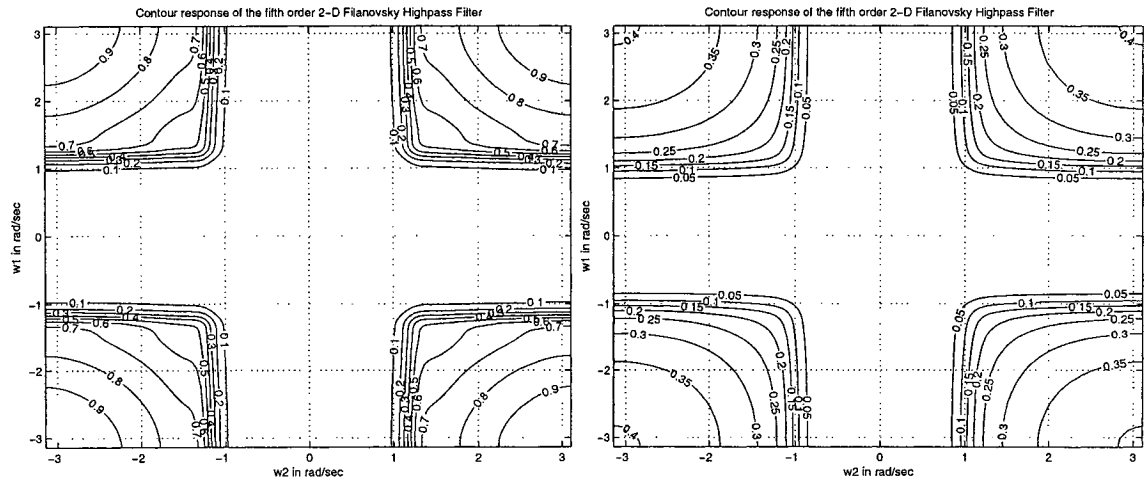

(e) When k1=k2=0.7, a1=a2=1 and b1=b2=-1

(f) When k1=k2=0.7, a1=a2=0.7 and b1=b2=-1

Figure 5.13: Contour response of the fifth order 2-D digital Filanovsky highpass filter

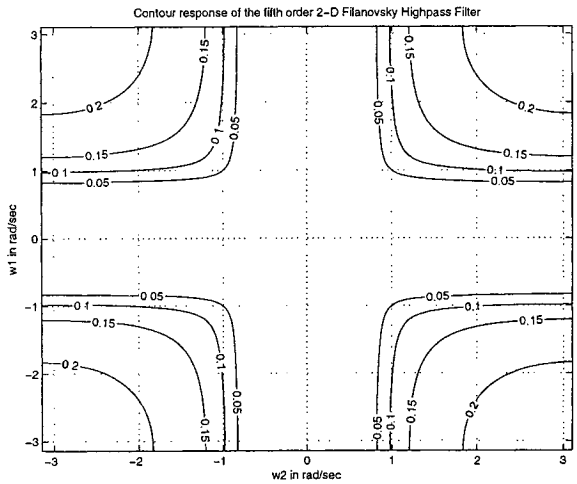

(a) When k1=k2=0.7, a1=a2=0.5 and b1=b2=-1

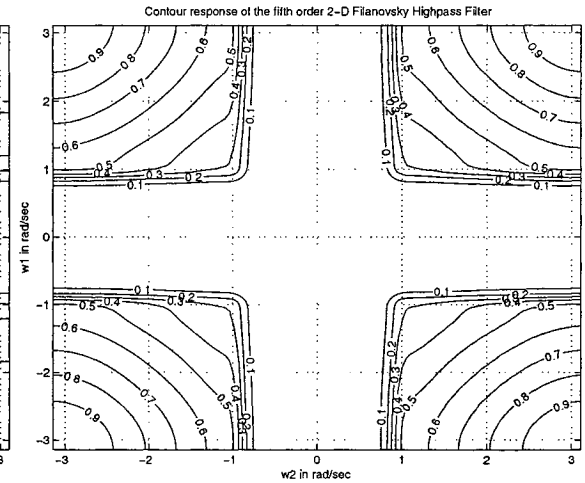

(b) When k1=k2=0.5, a1=a2=1 and b1=b2=-1

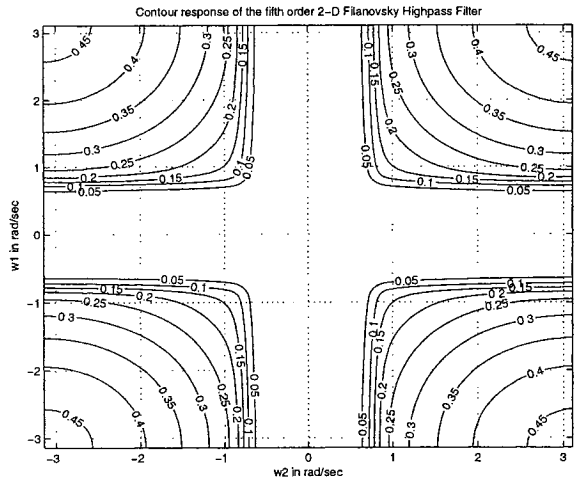

(c) When k1=k2=0.5, a1=a2=0.7 and b1=b2=-1

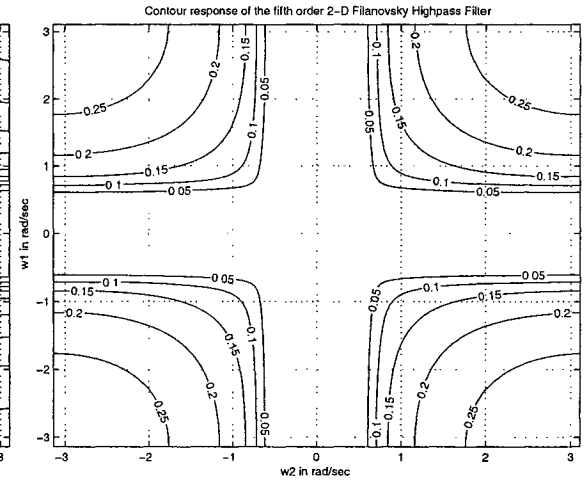

(d) When k1=k2=0.5, a1=a2=0.5 and b1=b2=-1

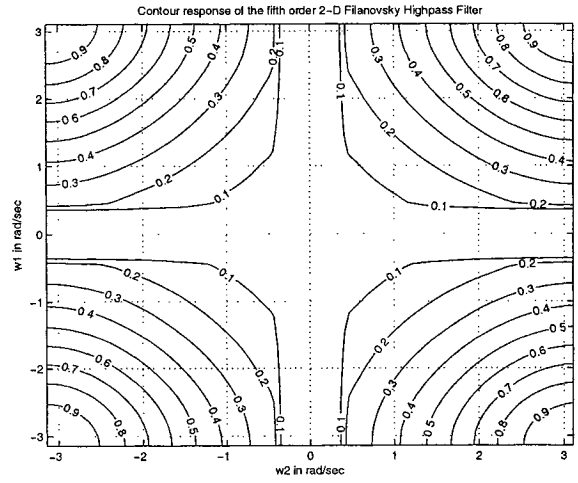

(e) When k1=k2=0.2, a1=a2=1 and b1=b2=-1

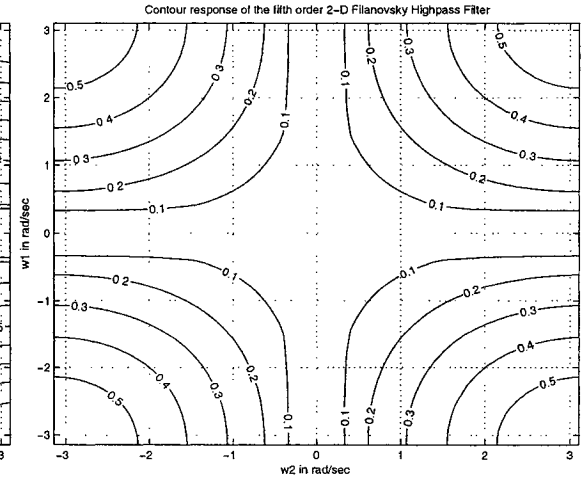

(f) When k1=k2=0.2, a1=a2=0.7 and b1=b2=-1

Figure 5.14: Contour response of the fifth order 2-D digital Filanovsky highpass filter

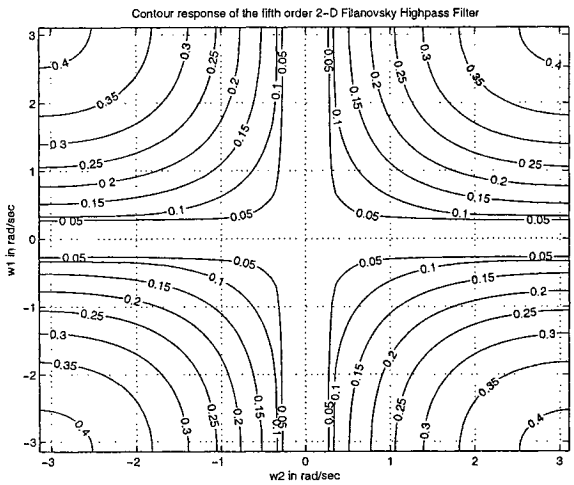

(a) When k1=k2=0.2, a1=a2=0.5 and b1=b2=-1

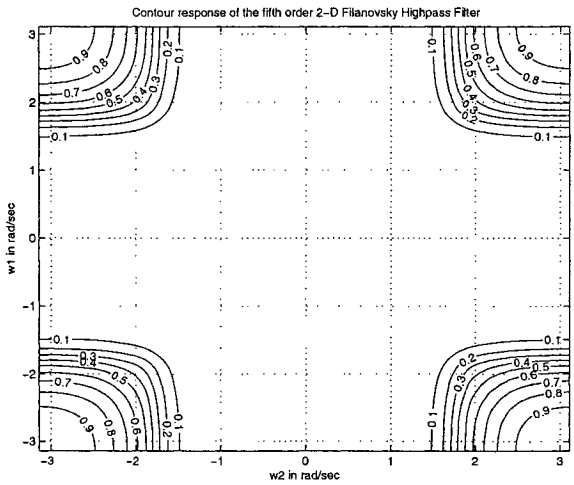

(b) When k1=k2=1, a1=a2=1 and b1=b2=-0.7

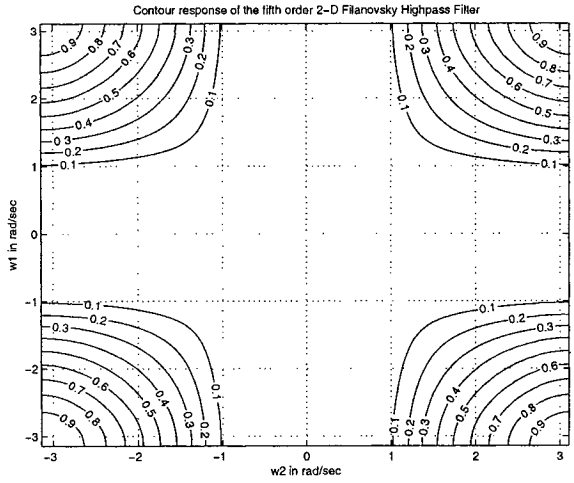

(c) When k1=k2=0.5, a1=a2=1 and b1=b2=-0.7

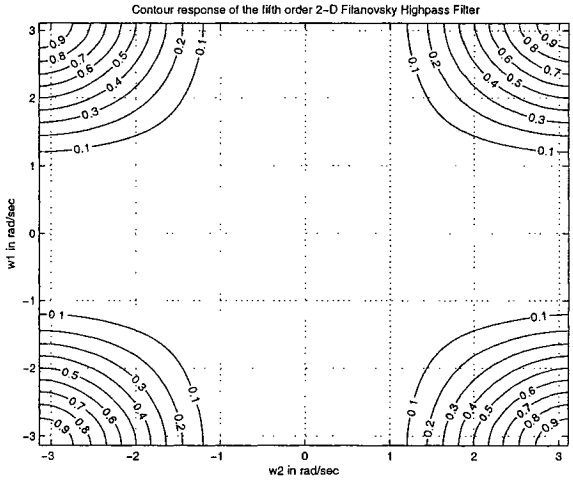

(d) When k1=k2=0.5, a1=a2=1 and b1=b2=-0.5

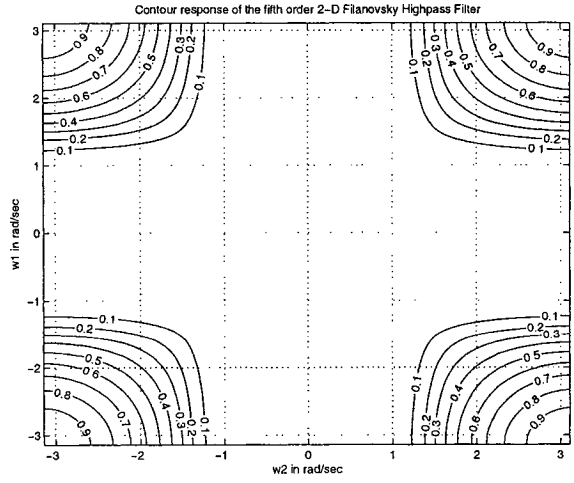

(e) When k1=k2=0.7, a1=a2=1 and b1=b2=-0.7

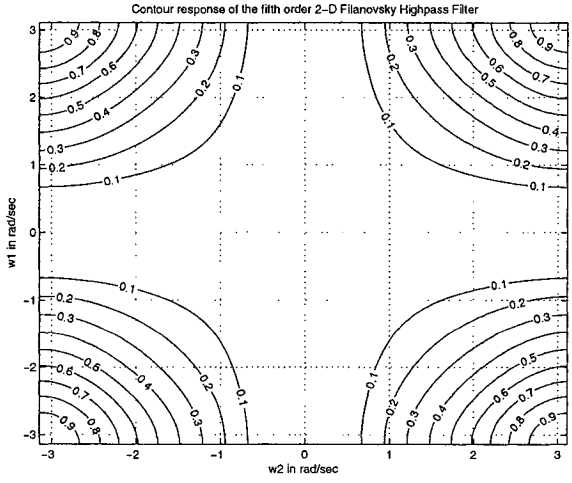

(f) When k1=k2=0.2, a1=a2=1 and b1=b2=-0.7

Figure 5.15: Contour response of the fifth order 2-D digital Filanovsky highpass filter

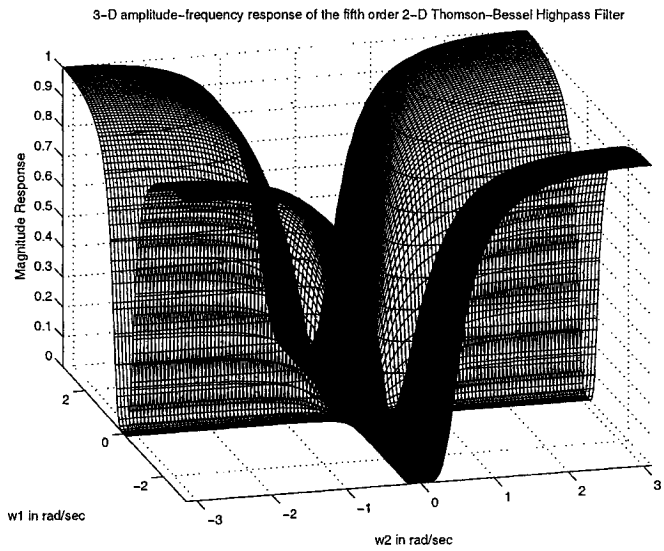

Figure 5.16: 3-D amplitude-frequency response of the fifth order 2-D digital Thomson-Bessel highpass filter (When $k_1 = k_2 = a_1 = a_2 = 1$ and $b_1 = b_2 = -1$)

increases. For example, in fig. 5.17 (b), (f) and fig. 5.18 (c), (f), as k_1, k_2, are decreased from 1 to 0.2, for same values of $a_1 = a_2 = 0.7$ and $b_1 = b_2 = -1$, the passband width of 2-D highpass filter increases. Similarly, in fig. 5.17 (a), (e) and fig. 5.18 (b), (e), as k_1, k_2, are decreased from 1 to 0.2, for same values of $a_1 = a_2 = 1$ and $b_1 = b_2 = -1$, the passband width of 2-D highpass filter increases. As the coefficients a_1, a_2, values are decreased, the magnitude of the amplitude-frequency response of the 2-D highpass filter decreases. For example, in fig. 5.17 (a), (b), (c) and (d), as a_1, a_2, are decreased from 1 to 0.2, for same values of $k_1 = k_2 = 1$ and $b_1 = b_2 = -1$, the magnitude of the passband decreases. Similarly, in fig. 5.18 (b), (c) and (d), as a_1, a_2, are decreased from 1 to 0.5, for same values of $k_1 = k_2 = 0.5$ and $b_1 = b_2 = -1$, the magnitude of the passband decreases. As b_1, b_2, are decreased to -0.7 and -0.5 in fig. 5.19 from -1 in fig. 5.17 and 5.18, the polarity of the amplitude-frequency response changes, and there is rounding of contour edges with decrease in passband. In all the cases discussed, the fifth order 2-D digital Thomson-Bessel highpass filter inhibits monotonic amplitude-frequency response.

Algorithm 37 The MATLAB code to plot the 3-D amplitude-frequency response and contour response of the fifth order 2-D digital Thomson-Bessel highpass filters having monotonic characteristics.

```
% Under Guidance of Prof. Dr. V. Ramachandran
% Student's name : Ajit Singh Sandhu..... ID:4841492.
clc; clear all;
%————Lowpass filter————————
k1=input('Give the value of the constant k1 for the bilinear LP transformation => ');
k2=input('Give the value of the constant k2 for the bilinear LP transformation => ');
a1L=input('Give the value of the constant a1L for the bilinear LP transformation => ');
a2L=input('Give the value of the constant a2L for the bilinear LP transformation => ');
% Creates two dimensional square matrix (mesh grid) of angular frequency w1 and w2.
[w1,w2] = meshgrid(-pi:0.05:pi,-pi:0.05:pi);
% Apply Z1=r1*exp(jw1) and Z2=r2*exp(jw2) with r1 = r2 =1
z1=exp(j.*w1); z2=exp(j.*w2);
% h1 is the required digital transfer function and its value is evaluated as follows.
a=z1-a1L; b=z2-a2L; c=z1+1; d=z2+1;
h1_1=((k1.^5).*(a.^5))+((k1.^4).*15.*(a.^4).*c)+((k1.^3).*105.*(a.^3).*(c.^2))
+((k1.^2).*420.*(a.^2).*(c.^3))+(k1.*945.*a.*(c.^4))+(945.*(c.^5));
h1_2=((k2.^5).*(b.^5))+((k2.^4).*15.*(b.^4).*d)+((k2.^3).*105.*(b.^3).*(d.^2))
+((k2.^2).*420.*(b.^2).*(d.^3))+(k2.*945.*b.*(d.^4))+(945.*(d.^5));
h_lpf=((c.^5).*(d.^5).*(945^2))./(h1_1.*h1_2);
h1=abs(h_lpf);
%————————Highpass Filter————————————%
k1=input('Give the value of the constant k1 for the bilinear LP transformation => ');
k2=input('Give the value of the constant k2 for the bilinear LP transformation => ');
a1=input('Give the value of the constant a1 for the bilinear LP transformation => ');
a2=input('Give the value of the constant a2 for the bilinear LP transformation => ');
b1=input('Give the value of the constant b1 for the bilinear LP transformation => ');
b2=input('Give the value of the constant b2 for the bilinear LP transformation => ');
% hh1 is the required digital transfer function and its value is evaluated as follows.
a=z1+a1; b=z2+a2; c=z1+b1; d=z2+b2;
hh1_1=((k1.^5).*(a.^5))+((k1.^4).*15.*(a.^4).*c)+((k1.^3).*105.*(a.^3).*(c.^2))
+((k1.^2).*420.*(a.^2).*(c.^3))+(k1.*945.*a.*(c.^4))+(945.*(c.^5));
hh1_2=((k2.^5).*(b.^5))+((k2.^4).*15.*(b.^4).*d)+((k2.^3).*105.*(b.^3).*(d.^2))
+((k2.^2).*420.*(b.^2).*(d.^3))+(k2.*945.*b.*(d.^4))+(945.*(d.^5));
h_hpf=((c.^5).*(d.^5).*(945^2))./(hh1_1.*hh1_2);
hh1=abs(h_hpf);
figure(1);
contour3(w1,w2,hh1);
surface(w1,w2,abs(hh1),'EdgeColor',[.8 .8 .8],'FaceColor','none');
grid on; view(-15,25);
title('3-D amplitude-frequency response of the fifth order 2-D Thomson-Bessel Highpass Filter');
xlabel(' w2 in rad/sec ');
ylabel(' w1 in rad/sec ');
zlabel(' Magnitude Response ');
figure(2);
[C,h] = contour(w1,w2,hh1);
clabel(C,h); grid on;
title('Contour response of the fifth order 2-D Thomson-Bessel Highpass Filter');
xlabel(' w2 in rad/sec ');
ylabel(' w1 in rad/sec ');
```

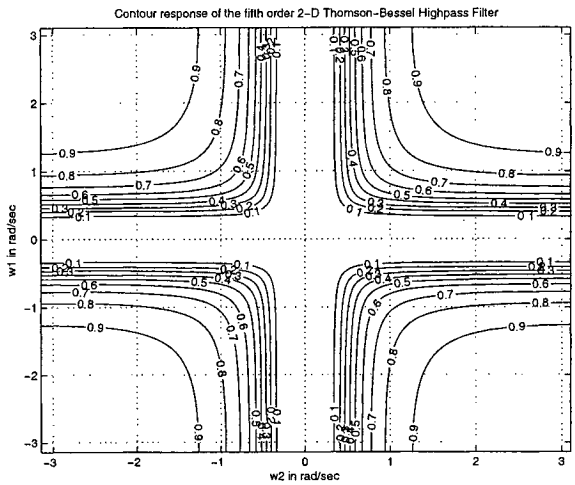

(a) When k1=k2=1, a1=a2=1 and b1=b2=-1

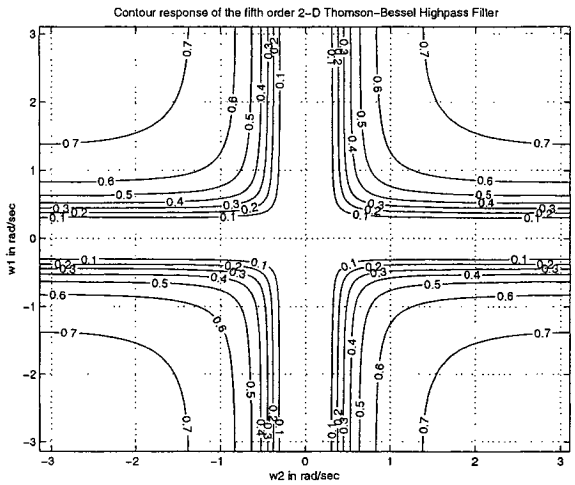

(b) When k1=k2=1, a1=a2=0.7 and b1=b2=-1

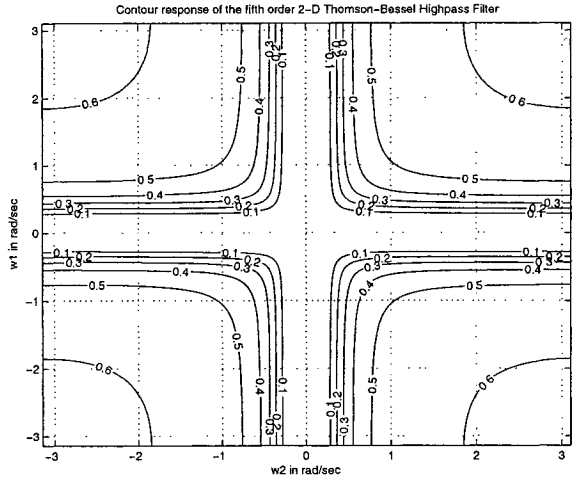

(c) When k1=k2=1, a1=a2=0.5 and b1=b2=-1

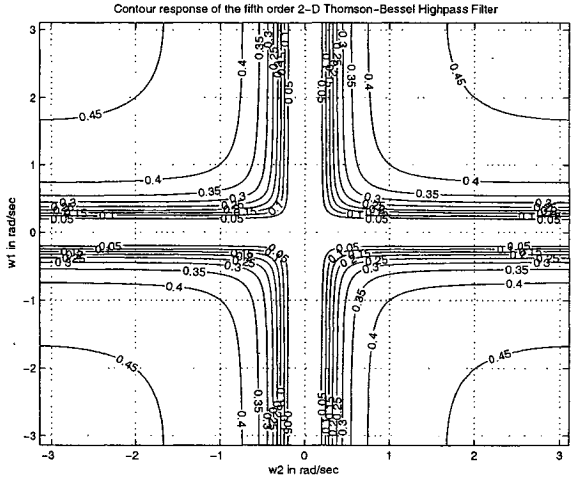

(d) When k1=k2=1, a1=a2=0.2 and b1=b2=-1

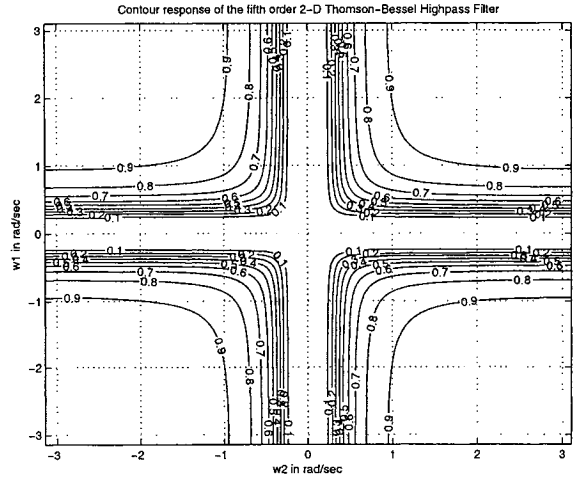

(e) When k1=k2=0.7, a1=a2=1 and b1=b2=-1

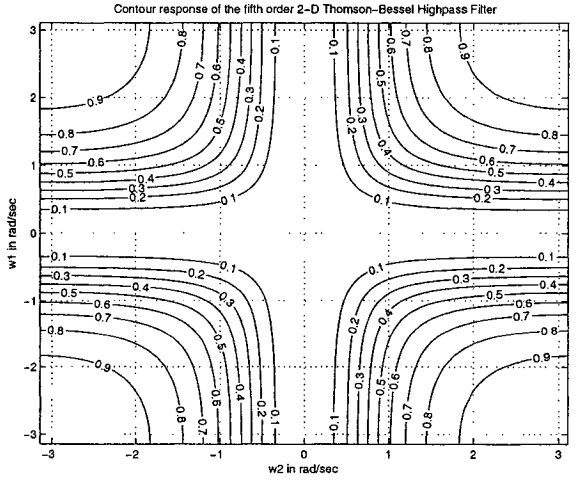

(f) When k1=k2=0.7, a1=a2=0.7 and b1=b2=-1

Figure 5.17: Contour response of the fifth order 2-D digital Thomson-Bessel highpass filter

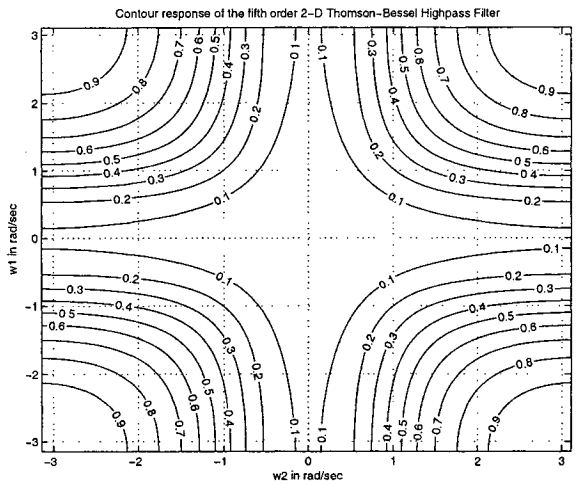

(a) When k1=k2=0.7, a1=a2=0.5 and b1=b2=-1

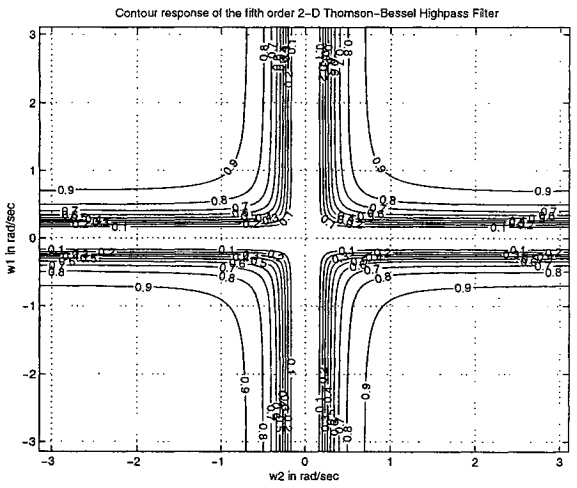

(b) When k1=k2=0.5, a1=a2=1 and b1=b2=-1

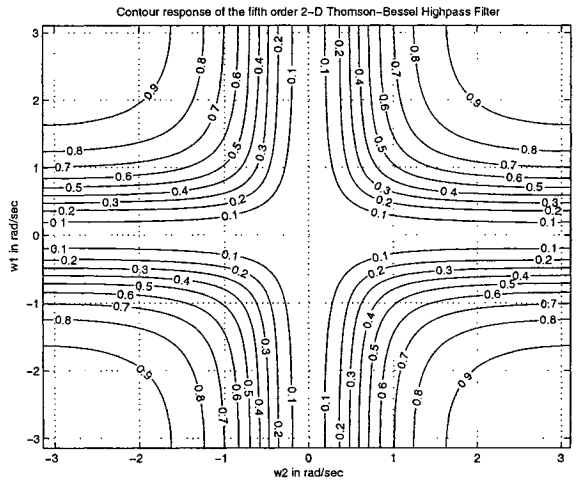

(c) When k1=k2=0.5, a1=a2=0.7 and b1=b2=-1

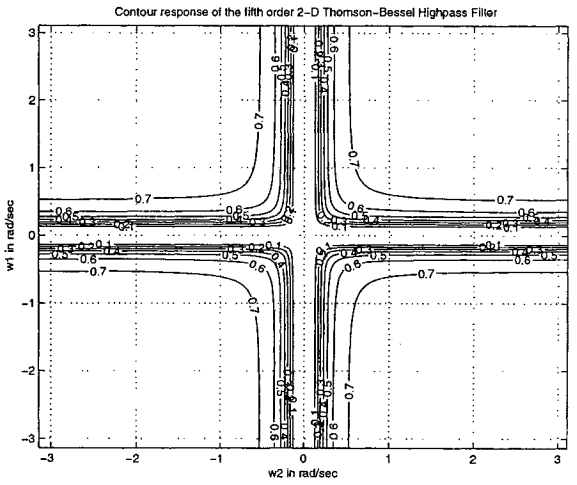

(d) When k1=k2=0.5, a1=a2=0.5 and b1=b2=-1

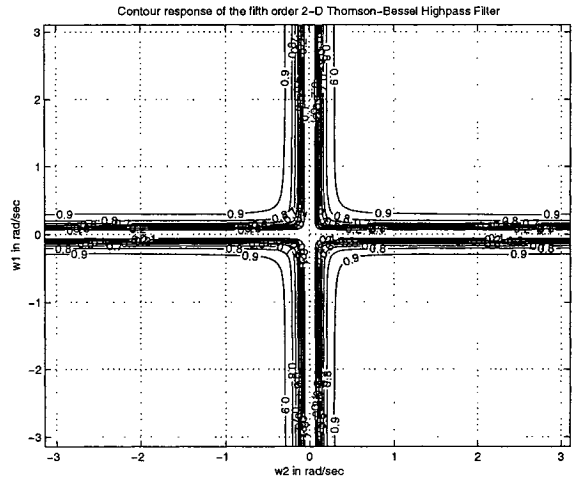

(e) When k1=k2=0.2, a1=a2=1 and b1=b2=-1

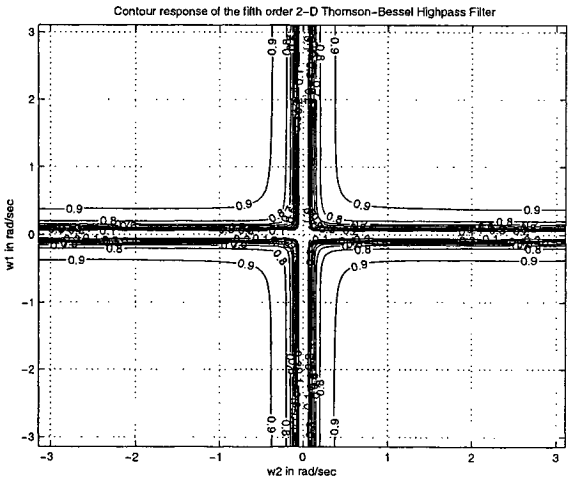

(f) When k1=k2=0.2, a1=a2=0.7 and b1=b2=-1

Figure 5.18: Contour response of the fifth order 2-D digital Thomson-Bessel highpass filter

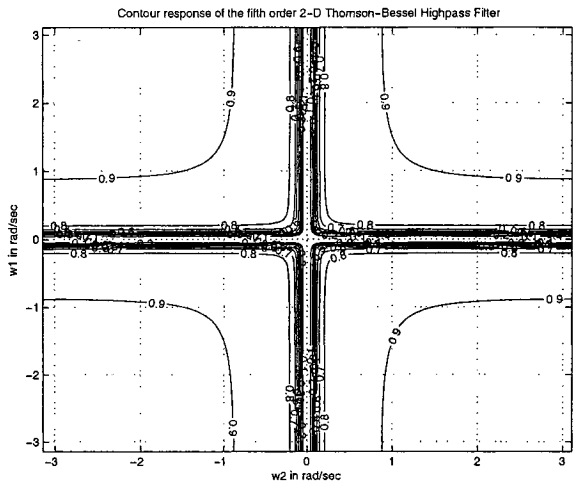

(a) When k1=k2=0.2, a1=a2=0.5 and b1=b2=-1

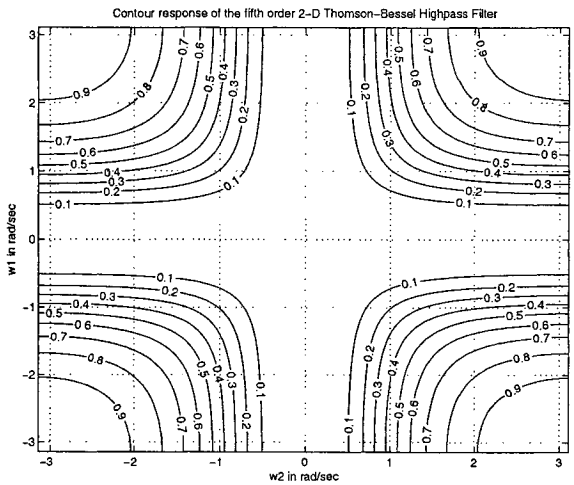

(b) When k1=k2=1, a1=a2=1 and b1=b2=-0.7

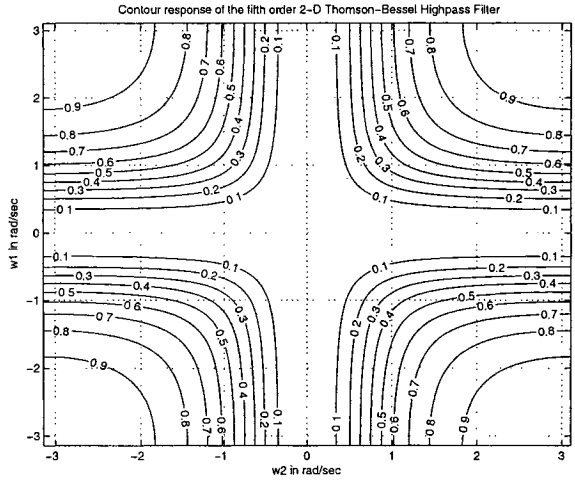

(c) When k1=k2=0.7, a1=a2=1 and b1=b2=-0.7

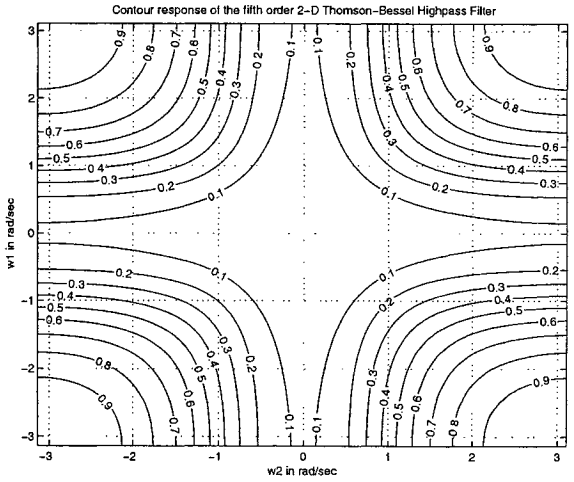

(d) When k1=k2=0.7, a1=a2=1 and b1=b2=-0.5

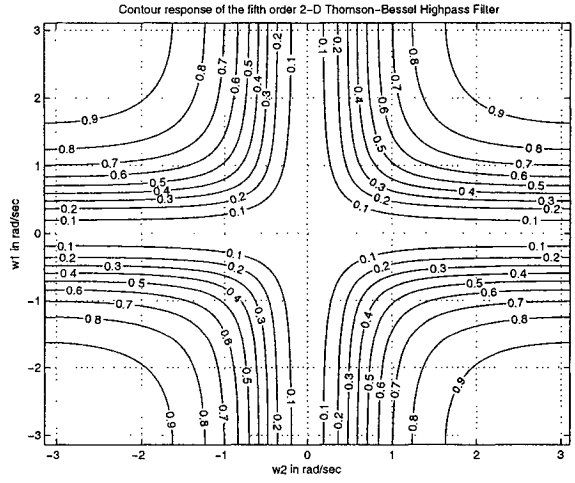

(e) When k1=k2=0.5, a1=a2=1 and b1=b2=-0.7

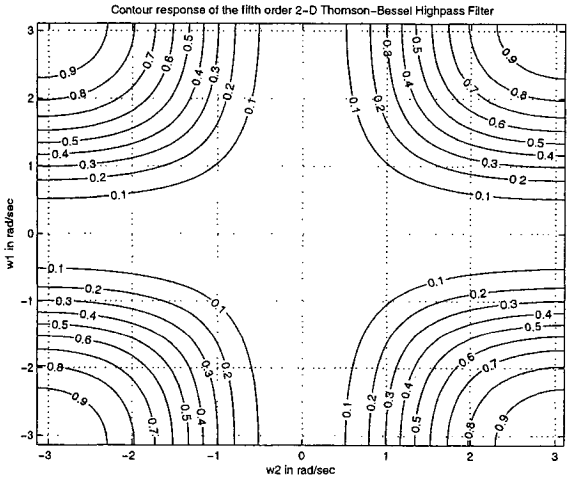

(f) When k1=k2=1, a1=a2=1 and b1=b2=-0.5

Figure 5.19: Contour response of the fifth order 2-D digital Thomson-Bessel highpass filter

5.3 Generation of 2-D digital bandpass filters with monotonic amplitude-frequency response

There are various ways to obtain bandpass filter from the lowpass filters. A common method is by using lowpass filter and highpass filter (obtained from the equivalent lowpass filter). By cascading 2-D digital highpass and lowpass filters in series, we can obtain bandpass filters, provided that the passband of both the filters overlap. In this section, we will propose some examples of implementation of 2-D digital Butterworth, Papoulis, Filanovsky and Thomson-Bessel bandpass filters, from their equivalent 2-D analog lowpass filters, having monotonic characteristics. We will implement fifth order 2-D digital Papoulis, Butterworth, Filanovsky and Thomson-Bessel bandpass filters by using the transfer functions of lowpass filters and highpass filters proposed in Chapter 3 and Sec. 5.2, respectively. Furthermore, we will also implement 2-D digital Butterworth bandpass filter by utilizing the lowpass and highpass filter transfer functions proposed in Chapter 4 and Sec. 5.2, respectively.

5.3.1 Generation of fifth order 2-D digital Papoulis bandpass filter with monotonic characteristics

The fifth order 2-D analog and digital Papoulis lowpass filter proposed in Chapter 3 are given by eqn. 3.4 and 3.6. By applying generalized bilinear transformation (eqn. 5.1) to eqn. 3.4, we got 2-D digital Papoulis lowpass filter in Sec. 5.2.1 (i.e. eqn. 5.2). By cascading the 2-D digital lowpass and highpass filters in series, we can get combinational 2-D digital Papoulis bandpass filter.

The 3-D amplitude-frequency response and contour plots of the fifth order 2-D digital Papoulis bandpass filter with monotonic amplitude-frequency response for different combination values of the coefficients of generalized bilinear transformation are shown in the fig. 5.20, 5.21 and 5.22. The MATLAB code to plot the 3-D amplitude-frequency response

and contour plots of the frequency response of the fifth order 2-D digital Papoulis bandpass filter is in algorithm 38.

From the simulation results we can see that the coefficients k_1, k_2, affects passband width and a_{1L}, a_{2L}, a_1, a_2, affects gain of the amplitude-frequency response in fig. 5.20 and 5.21, for $b_1 = b_2 = -1$. It may be noted that as the coefficients k_1, k_2, values are decreased, the passband width of the 2-D bandpass filter increases. In fig. 5.20 (c), (d) and fig. 5.21 (a), (b), (e) and (f), as k_1, k_2 are decreased from 0.7 to 0.2, for same values of $a_{1L} = a_{2L} = a_1 = a_2 = 0.9$ and $b_1 = b_2 = -1$, the passband width of 2-D bandpass filter increases. As the coefficients, a_{1L}, a_{2L}, a_1, a_2, values are decreased, the magnitude of the amplitude-frequency response of the 2-D bandpass filter decreases. In fig. 5.20 (c), (d) and fig. 5.21 (e), (f), as a_{1L}, a_{2L}, a_1, a_2, are decreased from 0.9 to 0.7, for same values of $k_1 = k_2 = 0.7$ and $b_1 = b_2 = -1$, the magnitude of the passband decreases. Similarly, in fig. 5.21 (a), (b) and fig. 5.21 (c), (d), as a_{1L}, a_{2L}, a_1, a_2 are decreased from 0.9 to 0.7, for same values of $k_1 = k_2 = 0.5$ and $b_1 = b_2 = -1$, the magnitude of the passband decreases. As b_1, b_2, are decreased to -0.7 in fig. 5.22 from -1 in fig. 5.20 and 5.21, the shape and polarity of the amplitude-frequency response changes. In all the cases discussed, the 2-D Papoulis bandpass filter inhibits monotonic amplitude-frequency response.

5.3.2 Generation of 2-D digital Butterworth bandpass filters with monotonic characteristics

In this section, we will generate 2-D digital Butterworth bandpass filters by utilizing, *(i)* the fifth order 2-D Butterworth lowpass and highpass filters proposed in Sec. 3.3.1.2 and Sec. 5.2.2.1, respectively, and *(ii)* second order 2-D Butterworth lowpass and highpass filters proposed in Sec. 4.6.2 and Sec. 5.2.2.2, respectively.

Algorithm 38 The MATLAB code to plot the 3-D amplitude-frequency response and contour response of the fifth order 2-D digital Papoulis bandpass filters having monotonic characteristics.

```
% % Under Guidance of Prof. Dr. V. Ramachandran
% Student's name : Ajit Singh Sandhu..... ID:4841492.
clc; clear all;
%----------Lowpass filter----------
k1=input('Give the value of the constant k1 for the bilinear LP transformation => ');
k2=input('Give the value of the constant k2 for the bilinear LP transformation => ');
a1L=input('Give the value of the constant a1L for the bilinear LP transformation => ');
a2L=input('Give the value of the constant a2L for the bilinear LP transformation => ');
% Creates two dimensional square matrix (mesh grid) of angular frequency w1 and w2.
[w1,w2] = meshgrid(-pi:0.05:pi,-pi:0.05:pi);
% Apply Z1=r1*exp(jw1) and Z2=r2*exp(jw2) with r1 = r2 =1
z1=exp(j.*w1); z2=exp(j.*w2);
% h1 is the required digital transfer function and its value is evaluated as follows.
a=z1-a1L; b=z2-a2L; c=z1+1; d=z2+1;
h1_1=(((k1.^2).*(a.^2))+(k1.*0.7762.*a.*c)+(0.4971.*(c.^2))).*(((k1.^2).*(a.^2))
+(k1.*0.3072.*a.*c)+(0.9608.*(c.^2))).*(a+(0.4681.*c));
h1_2=(((k2.^2).*(b.^2))+(k2.*0.7762.*b.*d)+(0.4971.*(d.^2))).*(((k2.^2).*(b.^2))
+(k2.*0.3072.*b.*d)+(0.9608.*(d.^2))).*(b+(0.4681.*d));
h_lpf=((c.^5).*(d.^5).*(0.2235.^2))./(h1_1.*h1_2); h1=abs(h_lpf);
% ---------- High Pass filter----------
k1=input('Give the value of the constant k1 for the bilinear LP transformation => ');
k2=input('Give the value of the constant k2 for the bilinear LP transformation => ');
a1=input('Give the value of the constant a1 for the bilinear LP transformation => ');
a2=input('Give the value of the constant a2 for the bilinear LP transformation => ');
b1=input('Give the value of the constant b1 for the bilinear LP transformation => ');
b2=input('Give the value of the constant b2 for the bilinear LP transformation => ');
% hh1 is the required digital transfer function and its value is evaluated as follows.
a=z1+a1; b=z2+a2; c=z1+b1; d=z2+b2;
hh1_1=(((k1.^2).*(a.^2))+(k1.*0.7762.*a.*c)+(0.4971.*(c.^2))).*(((k1.^2).*(a.^2))
+(k1.*0.3072.*a.*c)+(0.9608.*(c.^2))).*(a+(0.4681.*c));
hh1_2=(((k2.^2).*(b.^2))+(k2.*0.7762.*b.*d)+(0.4971.*(d.^2))).*(((k2.^2).*(b.^2))
+(k2.*0.3072.*b.*d)+(0.9608.*(d.^2))).*(b+(0.4681.*d));
h_hpf=((c.^5).*(d.^5).*(0.2235.^2))./(hh1_1.*hh1_2); hh1=abs(h_hpf);
% ---------- Bandpass filter----------
% hb is the required digital transfer function and its value is evaluated as follows.
h_bpf=h_lpf.*h_hpf; hb=abs(h_bpf);
figure(1);
contour3(w1,w2,hb);
surface(w1,w2,abs(hb),'EdgeColor',[.8 .8 .8],'FaceColor','none');
grid on; view(-15,25);
title('3-D amplitude-frequency response of the fifth order 2-D Papoulis Bandpass Filter');
xlabel(' w2 in rad/sec '); ylabel(' w1 in rad/sec ');
zlabel(' Magnitude Response ');
figure(2);
contour(w1,w2,hb);
grid on;
title('Contour response of the fifth order 2-D Papoulis Bandpass Filter');
xlabel(' w2 in rad/sec '); ylabel(' w1 in rad/sec ');
```

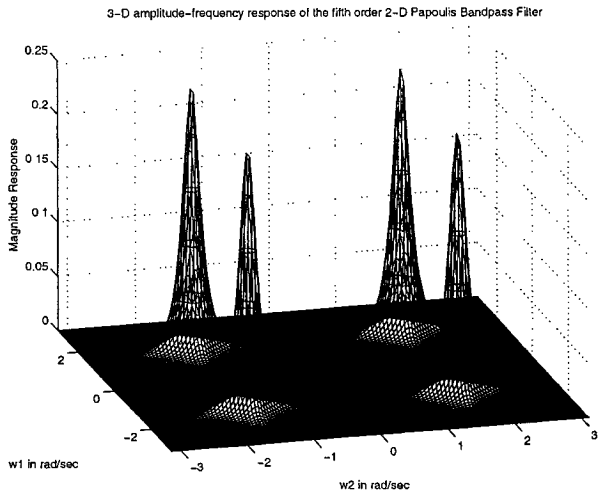

(a) k1=k2=1, a1L=a2L=a1=a2=1 and b1=b2=-1

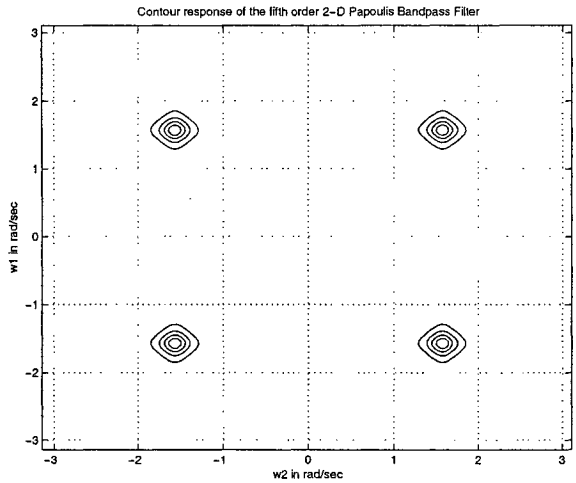

(b) k1=k2=1, a1L=a2L=a1=a2=1 and b1=b2=-1

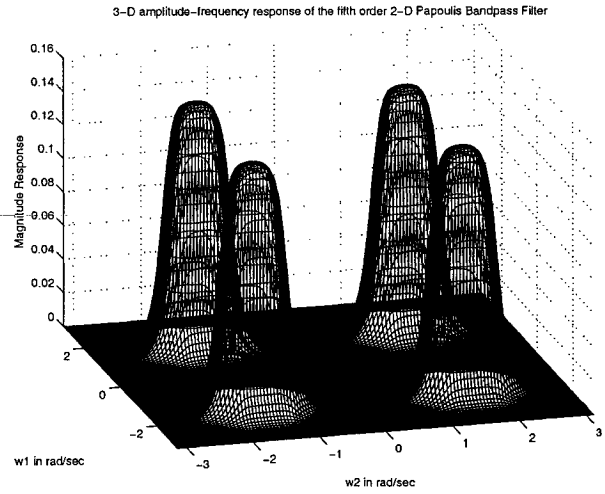

(c) k1=k2=0.7, a1L=a2L=a1=a2=0.9 and b1=b2=-1

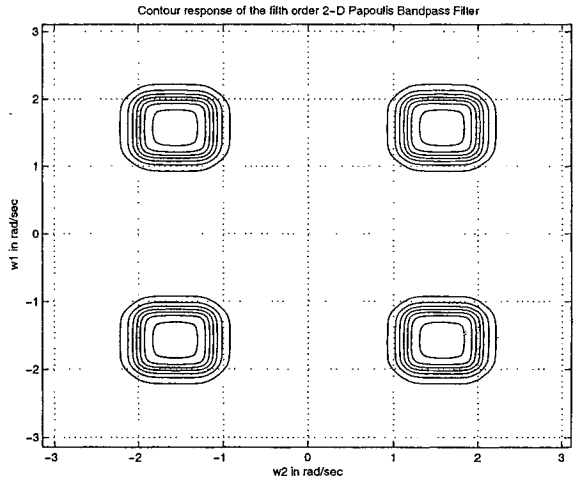

(d) k1=k2=0.7, a1L=a2L=a1=a2=0.9 and b1=b2=-1

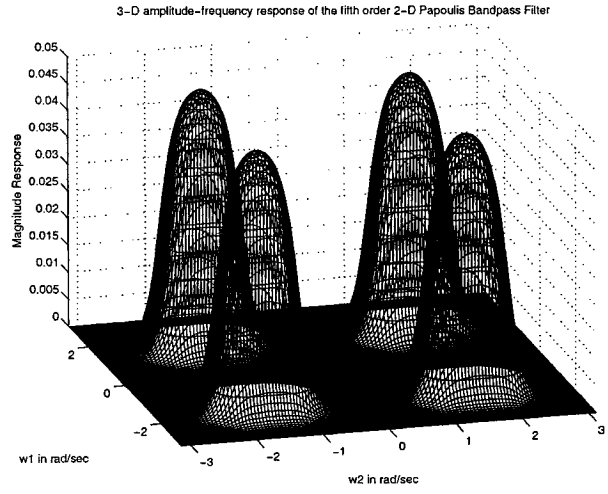

(e) k1=k2=0.7, a1L=a2L=a1=a2=0.7 and b1=b2=-1

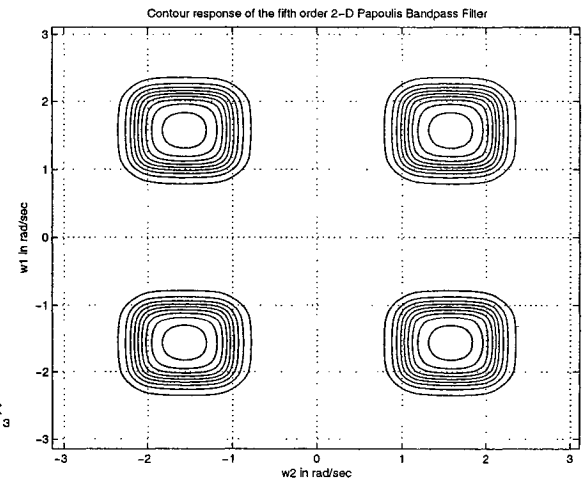

(f) k1=k2=0.7, a1L=a2L=a1=a2=0.7 and b1=b2=-1

Figure 5.20: 3-D amplitude-frequency and contour response of the fifth order 2-D digital Papoulis bandpass filter

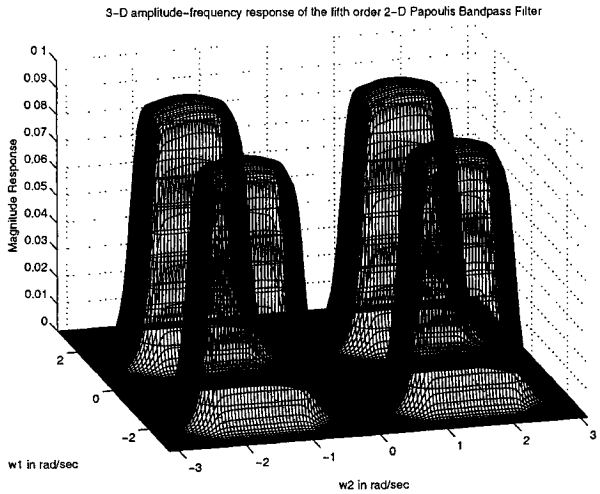

(a) k1=k2=0.5, a1L=a2L=a1=a2=0.9 and b1=b2=-1

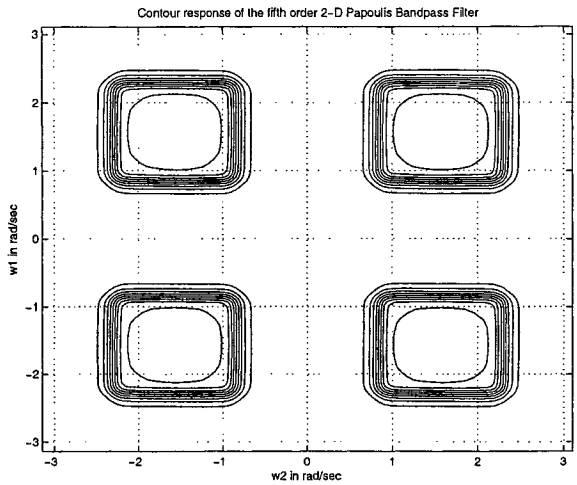

(b) k1=k2=0.5, a1L=a2L=a1=a2=0.9 and b1=b2=-1

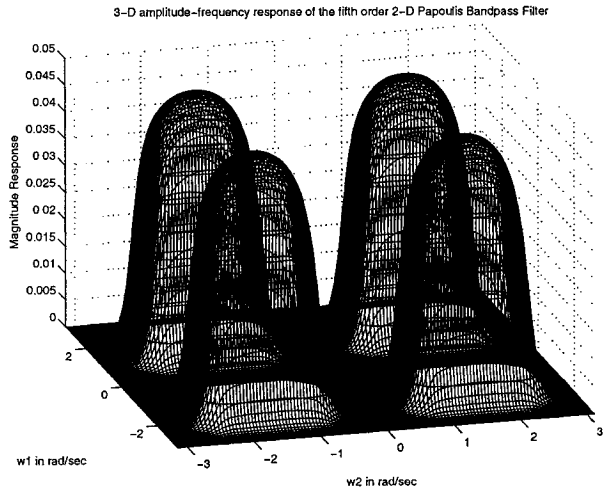

(c) k1=k2=0.5, a1L=a2L=a1=a2=0.7 and b1=b2=-1

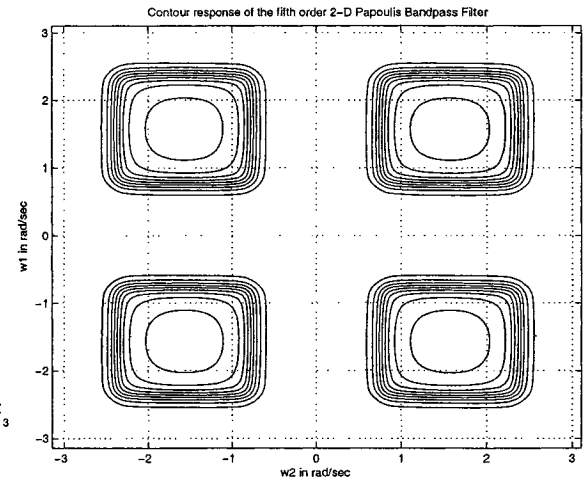

(d) k1=k2=0.5, a1L=a2L=a1=a2=0.7 and b1=b2=-1

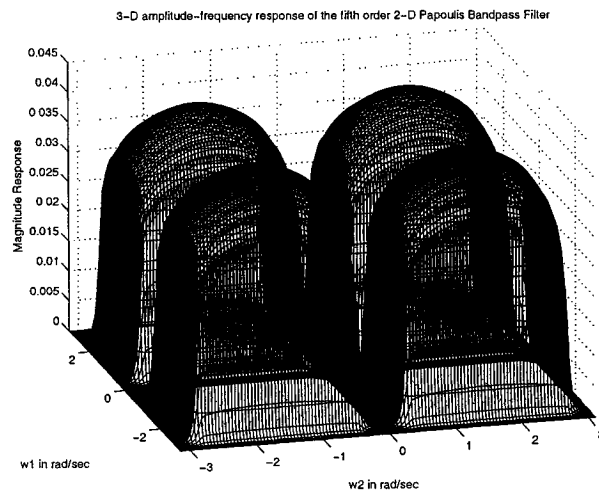

(e) k1=k2=0.2, a1L=a2L=a1=a2=0.9 and b1=b2=-1

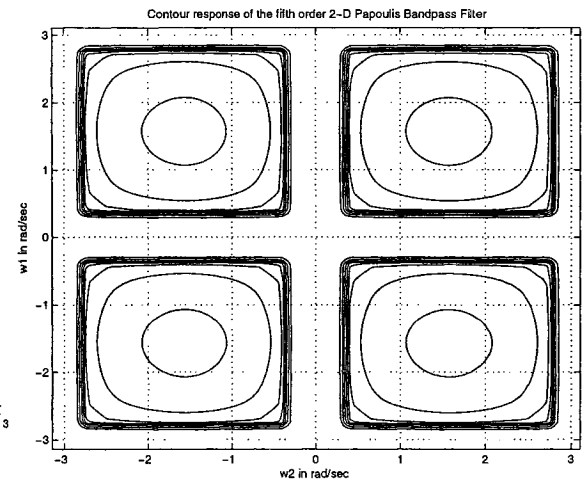

(f) k1=k2=0.2, a1L=a2L=a1=a2=0.9 and b1=b2=-1

Figure 5.21: 3-D amplitude-frequency and contour response of the fifth order 2-D digital Papoulis bandpass filter

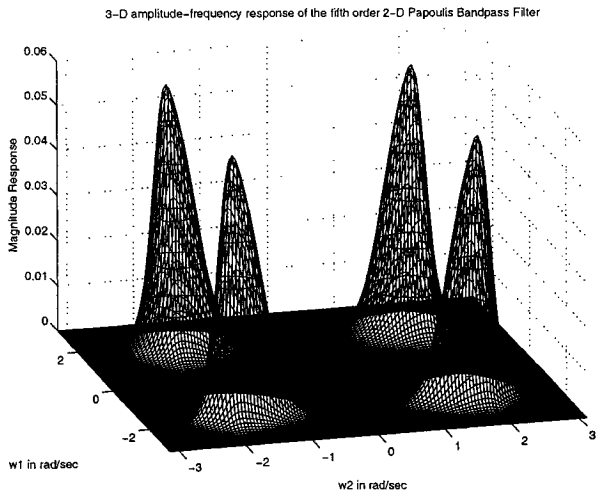

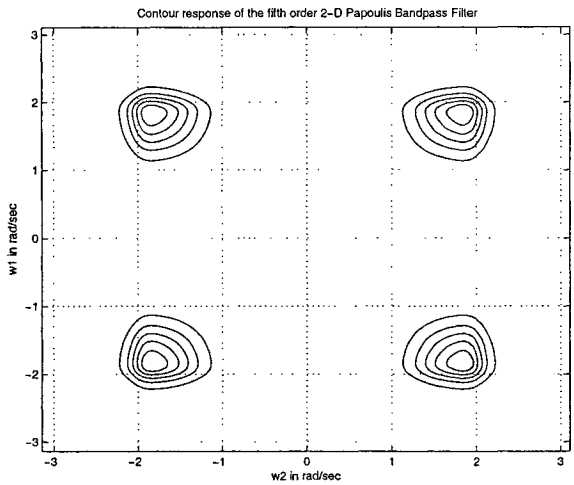

(a) k1=k2=0.7, a1L=a2L=a1=a2=0.9 and b1=b2=-0.7 (b) k1=k2=0.7, a1L=a2L=a1=a2=0.9 and b1=b2=-0.7

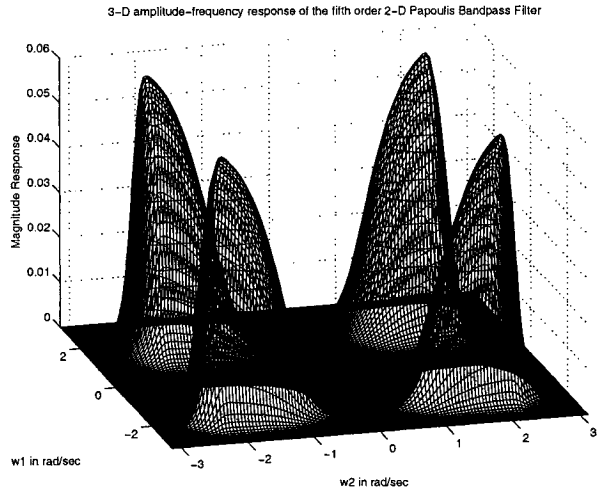

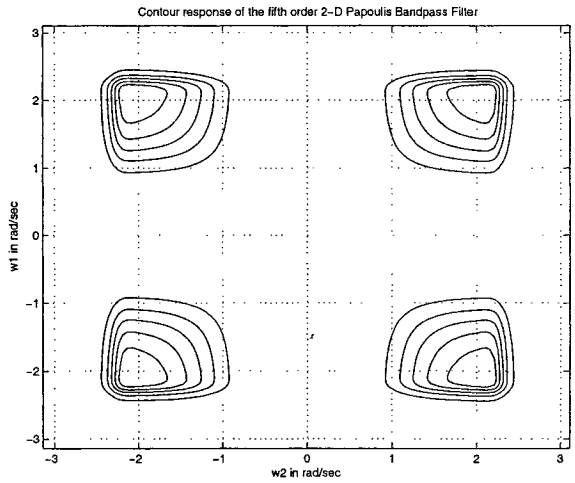

(c) k1=k2=0.5, a1L=a2L=a1=a2=0.9 and b1=b2=-0.7 (d) k1=k2=0.5, a1L=a2L=a1=a2=0.9 and b1=b2=-0.7

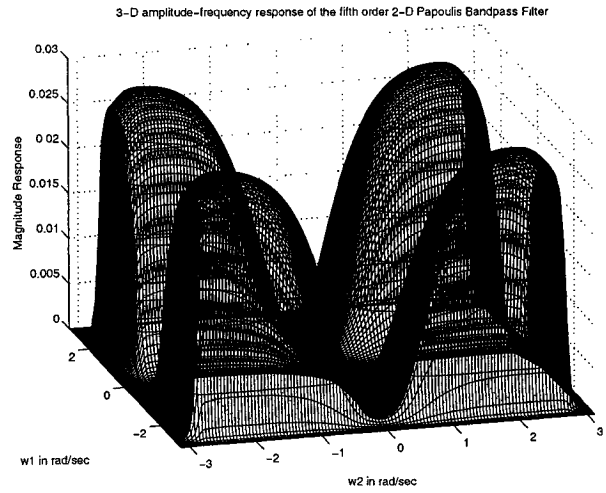

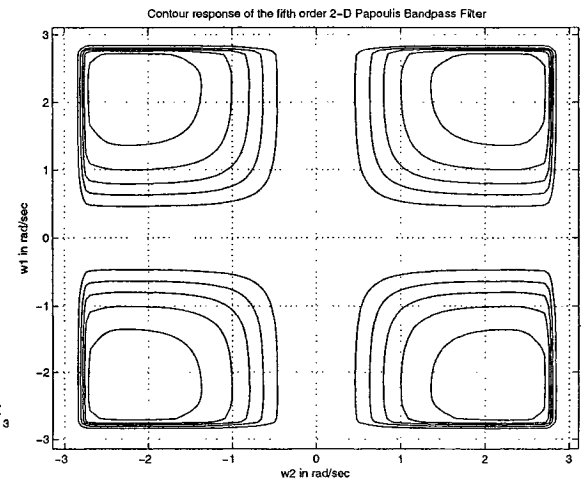

(e) k1=k2=0.2, a1L=a2L=a1=a2=0.9 and b1=b2=-0.7 (f) k1=k2=0.2, a1L=a2L=a1=a2=0.9 and b1=b2=-0.7

Figure 5.22: 3-D amplitude-frequency and contour response of the fifth order 2-D digital Papoulis bandpass filter

5.3.2.1 Generation of fifth order 2-D digital Butterworth bandpass filters with monotonic characteristics

The fifth order 2-D analog and digital Butterworth lowpass filter proposed in Chapter 3 are given by eqn. 3.8 and 3.10. By applying generalized bilinear transformation (eqn. 5.1) to eqn. 3.8, we got 2-D digital Butterworth highpass filter in Sec. 5.2.2.1 (i.e. eqn. 5.3). By cascading the 2-D digital lowpass and highpass filters in series, we can get combinational 2-D digital Butterworth bandpass filter.

The 3-D amplitude-frequency response and contour plots of the fifth order 2-D digital Butterworth bandpass filter for different combination values of the coefficients of generalized bilinear transformation are shown in the fig. 5.23, 5.24 and 5.25. The MATLAB code to plot the 3-D amplitude-frequency response and contour plots of the frequency response of the fifth order 2-D digital Butterworth bandpass filter is in algorithm 39.

From the simulation results we can see that the coefficients k_1, k_2, affects passband width and a_{1L}, a_{2L}, a_1, a_2, affects gain of the amplitude-frequency response in fig. 5.23 and 5.24, for $b_1 = b_2 = -1$. It may be noted that as the coefficients k_1, k_2, values are decreased, the passband width of the 2-D bandpass filter increases. In fig. 5.23 (c), (d) and fig. 5.24 (a), (b), (e) and (f), as k_1, k_2 are decreased from 0.7 to 0.2, for same values of $a_{1L} = a_{2L} = a_1 = a_2 = 0.9$ and $b_1 = b_2 = -1$, the passband width of the 2-D bandpass filter increases. As the coefficients, a_{1L}, a_{2L}, a_1, a_2, values are decreased, the magnitude of the amplitude-frequency response of the 2-D bandpass filter decreases. In fig. 5.23 (c), (d) and fig. 5.23 (e), (f), as a_{1L}, a_{2L}, a_1, a_2, are decreased from 0.9 to 0.7, for same values of $k_1 = k_2 = 0.7$ and $b_1 = b_2 = -1$, the magnitude of the passband decreases. Similarly, in fig. 5.24 (a), (b) and fig. 5.24 (c), (d), as a_{1L}, a_{2L}, a_1, a_2 are decreased from 0.9 to 0.7, for same values of $k_1 = k_2 = 0.5$ and $b_1 = b_2 = -1$, the magnitude of the passband decreases. As b_1, b_2, are decreased to -0.7 in fig. 5.25 from -1 in fig. 5.23 and 5.24, the shape and polarity of the amplitude-frequency response changes. In all the cases discussed, the fifth order 2-D Butterworth bandpass filter inhibits monotonic amplitude-frequency response.

Algorithm 39 The MATLAB code to plot the 3-D amplitude-frequency response and contour response of the fifth order 2-D digital Butterworth bandpass filters having monotonic characteristics.

```
% Under Guidance of Prof. Dr. V. Ramachandran
% Student's name : Ajit Singh Sandhu..... ID:4841492.
clc; clear all;
% ————Lowpass Filter————
k1=input('Give the value of the constant k1 for the bilinear LP transformation => ');
k2=input('Give the value of the constant k2 for the bilinear LP transformation => ');
a1L=input('Give the value of the constant a1L for the bilinear LP transformation => ');
a2L=input('Give the value of the constant a2L for the bilinear LP transformation => ');
% Creates two dimensional square matrix (mesh grid) of angular frequency w1 and w2.
[w1,w2] = meshgrid(-pi:0.05:pi,-pi:0.05:pi);
% Apply Z1=r1*exp(jw1) and Z2=r2*exp(jw2) with r1 = r2 =1
z1=exp(j.*w1); z2=exp(j.*w2);
% h1 is the required digital transfer function and its value is evaluated as follows.
a=z1-a1L; b=z2-a2L; c=z1+1; d=z2+1;
h1_1=(((k1.^2).*(a.^2))+(k1.*1.618.*a.*c)+(c.^2)).*(((k1.^2).*(a.^2))+(k1.*0.618.*a.*c)+(c.^2)).*(a+c);
h1_2=(((k2.^2).*(b.^2))+(k2.*1.618.*b.*d)+(d.^2)).*(((k2.^2).*(b.^2))+(k2.*0.618.*b.*d)+(d.^2)).*(b+d);
h_lpf=((c.^5).*(d.^5))./(h1_1.*h1_2);
h1=abs(h_lpf);
%————————Highpass filter————————
k1=input('Give the value of the constant k1 for the bilinear LP transformation => ');
k2=input('Give the value of the constant k2 for the bilinear LP transformation => ');
a1=input('Give the value of the constant a1 for the bilinear LP transformation => ');
a2=input('Give the value of the constant a2 for the bilinear LP transformation => ');
b1=input('Give the value of the constant b1 for the bilinear LP transformation => ');
b2=input('Give the value of the constant b2 for the bilinear LP transformation => ');
% hh1 is the required digital transfer function and its value is evaluated as follows.
a=z1+a1; b=z2+a2; c=z1+b1; d=z2+b2;
hh1_1=(((k1.^2).*(a.^2))+(k1.*1.618.*a.*c)+(c.^2)).*(((k1.^2).*(a.^2))+(k1.*0.618.*a.*c)+(c.^2)).*(a+c);
hh1_2=(((k2.^2).*(b.^2))+(k2.*1.618.*b.*d)+(d.^2)).*(((k2.^2).*(b.^2))+(k2.*0.618.*b.*d)+(d.^2)).*(b+d);
h_hpf=((c.^5).*(d.^5))./(hh1_1.*hh1_2); hh1=abs(h_hpf);
%————————Bandpass filter————————
h_bpf=h_lpf.*h_hpf; hb=abs(h_bpf);
figure(1);
contour3(w1,w2,hb);
surface(w1,w2,abs(hb),'EdgeColor',[.8 .8 .8],'FaceColor','none');
grid on; view(-15,25);
title('3-D amplitude-frequency response of the fifth order 2-D digital Butterworth Bandpass Filter');
xlabel(' w2 in rad/sec '); ylabel(' w1 in rad/sec ');
zlabel(' Magnitude Response ');
figure(2);
contour(w1,w2,hb); grid on;
title('Contour response of the fifth order 2-D digital Butterworth Bandpass Filter');
xlabel(' w2 in rad/sec '); ylabel(' w1 in rad/sec ');
```

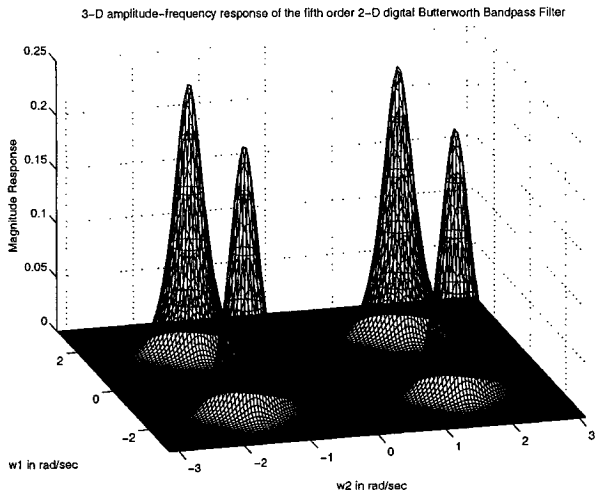

(a) k1=k2=1, a1L=a2L=a1=a2=1 and b1=b2=-1

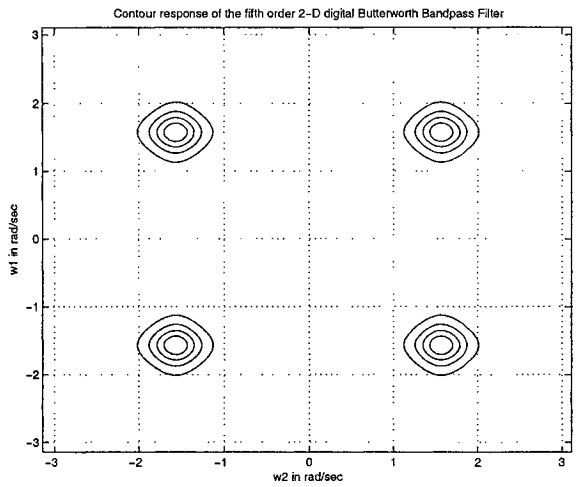

(b) k1=k2=1, a1L=a2L=a1=a2=1 and b1=b2=-1

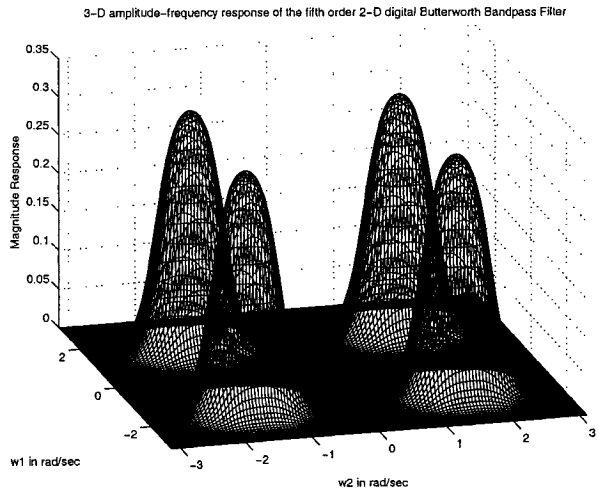

(c) k1=k2=0.7, a1L=a2L=a1=a2=0.9 and b1=b2=-1

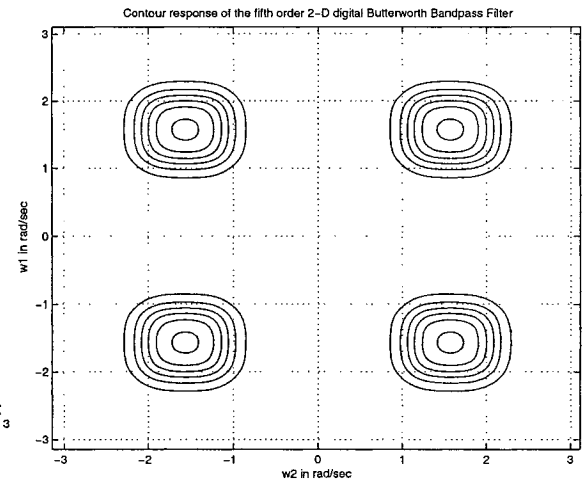

(d) k1=k2=0.7, a1L=a2L=a1=a2=0.9 and b1=b2=-1

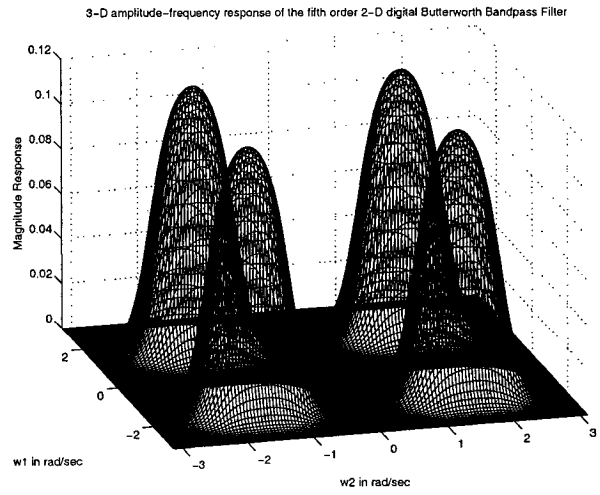

(e) k1=k2=0.7, a1L=a2L=a1=a2=0.7 and b1=b2=-1

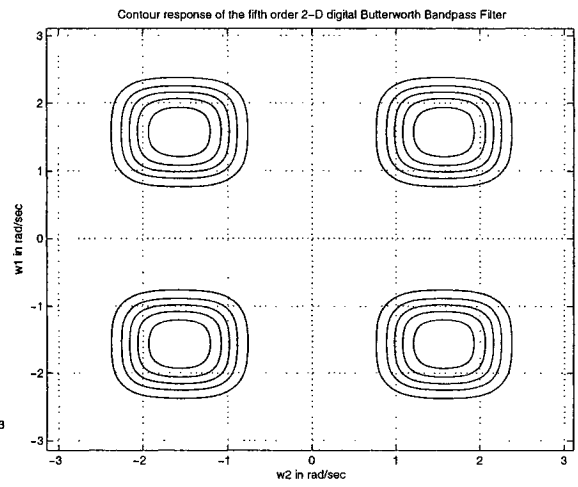

(f) k1=k2=0.7, a1L=a2L=a1=a2=0.7 and b1=b2=-1

Figure 5.23: 3-D amplitude-frequency and contour response of the fifth order 2-D digital Butterworth bandpass filter

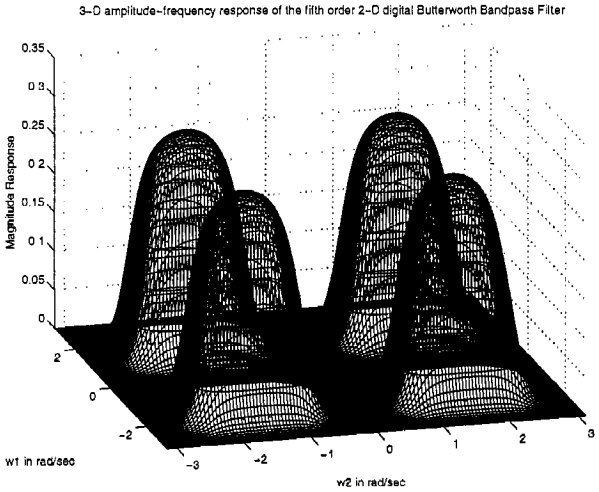

(a) k1=k2=0.5, a1L=a2L=a1=a2=0.9 and b1=b2=-1

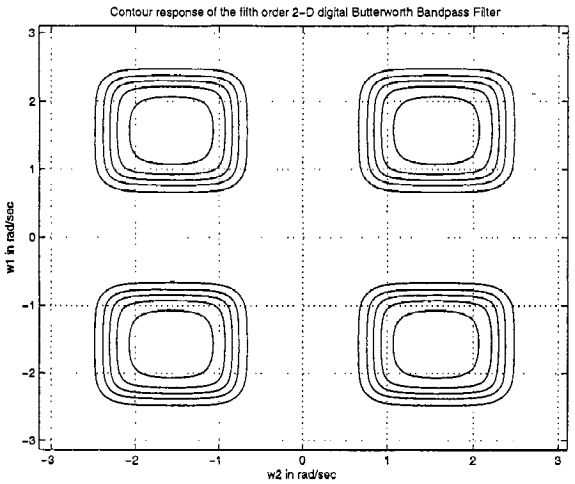

(b) k1=k2=0.5, a1L=a2L=a1=a2=0.9 and b1=b2=-1

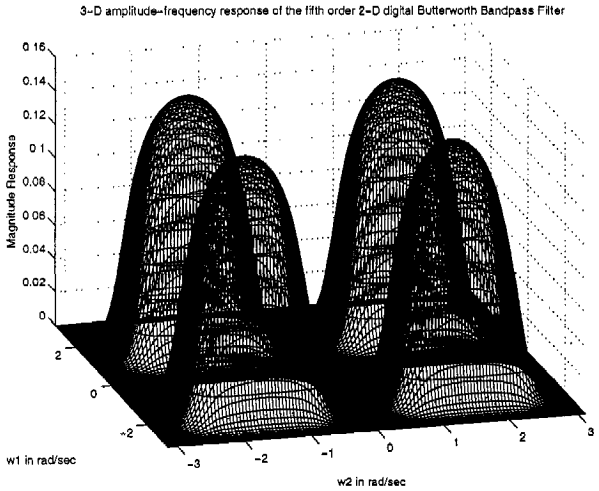

(c) k1=k2=0.5, a1L=a2L=a1=a2=0.7 and b1=b2=-1

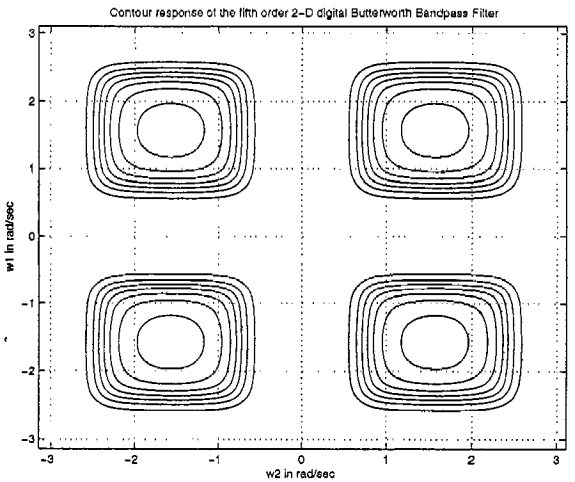

(d) k1=k2=0.5, a1L=a2L=a1=a2=0.7 and b1=b2=-1

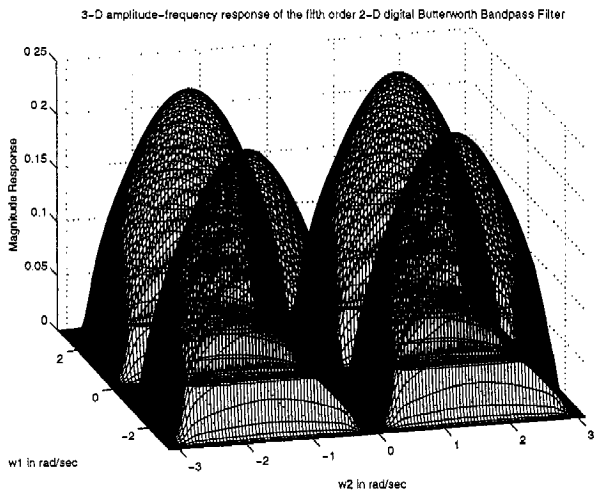

(e) k1=k2=0.2, a1L=a2L=a1=a2=0.9 and b1=b2=-1

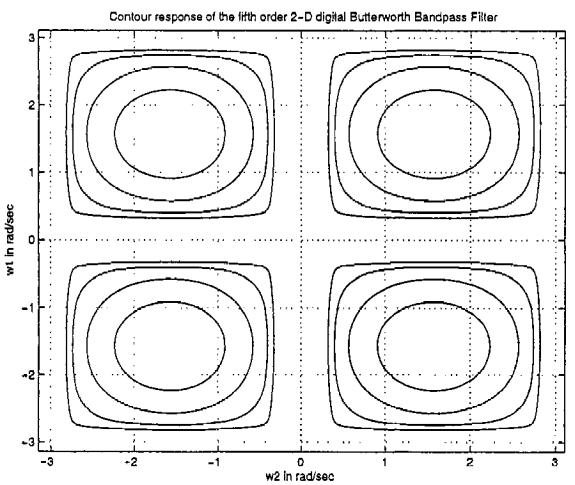

(f) k1=k2=0.2, a1L=a2L=a1=a2=0.9 and b1=b2=-1

Figure 5.24: 3-D amplitude-frequency and contour response of the fifth order 2-D digital Butterworth bandpass filter

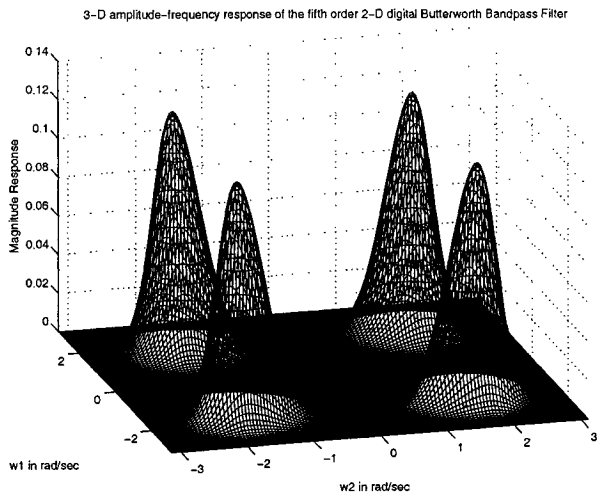

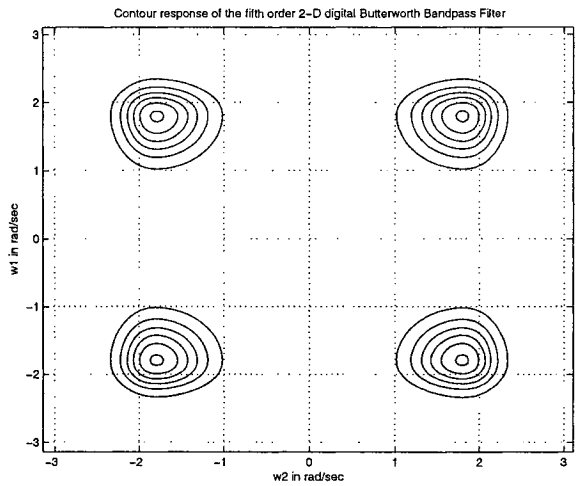

(a) k1=k2=0.7, a1L=a2L=a1=a2=0.9 and b1=b2=-0.7 (b) k1=k2=0.7, a1L=a2L=a1=a2=0.9 and b1=b2=-0.7

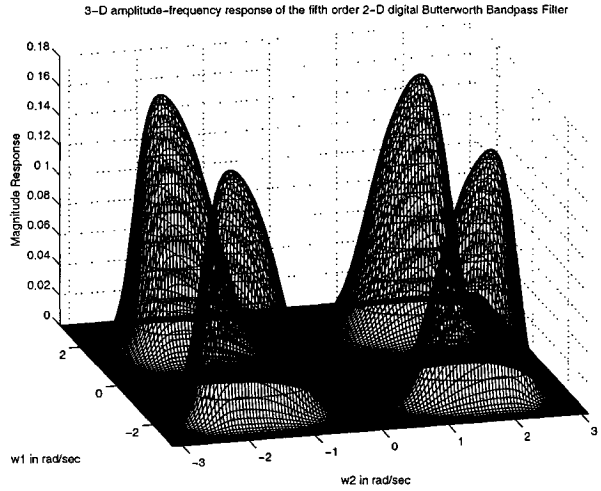

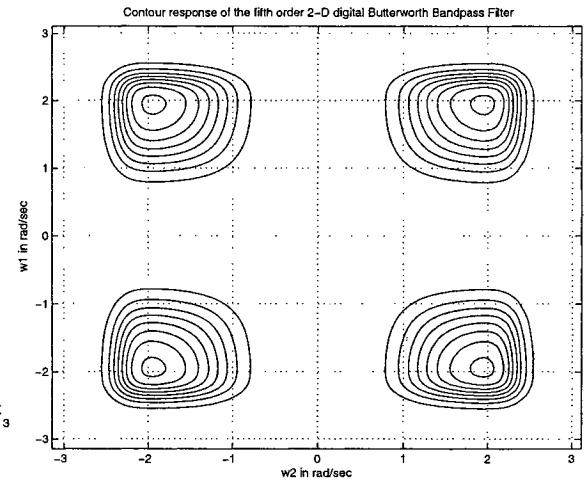

(c) k1=k2=0.5, a1L=a2L=a1=a2=0.9 and b1=b2=-0.7 (d) k1=k2=0.5, a1L=a2L=a1=a2=0.9 and b1=b2=-0.7

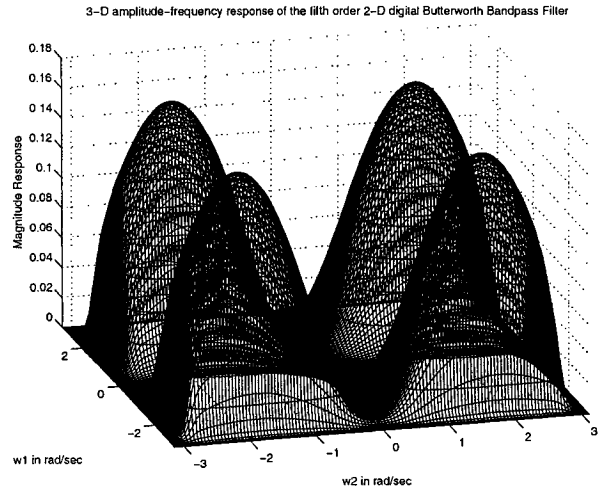

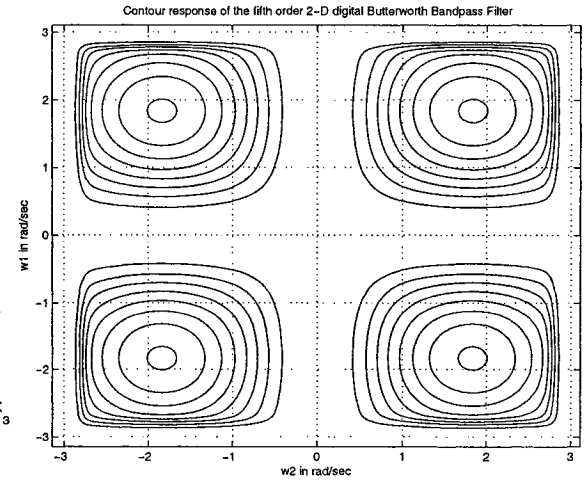

(e) k1=k2=0.2, a1L=a2L=a1=a2=0.9 and b1=b2=-0.7 (f) k1=k2=0.2, a1L=a2L=a1=a2=0.9 and b1=b2=-0.7

Figure 5.25: 3-D amplitude-frequency and contour response of the fifth order 2-D digital Butterworth bandpass filter

5.3.2.2 Generation of second order 2-D digital Butterworth bandpass filters with monotonic characteristics

The second order 2-D analog and digital Butterworth lowpass filter proposed in Chapter 4 are given by eqn. 4.14 and 4.15. By applying generalized bilinear transformation (eqn. 5.1) to eqn. 4.14, we got 2-D digital Butterworth highpass filter in Sec. 5.2.2.2 (i.e. eqn. 5.4). By cascading the 2-D digital lowpass and highpass filters in series, we can get combinational 2-D digital Butterworth bandpass filter.

The 3-D amplitude-frequency response and contour plots of the second order 2-D digital Butterworth bandpass filter for different combination values of the coefficients of generalized bilinear transformation are shown in the fig. 5.26, 5.27 and 5.28. The MATLAB code to plot the 3-D amplitude-frequency response and contour plots of the frequency response of the second order 2-D digital Butterworth bandpass filter is in algorithm 40.

From the simulation results we can see that the coefficients k_1, k_2, affects passband width and a_{1L}, a_{2L}, a_1, a_2, affects gain of the amplitude-frequency response in fig. 5.26 and 5.27, for $b_1 = b_2 = -1$. It may be noted that as the coefficients k_1, k_2, values are decreased, the passband width of the 2-D bandpass filter increases. In fig. 5.26 (c), (d) and fig. 5.27 (a) and (b), as k_1, k_2 are decreased from 0.7 to 0.5, for same values of $a_{1L} = a_{2L} = a_1 = a_2 = 0.9$ and $b_1 = b_2 = -1$, the passband width of the 2-D bandpass filter increases. As the coefficients, a_{1L}, a_{2L}, a_1, a_2, values are decreased, the magnitude of the amplitude-frequency response of the 2-D bandpass filter decreases. In fig. 5.26 (c), (d) and fig. 5.26 (e), (f), as a_{1L}, a_{2L}, a_1, a_2, are decreased from 0.9 to 0.7, for same values of $k_1 = k_2 = 0.7$ and $b_1 = b_2 = -1$, the magnitude of the passband decreases. Similarly, in fig. 5.27 (a), (b) and fig. 5.27 (c), (d), as a_{1L}, a_{2L}, a_1, a_2 are decreased from 0.9 to 0.7, for same values of $k_1 = k_2 = 0.5$ and $b_1 = b_2 = -1$, the magnitude of the passband decreases. As b_1, b_2, are decreased to -0.7 in fig. 5.28 from -1 in fig. 5.26 and 5.27, the shape and polarity of the amplitude-frequency response changes. In all the cases discussed, the second order 2-D Butterworth bandpass filter inhibits monotonic amplitude-

frequency response. We can see two pair of lobes with different magnitude in the frequency response, because of unequal overlapping of second order 2-D digital Butterworth lowpass and highpass filters.

5.3.3 Generation of fifth order 2-D digital Filanovsky bandpass filter with monotonic characteristics

The fifth order 2-D analog and digital Filanovsky lowpass filter proposed in Chapter 3 are given by eqn. 3.11 and 3.12. By applying generalized bilinear transformation (eqn. 5.1) to eqn. 3.11, we got 2-D digital Filanovsky highpass filter in Sec. 5.2.3 (i.e. eqn. 5.5). By cascading the 2-D digital lowpass and highpass filters in series, we can get combinational 2-D digital Filanovsky bandpass filter.

The 3-D amplitude-frequency response and contour plots of the fifth order 2-D digital Filanovsky bandpass filter for different combination values of the coefficients of generalized bilinear transformation are shown in the fig. 5.29, 5.30 and 5.31. The MATLAB code to plot the 3-D amplitude-frequency response and contour plots of the frequency response of the fifth order 2-D digital Filanovsky bandpass filter is in algorithm 41.

From the simulation results we can see that the coefficients k_1, k_2, affects passband width and a_{1L}, a_{2L}, a_1, a_2, affects gain of the amplitude-frequency response in fig. 5.29 and 5.30, for $b_1 = b_2 = -1$. It may be noted that as the coefficients k_1, k_2, values are decreased, the passband width of the 2-D bandpass filter increases. In fig. 5.29 (c), (d) and fig. 5.30 (a), (b), (e) and (f), as k_1, k_2 are decreased from 0.7 to 0.2, for same values of $a_{1L} = a_{2L} = a_1 = a_2 = 0.9$ and $b_1 = b_2 = -1$, the passband width of the 2-D bandpass filter increases. As the coefficients, a_{1L}, a_{2L}, a_1, a_2, values are decreased, the magnitude of the amplitude-frequency response of the 2-D bandpass filter decreases. In fig. 5.29 (c), (d) and fig. 5.29 (e), (f), as a_{1L}, a_{2L}, a_1, a_2, are decreased from 0.9 to 0.7, for same values of $k_1 = k_2 = 0.7$ and $b_1 = b_2 = -1$, the magnitude of the passband decreases. Similarly, in fig. 5.30 (a), (b) and fig. 5.30 (c), (d), as a_{1L}, a_{2L}, a_1, a_2 are decreased from 0.9 to 0.7, for

Algorithm 40 The MATLAB code to plot the 3-D amplitude-frequency response and contour response of the second order 2-D digital Butterworth bandpass filters having monotonic characteristics.

```
% Under Guidance of Prof. Dr. V. Ramachandran
% Student's name : Ajit Singh Sandhu..... ID:4841492.
clear all; clc;
a11=1; a10=1/sqrt(2); a01=1/sqrt(2); a00=1;
b11=1; b10=1/sqrt(2); b01=1/sqrt(2); b00=1;
%-----------Lowpass Filter-----------
% Input the values of the constants in the LP bilinear transformation.
k1=input('Give the value of the constant k1 for the bilinear LP transformation => ');
k2=input('Give the value of the constant k2 for the bilinear LP transformation => ');
a1L=input('Give the value of the constant a1L for the bilinear LP transformation => ');
a2L=input('Give the value of the constant a2L for the bilinear LP transformation => ');
% Create two dimensional square matrix (mesh grid) of angular frequency w1 and w2.
[w1,w2] = meshgrid(-pi:0.05:pi,-pi:0.05:pi);
% Apply Z1=r1*exp(jw1) and Z2=r2*exp(jw2) with r1 = r2 =1
z1=exp(j.*w1); z2=exp(j.*w2);
% hd is the required digital transfer function and its value is evaluated as follows.....
a=z1-a1L; b=z2-a2L; c=z1+1; d=z2+1;
hd1=((a11.*k1.*k2.*a.*b)+(a10.*k1.*a.*d)+(a01.*k2.*b.*c)
+(a00.*c.*d)).*((b11.*k1.*k2.*a.*b)+(b10.*k1.*a.*d)+(b01.*k2.*b.*c)+(b00.*c.*d));
hd2=((a10.*k1.*a.*d)+(a01.*k2.*b.*c)).*((b10.*k1.*a.*d)+(b01.*k2.*b.*c));
h_lpf=((c.^2).*(d.^2).*(a00.*b00))./(hd1+hd2);
hd=abs(h_lpf);
%-----------Highpass Filter-----------
k1=input('Give the value of the constant k1 for the bilinear LP transformation => ');
k2=input('Give the value of the constant k2 for the bilinear LP transformation => ');
a1=input('Give the value of the constant a1 for the bilinear LP transformation => ');
a2=input('Give the value of the constant a2 for the bilinear LP transformation => ');
b1=input('Give the value of the constant b1 for the bilinear LP transformation => ');
b2=input('Give the value of the constant b2 for the bilinear LP transformation => ');
% hhd is the required digital transfer function and its value is evaluated as follows.
a=z1+a1; b=z2+a2; c=z1+b1; d=z2+b2;
hhd1=((a11.*k1.*k2.*a.*b)+(a10.*k1.*a.*d)+(a01.*k2.*b.*c)
+(a00.*c.*d)).*((b11.*k1.*k2.*a.*b)+(b10.*k1.*a.*d)+(b01.*k2.*b.*c)+(b00.*c.*d));
hhd2=((a10.*k1.*a.*d)+(a01.*k2.*b.*c)).*((b10.*k1.*a.*d)+(b01.*k2.*b.*c));
h_hpf=((c.^2).*(d.^2).*(a00.*b00))./(hhd1+hhd2); hhd=abs(h_hpf);
%-----------Bandpass Filter-----------
h_bpf=h_lpf.*h_hpf; hb=abs(h_bpf);
figure(1);
contour3(w1,w2,hb);
surface(w1,w2,abs(hb),'EdgeColor',[.8 .8 .8],'FaceColor','none');
grid on; view(-15,25);
title('3-D amplitude-frequency response of the 2-D digital Butterworth Bandpass filter');
xlabel(' w2 in rad/sec '); ylabel(' w1 in rad/sec ');
zlabel(' Magnitude Response ');
figure(6);
contour(w1,w2,hb);
grid on;
title('Contour response of the 2-D digital Butterworth Bandpass filter');
xlabel(' w2 in rad/sec '); ylabel(' w1 in rad/sec ');
```

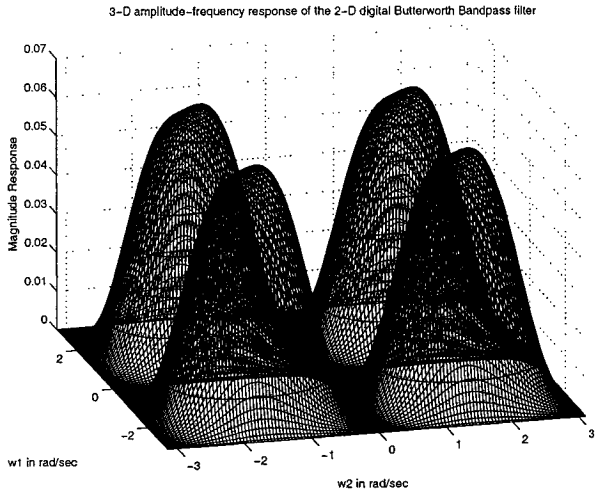

(a) k1=k2=1, a1L=a2L=a1=a2=1 and b1=b2=-1

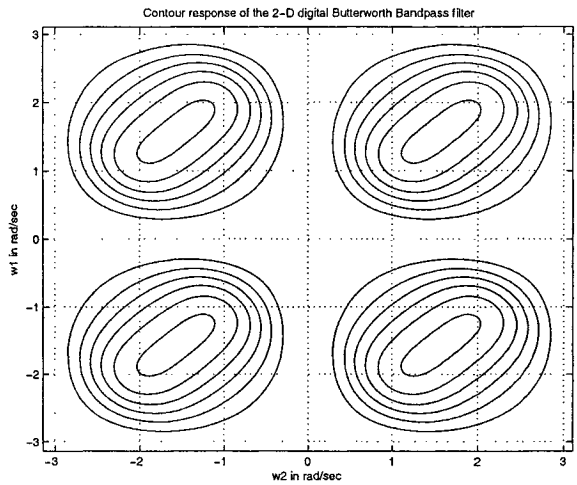

(b) k1=k2=1, a1L=a2L=a1=a2=1 and b1=b2=-1

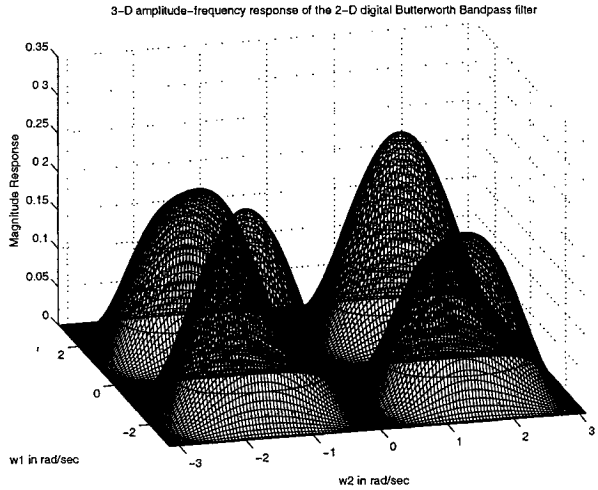

(c) k1=k2=0.7, a1L=a2L=a1=a2=0.9 and b1=b2=-1

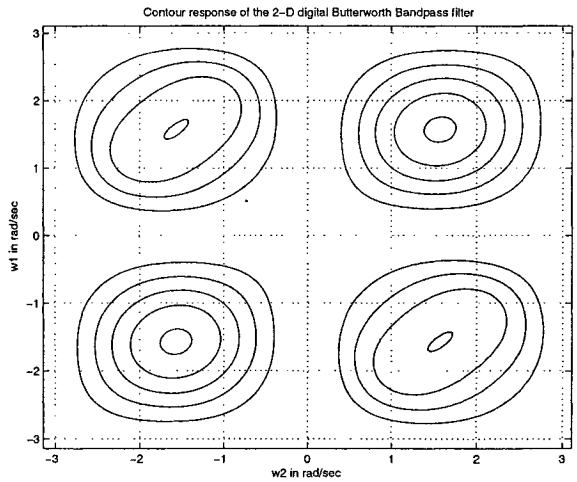

(d) k1=k2=0.7, a1L=a2L=a1=a2=0.9 and b1=b2=-1

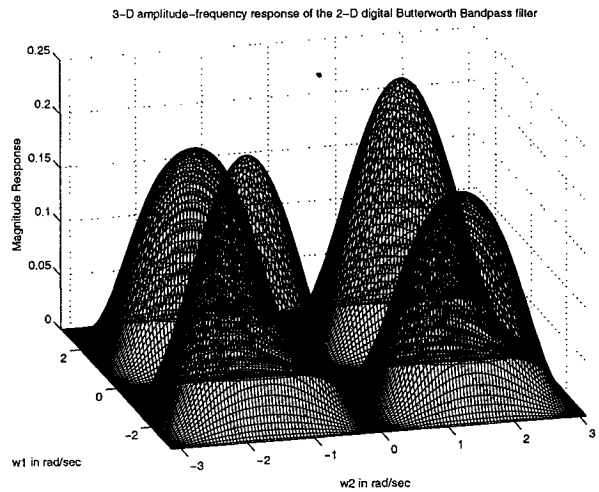

(e) k1=k2=0.7, a1L=a2L=a1=a2=0.7 and b1=b2=-1

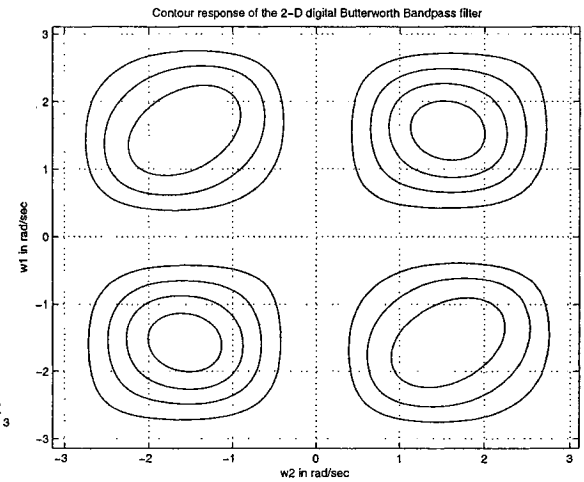

(f) k1=k2=0.7, a1L=a2L=a1=a2=0.7 and b1=b2=-1

Figure 5.26: 3-D amplitude-frequency and contour response of the second order 2-D digital Butterworth bandpass filter

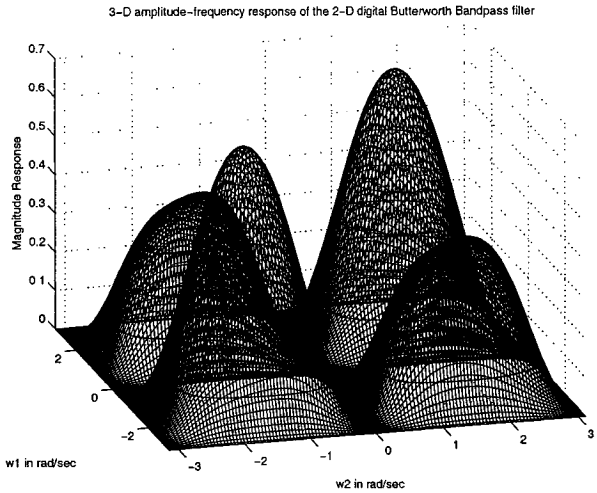

(a) k1=k2=0.5, a1L=a2L=a1=a2=0.9 and b1=b2=-1

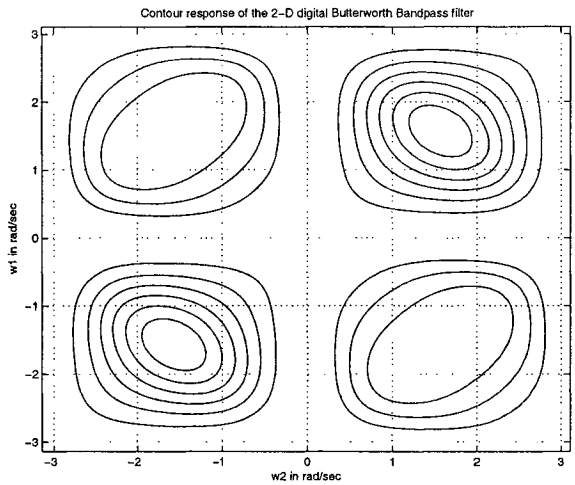

(b) k1=k2=0.5, a1L=a2L=a1=a2=0.9 and b1=b2=-1

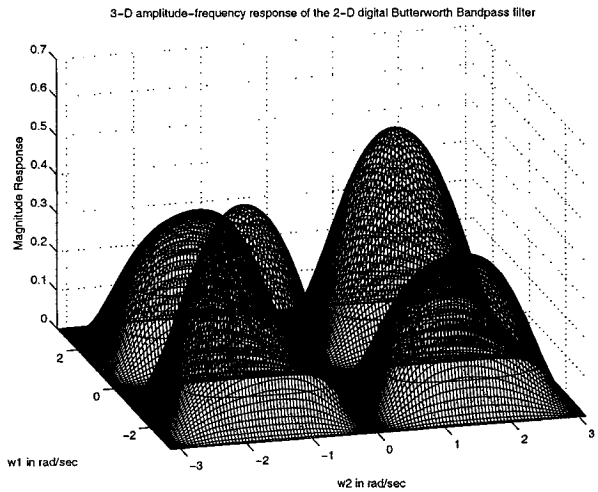

(c) k1=k2=0.5, a1L=a2L=a1=a2=0.7 and b1=b2=-1

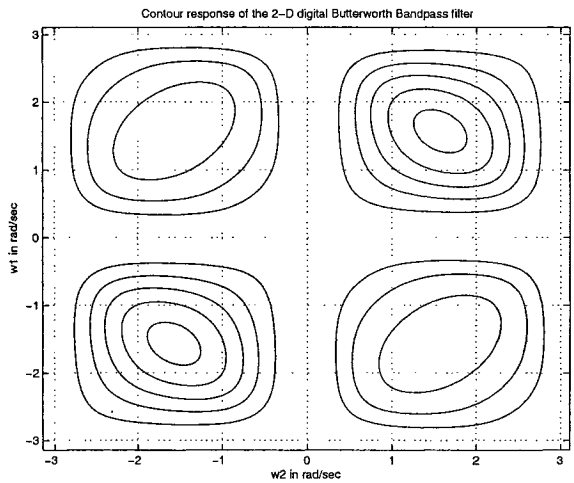

(d) k1=k2=0.5, a1L=a2L=a1=a2=0.7 and b1=b2=-1

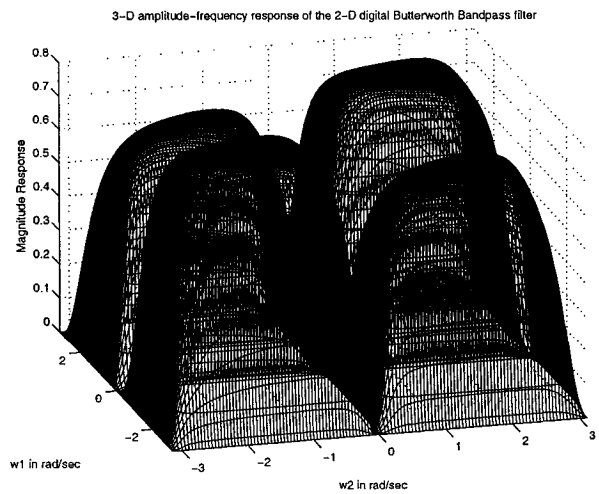

(e) k1=k2=0.2, a1L=a2L=a1=a2=0.5 and b1=b2=-1

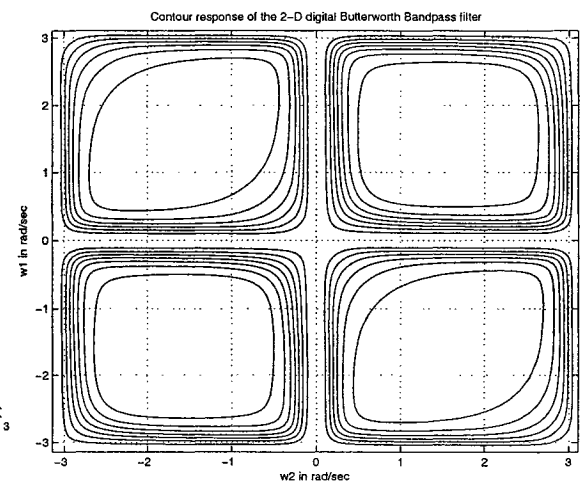

(f) k1=k2=0.2, a1L=a2L=a1=a2=0.5 and b1=b2=-1

Figure 5.27: 3-D amplitude-frequency and contour response of the second order 2-D digital Butterworth bandpass filter

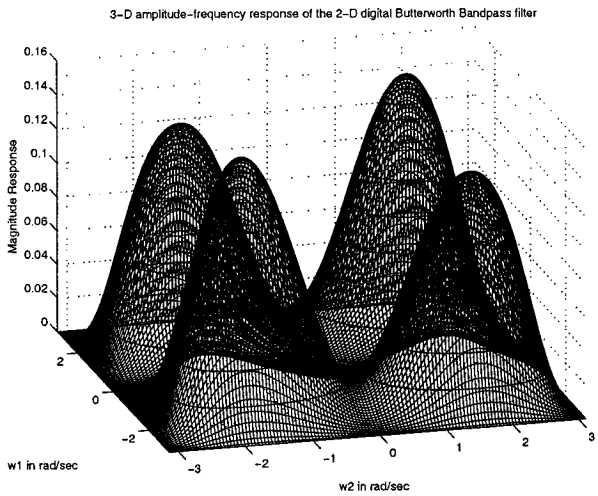

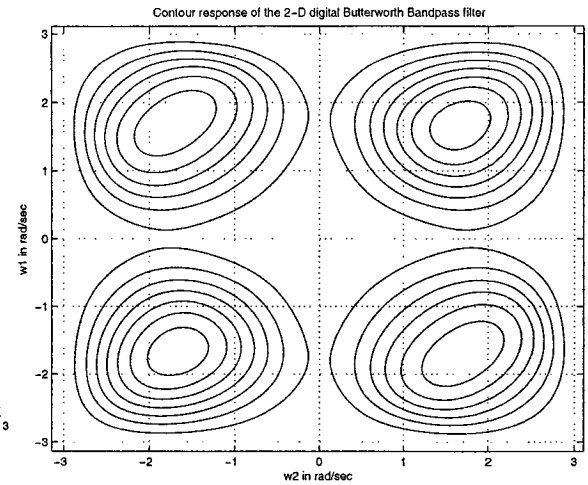

(a) k1=k2=0.7, a1L=a2L=a1=a2=0.9 and b1=b2=-0.7 (b) k1=k2=0.7, a1L=a2L=a1=a2=0.9 and b1=b2=-0.7

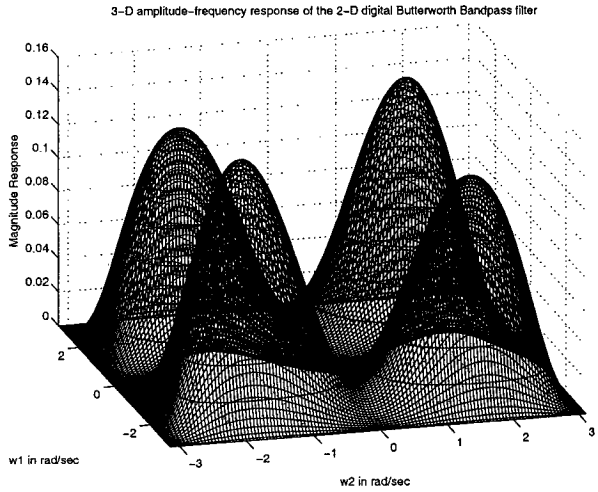

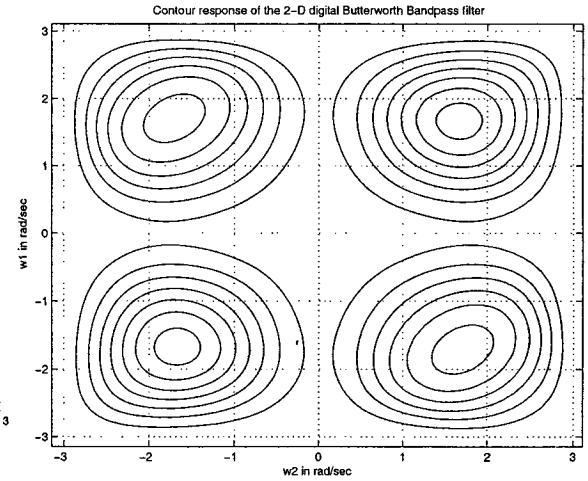

(c) k1=k2=0.7, a1L=a2L=a1=a2=0.7 and b1=b2=-0.7 (d) k1=k2=0.7, a1L=a2L=a1=a2=0.7 and b1=b2=-0.7

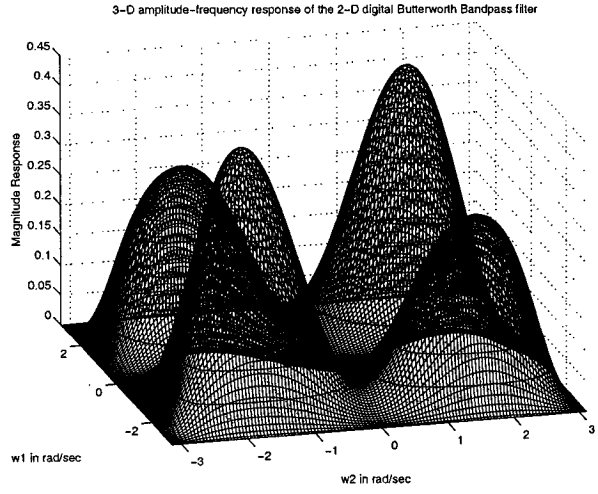

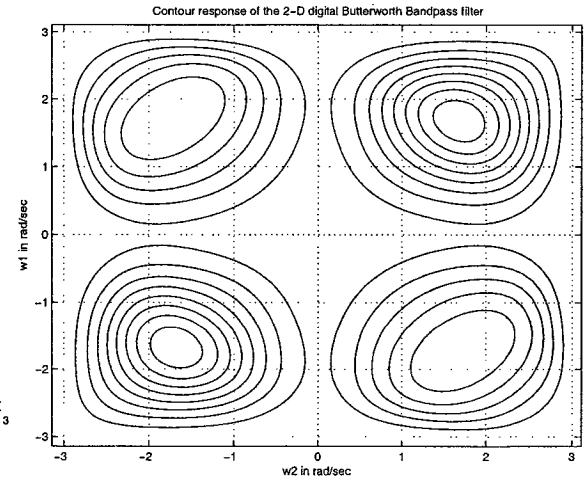

(e) k1=k2=0.5, a1L=a2L=a1=a2=0.9 and b1=b2=-0.7 (f) k1=k2=0.5, a1L=a2L=a1=a2=0.9 and b1=b2=-0.7

Figure 5.28: 3-D amplitude-frequency and contour response of the second order 2-D digital Butterworth bandpass filter

same values of $k_1 = k_2 = 0.5$ and $b_1 = b_2 = -1$, the magnitude of the passband decreases. As b_1, b_2, are decreased to -0.7 in fig. 5.31 from -1 in fig. 5.29 and 5.30, the shape and polarity of the amplitude-frequency response changes. In all the cases discussed, the fifth order 2-D Filanovsky bandpass filter inhibits monotonic amplitude-frequency response.

5.3.4 Generation of fifth order 2-D digital Thomson-Bessel bandpass filter with monotonic characteristics

The fifth order 2-D analog and digital Thomson-Bessel lowpass filter proposed in Chapter 3 are given by eqn. 3.14 and 3.16. By applying generalized bilinear transformation (eqn. 5.1) to eqn. 3.14, we got 2-D digital Thomson-Bessel highpass filter in Sec. 5.2.4 (i.e. eqn. 5.6). By cascading the 2-D digital lowpass and highpass filters in series, we can get combinational 2-D digital Thomson-Bessel bandpass filter.

The 3-D amplitude-frequency response and contour plots of the fifth order 2-D digital Thomson-Bessel bandpass filter for different combination values of the coefficients of generalized bilinear transformation are shown in the fig. 5.32, 5.33 and 5.34. The MATLAB code to plot the 3-D amplitude-frequency response and contour plots of the frequency response of the fifth order 2-D digital Thomson-Bessel bandpass filter is in algorithm 42.

From the simulation results we can see that the coefficients k_1, k_2, affects passband width and a_{1L}, a_{2L}, a_1, a_2, affects gain of the amplitude-frequency response in fig. 5.32 and 5.33, for $b_1 = b_2 = -1$. It may be noted that as the coefficients k_1, k_2, values are decreased, the passband width of the 2-D bandpass filter increases. In fig. 5.32 (c), (d) and fig. 5.33 (a), (b), (e) and (f), as k_1, k_2 are decreased from 0.7 to 0.2, for same values of $a_{1L} = a_{2L} = a_1 = a_2 = 0.9$ and $b_1 = b_2 = -1$, the passband width of the 2-D bandpass filter increases. As the coefficients, a_{1L}, a_{2L}, a_1, a_2, values are decreased, the magnitude of the amplitude-frequency response of the 2-D bandpass filter decreases. In fig. 5.32 (c), (d) and fig. 5.32 (e), (f), as a_{1L}, a_{2L}, a_1, a_2, are decreased from 0.9 to 0.7, for same values of $k_1 = k_2 = 0.7$ and $b_1 = b_2 = -1$, the magnitude of the passband decreases. Similarly, in

Algorithm 41 The MATLAB code to plot the 3-D amplitude-frequency response and contour response of the fifth order 2-D digital Filanovsky bandpass filters having monotonic characteristics.

```
% Under Guidance of Prof. Dr. V. Ramachandran
% Student's name : Ajit Singh Sandhu..... ID:4841492.
clc; clear all;
%————Lowpass filter————
k1=input('Give the value of the constant k1 for the bilinear LP transformation => ');
k2=input('Give the value of the constant k2 for the bilinear LP transformation => ');
a1L=input('Give the value of the constant a1L for the bilinear LP transformation => ');
a2L=input('Give the value of the constant a2L for the bilinear LP transformation => ');
% Creates two dimensional square matrix (mesh grid) of angular frequency w1 and w2.
[w1,w2] = meshgrid(-pi:0.05:pi,-pi:0.05:pi);
% Apply Z1=r1*exp(jw1) and Z2=r2*exp(jw2) with r1 = r2 =1
z1=exp(j.*w1); z2=exp(j.*w2);
% h1 is the required digital transfer function and its value is evaluated as follows.
a=z1-a1L; b=z2-a2L; c=z1+1; d=z2+1;
h1_1=(((k1.^2).*(a.^2))+(k1.*0.9508.*a.*c)+(0.5116.*(c.^2))).*(((k1.^2).*(a.^2))
+(k1.*0.3492.*a.*c)+(0.9592.*(c.^2))).*(a+(0.6445.*c));
h1_2=(((k2.^2).*(b.^2))+(k2.*0.9508.*b.*d)+(0.5116.*(d.^2))).*(((k2.^2).*(b.^2))
+(k2.*0.3492.*b.*d)+(0.9592.*(d.^2))).*(b+(0.6445.*d));
h_lpf=((c.^5).*(d.^5).*(0.3162^2))./(h1_1.*h1_2); h1=abs(h_lpf);
%————————Highpass filter————————
k1=input('Give the value of the constant k1 for the bilinear LP transformation => ');
k2=input('Give the value of the constant k2 for the bilinear LP transformation => ');
a1=input('Give the value of the constant a1 for the bilinear LP transformation => ');
a2=input('Give the value of the constant a2 for the bilinear LP transformation => ');
b1=input('Give the value of the constant b1 for the bilinear LP transformation => ');
b2=input('Give the value of the constant b2 for the bilinear LP transformation => ');
% hh1 is the required digital transfer function and its value is evaluated as follows.
a=z1+a1; b=z2+a2; c=z1+b1; d=z2+b2;
hh1_1=(((k1.^2).*(a.^2))+(k1.*0.9508.*a.*c)+(0.5116.*(c.^2))).*(((k1.^2).*(a.^2))
+(k1.*0.3492.*a.*c)+(0.9592.*(c.^2))).*(a+(0.6445.*c));
hh1_2=(((k2.^2).*(b.^2))+(k2.*0.9508.*b.*d)+(0.5116.*(d.^2))).*(((k2.^2).*(b.^2))
+(k2.*0.3492.*b.*d)+(0.9592.*(d.^2))).*(b+(0.6445.*d));
h_hpf=((c.^5).*(d.^5).*(0.3162^2))./(hh1_1.*hh1_2); hh1=abs(h_hpf);
%————————Bandpass filter————————
h_bpf=h_lpf.*h_hpf; hb=abs(h_bpf);
figure(1);
contour3(w1,w2,hb);
surface(w1,w2,abs(hb),'EdgeColor',[.8 .8 .8],'FaceColor','none');
grid on; view(-15,25);
title('3-D amplitude-frequency response of the fifth order 2-D Filanovsky Bandpass Filter');
xlabel(' w2 in rad/sec '); ylabel(' w1 in rad/sec ');
zlabel(' Magnitude Response ');
figure(2);
contour(w1,w2,hb);
grid on;
title('Contour response of the fifth order 2-D Filanovsky Bandpass Filter');
xlabel(' w2 in rad/sec '); ylabel(' w1 in rad/sec ');
```

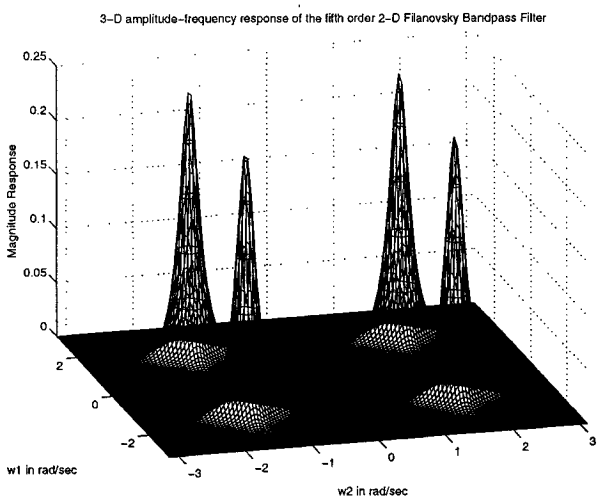

(a) k1=k2=1, a1L=a2L=a1=a2=1 and b1=b2=-1

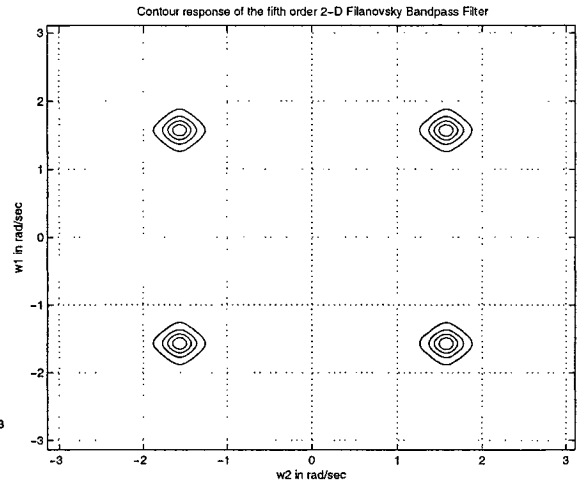

(b) k1=k2=1, a1L=a2L=a1=a2=1 and b1=b2=-1

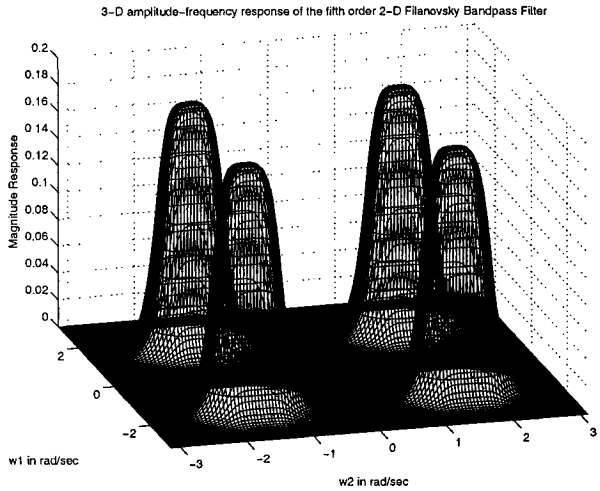

(c) k1=k2=0.7, a1L=a2L=a1=a2=0.9 and b1=b2=-1

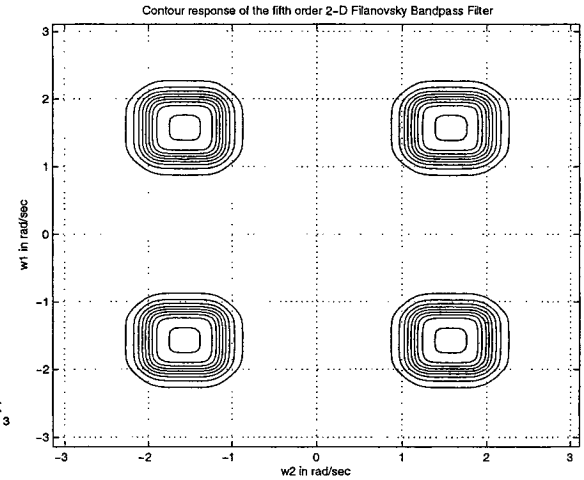

(d) k1=k2=0.7, a1L=a2L=a1=a2=0.9 and b1=b2=-1

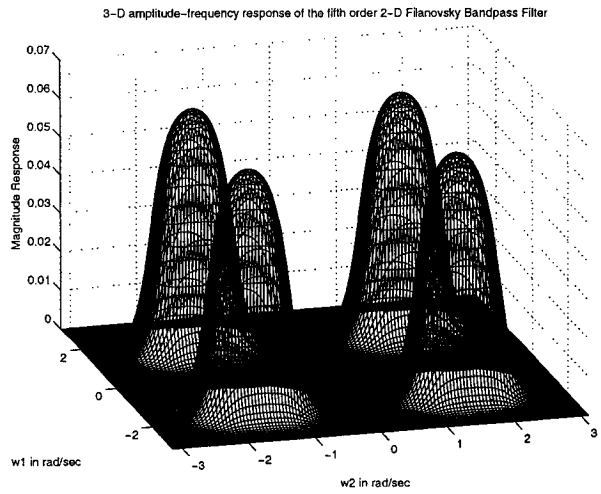

(e) k1=k2=0.7, a1L=a2L=a1=a2=0.7 and b1=b2=-1

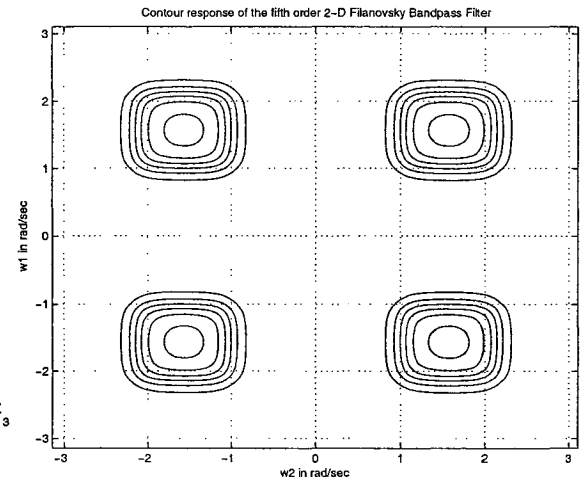

(f) k1=k2=0.7, a1L=a2L=a1=a2=0.7 and b1=b2=-1

Figure 5.29: 3-D amplitude-frequency and contour response of the fifth order 2-D digital Filanovsky bandpass filter

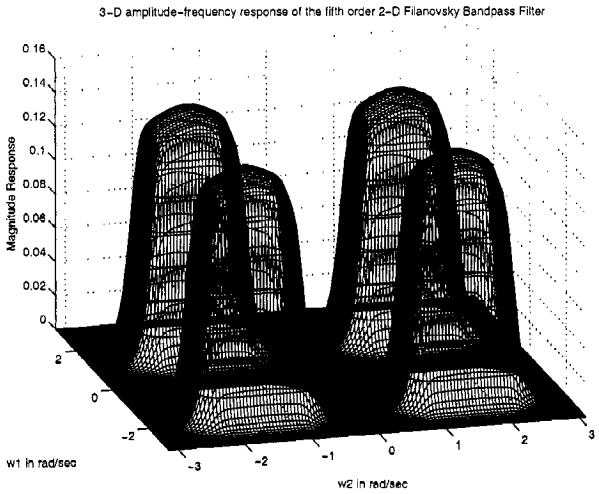

(a) k1=k2=0.5, a1L=a2L=a1=a2=0.9 and b1=b2=-1

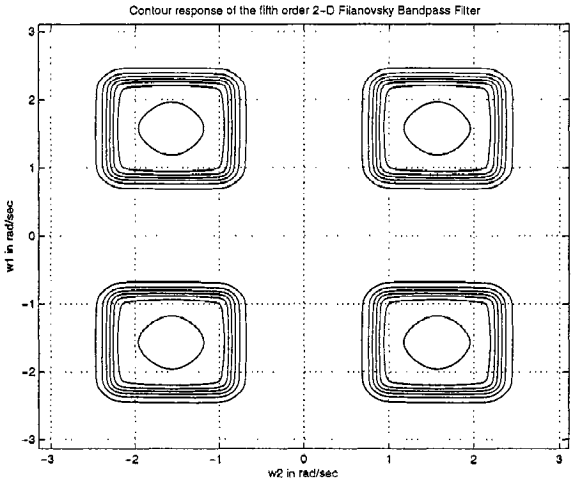

(b) k1=k2=0.5, a1L=a2L=a1=a2=0.9 and b1=b2=-1

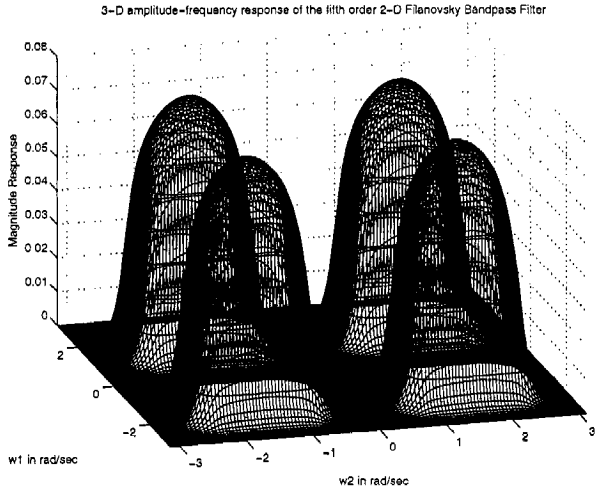

(c) k1=k2=0.5, a1L=a2L=a1=a2=0.7 and b1=b2=-1

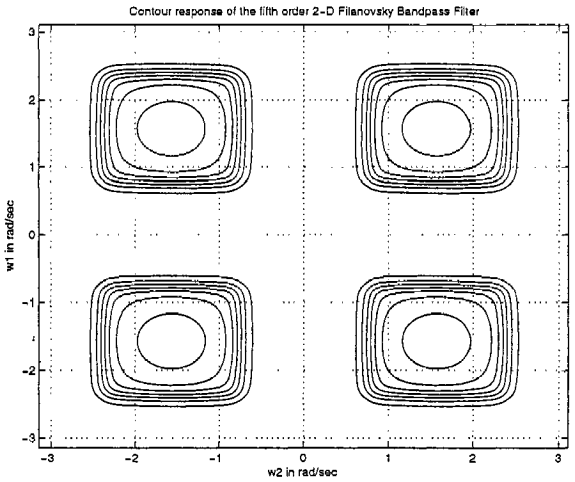

(d) k1=k2=0.5, a1L=a2L=a1=a2=0.7 and b1=b2=-1

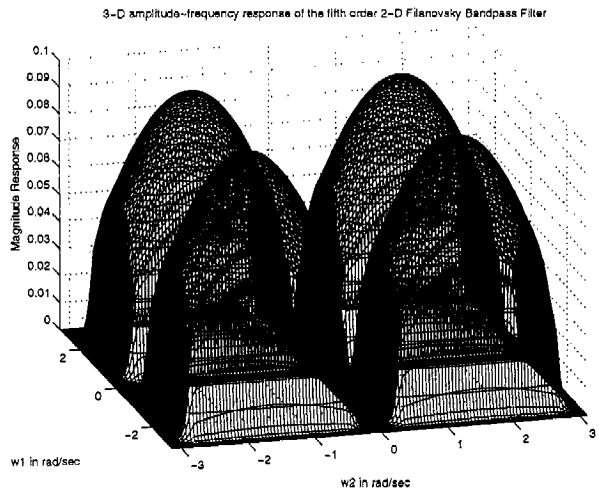

(e) k1=k2=0.2, a1L=a2L=a1=a2=0.9 and b1=b2=-1

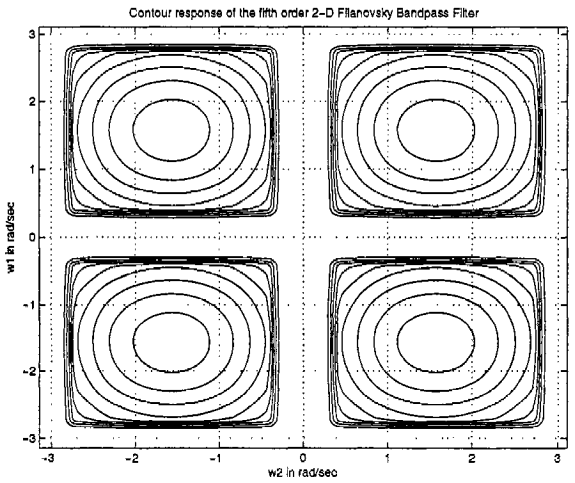

(f) k1=k2=0.2, a1L=a2L=a1=a2=0.9 and b1=b2=-1

Figure 5.30: 3-D amplitude-frequency and contour response of the fifth order 2-D digital Filanovsky bandpass filter

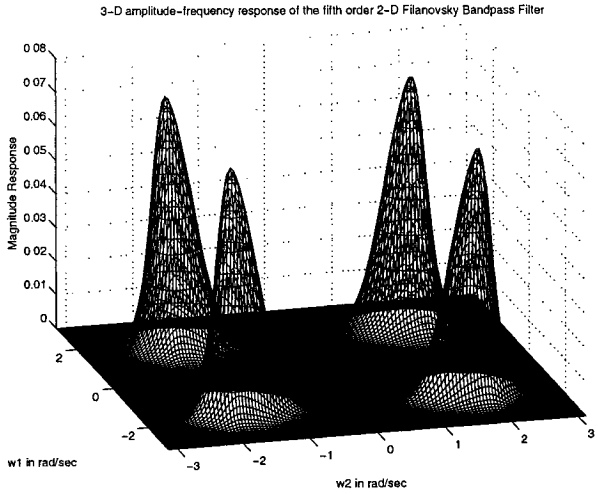

(a) k1=k2=0.7, a1L=a2L=a1=a2=0.9 and b1=b2=-0.7

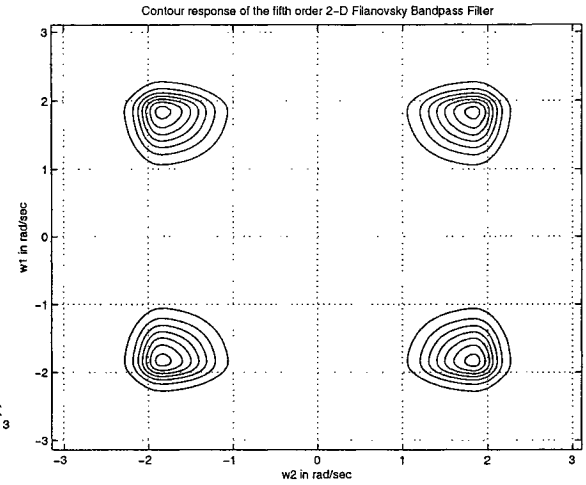

(b) k1=k2=0.7, a1L=a2L=a1=a2=0.9 and b1=b2=-0.7

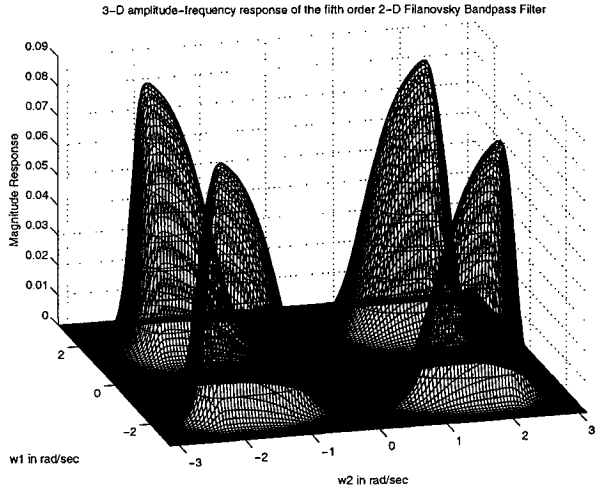

(c) k1=k2=0.5, a1L=a2L=a1=a2=0.9 and b1=b2=-0.7

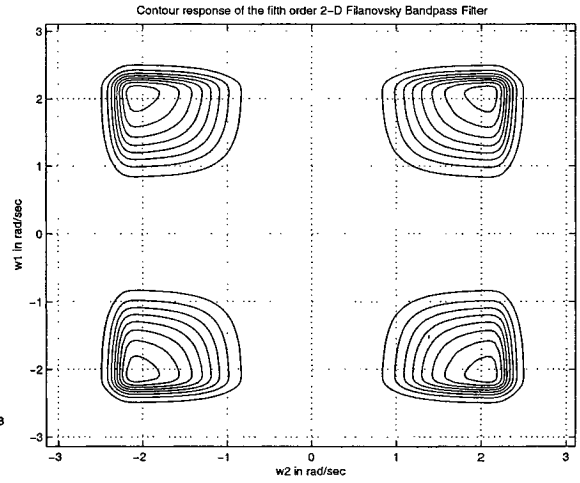

(d) k1=k2=0.5, a1L=a2L=a1=a2=0.9 and b1=b2=-0.7

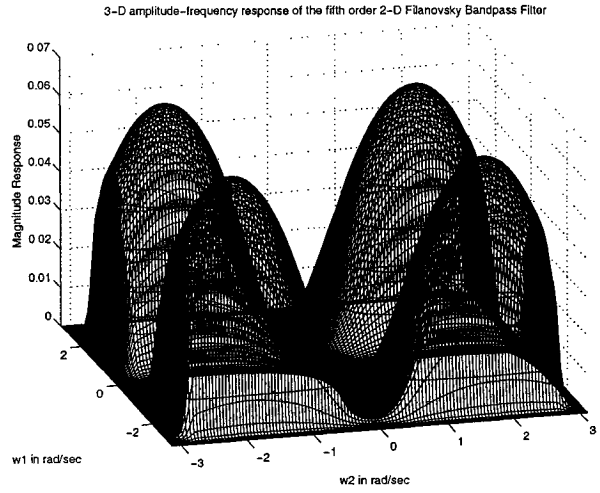

(e) k1=k2=0.2, a1L=a2L=a1=a2=0.9 and b1=b2=-0.7

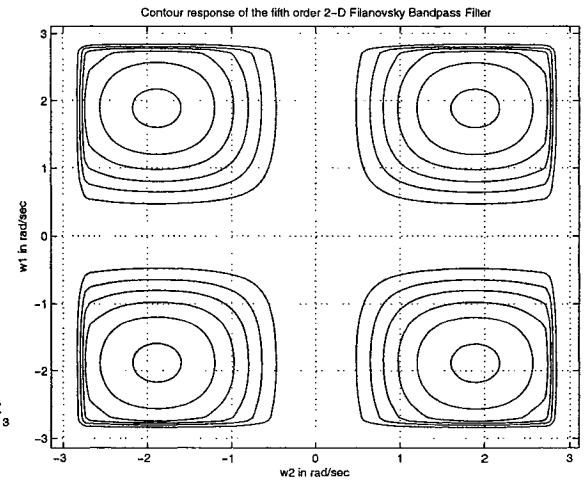

(f) k1=k2=0.2, a1L=a2L=a1=a2=0.9 and b1=b2=-0.7

Figure 5.31: 3-D amplitude-frequency and contour response of the fifth order 2-D digital Filanovsky bandpass filter

fig. 5.33 (a), (b) and fig. 5.33 (c), (d), as a_{1L}, a_{2L}, a_1, a_2 are decreased from 0.9 to 0.7, for same values of $k_1 = k_2 = 0.5$ and $b_1 = b_2 = -1$, the magnitude of the passband decreases. As b_1, b_2, are decreased to -0.7 in fig. 5.34 from -1 in fig. 5.32 and 5.33, the shape and polarity of the amplitude-frequency response changes. In all the cases discussed, the fifth order 2-D Thomson-Bessel bandpass filter inhibits monotonic amplitude-frequency response.

5.4 Summary

In this Chapter, we generated 2-D digital Papoulis, Butterworth, Filanovsky and Thomson-Bessel highpass and bandpass filters, with monotonic amplitude-frequency response and studied their characteristics.

We implemented fifth order 2-D digital Papoulis, Butterworth, Filanovsky and Thomson-Bessel highpass filters with monotonic characteristics, by using one of the corresponding 2-D lowpass filter transfer functions proposed in Chapter 3. Furthermore, we also implemented second order 2-D digital Butterworth highpass filter by utilizing the 2-D lowpass filter transfer function proposed in Chapter 4, having monotonic amplitude-frequency response.

We implemented fifth order 2-D digital Papoulis, Butterworth, Filanovsky and Thomson-Bessel bandpass filters with monotonic characteristics, by using one of the corresponding 2-D lowpass filter and highpass filters proposed in Chapter 3 and Chapter 5, respectively. Furthermore, we also implemented second order 2-D digital Butterworth bandpass filter by utilizing the 2-D lowpass filter and highpass filters proposed in Chapter 4 and Chapter 5, respectively, having monotonic amplitude-frequency response.

The affect of the digital filter coefficients on the 2-D highpass and bandpass filter design were studied. Overall in this Chapter, we proposed different types of 2-D digital highpass and bandpass filters with monotonic amplitude-frequency response.

Algorithm 42 The MATLAB code to plot the 3-D amplitude-frequency response and contour response of the fifth order 2-D digital Thomson-Bessel bandpass filters having monotonic characteristics.

```
% Under Guidance of Prof. Dr. V. Ramachandran
% Student's name : Ajit Singh Sandhu..... ID:4841492.
clc; clear all;
%———Lowpass filter————
k1=input('Give the value of the constant k1 for the bilinear LP transformation => ');
k2=input('Give the value of the constant k2 for the bilinear LP transformation => ');
a1L=input('Give the value of the constant a1L for the bilinear LP transformation => ');
a2L=input('Give the value of the constant a2L for the bilinear LP transformation => ');
% Creates two dimensional square matrix (mesh grid) of angular frequency w1 and w2.
[w1,w2] = meshgrid(-pi:0.05:pi,-pi:0.05:pi);
% Apply Z1=r1*exp(jw1) and Z2=r2*exp(jw2) with r1 = r2 =1
z1=exp(j.*w1); z2=exp(j.*w2);
% h1 is the required digital transfer function and its value is evaluated as follows.
a=z1-a1L; b=z2-a2L; c=z1+1; d=z2+1;
h1_1=((k1.^5).*(a.^5))+((k1.^4).*15.*(a.^4).*c)+((k1.^3).*105.*(a.^3).*(c.^2))
+((k1.^2).*420.*(a.^2).*(c.^3))+(k1.*945.*a.*(c.^4))+(945.*(c.^5));
h1_2=((k2.^5).*(b.^5))+((k2.^4).*15.*(b.^4).*d)+((k2.^3).*105.*(b.^3).*(d.^2))
+((k2.^2).*420.*(b.^2).*(d.^3))+(k2.*945.*b.*(d.^4))+(945.*(d.^5));
h_lpf=((c.^5).*(d.^5).*(945^2))./(h1_1.*h1_2); h1=abs(h_lpf);
%————————Highpass Filter————————————%
k1=input('Give the value of the constant k1 for the bilinear LP transformation => ');
k2=input('Give the value of the constant k2 for the bilinear LP transformation => ');
a1=input('Give the value of the constant a1 for the bilinear LP transformation => ');
a2=input('Give the value of the constant a2 for the bilinear LP transformation => ');
b1=input('Give the value of the constant b1 for the bilinear LP transformation => ');
b2=input('Give the value of the constant b2 for the bilinear LP transformation => ');
% hh1 is the required digital transfer function and its value is evaluated as follows.
a=z1+a1; b=z2+a2; c=z1+b1; d=z2+b2;
hh1_1=((k1.^5).*(a.^5))+((k1.^4).*15.*(a.^4).*c)+((k1.^3).*105.*(a.^3).*(c.^2))
+((k1.^2).*420.*(a.^2).*(c.^3))+(k1.*945.*a.*(c.^4))+(945.*(c.^5));
hh1_2=((k2.^5).*(b.^5))+((k2.^4).*15.*(b.^4).*d)+((k2.^3).*105.*(b.^3).*(d.^2))
+((k2.^2).*420.*(b.^2).*(d.^3))+(k2.*945.*b.*(d.^4))+(945.*(d.^5));
h_hpf=((c.^5).*(d.^5).*(945^2))./(hh1_1.*hh1_2); hh1=abs(h_hpf);
%————————Bandpass Filter————————————%
h_bpf=h_lpf.*h_hpf; hb=abs(h_bpf);
figure(1);
contour3(w1,w2,hb);
surface(w1,w2,abs(hb),'EdgeColor',[.8 .8 .8],'FaceColor','none');
grid on; view(-15,25);
title('3-D amplitude-frequency response of the fifth order 2-D Thomson-Bessel Bandpass Filter');
xlabel(' w2 in rad/sec '); ylabel(' w1 in rad/sec ');
zlabel(' Magnitude Response ');
figure(2);
[C,h] = contour(w1,w2,hb);
clabel(C,h);
grid on;
title('Contour response of the fifth order 2-D Thomson-Bessel Bandpass Filter');
xlabel(' w2 in rad/sec '); ylabel(' w1 in rad/sec ');
```

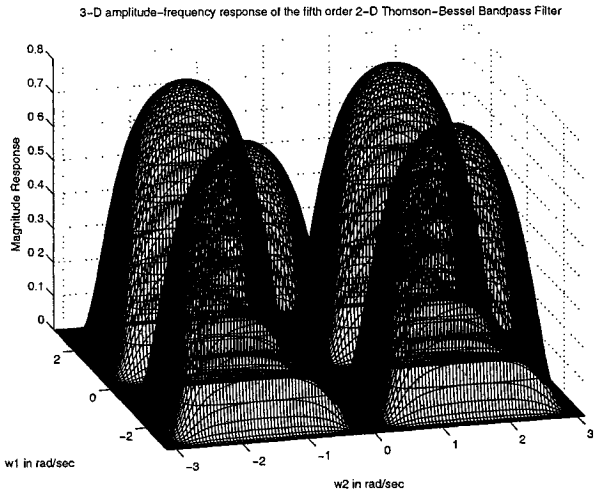

(a) k1=k2=1, a1L=a2L=a1=a2=1 and b1=b2=-1

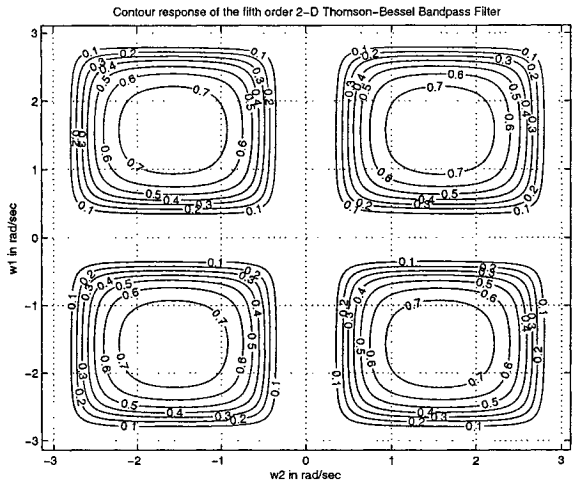

(b) k1=k2=1, a1L=a2L=a1=a2=1 and b1=b2=-1

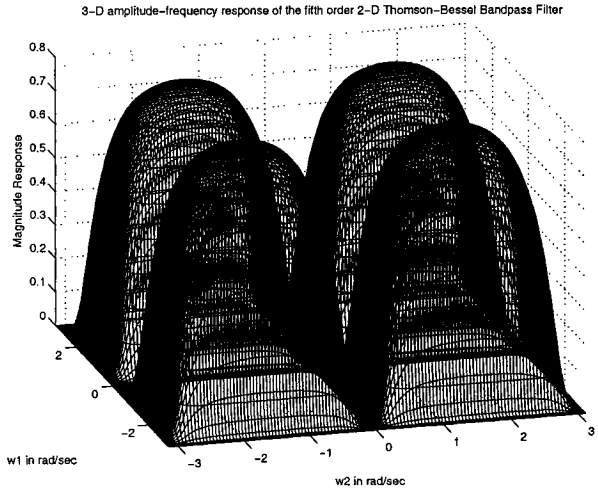

(c) k1=k2=0.7, a1L=a2L=a1=a2=0.9 and b1=b2=-1

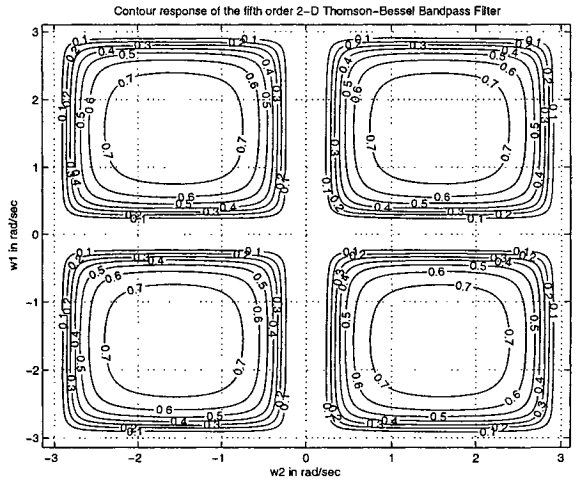

(d) k1=k2=0.7, a1L=a2L=a1=a2=0.9 and b1=b2=-1

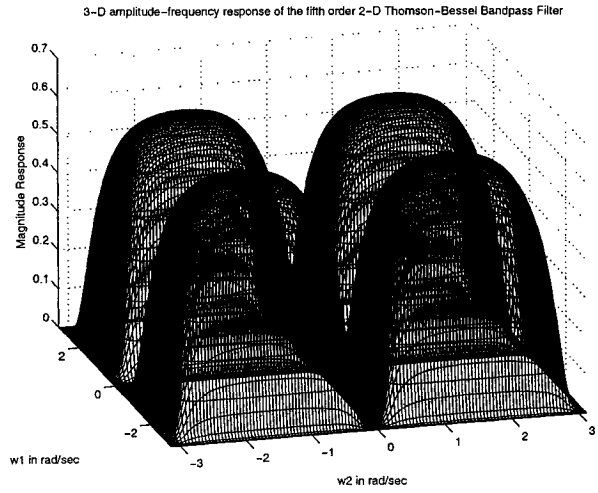

(e) k1=k2=0.7, a1L=a2L=a1=a2=0.7 and b1=b2=-1

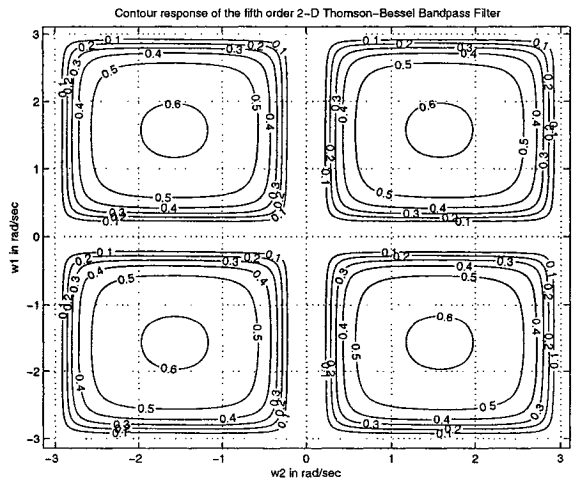

(f) k1=k2=0.7, a1L=a2L=a1=a2=0.7 and b1=b2=-1

Figure 5.32: 3-D amplitude-frequency and contour response of the fifth order 2-D digital Thomson-Bessel bandpass filter

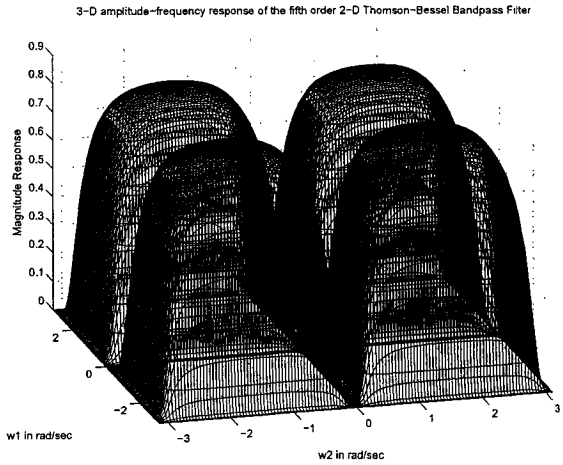

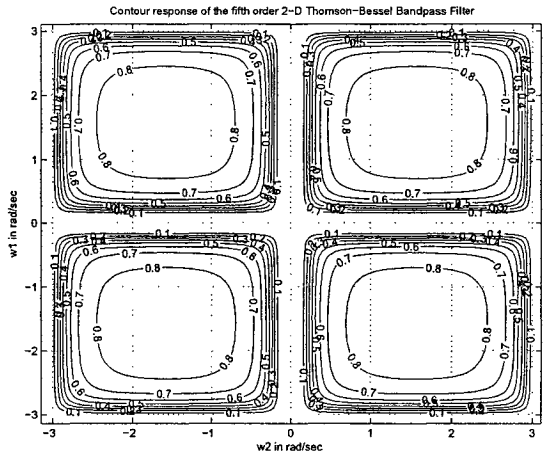

(a) k1=k2=0.5, a1L=a2L=a1=a2=0.9 and b1=b2=-1 (b) k1=k2=0.5, a1L=a2L=a1=a2=0.9 and b1=b2=-1

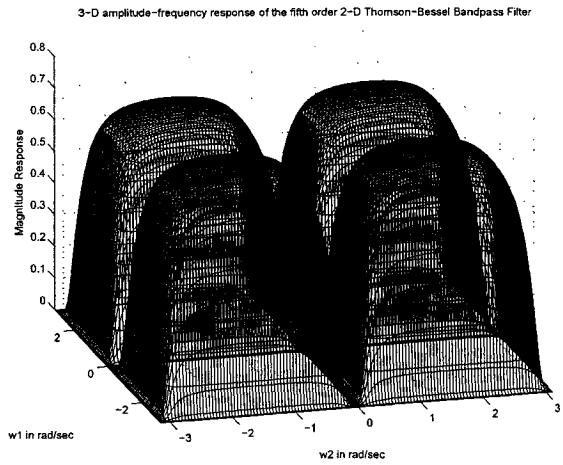

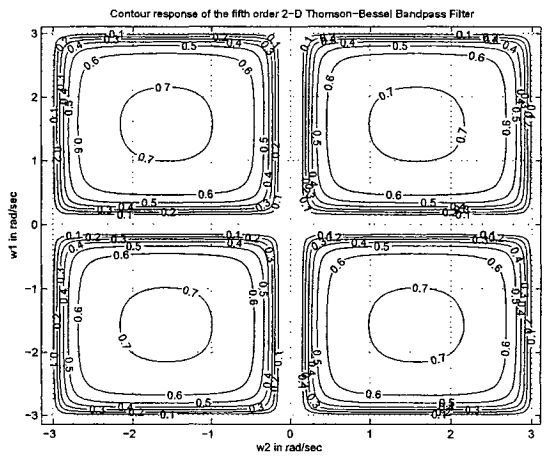

(c) k1=k2=0.5, a1L=a2L=a1=a2=0.7 and b1=b2=-1 (d) k1=k2=0.5, a1L=a2L=a1=a2=0.7 and b1=b2=-1

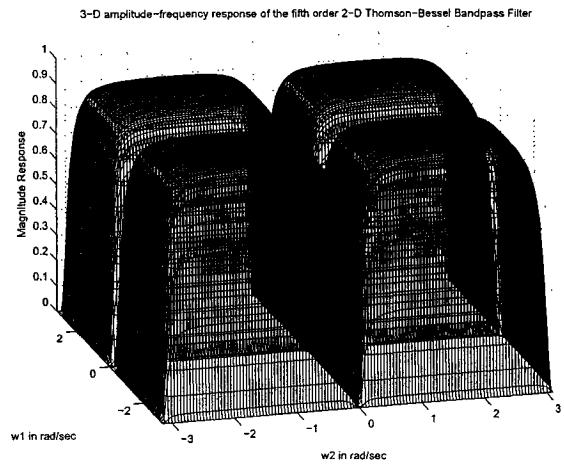

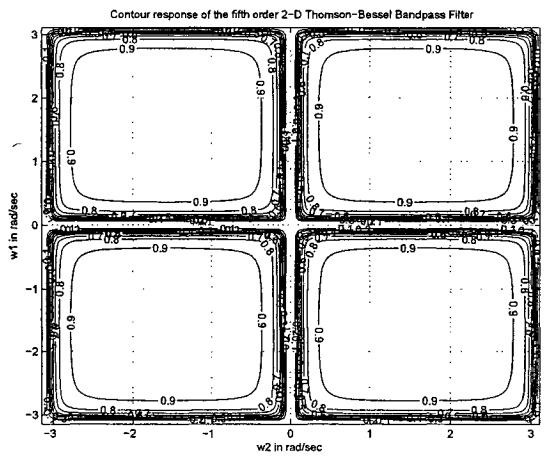

(e) k1=k2=0.2, a1L=a2L=a1=a2=0.9 and b1=b2=-1 (f) k1=k2=0.2, a1L=a2L=a1=a2=0.9 and b1=b2=-1

Figure 5.33: 3-D amplitude-frequency and contour response of the fifth order 2-D digital Thomson-Bessel bandpass filter

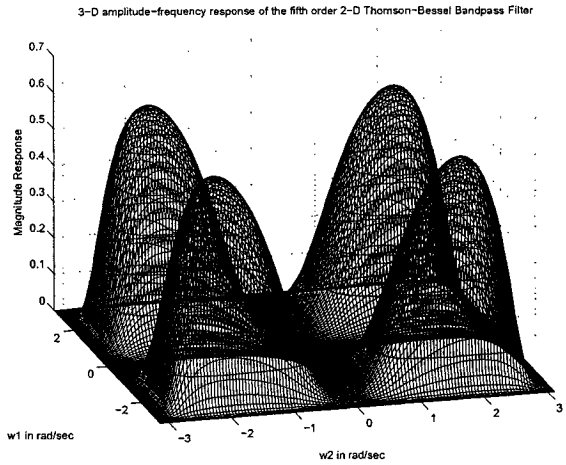

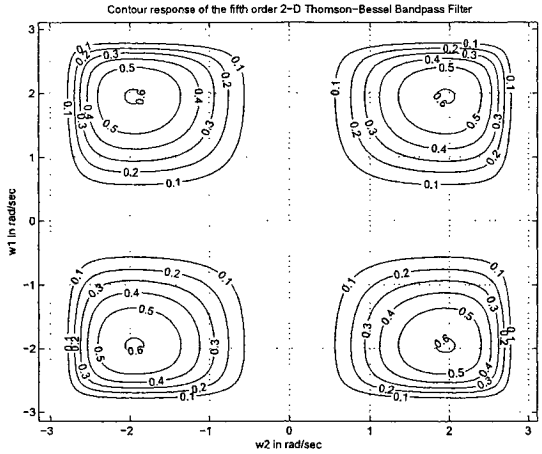

(a) k1=k2=1, a1L=a2L=a1=a2=1 and b1=b2=-0.7 (b) k1=k2=0.2, a1L=a2L=a1=a2=0.9 and b1=b2=-0.7

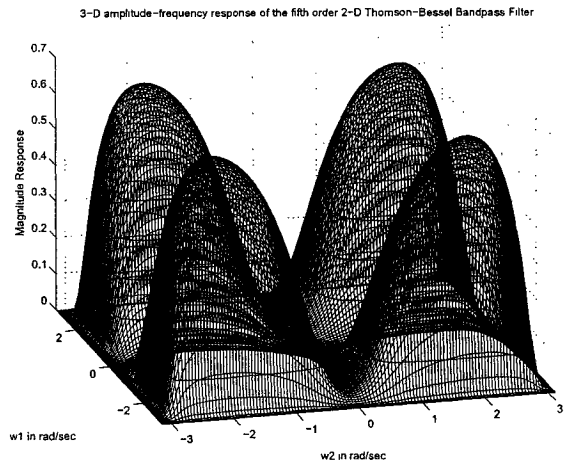

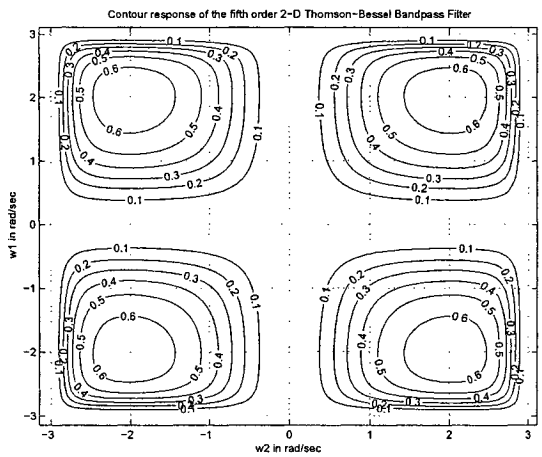

(c) k1=k2=0.7, a1L=a2L=a1=a2=0.9 and b1=b2=-0.7 (d) k1=k2=0.7, a1L=a2L=a1=a2=0.9 and b1=b2=-0.7

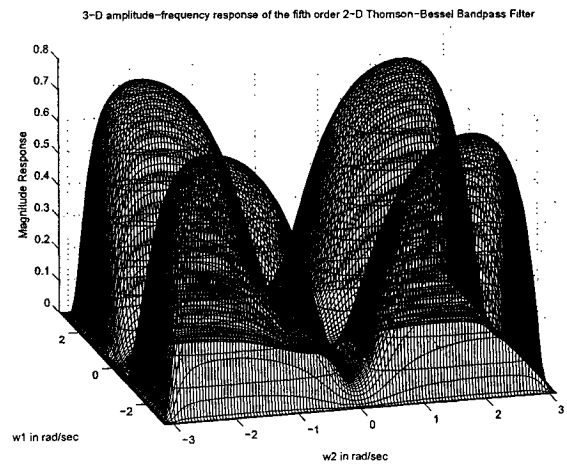

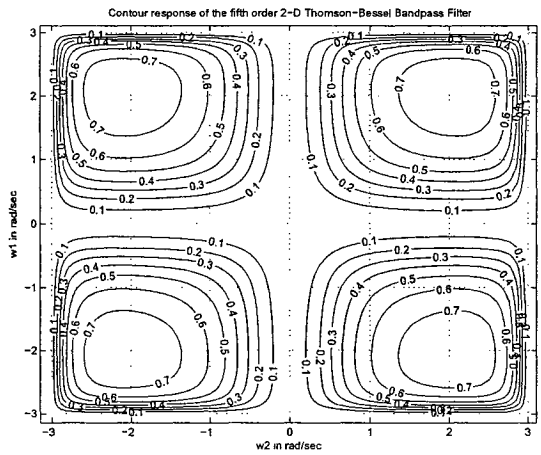

(e) k1=k2=0.5, a1L=a2L=a1=a2=0.9 and b1=b2=-0.7 (f) k1=k2=0.5, a1L=a2L=a1=a2=0.9 and b1=b2=-0.7

Figure 5.34: 3-D amplitude-frequency and contour response of the fifth order 2-D digital Thomson-Bessel bandpass filter

Chapter 6

Some examples of 2-D digital filter application in image and video processing

6.1 Introduction

An image may be defined as a 2-D function with amplitude $f(x, y)$ at any pair of coordinates (x, y) called as intensity or gray level of the image [44]. When these values are all finite and discrete quantities, we call the image digital image. A digital video constitutes frames (digital images) changing at a frame rate, giving perception as moving objects in continuation according to human vision [45].

Fourier transforms are widely used in the field of image processing, where one commonly describe an image in terms of intensity values in a 2-D matrix. The 2-D digital filters can be applied in frequency domain for various standard applications, e.g., image enhancement, image restoration, etc [44, 46]. The 2-D Discrete Fourier Transform (DFT) and Inverse Discrete Fourier transform (IDFT) are effective tools for image processing.

In this Chapter, to show some examples of possible applications of 2-D digital fil-

ters, we will show some examples in image and video processing by using standard image(s)/video(s). In Sec. 6.2, we will study the effect of 2-D digital lowpass filtering in image restoration, by applying it on images/videos corrupted with known amount of noise. We will use Gaussian noise and vary its variance to see the effect of filtering on images, and discuss the results. In Sec. 6.3, we will show an example of extracting different frequency bands/components by applying 2-D lowpass, highpass and bandpass filters.

6.2 Study of 2-D digital lowpass filtering in image restoration

The ultimate goal of image restoration techniques is to improve an image in some predefined sense. Restoration attempts to reconstruct or recover an image that has been degraded by using a priori knowledge of the degradation phenomenon. The restoration techniques are oriented toward modeling the degradation, and applying the inverse process in order to recover the original image. The noise in digital images arise during image acquisition (digitization) and/or transmission. We introduce image degradation artificially by adding noise, which is assumed to be independent of spatial coordinates and uncorrelated with respect to the image itself, i.e., there is no correlation between pixel values of image and the values of noise components [44, 46]. The lowpass filter in the spatial domain is equivalent to that of a smoothing filter, as it blocks high frequencies corresponding to sharp intensity changes, i.e., to the fine-scale details and noise in the spatial domain image.

There are various noise models, e.g., Gaussian noise, Rayleigh noise, Erlang (Gamma) noise, exponential noise, uniform noise, impulse (salt and pepper) noise, periodic noise, etc, available in literature [44]. We will consider Gaussian noise model for our analysis, as its mathematical tractability in both spatial and frequency domains are used frequently in practice. Gaussian noise with zero mean, $n(x, y)$, is added to the image, $f(x, y)$, to get the

degraded image, $f_d(x,y)$, i.e.,

$$f_d(x,y) = f(x,y) + n(x,y) \tag{6.1}$$

We can apply any 2-D lowpass digital filter proposed in Chapter 3, 4 and 5, to remove/reduce the effect of noise, effectively. Let us use the fifth order 2-D digital Butterworth lowpass filter, $H_d(w_1,w_2)$ with $z_1 = e^{jw_1}$ and $z_2 = e^{jw_2}$, proposed in Sec. 3.3.2.2. By applying 2-D IDFT to $H_d(w_1,w_2)$ we get, the 2-D filter function, $h_d(x,y)$, in spatial domain. There are two approaches to apply the 2-D filter,

(i) By convolution of the 2-D lowpass filter, $h_d(x,y)$, with the degraded image, $f(x,y)$, in spatial domain, we expect to recover the image, $f_r(x,y)$,

$$f_r(x,y) = f_d(x,y) * h_d(x,y) \tag{6.2}$$

(ii) By multiplication of the filter, $H_d(w_1,w_2)$, and degraded image, $F_d(w_1,w_2) = DFT[f_d(x,y)]$, in frequency domain, and then 2-D IDFT to get filtered image,

$$f_r(x,y) = IDFT[F_d(w_1,w_2).H_d(w_1,w_2)] \tag{6.3}$$

Although various quality measures are available in literature, those that correlate well with visual perception are quite complicated to compute. Most image/video processing systems of today are designed to minimise the Mean Square Error (MSE), as the quantitative measure, between two images/frames, $f_1(x,y)$, $f_2(x,y)$, which is defined as

$$MSE = \frac{1}{MN}\sum_{x=0}^{M-1}\sum_{y=0}^{N-1}[f_1(x,y) - f_2(x,y)]^2 \tag{6.4}$$

where, M X N is the image dimension, and its product gives total number of pixels in the image. Instead of the MSE, the Peak Signal-to-Noise Ratio ($PSNR$) in decibels (dB) is

more often used as a quality measure. The $PSNR$ is defined as

$$PSNR = 10log_{10}\frac{\Psi_{max}^2}{MSE} \tag{6.5}$$

where, Ψ_{max} is the peak (maximum) intensity value of the image. For the most common eight bit gray image, $\Psi_{max} = 255$.

We have considered images of 8-bit gray levels and added Gaussian noise with zero mean and standard deviation of σ x 255 gray levels. The corrupted image is passed through the 2-D digital lowpass filter, based on (i) approach. The (a) Original image, (b) Degraded image and (c) Recovered/filtered output images are shown in fig. 6.1, 6.2, 6.3 and 6.4. The MSE and $PSNR$ of the output and corrupted images are calculated with respect to the original image as reference. It is observed in the corrupted image that the MSE decreases, and $PSNR$ increases with decrease in noise level (i.e. Standard deviation σ or the noise variance σ^2) of the added Gaussian noise. The recovered image is having blurring effect because of 2-D lowpass filtering. It can be seen that when noise level (i.e. σ) is not high, the MSE, $PSNR$, of the corrupted and output recovered image are closer to each other with small improvement in the recovered image. For example, in fig. 6.4, the noise level is not high (i.e. σ is a smaller value), and the MSE = 163.68 and 144.95 for the degraded (fig. 6.4 (b)) and recovered (fig. 6.4 (c)) image, respectively. Since we are applying 2-D lowpass filtering the sharpness of the image goes down and it can be easily seen in the eyes and the hair of the Linna image. But the effect of the noise is reduced effectively with a blurring effect in the output recovered image. When σ is increased, there is higher level of degradation (noise variance σ^2) in the image and the filtered results have considerable amount of improvement with the 2-D lowpass filtering. For example, in fig. 6.1, since noise level is high (i.e. σ is a comparatively larger value), the MSE = 7974.6 and 628.19 for the degraded (fig. 6.1 (b)) and recovered (fig. 6.1 (c)) image, respectively. In this example, there is significant amount of improvement in the recovered image, and effectiveness of the

2-D lowpass digital filtering can be easily observed, in terms of quantitative measure. The MATLAB code to plot these results is in algorithm 43.

6.3 Determine different frequency bands of images by applying 2-D digital lowpass, highpass and bandpass filters

In the previous section, we showed that an image can be blurred by attenuating the high frequency components of its Fourier transform. Because edges and other abrupt changes in gray levels are associated with high frequency components, image sharpening can be achieved in the frequency domain by a highpass filtering process, which attenuates the low frequency components without disturbing high frequency information in the Fourier transform. A highpass filter, yields edge enhancement or edge detection in the spatial domain, because edges contain many high frequencies. Areas of rather constant gray level consist of mainly low frequencies and are therefore suppressed. A bandpass filter attenuates very low and very high frequencies, but retains a middle range band of frequencies. Bandpass filtering can be used to enhance edges (suppressing low frequencies) while reducing the noise at the same time (attenuating high frequencies). In this section, we will consider fifth order 2-D digital Butterworth lowpass, highpass and bandpass filters proposed in Chapter 3 and 5 to show an example of 2-D filtering in image processing.

We have applied 2-D digital lowpass filter, based on approach (ii) mentioned in Sec. 6.2. We have taken product of the Fourier transform of the image and the 2-D digital filter, to get different frequency bands of the image. The 2-D digital filters considered are fifth order 2-D digital Butterworth lowpass (Sec. 3.3.2.2), highpass (Sec. 5.2.2.1) and bandpass (Sec. 5.3.2.1) filters. Then, the corresponding filtered images in spatial domain are obtained in spatial domain by applying IDFT (eqn. 6.3). The (a) Original image, (b)

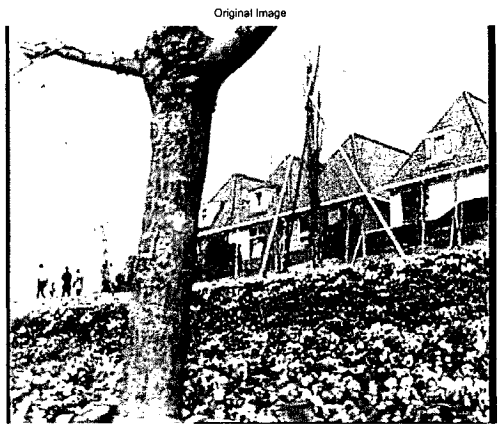

(a) The Original Image

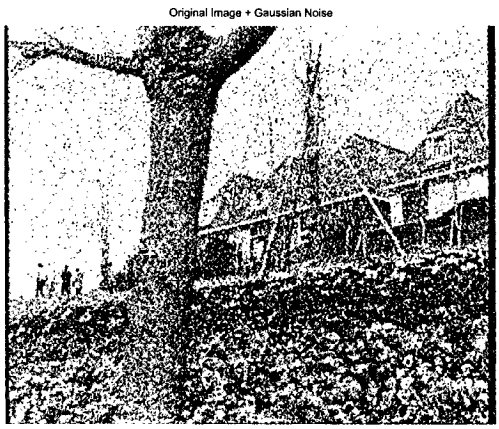

(b) Degraded image with Gaussian Noise

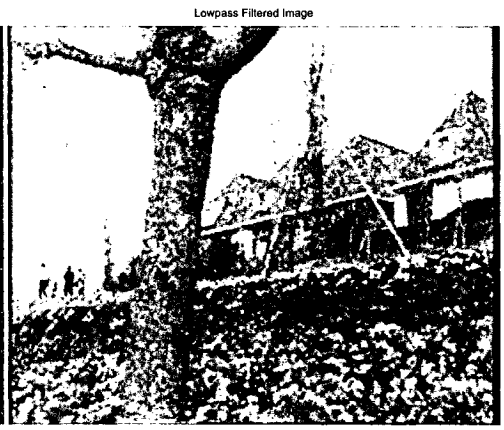

(c) Recovered output image

Figure 6.1: An output of Flower Garden video sequence (Frame: 40, size: 720 X 576) when degraded by added Gaussian noise, and passed through fifth order 2-D digital Butterworth lowpass filter (with $k_1 = k_2 = 0.9$, $a_{1L} = a_{2L} = 1$).
(a) Original Image
(b) Degraded Image, with added Gaussian noise of standard deviation $\sigma = 0.35$, MSE = 7974.6 & PSNR = 9.11 db
(c) Output Image, MSE = 628.19 and PSNR = 20.15 db.

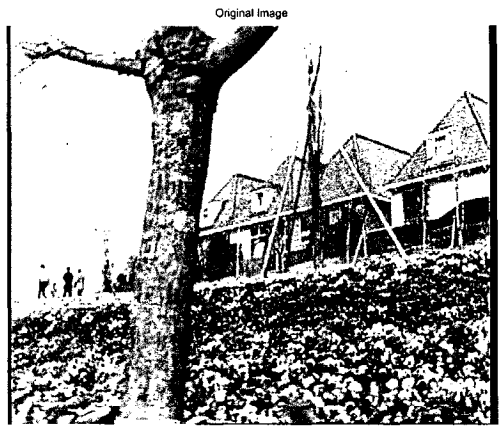

(a) The Original Image

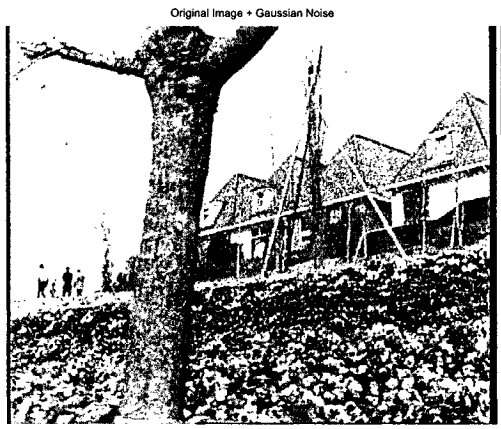

(b) Degraded image with Gaussian Noise

(c) Recovered output image

Figure 6.2: The output of Flower Garden video sequence (Frame: 40, size: 720 X 576) when degraded by added Gaussian noise, and passed through fifth order 2-D digital Butterworth lowpass filter (with $k_1 = k_2 = 0.9$, $a_{1L} = a_{2L} = 1$).
(a) Original Image
(b) Degraded Image, with added Gaussian noise of standard deviation σ = 0.1, MSE = 651.61 & PSNR = 19.99 db
(c) Output Image, MSE = 314.83 and PSNR = 23.15 db.

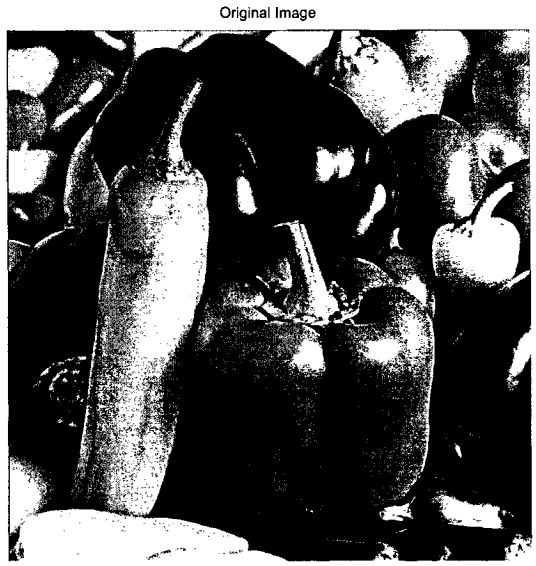

(a) The Original Image

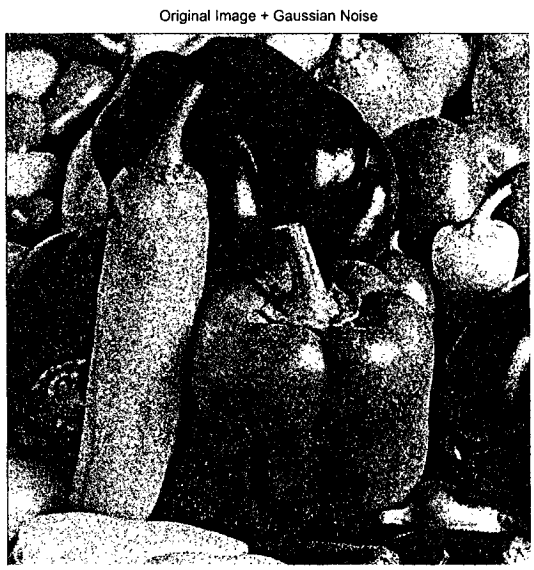

(b) Degraded image with Gaussian Noise

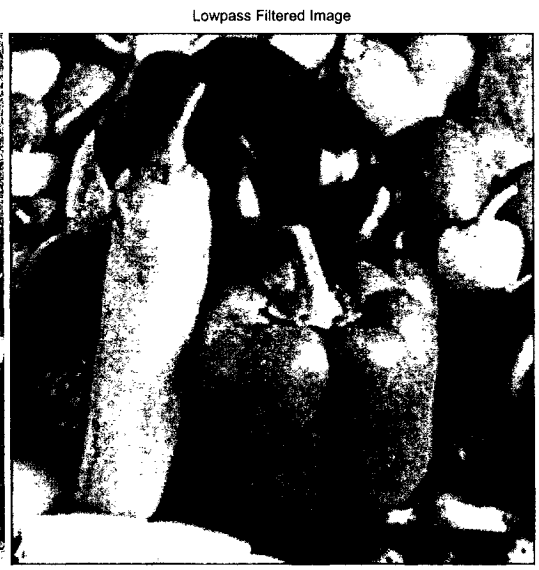

(c) Recovered output image

Figure 6.3: The output of Peppers image (Size: 512 X 512) when degraded by added Gaussian noise, and passed through fifth order 2-D digital Butterworth lowpass filter (with $k_1 = k_2 = 0.9$, $a_{1L} = a_{2L} = 1$).
(a) Original Image
(b) Degraded Image, with added Gaussian noise of standard deviation σ = 0.1, MSE = 649.38 & PSNR = 20.00 db
(c) Output Image, MSE = 132.83 and PSNR = 26.90 db.

(a) The Original Image

(b) Degraded image with Gaussian Noise

(c) Recovered output image

Figure 6.4: The output of Linna image (Size: 256 X 256) when degraded by added Gaussian noise, and passed through fifth order 2-D digital Butterworth lowpass filter (with $k_1 = k_2 = 0.9$, $a_{1L} = a_{2L} = 1$).
(a) Original Image
(b) Degraded Image, with added Gaussian noise of standard deviation σ = 0.05, MSE = 163.68 & PSNR = 25.99 db
(c) Output Image, MSE = 144.95 and PSNR = 26.52 db.

Algorithm 43 The MATLAB code to corrupt the image (or video sequence) by added Gaussian noise and recover the same by applying the fifth order 2-D digital Butterworth lowpass filter.

```
% Image restoration by using fifth order 2-D digital Butterworth Lowpass filter
clc; clear all;
L=5; W=5; miss=floor(L/2);
% Read the image and get pixel values between 0 to 1 value
% imgTemp =imread('peppers.jpg','jpg'); img = double(imgTemp)./255;
% FOR—Video Sequences————————
avi_info = aviinfo('flowerg.avi');
startframe =1; endframe = avi_info.NumFrames
for i = startframe:endframe
avi_frame = aviread('flowerg.avi',i);
img = frame2im(avi_frame);
y = 0.299*double(img(:,:,1))+0.587*double(img(:,:,2))+0.114*double(img(:,:,3));
img=y./255;
% Display the original image/Frame.
figure(1); imshow(img);
title('Original Image');
mxSize = size(img); M = mxSize(1); N = mxSize(2);
% Introducing normal/Gaussian noise with standard deviation - SD and mean - 0
SD=0.1; imgdeg=img+SD*randn(M,N);
% Display the degraded image with known noise value
figure(2); imshow(imgdeg);
title('Original Image + Gaussian Noise');
tot=0; for i = 1:M
for j= 1:N
tot=tot+(imgdeg(i,j)*255-img(i,j)*255)^2;
end; end; mserror=tot*(1/(M*N))
psnr=10*log10((255^2)/mserror)
k1=0.9; k2=0.9; a1L=1; a2L=1;
[w1,w2] = meshgrid(0:((2*pi)/N):(2*pi)-((2*pi)/N),0:((2*pi)/M):(2*pi)-(2*pi/M));
% Creates two dimensional square matrix (mesh grid) of angular frequency w1 and w2.
% Apply Z1=r1*exp(jw1) and Z2=r2*exp(jw2) with r1 = r2 =1
z1=exp(j.*w1); z2=exp(j.*w2);
% h1 is the required digital transfer function and its value is evaluated as follows.
a=z1-a1L; b=z2-a2L; c=z1+1; d=z2+1;
h1_1=(((k1.^2).*(a.^2))+(k1.*1.618.*a.*c)+(c.^2)).*(((k1.^2).*(a.^2))+(k1.*0.618.*a.*c)+(c.^2)).*(a+c);
h1_2=(((k2.^2).*(b.^2))+(k2.*1.618.*b.*d)+(d.^2)).*(((k2.^2).*(b.^2))+(k2.*0.618.*b.*d)+(d.^2)).*(b+d);
% Transfer Function of the Lowpass filter.
h_lpf=((c.^5).*(d.^5))./(h1_1.*h1_2);
h1=abs(h_lpf);
%Taking IFFT of the digital lowpass filter
imgLPF_S = real(ifft2(h_lpf,L,W));
% Convoluting degraded image and lowpass filter in spatial domain
img_out=conv2(imgdeg,imgLPF_S);
% Extracting the image from the enlarged image because of convolution
sz=size(img_out); imgLowpassFiltered=[];
imgLowpassFiltered=img_out(miss+1:sz(1)-miss,1+miss:sz(2)-miss);
figure(3); imshow(imgLowpassFiltered);
title('Lowpass Filtered Image');
mse_LP=mse(imgLowpassFiltered,img)
psnr_LP=10*log10((255^2)/mse_LP)
pause; end;
```

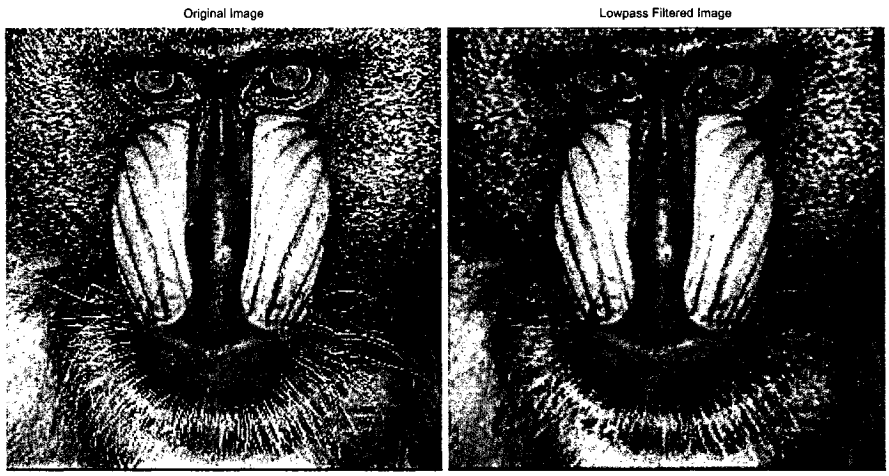

(a) The Original Image (b) Lowpass Filtered Image

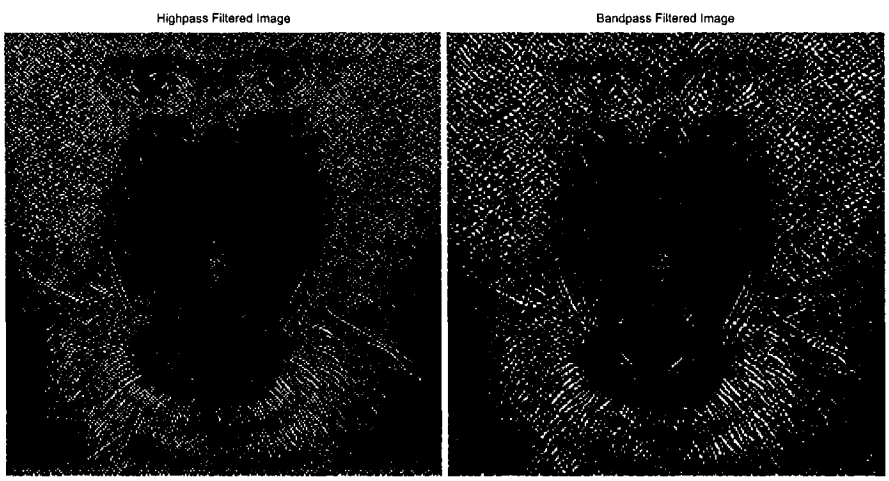

(c) Highpass Filtered Image (d) Bandpass Filtered Image

Figure 6.5: The output of Baboon image (size: 256 X 256) when passed through fifth order 2-D digital Butterworth lowpass, highpass and bandpass filters (with $k_1 = k_2 = 0.3$, $a_{1L} = a_{2L} = a_1 = a_2 = 1$).

(a) The Original Image (b) Lowpass Filtered Image

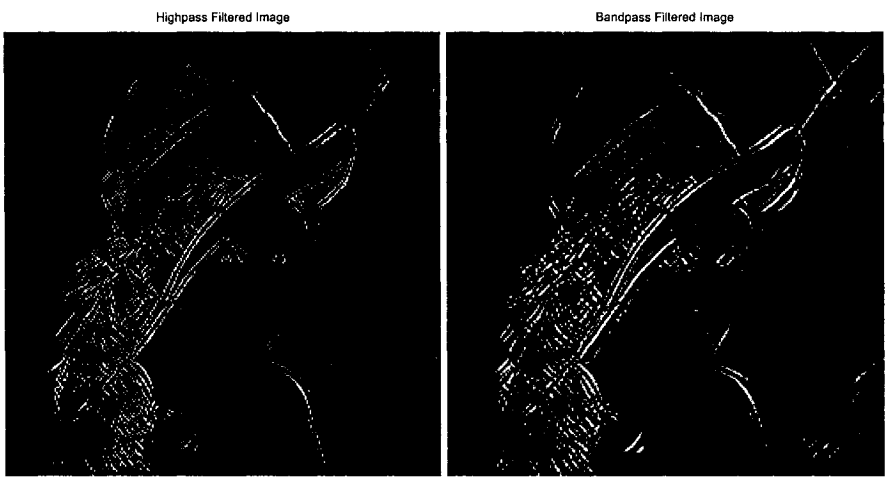

(c) Highpass Filtered Image (d) Bandpass Filtered Image

Figure 6.6: The output of Lenna image (size: 256 X 256) when passed through fifth order 2-D digital Butterworth lowpass, highpass and bandpass filters (with $k_1 = k_2 = 0.3$, $a_{1L} = a_{2L} = a_1 = a_2 = 1$).

Lowpass filtered image, (c) Highpass filtered image and (d) Bandpass filtered image for the Baboon and Lenna images by applying the mentioned methodology are shown in fig. 6.5 and 6.6. The lowpass filtered output is having blurring effect as the high frequency information (the sharpness of the edges) is lost. Since most of the energy of the image is concentrated at low frequencies, the lowpass filtered image output is similar to the original image. The highpass filtered output is having sharp edge information of the image. The bandpass filtered output is having enhanced edge information of the image. The MATLAB code to plot the same is in algorithm 44.

6.4 Summary and Discussions

In image and video processing it is observed that most of the energy of a typical image is located at the low frequencies. On the other hand, energy of the noise is often spread across the frequency axes (e.g. white noise), or in the higher frequency range, depending on its distribution function. One should expect to obtain good noise removal properties from 2-D lowpass filters. The high frequency content of an image constitutes the edges and applying 2-D lowpass filtering will result in blurring of the recovered image.

In Sec. 6.2, standard images are corrupted by additive Gaussian noise with known variance and mean. The 2-D Butterworth lowpass digital filter with same coefficients is used to remove noise from each corrupted image. The MSE and $PSNR$ of the corrupted and recovered images are compared for quantitative measures of the image restoration. In Sec. 6.3, lowpass, highpass and bandpass 2-D Butterworth digital filters are applied to standard original images. The low, high and band of frequencies of the images are extracted and these different bands of images are shown in spatial domain as output. It is interesting to note that by changing the digital filter coefficients a_1, a_2, b_1 and b_2, we are able to obtain different frequency bands of the images. Extraction of different frequency bands can be used in various applications, e.g., contrast improvement, edge detection, image sharpening,

Algorithm 44 The MATLAB code to extract different frequency bands of the image by applying fifth order 2-D digital Butterworth lowpass, highpass and bandpass filters.

```
clc; clear all;
imgTemp =imread('baboon.jpg','jpg');
miss=5;
% Normalize Image
img = double(imgTemp)./255;
mxLennaSize = size(img);
M = mxLennaSize(1); N = mxLennaSize(2);
figure(20); imshow(img);
title('Original Image');
imgLenna=img;
k1=0.3; k2=0.3; a1L=1; a2L=1;
imgSpectrum = FFT2(img);
[w1,w2] = meshgrid(0:((2*pi)/(N)):(2*pi)-((2*pi)/(N)),0:((2*pi)/(M)):(2*pi)-(2*pi/(M)));
% Creates two dimensional square matrix (mesh grid) of angular frequency w1 and w2.
% Apply Z1=r1*exp(jw1) and Z2=r2*exp(jw2) with r1 = r2 =1
z1=exp(j.*w1); z2=exp(j.*w2);
% h1 is the required digital transfer function and its value is evaluated as follows.
a=z1-a1L; b=z2-a2L; c=z1+1; d=z2+1;
h1_1=(((k1.^2).*(a.^2))+(k1.*1.618.*a.*c)+(c.^2)).*(((k1.^2).*(a.^2))+(k1.*0.618.*a.*c)+(c.^2)).*(a+c);
h1_2=(((k2.^2).*(b.^2))+(k2.*1.618.*b.*d)+(d.^2)).*(((k2.^2).*(b.^2))+(k2.*0.618.*b.*d)+(d.^2)).*(b+d);
h_lpf=((c.^5).*(d.^5))./(h1_1.*h1_2);
h1=abs(h_lpf);
imgFiltered=imgSpectrum.*h_lpf;
imgLowpassFiltered = abs(ifft2(imgFiltered));
imgout_LP=imgFiltered;
imgout_LP = circshift(imgLowpassFiltered,[-1 -1]);
figure(3); imshow(imgout_LP);
title('Lowpass Filtered Image');
% For the High PAss filter.....
k1=0.3; k2=0.3; a1=1; a2=1; b1=-1; b2=-1;
% hh1 is the required digital transfer function and its value is evaluated as follows.
a=z1+a1; b=z2+a2; c=z1+b1; d=z2+b2;
hh1_1=(((k1.^2).*(a.^2))+(k1.*1.618.*a.*c)+(c.^2)).*(((k1.^2).*(a.^2))+(k1.*0.618.*a.*c)+(c.^2)).*(a+c);
hh1_2=(((k2.^2).*(b.^2))+(k2.*1.618.*b.*d)+(d.^2)).*(((k2.^2).*(b.^2))+(k2.*0.618.*b.*d)+(d.^2)).*(b+d);
h_hpf=((c.^5).*(d.^5))./(hh1_1.*hh1_2);
hh1=abs(h_hpf);
imgFiltered_HP=FFT2(img).*h_hpf;
imgHighpassFiltered = real(ifft2(imgFiltered_HP));
imgout_HP = circshift(imgHighpassFiltered,[-4 -4]);
figure(6); imshow(imgout_HP./(max(max(imgout_HP))));
title('Highpass Filtered Image');
% Band Pass Filter.....
h_bpf=h_lpf.*h_hpf;
hb=abs(h_bpf);
imgFiltered_BP=FFT2(img).*h_bpf;
imgBandpassFiltered = real(ifft2(imgFiltered_BP));
imgout_BP = circshift(imgBandpassFiltered,[-4 -4]);
figure(9); imshow(imgout_BP./(max(max(imgout_BP))));
title('Bandpass Filtered Image');
```

image segmentation, video processing, etc.

Therefore, in this Chapter, we have shown examples of implementation of 2-D digital lowpass, highpass and bandpass filters in image and video processing. The 2-D lowpass filters are used to remove added Gaussian noise from standard images, or frames of videos. We also showed that how different types of filters can be used to extract different frequency bands from images, which can be furthermore used in various applications like, image enhancement, image restoration, etc [44, 45, 46].

Chapter 7

Conclusions

There has been significant amount of research in 1-D filters with monotonic amplitude-frequency response in the passband and transition band, e.g., Papoulis, Butterworth, Thomson-Bessel, Filanovsky filters to name a few. Multi-dimensional filters with monotonic amplitude-frequency response have not been explored in literature till now. In this thesis, keeping monotonic amplitude-frequency response as the primary aspect, we have explored various possibilities in the 1-D and 2-D analog and digital filters. The monotonic filters of various types, namely, Butterworth, Filanovsky, Papoulis and Thomson-Bessel filters have been studied. We started with study of monotonic 1-D filters and reviewed a generalized design criterion proposed by Filanovsky [14]. We proposed analog lowpass 1-D filters of different orders with monotonic amplitude-frequency response by judiciously combining the poles of the mentioned 1-D filters. The 1-D filters of different types and orders were extended to 2-D analog and digital lowpass filters, and the constraints/conditions to achieve these monotonic 2-D filters were discussed. Another approach to generate 2-D filters is to start with a doubly terminated network. So, we considered a Continued Fractional Expansion, defined its stability, conditions for monotonicity, and implemented it as stable 2-D analog and digital lowpass filters with monotonic amplitude-frequency response. All the 2-D low-pass filters were furthermore, extended to highpass and bandpass digital filters of different

orders with monotonic amplitude-frequency response. In the end, we showed a few basic examples of 2-D filter application in image and video processing.

In Chapter 2, we generated analog 1-D lowpass filters with monotonic amplitude-frequency response. We started with literature review of few monotonic filters, and then discussed a design technique for generation of Butterworth, Papoulis and Filanovsky lowpass filters of any order with arbitrary flatness [14]. We derived the filtering transfer function for the fourth and fifth order Butterworth and Papoulis filters, and also for the fifth order Filanovsky filters. By using the filtering functions, the corresponding 1-D analog stable lowpass filters with monotonic amplitude-frequency response were designed and implemented. Furthermore, Thomson-Bessel filters of fourth and fifth order with monotonic response were also designed. The characteristics of all the designed filters were compared, and results were discussed.

After studying the standard 1-D lowpass analog filters, namely, Butterworth, Papoulis, Filanovsky and Thomson-Bessel filters, we proposed two concepts for monotonic 1-D filters. Firstly, we proposed extraction of all possible lower order 1-D lowpass filters from the implemented filters, namely, Butterworth, Papoulis, Filanovsky and Thomson-Bessel filters. They were based on the real or complex conjugate poles of the higher order 1-D filters implemented. The characteristics of all the lower order 1-D filters were studied and the one with monotonic amplitude-frequency response were segregated. Secondly, we proposed few cascaded combinations of the extracted monotonic lower order filters to attain higher order 1-D lowpass filters. It was verified that these higher order cascaded lowpass 1-D filters of different orders (obtained from different types of filters) also inhibit monotonic amplitude-frequency response.

All the filters discussed and proposed in Chapter 2, were extended to 2-D analog and digital lowpass filters with monotonic characteristics, in Chapter 3. The 2-D analog lowpass filters with monotonic characteristics were derived by cascade realization of the corresponding 1-D lowpass filters. The 2-D digital lowpass filters were generated by applying

generalized lowpass filter bilinear transformation to the corresponding 2-D analog lowpass filters. We generated fourth and fifth order Papoulis, Butterworth and Thomson-Bessel 2-D analog lowpass filters with monotonic characteristics by cascading the corresponding 1-D lowpass filters (derived in Chapter 2), and their results were discussed. The 2-D lowpass filters were also realized in digital (z) domain, and their properties based on different values of coefficients of the generalized bilinear transformation were studied. Similarly, fifth order 2-D Filanovsky lowpass analog and digital filters were generated and their properties were studied. We also generated all possible first to fourth order 2-D analog lowpass filters with monotonic characteristics, by cascade combination of the corresponding extracted lower order 1-D lowpass filters (proposed in Chapter 2) with monotonic amplitude-frequency response. Furthermore, we also realized few fourth, sixth and eighth order 2-D analog lowpass filters, by cascading higher order combinational monotonic 1-D lowpass filters (derived in Chapter 2), with monotonic amplitude-frequency response.

In Chapter 4, we considered a Continued Fraction Expansion (CFE), and starting from this generalized doubly terminated network, we generated 2-D analog and digital lowpass filters, with monotonic amplitude-frequency response and studied their characteristics. The stability of the 2-D analog lowpass filter was defined and proved by checking the transfer function polynomial to be a Very Stable Hurwitz Polynomial (VSHP). Some conditions to be satisfied by the coefficients of the 2-D filter to achieve monotonicity in the amplitude-frequency response were derived. The generalized 2-D analog filter was implemented, and constraints on the coefficients to achieve monotonic characteristics were defined, and verified by simulation results. Furthermore, the coefficients of the generalized 2-D analog lowpass filter required to generate 2-D Butterworth analog lowpass filter were derived by using Koga's technique [29], and the corresponding 2-D analog lowpass filter was implemented. The 2-D lowpass analog filters were implemented in digital domain by applying generalized lowpass bilinear transformation. The effect of the coefficients were studied, and their impact to achieve monotonic amplitude-frequency response were discussed. Also, a sim-

plified relationship between cutoff frequencies and gain of the 2-D Butterworth filter was established. Overall, we proposed a methodology to obtain monotonic analog and digital 2-D lowpass filters by considering a generalized doubly terminated network.

In Chapter 5, we proposed 2-D digital Papoulis, Butterworth, Filanovsky and Thomson-Bessel highpass and bandpass filters, with monotonic amplitude-frequency response, and studied their characteristics. We implemented fifth order 2-D digital Papoulis, Butterworth, Filanovsky and Thomson-Bessel highpass filters with monotonic characteristics, by using the corresponding 2-D lowpass filter transfer functions proposed in Chapter 3. We also implemented second order 2-D digital Butterworth highpass filter by utilizing the 2-D low-pass filter transfer function proposed in Chapter 4, having monotonic amplitude-frequency response. Furthermore, we implemented fifth order 2-D digital Papoulis, Butterworth, Filanovsky and Thomson-Bessel bandpass filters with monotonic characteristics, by cascading the corresponding 2-D lowpass filter and highpass filters proposed in Chapter 3 and 5, respectively. We also implemented second order 2-D digital Butterworth bandpass filter by cascading the 2-D lowpass filter and highpass filters proposed in Chapter 4 and 5, respectively, having monotonic amplitude-frequency response. The effect of digital filter coefficients on the 2-D highpass and bandpass filters, to obtain monotonic characteristics were studied.

In Chapter 6, we have shown examples of implementation of 2-D digital lowpass, high-pass and bandpass filters in image and video processing. The 2-D lowpass filters were used to remove the added Gaussian noise corrupting standard images, or frames of videos. We also showed that how different types of filters can be used to extract different frequency bands from images, which can be furthermore used in various applications like, image enhancement, image restoration, etc [44, 45].

Scope for Future Work

In Chapter 2, we restricted Butterworth, Papoulis, Filanovsky and Thomson-Bessel filter implementation till fifth order because the possible number of lower order 1-D filters to extract and study increases, as there are more pole combinations. As can be readily observed, as the orders increase, the number of combinations increases enormously, and hence, a very large number will be possible. In future, all the 1-D filters can be studied for higher order and a design technique to obtain extracted and combinational 1-D lowpass filters with a specific cutoff frequency can be explored. We can explore the correlation between the coefficients of the monotonic 2-D filters obtained from cascaded equivalent 1-D filters, and monotonic 2-D filters obtained from doubly terminated network, of the same order. Therefore, same type of monotonic 2-D filter can be obtained from both the possible approaches. We can study the 2-D filters obtained from other types of transformations, e.g., impulse invariance method, to obtain 2-D filters monotonic characteristics and study the effect of the coefficients on the filter characteristics. Design of 2-D bandstop filters with a predefined cutoff frequency in both analog and digital domain having monotonic amplitude-frequency response can be explored. The phase response of the filters are not studied in this thesis, and they can be explored in future. The design of standard 2-D monotonic filters, e.g., Butterworth, Papoulis, Filanovsky or Thomson-Bessel filters having a particular type of symmetry in frequency response can also be explored in future. In addition, it is possible that 2-D separable polynomials can be associated with such functions to obtain different monotonic responses.

Bibliography

[1] D.Goodman, "Some stability properties of two - dimensional linear shift-invariant digital filters, IEEE Transactions on Circuits and Systems.", vol.CAS-24, no.4, pp.201-208, April 1977.

[2] D.Goodman, "Some difficulties with double bilinear transformation in 2-D digital filter design.", Proc. IEEE, vol.66, no.7, pp.796-797 , July 1978.

[3] V.Ramachandran, "Some similarities and dissimilarities between single-variable and two- variable reactance functions", IEEE Circuits and Systems Newsletter, vol.10, no.1, pp.11-14, February 1976.

[4] M.Marden, "Geometry of Polynomials", American Mathematical Society, pp.22, 1966.

[5] P. Karivaratharajan, M.N.S. Swamy, "Symmetry Constraints on Two- dimensional Half - Plane digital transfer functions.", IEEE Transactions on acoustics, speech and signal processing, 27(5), pp.506- 511, 1979.

[6] H.C. Reddy, P.K. Rajan, "A comprehensive study of two-variable Hurwitz polynomials", IEEE Transactions on Education, vol.32, Issue: 3, pp.198 -209, Aug. 1989.

[7] V. Ramachandran and C.S. Gargour, "Generation of Very Strict Hurwitz Polynomial and applications to 2-D filter design", Control and Dynamic Systems, Academic Press Inc. vol.69, pp.211-254, 1995.

[8] H.C. Reddy et al., "Generation of two-dimensional digital transfer functions without nonessential singularities of the second kind.", Proc. IEEE Int. Conf. Acoust., Speech, Signal Processing, pp.13 19, April 1979.

[9] Ph. Delsarte, Y. Genin and Y. Kamp, "Two-variable stability criteria", Proc. IEEE Int. Symp. Circuits Syst., pp. 495-498, July 1979.

[10] P.A. Ramamorthy and L.T.Bruton, "Design of stable two dimensional analog and digital filters with application in image processing", Int. J. Circuit Theory Appl., vol. 7, pp.229-245, 1979.

[11] V. Ramachandran and M. Ahmadi, "Design of stable 2-D recursive filters by generation of VSHP using terminated n-port gyrator networks", J. Franklin Inst., vol.316, pp. 373-383, Nov 1983.

[12] S. Basu and A. Fettweis, "Test for two dimensional scattering Hurwitz polynomials.", Circuits, Syst., Signal Processing, vol.3, no. 2, pp. 225-242, 1984.

[13] P. Kavitharajan and M.N.S. Swamy, "Some results on the Nature of a 2-Dimensional Filter functions possessing certain symmetry in its magnitude response.", IEEE Journal on Electronic Circuits and System, vol.2, no.5, pp.147-153, September, 1978.

[14] I. M. Filanovsky, "A Generalization of Filters with Monotonic Amplitude Frequency Response.", IEEE Transactions on Circuits and Systems-I, vol. 46, no.11, Nov, 1999.

[15] A. Papoulis, "Optimum filters with monotonic response", Proc. IRE, vol. 46, pp. 606-609, 1958.

[16] A. Papoulis, "On monotonic response filters", Proc. IRE, vol. 47, pp. 332-333, 1959.

[17] M. Fukada, "Optimum filters of even orders with monotonic response", IRE Trans. Circuit Theory, vol. CT-6, pp. 277-281, 1959.

[18] M.N.S. Swamy, L.M. Roytman, N. Marinovic, S. Huang, "Stability of two-dimensional recursive digital filters", IEEE Trans. Audio Electroacoust., vol. AU-20, pp. 158 - 163, June, 1972.

[19] C.S.Gargour, V.Ramachandran, Ravi P.Ramachandran and F.Awad, "Variable Magnitude characteristics of 1-D IIR discrete filters by a generalized bilinear transformation", Proceedings of the IEEE Canadian Conference on Electrical and Computer Engineering, pp. 1036-1039, 2002.

[20] J.L. Shanks, S. Treitel and J.H. Justice, "Stability of two-dimensional Recursive Filters.", IEEE Trans. Audio-Acoustics, vol. AU-20, June 1972.

[21] Anjit K. Mitra, Michael P. Ekstrom, "Two-dimensional digital signal processing.", Benchmark Papers in Electrical and Computer Science V.20, Dowden, Hutchinson & Ross, Inc., copyright - 1978.

[22] E. Dubois and M.L. Blostein, "A circuit analog method for the design of recursive two-dimensional digital filters.", Proc. IEEE Internet. Symp. Circuits Syst., pp.451 - 454, 1975.

[23] P.A. Ramamoorthy, L.T. Bruton, "Frequency Domain Approximation of stable multi-dimensional discrete filters", Proc. IEEE Internat. Symp. Circuits Syst., pp. 654-657, 1977.

[24] Richard E. Twogood, Sanjit K. Mitra, "Computer-aided design of separable two-dimensional digital filters.", Proc. IEEE Trans. Acoust., Speech, Signal Process. ASSP-25(2), pp.165-169, 1977.

[25] R.L. Rabiner and B. Gold, "Theory and applications of Digital Signal Processing.", Prentice Hall, 1975.

[26] E.I. Jury, "Inners and stability of Dynamic Systems.", John Wiley and Sons, 1974.

[27] S.G. Tzafestas, "Multidimensional Systems: Techniques and Applications", Publisher: New York: M. Dekker, 1986.

[28] M.N.S. Swamy, L.M. Roytman, N. Marinovic, "A necessary condition for the BIBO stability of 2-D filters.", IEEE Transactions on Circuits and Systems II: Analog and Digital Signal Processing, vol. 39, Issue: 7, pp.475 - 476, July 1992.

[29] T. Koga, "Synthesis of Finite Passive n-Ports with Prescribed Positive Real Matrices of Several Variables.", IEEE Transactions on Circuits and Systems, vol. 15, Issue: 1, pp.2 - 23, Mar 1968.

[30] Harry Y-F. Lam, "Analog and Digital filters: Design and Realization.", Prentice-Hall Inc. 1979.

[31] T. Ueda, N. Aikawa, M. Sato, "Design method of analog lowpass filters with monotonic response and arbitrary flatness.", IEEE International Conference on Electronics, Circuits and Systems, vol. 3, pp.15 - 18, Sept. 1998.

[32] P. Halpern, "Optimum Monotonic Low-Pass Filters", IEEE Transactions on Circuits and Systems, vol. 16, Issue: 2, pp.240 - 242, May 1969 .

[33] B. Rakovich and B. Litovski, "Least squares monotonic low-pass filters with sharp cutoff ", Electron. Left., vol. 9, pp. 75-76, Feb. 22, 1973.

[34] D. Rabrenovic, and V. Jovanovid, "Lowpass filters with critical monotonic magnitude", Publications of the Faculty of Electrical Eng., Belgrade,Yugoslavia, no. 84, 1973.

[35] D. Rabrenovic, Z. Aleksic, "Monotonic magnitude response with equal ripple sensitivity", IEEE Transactions on Circuits and Systems, vol. 26, Issue: 11, pp.980 - 983, Nov 1979.

[36] W. Magnus, F. Oberhettinger, and R. P. Soni, "Formulas and Theorems for the Special Features of Mathematical Physics ", New York: Springer-Verlag, 1966.

[37] B. Rakovich, V. Litovski, "Monotonic passband low-pass filters with Chebyshev stop-band attenuation ", IEEE Transactions on Acoustics, Speech, and Signal Processing, vol. 22, Issue: 1, pp.39 - 44, Feb 1974.

[38] A.V. Oppenheim and R.W. Schafer, "Digital Signal Processing" , Prentice-Hall, 1975.

[39] S.K. Mitra, " Digital Signal Processing A Computer-based Approach", McGraw Hill, 1998.

[40] J.G. Proakis and D.G. Manolakis, "Digital Signal Processing Principles, Algorithms and Applications", Prentice-Hall, 1996.

[41] I.W. Selesnick, C.S. Burrus, "Generalized digital Butterworth filter design", IEEE Transactions on Signal Processing, vol. 46, Issue: 6, pp.1688 - 1694, June 1998.

[42] A. Papoulis, "Attenuation Limits for Filters with Monotonic Step Response", IRE Transactions on Circuit Theory, vol. 9, Issue: 1, pp.86 - 86, Mar 1962.

[43] M. E. Van Valkenburg, "Analog Filter Design", CBS College Publishing, 1982.

[44] Rafael C. Gonzalez, Richard E. Woods, " Digital Image Processing", Pearson Education, Inc., Second Edition, 2002

[45] Yao Wang, Jorn Ostermann, YA-Qin Zhang, "Video Processing and Communications", Prentice-Hall, 2002.

[46] Tamal Bose, "Digital Signal and Image Processing", John Wiley and Sons, Inc., 2004.

[47] V Ramachandran, A Rao, "A multivariable array and its applications to ladder networks", IEEE Transactions on Circuits and Systems, vol. 20, Issue: 5, pp.511 - 518, Sep 1973.